Satellite measurements of air quality and greenhouse gases: application to regulatory activities

Chief Scientist's Group report

Date: May 2021

Version: SC200001/R

We are the Environment Agency. We protect and improve the environment.

We help people and wildlife adapt to climate change and reduce its impacts, including flooding, drought, sea level rise and coastal erosion.

We improve the quality of our water, land and air by tackling pollution. We work with businesses to help them comply with environmental regulations. A healthy and diverse environment enhances people's lives and contributes to economic growth.

We can't do this alone. We work as part of the Defra group (Department for Environment, Food & Rural Affairs), with the rest of government, local councils, businesses, civil society groups and local communities to create a better place for people and wildlife.

Author(s):
Andrew Brown[1], Ty Hayward[1], Roger Timmis[1], Kate Wade[2,4], Richard Pope[2,4], Tim Trent[3,4], Hartmut Boesch[3,4] and Rocio Barrio Guillo[3,4]

[1] Environment Agency
[2] School of Earth and Environment, University of Leeds
[3] Department of Physics and Astronomy, University of
  Leicester
[4] National Centre for Earth Observation

Research at the Environment Agency

Scientific research and analysis underpins everything the Environment Agency does. It helps us to understand and manage the environment effectively. Our own experts work with leading scientific organisations, universities and other parts of the Defra group to bring the best knowledge to bear on the environmental problems that we face now and in the future. Our scientific work is published as summaries and reports, freely available to all.

This report is the result of research commissioned by the Environment Agency's Chief Scientist's Group.

You can find out more about our current science programmes at
https://www.gov.uk/government/organisations/environment-agency/about/research

If you have any comments or questions about this report or the Environment Agency's other scientific work, please contact research@environment-agency.gov.uk.

Professor Doug Wilson
Chief Scientist

Executive summary

This report presents the findings of an exploratory Environment Agency project delivered in 2020 to investigate how satellite measurements of air pollutants and greenhouse gases might be applied to the Environment Agency's regulatory activities.

At the time of the work, the Environment Agency was not utilising satellite measurements of air quality or greenhouses gases in any of its regulatory activities. The use of such data was however becoming more widespread in the research and scientific communities, and the potential applicability of the data to regulatory activities was thought to be increasing. For example, the Tropospheric Measuring Instrument (TROPOMI) on the European Space Agency (ESA) Sentinel-5 Precursor ('Sentinel-5P') satellite was providing air pollutant data with higher spatial resolution than previously available. Looking ahead, the 'next generation' of satellite instruments (including geostationary satellites, miniaturised satellites and constellation satellites) also soon promised significant improvements in temporal resolution, spatial resolution and sensitivity.

The work had two main goals: (1) to determine whether current satellite data could be used to detect Environment Agency regulated sites and activities; (2) to develop analysis techniques that might be used in the future to track regulated activity from the next generation of satellites. To deliver these goals, an extensive stakeholder engagement campaign and review of the literature was undertaken, and three proof-of-concept case studies were delivered. The case studies investigated whether measurements of ammonia (using the Infrared Atmospheric Sounded Interferometer (IASI) instrument), nitrogen dioxide and methane (both using TROPOMI) could currently be applied to regulatory activities.

In the ammonia / IASI case study, we identified clear monthly and seasonal variations in measured ammonia over the UK. The monthly and seasonal variations in ammonia measured by the IASI instrument could also be observed in data from the UK ammonia monitoring network. When investigating annual changes in ammonia using the IASI instrument, no overall trend could be identified over 11 years due to the large inter-annual variability of the data, which was probably a result of the limited and sparse number of valid measurements comprising each annual average value.

UK emissions inventories show that ammonia emissions from intensive agriculture have increased in recent years. The IASI satellite data were analysed to see if they could confirm these increases, based on long-term changes and multi-year averages. We found that the IASI data detected above-UK-average increases in ammonia in parts of Powys (Wales) and Shropshire (England) where the growth in intensive agriculture has been especially marked. Satellite data can therefore be used to detect increases in ammonia emissions from intensive agriculture in parts of the UK where these increases are relatively prominent. However, data from current satellite instruments cannot identify ammonia emissions from individual sites as the data is too sparse, its spatial resolution too large and measurements over the UK are not sufficiently sensitive (there is a lack of large ammonia point sources in the UK). Outside the UK, there are larger and less disperse point sources of ammonia that other groups have identified using IASI data with signal sharpening techniques.

In the nitrogen dioxide / TROPOMI case study, we found that satellite data could be used to identify elevated levels of tropospheric column nitrogen dioxide ($TCNO_2$) around three large UK point source emitters of NO_x (Drax power station, Port Talbot Steel Works and Grangemouth refinery), even when averaging only three months of TROPOMI data. The relative strength of the $TCNO_2$ signals from each source was

found to correspond to the size order of their NO_x emissions reported in emissions inventories, *i.e.* Drax > Port Talbot > Grangemouth.

The use of wind-directional conditional aggregation enabled directional NO_2 plumes from Drax and Port Talbot to be identified. When using wind-speed and wind-direction conditional aggregation, directional NO_2 plumes from these point sources could be identified for most wind speed groups. Although visual identification of plumes from these large sources was possible, a brief investigation to quantify the emissions contributing to the plumes was unsuccessful.

The methane / TROPOMI case study was unable to detect elevated levels or plumes of methane from UK landfills. Methane emissions from even the largest UK sources are relatively low compared to sources outside the UK where methane has been successfully detected from TROPOMI data. The case study did however identify a striping issue in the ESA TROPOMI Level 2 methane product, and significantly advanced the Environment Agency's tools, skills and knowledge. This will be beneficial for application to future satellites that are designed for detecting methane point sources: these are expected to be much more capable of detecting UK sources.

Considering the outcome of all three case studies, although we found some evidence of regulated activity in the ammonia and nitrogen dioxide case studies, we concluded that current satellite instruments and their air quality and greenhouse gas data products are not at present readily applicable to assessing regulated processes at individual sites. This conclusion applies to *current satellites* and to *our data analysis methods*, which were relatively simple *i.e.* not combined with other data or modelling. It is important to note that this conclusion may not apply to future satellite instruments or to more complex analysis methods. The 'next generation' of satellite instruments (including geostationary satellites, miniaturised satellites and constellation satellites) promise significant improvements in temporal resolution, spatial resolution and sensitivity and these instruments are much more likely to be applicable to regulation.

The continued development of data products from current satellite instruments and techniques for their use will also increase the potential usefulness of data from current satellites to regulators. Expected developments include: (1) improved signal sharpening techniques to enhance spatial resolution and/or enhance signal strength; (2) improvements to existing Level 2 satellite products (*e.g.* improved bias correction); and (3) more robust determination of uncertainties in Level 3 products. The use of satellite data in combination with other data sources (*e.g.* ground-based instruments and sensors) also has considerable potential.

These future developments mean that in the near future satellite measurements of air quality and greenhouse gases are likely to be applied to a wide range of outcomes including health, ecosystems, climate change and net zero carbon emissions.

As the use and availability of satellite air quality and greenhouse gas data continues to grow, the Environment Agency and other government bodies can expect to be presented with satellite data from industry, campaign groups and members of the public. It is therefore important for the Environment Agency to stay abreast of the ongoing developments satellite data and analysis methods.

This project has enabled the Environment Agency to understand the current and future landscape of satellite measurements of air pollutants and greenhouse gases. It has also enabled data processing methods, including signal-sharpening techniques such as oversampling, to be explored. These methods could be further developed, adapted and applied to data from the next-generation satellites. The Environment Agency is now therefore well positioned to understand, adopt and respond to future developments in this area.

Acknowledgements

The authors would like to acknowledge the following invaluable support in delivering this work described in this report:

Contents

1   Introduction

1.1   Overview

This report is an output from an Environment Agency project delivered in 2020 to investigate how satellite-based measurements (hereafter referred to as 'satellite measurements') of air pollutants and greenhouse gases might be applied to the Environment Agency's regulatory activities.

It should be noted that work described in this report was an *exploratory* study of the potential regulatory use of satellite measurements of air pollutants and greenhouse gases, and the findings of the work are therefore indicative rather than conclusive and definitive. Similarly, the conclusions drawn and recommendations for future work are based on expert judgement, rather than a firm forecast of the use of satellite data in regulatory applications.

The high-level objectives of the work were to:

- Understand the external landscape of satellite measurements of air pollutants and greenhouse gases. Specifically:
    - The current state-of-the-art and how this might be applied to regulation
    - How the measurements are used by research groups and Government bodies
    - What capabilities will be available in the near future and how these might be applied to regulation
    - The advantages and disadvantages of using satellite measurements compared to ground-based monitors
- Suggest how current and future satellite measurements might improve the Environment Agency's ways of working
- Position the Environment Agency to understand if and how it can use data from future satellite instruments

This report starts with this Introduction section (Section 1), which consists of five sub-sections. These set out an overview of this report (sub-section 1.1), the drivers for the work (sub-section 1.2), the role of the Environment Agency in regulating air pollutants and greenhouse gases (sub-section 1.3), an introduction to air quality (sub-section 1.4) and an introduction to greenhouse gases (sub-section 1.5). The latter two of these sub-sections (1.4 and 1.5) are designed as introductory material for the non-specialist.

Section 2 describes the external landscape of satellite measurements of air quality and greenhouse gases and is also designed as introductory material for the non-specialist. This information summarised in this section of the report was delivered through an extensive stakeholder engagement campaign (details of the stakeholders consulted are given in the Annex) and reviews of the literature.

The project delivered three proof-of-concept case studies to investigate whether current satellite data can provide evidence of regulated activity and to understand what further developments are required before satellite measurements might be introduced to provide evidence to support regulation. An overview of the case studies, which investigated satellite measurements of ammonia, nitrogen dioxide and methane, is given in Section 3 of the report. The findings of the case studies are presented in detail in Sections 4, 5 and 6. Section 7 summarises the conclusions of the work.

Disclaimer: During the course of this report, we refer to a number of satellite instruments and data products, data processing methods, ancillary data sources and commercial products. These are used as examples to illustrate the potential of using satellite data for air and greenhouse gas applications only, and are in no way recommendations or endorsements for any instrument, product, data source or method.

1.2 Drivers

The main drivers for this project were:

- The recent increase in the use of Earth observation measurements of air quality and greenhouse gases in the research[1] and wider scientific community. For example, in 2020, a widely communicated use of satellite air quality data was to observe improvements in air quality during the early stages of Covid-19 lockdowns in 2020 (*e.g.* National Centre for Earth Observation 2020). Satellite air quality data were also used widely to report improvements in air quality in the popular media (*e.g.* BBC News 2020).

- The increased awareness of the availability of satellite air quality and greenhouse gas data and its potential use by - for example - industry, public interest groups, scientific committees and members of the public. This has recently increased the possibility of regulators being presented with such data.

- An awareness that the Environment Agency was, at the time of the project, not utilising satellite measurements of air pollutants or greenhouse gases in any of its regulatory activities.

- The recent improvement in the spatial resolution available from satellites measurements of some air pollutants and methane delivered by the Tropospheric Measuring Instrument (TROPOMI) on the European Space Agency (ESA) Sentinel-5 Precursor ('Sentinel-5P') satellite (European Space Agency 2020a). Launched in October 2017, TROPOMI has a spatial resolution as small as 7 x 3.5 km. Data at these scales are more likely to be of use in supporting regulatory activities and permitting decisions than those available from earlier instruments, because such scales are approaching the dimensions of air-pollution plumes from large regulated industrial sites.

- The launch, or impending launch, of instruments on geostationary satellites, which are set to provide a step-change in the temporal resolution of Earth observation measurements of air quality. For example, the ESA Sentinel-4 instrument (European Space Agency 2020b), which is due to be launched on the Meteosat Third Generation - Sounding 1 (MTG-S1) satellite in 2023, will monitor a range of key air quality trace gases and aerosols over Europe with a repeat measurement frequency of approximately one hour (compared to typically two overpasses per day for polar orbiting or sun synchronous-orbiting satellites). More detailed information about current and future Earth observation air quality and greenhouse gas capabilities is given in Section 2.5 and Section 2.6.

---

[1] The number of published journal papers on the Web of Science database containing one or both of the following phrases in the 'topic' field: (a) Air quality, air pollution, air pollutant or air pollutants, (b) satellite, Earth observation or remote sensing, has increased as follows over the last two decades: 24 in 2000, 73 in 2005, 171 in 2010, 309 in 2015, 684 in 2020.

1.3 Air quality and greenhouses gases: the role of the Environment Agency

The Environment Agency plays a key role in ensuring that air quality and greenhouse gas policy and legislation is implemented throughout England[2]. For air quality, the Environment Agency's activities can be summarised as:

- Ensuring that emissions to air from Environment Agency regulated facilities comply with Environmental Permitting Regulations (Legislation 2010). For air quality, these are driven by UK requirements such as the UK Air Quality Strategy (Department for Environment, Food & Rural Affairs 2007) and European Union (EU) requirements such as the Ambient Air Quality Directive (Council of the European Communities 2004), the Fourth Air Quality Daughter Directive (Council of the European Communities 2008), the National Emissions Ceilings Directive (Council of the European Communities 2016), and the Industrial Emissions Directive (Council of the European Communities 2010).

- Supporting local authorities in improving air quality, particularly through the provision technical guidance on behalf of Defra (Department for Environment, Food & Rural Affairs) to local authorities in respect of industrial facilities they regulate.

- Coordinating ambient air quality monitoring for incidents that may have a significant impact on air quality.

- Monitoring ambient air quality around selected regulated installations.

- Delivering the contract management for the UK's ambient air quality monitoring networks (Department for Environment, Food & Rural Affairs 2020a) and providing some of the local site operations for these networks.

- Delivering novel air quality research to underpin current and future legislative activities.

The Environment Agency's greenhouse gas activities can be summarised as:

- Regulating emissions under the Environmental Permitting Regulations (Legislation 2010) and the Industrial Emissions Directive (Council of the European Communities 2010). In 2018, 89% of all methane emissions from Environment Agency permitted sites were from landfills (Environment Agency 2019).

- Administering energy efficiency and greenhouse gas reduction schemes for the UK and regulating these for England, namely: the EU Emissions Trading Scheme for installations (European Commission 2020), the EU Emissions Trading Scheme for aviation (European Commission 2020), the CRC (formerly the Carbon Reduction Commitment) Energy Efficiency Scheme (Department for Business, Energy & Industrial Strategy 2017), the Energy Saving Opportunity Scheme (Department for Business, Energy & Industrial Strategy 2019), Climate Change Agreements (Environment Agency 2020), the

---

[2] In Scotland, Wales and Northern Ireland, the equivalent bodies to the Environment Agency are, respectively: Scottish Environment Protection Agency (SEPA), Natural Resources Wales (NRW) and the Northern Ireland Environment Agency (NIEA) which is part of the Department of Agriculture, Environment and Rural Affairs (DAERA).

Fluorinated Greenhouse Gases Scheme (European Parliament 2014) and the Ozone Depleting Substances Scheme (European Parliament 2009).

- Undertaking novel air quality research to underpin current and future legislative activities.

The Environment Agency's regulation of industrial installations covers several spatial scales, which affect the potential to use satellite data to detect emissions performance:

Most regulated installations are of the individual site scale, usually involving a single permitted installation (*e.g.* an incinerator, cement works or poultry unit). Almost all individual sites are likely to be too small – both geographically and in the scale of their emissions - to be detectable by satellite instruments. A few individual installations such as a large power station may have large enough emissions to be detectable above the background signals. Larger scale areas of interest are industrial complexes or district-scale emissions. These can involve a group of several permitted activities within a defined perimeter (*e.g.* a large refinery or a steelworks with associated industries) or multiple sites that occur in the same district *(e.g.* intensive agricultural facilities in close proximity). The emissions from sites in a group can combine in a single plume and regulation needs to consider the combined (as well as individual) impact of the sites. For these sources, it may be possible to distinguish the combined plume from satellite instruments even though the plumes of individual sites are not discernible.

At a slightly larger scale, satellite data may have potential for estimating the upwind concentration of pollution before air reaches a regulated site, so it can be compared with the downwind concentration, thus allowing the incremental impact of a complex or group of sites to be inferred.

1.4 Air quality – an introduction

1.4.1 Introduction

Poor air quality has been described as the top environmental risk to human health in the UK (Department for Environment, Food & Rural Affairs 2019), and has been linked to around 40,000 deaths per year in the UK (Royal College of Physicians 2016). More detailed information about air quality can be found in a wide range of documents, for example the Clean Air Strategy (Department for Environment, Food & Rural Affairs 2019) and a recent Environment Agency State of the Environment Report (Environment Agency 2018). An overview of the aims of Clean Air Strategy, and some background information on air pollutants and their measurement are however given in the remainder of this section.

Although ambient air quality in the UK has improved significantly since the middle of the twentieth century, and had continued to improve over the past few decades (National Statistics 2020), a number of significant challenges remain, for example:

- Legal limits for nitrogen dioxide are frequently exceeded in some parts of the UK, especially in urban areas.
- Levels of particulate matter are generally within legal limits but remain at levels of concern for human health in many locations.
- The majority of nitrogen-sensitive habitats in England are subject to excess nitrogen deposition.

1.4.2   Clean Air Strategy and key air pollutants

The Clean Air Strategy (Department for Environment, Food & Rural Affairs 2019) was published by the UK Government in January 2019, delivering on a key action in the 25 Year Environment plan (HM Government 2018). The Strategy set out the Government's plans for improving air quality and delivering the UK's emissions reductions commitments[3] under the National Emissions Ceilings Directive and the revised United Nations Economic Commission for Europe (UNECE) Gothenburg Protocol (United Nations Economic Commission for Europe 2020) by 2020 and 2030 with the overarching goals of protecting the nation's health, protecting the environment and securing clean growth and innovation. The Strategy sets out actions to reduce emissions that are focussed on transport, the home environment, farming and industry.

The Clean Air Strategy focuses on the following five pollutants. Some context about the sources and effects of each pollutant, and trends in their emissions is provided for background information.

- **Fine particulate matter (PM$_{2.5}$)** *i.e.* particles with an aerodynamic diameter of ≤ 2.5 μm. PM$_{2.5}$ is emitted from sources such as domestic wood and coal burning, industrial combustion, road transport, the use of solvents and other industrial processes, as well as non-anthropogenic sources such as pollen and sea spray (Department for Environment, Food & Rural Affairs 2020b). The emissions are termed primary particulate matter. Secondary particulate matter can also be formed through chemical reactions between pollutant gases. Particulate matter is readily transported around the body once inhaled and affects health due to the toxicity of the particles themselves, and also because particulate matter acts as a carrier for transporting toxic compounds to parts of the body where they can do harm. Emissions of PM$_{2.5}$ fell by 73% between 1970 and 2018.

- **Ammonia (NH$_3$)** is emitted predominantly from agricultural activities such as the storage and spreading of manures, slurries and fertilisers: 87% of all ammonia emissions in 2018 were from agriculture (Department for Environment, Food & Rural Affairs 2020c). Ammonia can be converted into particulate matter (via ammonium compounds) by mixing with nitrogen oxides (NO$_x$) and sulphur dioxide (SO$_2$). Ammonia, either directly or as ammonium compounds, can cause significant long-term damage to sensitive habitats through a process of nitrogen deposition – in 2015, 62% of sensitive habitats in the UK had more nitrogen deposition than they could effectively cope with. Compared to the other pollutants targeted by the Clean Air strategy, ammonia emissions have fallen by a relatively small amount over the last few decades, decreasing by only 13% between 1990 and 2018.

- **Nitrogen oxides (NO$_x$)**, predominantly nitric oxide (NO) and nitrogen dioxide (NO$_2$), are products of the combustion of fossil fuels, with the main UK sources being road transport, energy generation, domestic and industrial combustion and other transport such as shipping and rail (Department for Environment, Food & Rural Affairs 2020d). Exposure to NO$_2$ can cause inflammation of the airways and susceptibility to respiratory infections and allergens. NO$_x$ also reacts with other pollutants to form ground-level ozone, which is also an air

---

[3] Although emissions reduction commitments are agreed at a UK level, it is important to note that air quality is a devolved matter in the UK, so the Clean Air Strategy is focussed on improving air quality in England. The other nations of the UK (Scotland, Wales and Northern Ireland) have developed or are developing strategies to improve air quality within their territories.

pollutant harmful to health and the environment. Emissions of $PM_{2.5}$ fell by 74% between 1970 and 2018.

- **Sulphur dioxide (SO₂)** is a corrosive, acidic gas which is harmful to health and combines with water vapour in the atmosphere to produce acid rain, thereby damaging the environment and affecting biodiversity. The main sources of SO_2 are currently energy generation, industrial combustion and domestic burning (Department for Environment, Food & Rural Affairs 2020e). Emissions of SO_2 fell by 98% between 1970 and 2018.

- **Non-methane volatile organic compounds (NMVOCs)** are a group of organic compounds predominantly emitted from industrial processes, household products, agriculture, domestic burning and transport (Department for Environment, Food & Rural Affairs 2020f). NMVOCs are a significant component of indoor air pollution due to emissions from, *e.g.* air fresheners, cleaning products, furniture, floorings and perfumes. They react in the atmosphere with other air pollutants to produce ozone and other products that are harmful to health. Emissions of NMVOCs fell by 66% between 1970 and 2018. Of specific concern is formaldehyde, a NMVOC which is classified as a human carcinogen and can also cause irritation to the eyes and upper airways.

1.4.3   Measurements of air pollutants

In the UK, measurements of ambient air quality for the purposes of reporting against air quality legislation are performed by the UK ambient air quality monitoring networks. Comprising around 300 monitoring sites in total, the networks are classified as either 'automatic' (where measurements are performed *in situ* and reported automatically) or 'non-automatic' (where samples are returned to a laboratory for analysis). Full details of the networks, including descriptions of the instruments and measurement techniques used, and detailed information about the monitoring sites, are available on the UK-AIR website (Department for Environment, Food & Rural Affairs 2020a).

The measurement methods used in the ambient air quality monitoring networks are reference methods, *i.e.* methods specified in European standards, or those methods that have been proven to demonstrate equivalence to reference methods. In general, these are methods based on well-established air quality instrumentation, which are often bulky, expensive, non-mobile and required continuous resources (*e.g.* electricity, carrier gas or solvent) to operate.

In recent years, there has been a significant increase in the range of innovative air quality sensors available such as:

- Fixed-point sensors, *i.e.* analysers similar to the instruments currently used in the ambient air quality monitoring networks.

- Pervasive sensors (which are increasingly small in size and relatively low cost). These sensors, which take measurements at fixed points, are often highly portable and are deployable in locations that conventional instruments cannot be due to constraints in *e.g.* size and access to power and telemetry.

- Remote sensors deployed on *e.g.* drones, aircraft and high altitude platform stations, or based on the ground.

- Remote sensors deployed on satellites.

Fixed-point sensors and pervasive sensors have the potential to revolutionise air quality monitoring, although a number of requirements need to be overcome prior to their adoption in the ambient air quality monitoring networks remain. For example:

- Testing and validation of sensors against reference methods in order to demonstrate equivalence.

- The uncertainty of measurements from sensors needs to be reduced so that they comply with quality objectives in ambient air quality Directives.

In general, the above challenges are further from being overcome for pervasive sensors, than fixed-point sensors. Nonetheless, pervasive sensors are already useful for reconnaissance purposes.

Remote sensing of air pollution from ground-based instruments, drones, aircraft or high altitude platform-based instruments is another emerging area. These sensors typically measure pollutants in a path or column of air (rather than at a fixed point), so are not directly applicable to the current legislative requirements of ambient air monitoring. This constraint also applies to sensors on satellites, the subject of this report, although modelling methods may be applied to estimate the ground-level concentration of pollution within the column of air. Satellite measurements of air quality are discussed in much more detail in Section 2.

The advantages, disadvantages and barriers to the wider adoption of all the above sensor technologies are discussed in much more detail in a report by Ricardo Energy & Environment (2015). This concluded that although satellite sensors, ground-based sensors, airborne remote sensors or pervasive sensors are not foreseen to become part or the UK air quality monitoring network before at least 2025, they have a number of advantages over traditional air quality monitoring instrumentation that would be useful in supplementing these networks. For satellite measurements of air quality, these advantages include estimating pollutant concentrations across large areas between fixed-point sensors; identifying regional sources of air pollution that affect local air quality; and providing simultaneous and continuous measurement of multiple pollutants.

For assessing compliance with regulation more broadly (*i.e.* not focussing only on the ambient air quality networks) many instruments are available to measure air pollutants. A detailed discussion of these is outside the scope of this report, but it is important that the method chosen has the following characteristics suitable for the application in question, amongst other considerations:

- A sufficiently low limit of detection

- A sufficiently high upper measurement range

- An appropriate duration of measurement

- A method for ensuring that potentially cross-interfering species do not affect the measurement

- A traceable method of analysis

- An appropriate measurement uncertainty

- Robust measurement and quality assurance and quality control (QA/QC) procedures

As an example, a typical Environmental Agency air quality monitoring campaign might use the following instruments: a chemiluminescence analyser (for NO and NO_2), an optical aerosol spectrometer (for PM_{10} & $PM_{2.5}$), a gas chromatograph with a flame ionisation detector (for selected hydrocarbons) and a UV (ultraviolet) fluorescence analyser (for hydrogen sulphide).

1.5 Greenhouse gases - an introduction

1.5.1 Introduction

Climate change is currently one of the greatest threats to people and the environment. It is having and will continue to have far-reaching effects on economies and societies, and major impacts on habitats and species. The main contributor to climate change is the anthropogenic emissions of greenhouse gases such as carbon dioxide, methane, nitrous oxide and some fluorinated gases: further details are given below.

The UK has domestic targets for reducing greenhouse gases under the Climate Change Act 2008 (Legislation 2008), which initially committed the UK to a reduction in greenhouse gas emissions to at least 1990 baseline by 2050. The Act was subsequently amended in 2019 to a 'net zero' target, *i.e.* a 100% reduction in net emissions (emissions minus removals) from the baseline by 2050.

In the UK, emissions of the basket of the seven greenhouses gases covered by the Kyoto Protocol (carbon dioxide, methane, nitrous oxide, hydrofluorocarbons, perfluorocarbons, sulphur hexafluoride and nitrogen trifluoride) fell by 43% between 1990 and 2018 to an estimated 452 $MtCO_2e$ (megatonnes carbon dioxide equivalent) (Department for Business, Energy & Industrial Strategy 2020a).

1.5.2 Key greenhouse gases

The key greenhouse gases are detailed below. All emissions data referenced in this sub-section is taken from the Government's 2018 Greenhouse Gas Emissions data report (Department for Business, Energy & Industrial Strategy 2020a); all global warming potential data is taken from Myhre *et al.* (2013)/

- **Carbon dioxide (CO_2)** is the greenhouse gas emitted in the largest volume: net CO_2 emissions (*i.e.* CO_2 emissions minus CO_2 removals) in the UK in 2018 were 365.7 $MtCO_2e$ out of a total of 451.5 $MtCO_2e$ from all greenhouse gases. Major sources of CO_2 in the UK are the transport sector (33%), the energy supply industry (26%, approximately two-thirds of which is from power stations), residential combustion (18%) and industrial combustion (15%). Net emissions of CO_2 have decreased by 35% in the last 20 years and by 31% in the last 10 years.

- **Methane (CH_4)**. The global warming potential of methane is approximately 28 times greater than that of carbon dioxide on a 100-year timescale, so even small decreases in methane can have significant benefits in diminishing its contribution to climate change. Total methane emissions in the UK in 2018 were 51.5 $MtCO_2e$, 49% of which were from agricultural process. Waste management activities were the next largest source of methane at 37%, with landfills alone being responsible for 28% of UK methane emissions. Emissions of methane from landfills have decreased by 77% in the last 20 years and by 56% in the last 10 years largely as result of the introduction of the of the Landfill Tax and the Landfill Directive (Council of the European Communities 1999; Environment Agency 2010a), which has diverted biodegradable waste away from landfill and has led to a reduction in the number of operational sites. Total emissions of methane have decreased by 57% in the last 20 years and by 29% in the last 10 years.

- **Nitrous oxide (N_2O)**. The global warming potential of nitrous oxide is approximately 265 times greater than carbon dioxide on a 100-year timescale. Globally, natural sources of N_2O (from various processes associated with the

nitrogen cycle) account for approximately two-thirds of all emissions. In the UK, total emissions of N_2O in 2018 were 20.4 $MtCO_2e$, 70% of which were from agricultural processes, 7% from waste management activities and 7% from land use, land change or forestry activities. Total emissions of N_2O have decreased by 47% in the last 20 years and by 9% in the last 10 years.

- **Fluorinated gases** such as hydrofluorocarbons, perfluorocarbons, sulphur hexafluoride (SF_6) and nitrogen trifluoride (NF_3) are extremely powerful greenhouse gases, with global warning potentials of up to 17,500 times that of carbon dioxide on a 100-year timescale (for SF_6). In the UK, total emissions of fluorinated gases in 2018 were 13.8 $MtCO_2e$, 78% of which were from refrigeration and air conditioning processes and 11% from domestic use of aerosols and inhalers. Total emissions of fluorinated gases have decreased by 37% in the last 20 years and by 13% in the last 10 years.

1.5.3   Measurement of greenhouse gases

In the UK, networks for monitoring greenhouse gases are significantly less extensive that for air pollutants: they are mostly designed to measure background levels of greenhouse gases, whereas networks for monitoring air pollutants are generally designed to measure local impacts in places where such impacts could harm health or the natural environment. The data from the greenhouse gas networks can also be used (with modelling) to validate estimates of the emissions of greenhouse gases. The networks are also less well established than those for air pollutants, due to greenhouse gases being of more recent concern.

The current UK greenhouse gas monitoring networks are outlined in detail in a recent paper (Palmer *et al.* 2018), but in summary they are:

- A network of up to six (currently five) tall tower monitoring stations in the UK and Ireland. The station at Mace Head (Ireland) has been operating since 1987, the other five (Ridge Hill, Tacolnestion, Angus, Bilsdale and Heathfield) have all come online since 2011. The Angus station ceased operation in 2015. All of the currently active stations monitor, at different inlet heights: CO_2, methane, N_2O and SF_6, and all but Ridge Hill also measure CO. Methods used are cavity-ring down spectrometry (for CO_2 and most methane measurements) and gas chromatography (with a variety of detectors) for methane at Mace Head, and all other components at all stations.

- A regional network of five (currently three) monitoring stations across East Anglia, established by the Greenhouse gAs Uk and Global Emissions (GAUGE) project. The stations at Haddenham, Weybourne, and Tilney came online in 2012 and 2013, and are still operational, two other former stations were at Glatton (2014-2016) and Earls Halls (2014-2015). The stations at Haddenham and Tilney measure methane only; the Weybourne measures methane and N_2O; Earls Hall measured methane, N_2O and CO_2; Glatton measured methane, N_2O, CO_2 and CO. The measurement methods used are / were gas chromatography (with flame ionisation detection), FTIR (Fourier transform infrared) spectroscopy and cavity ring-down spectroscopy

A typical Environmental Agency methane monitoring campaign to demonstrate regulatory compliance might measure methane using an analyser based on off-axis integrated cavity output spectroscopy.

The methane case study reported in Section 6 investigated whether methane signals could be identified from landfill sites in the UK. Information about the methods used to quantify the rate of methane emission flux from landfill is given in Section 6.1.2.

2 Satellite measurements of air pollutants and greenhouse gases

2.1 Introduction

A detailed description of satellite measurements of air pollutants and greenhouse gases is beyond the scope of this report. This section does however provide an overview of some of the key aspects of satellite measurements of air quality and greenhouses gases and describes their current use in the UK by government bodies and research groups. It also provides information about the satellite instruments that can currently be used to measure the gases studies in the three case studies described later in this report: ammonia, nitrogen dioxide and methane. Future satellite capabilities for the measurement of air pollutants and greenhouse gases are also signposted.

2.2 Fundamentals

In simple terms, satellite measurements of air pollutants and greenhouse gases are performed by measuring solar backscattered radiation through the whole atmospheric column. Total column measurements can be converted to tropospheric column measurements by correcting for stratospheric contributions.

Conversions from total column measurements to near-surface concentrations are not routinely performed but may be carried out using a transport inversion model. This process is however non-routine and can add a significant uncertainty contribution to the measurement.

For the measurement of gases, the number of molecules in the total column of air is measured by spectroscopic and radiometric cameras (UV, visible, near-IR, and short-wave IR). Particles cannot be measured directly: instead aerosol optical depth (AOD) is measured and particulate matter concentrations are derived.

Air pollutants and greenhouse gases that are commonly measured from satellite instruments include: NO_2, NH_3, CO, O_3, CH_4, CO_2 and water vapour. Of these, NO_2 measurements are perhaps the most useful for UK applications due to their high sensitivity and are the most mature. Measurements of near-ground concentrations of NO_2 (rather than tropospheric column NO_2) are however very challenging to achieve due to issues in distinguishing near-ground NO_2 from, for example, higher-level plumes. The measurements of other gases such as ammonia and methane are more problematic due to lower intensity signals, but measurements of these still possible in the UK: see for example the case studies later in Sections 4 and 6.

To give an indication of the full range of air pollutants and greenhouse gases that can potentially be measured from satellite, the Committee on Earth Observation Satellites (CEOS) & ESA Earth Observation Handbook database (Committee on Earth Observation Satellites 2020) and World Meteorological Organization (WMO) Observing Systems Capability Analysis and Review Tool (OSCAR) database (Word Meteorological Organization 2020) list the following atmospheric chemistry products: 2-methylbutane, 3-carene, α-pinene, β-pinene, CFC-11, CFC-12, HCFC-22, acetone, acetonitrile, ammonia, benzene, bromomethane, butane, carbon dioxide, carbon monoxide, carbonyl sulphide, chlorine nitrate, cyclopentene, dimethylsulphide,

dinitrogen pentoxide, ethane dimethyl sulphide, ethanol, ethyne, formaldehyde, glyoxal, hydrogen, hydrogen chloride, hydrogen deuteride, hydrogen deuterium oxide, methane, methane-d1, methanol, methylbenzene, methylpropane, nitric acid, nitrogen dioxide, nitrogen oxide, nitrogen trioxide, nitrous oxide, ozone, pentane peroxyacetyl nitrate, propane, sulphur dioxide, sulphur hexafluoride and water.

2.3 Satellite products

Satellite products (*i.e.* data from satellite instruments) are disseminated at different 'levels'. Example definitions of the satellite products levels are given in Table 2.1.

Table 2.1   Satellite product levels

Level	Description
L0	Unprocessed instrument data
L1	Calibrated observed radiance or reflectance data at top of atmosphere
L2	Geophysical variables (*e.g.* NO_2, CH_4) at swath resolution.
L3u	Geophysical variables for an orbit or granule mapped onto a regular grid
L3	Geophysical variables averaged over *e.g.* daily or monthly timescales mapped onto a regular grid.
L4	Output or results from the analyses of L0 to L3 data

In practice, Level 2 (L2) products are usually downloaded and processed by end-users to produce Level 3 (L3) and Level 4 (L4) products. It is important to note that L2 and L3 products do are 'whole atmospheric column' data, and do not provide estimates of near-surface concentrations

L2 products are validated before release and are typically accompanied by documentation to support the user. Such documentation can vary in the amount of detail provided, from large 'user guides' produced for ESA L2 products, *e.g.* the L2 NO_2 product user guide for TROPOMI (Royal Netherlands Meteorological Institute (A)) to more brief documentation for some other products, *e.g.* the IASI (Infrared Atmospheric Sounded Interferometer) instrument L2 ammonia product developed by Université Libre de Bruxelles (Aeris 2020). The less complex user guides are however usually supported by detailed publications in the peer-reviewed literature *e.g.* Van Damme *et al.* (2017) for the IASI L2 ammonia product.

Differing data steams may also be available. Using TROPOMI as an example, three data streams are available for the 'official' L2 product for methane, which is disseminated through ESA:

- *Near-real-time data stream:* Available within 3 hours, provides quick access to data for operational applications, but is possibly incomplete and lacks full data quality.

- *Offline data stream:* Available a few days after measurement; suitable for most users.

- *Reprocessing data stream*: Intended for long-term analysis with the latest version to be used to ensure uniformity of data processing.

It is also important to note that more than one L2 product may be available for the same pollutant from the same an instrument. Using TROPOMI and methane again as an example, in addition to the 'official' product disseminated by ESA, two third-party research products are available from SRON (Netherlands Institute for Space Research), and IUP (Institute of Environmental Physics, University of Bremen). These

products and are discussed in more detail in the methane case study in this report (Section 6).

2.4   Advantages and disadvantages of satellite measurements

Satellite measurements of air pollutants and greenhouse gases provide the following advantages over ground-based monitors:

- A very large spatial coverage (global coverage for case of polar orbiting and sun-synchronous satellites; approximately continental coverage for geostationary satellites).

- Measurements can be made at locations where there are no ground-based monitors.

- Measurements of the whole atmospheric column from satellites are more applicable to monitoring plumes from *e.g.* stacks than ground-based monitors

- A consistent and continuous historic dataset, which therefore allows historic incidents to be investigated.

- Data is (generally) free to download and use.

- Simultaneous measurements of multiple pollutants and gases (this is also the case from some ground-based instruments)

The main disadvantages of satellite measurements include:

- A coarse spatial resolution, typically a pixel size of a few km. It should however be noted that:

  - o The spatial resolution of satellite measurements continues to improve. For example, the launch of Sentinel-5P TROPOMI in 2017 provides the capability to measure NO_2 with the best currently available pixel size to date (5.5 x 3.5 km since August 2019). Also, as described in Section 2.6.3, miniaturised satellites and constellation satellites have the potential of performing measurements at a temporal scale of a few metres resolution. These satellites however have limited spatial coverage and are often commercial endeavours, so the data may not be available free-of-charge.

  - o Sub-pixel size resolution can be achieved by application of methods such as oversampling and supersampling: see for example Clarisse *et al.* (2019). More details on these and other techniques to 'sharpen' pollutant signals from satellite data are given in Section 2.5.3.

  - o Satellite measurements can be combined with data from other sources (*e.g.* ground-based air quality monitoring stations, sensors, meterological data and atmospheric dispersion modelling) to produce modelled data outputs with a greater spatial and temporal resolution: see Section 2.10.

- A coarse temporal resolution, with polar orbiting and sun-synchronous satellite typically providing overpasses per day. The number of valid measurements over the UK is often significantly lower than this due to losses caused by cloud coverage and the use of other data quality filters. An effect of these data losses

is that calculated annual averages are likely to be non-representative of the 'real' annul average, as more valid measurements are typically obtained in summer than in winter. Geostationary satellites (see Section 2.6.2) and constellation satellites (see Section 2.6.3) do promise to provide a step-change in temporal resolution, although the issues with data losses due to cloud cover will remain.

- The uncertainty of the measurements is very difficult to determine and is often much larger than for ground-based monitors. For example, for NO_2 see Boersma *et al.* (2018).

- Underlying assumptions being used when processing data from for example, L2 to L3.

- Conversion of total column measurements (which are often provided in units of molecules.cm^{-2}) into more useful near-surface measurements (in units of *e.g.* µg.m^{-3}) requires complex chemical transport modelling techniques to be applied to determine vertical profiles: see *e.g.* for ammonia, Liu *et al.* (2019). This process adds additional uncertainty to the resulting data.

- Processing and interpretation of the data requires expert knowledge and skills

- Being reliant on an irreplaceable single source of satellite data for business-critical activities introduces the risks of the instrument failing or losing sensitivity affecting ongoing business activity. Some back-up data sources are however available in the form of other satellite instruments and ground-based monitors.

- For regulatory activities, there is currently a mismatch between the spatial and temporal resolution of the satellite data (which are large and infrequent) and regulated processes (which are typically small and continuous).

2.5 Current satellite air pollutant and greenhouse gas capabilities

2.5.1 Databases of satellite instruments and capabilities

A large volume of information about current satellite instruments and capabilities can be found online. Two of the most useful sources of information are:

- The WMO OSCAR database (World Meteorological Organization 2020). This database provides information on environmental satellite missions and therefore has a much wider scope that air quality and greenhouse gases. It contains search functions that, for example, allow a timeline of satellite instruments having the potential to measure specific pollutants to be produced.

- The CEOS / ESA Earth Observation Handbook database (Committee on Earth Observation Satellites 2020). This database presents the main capabilities of satellite Earth observations, their applications and a systematic overview of present and planned CEOS Earth observation satellite missions and their instruments. The database is updated annually and is fully searchable.

2.5.2 Current and former satellite capabilities for measuring ammonia, nitrogen dioxide and methane

As an illustration of the range of satellite instruments available for measuring air pollutants and greenhouse gases, tables of the most widely-used current and former instruments measuring the three gases studies in the case studies presented later in this report (ammonia, nitrogen dioxide and methane) are presented in Table 2.2, Table 2.3 and Table 2.4. When viewing these tables, it should be noted that:

- The stated spatial resolution is the best available 'pixel size' (before any application of over sampling techniques) and does not necessarily represent the spatial resolution available over the UK for some or all measurements.

- The stated temporal resolution indicates the approximate measurement frequency over the UK.

- N/A indicates that the information was not be able to be found in publically-available resources at the time of writing.

- Full (non-abbreviated) names of the satellite platforms and instruments can be found in the list of abbreviations at the end of this report.

- More detailed information about these instruments is available through the WMO OSCAR and CEOS / ESA Earth Observation Handbook databases, or websites dedicated to the instruments.

Table 2.2   Satellite measurements of ammonia: current and former capabilities

Satellite platform	Instrument	Operational dates	Approx. spatial resolution	Temporal resolution
Aqua	AIRS	2002 - 2020	50 km	Daily
MetOp-A	IASI	2006 - 2021	12 km	Twice daily
MetOp-B	IASI	2012 - 2024	12 km	Twice daily
MetOp-C	IASI	2018 - 2025	12 km	Twice daily
Suomi-NPP	CrIS	2011 - 2020	14 km	Twice daily
NOAA-20	CrIS	2017 - 2024	14 km	Twice daily

Table 2.3   Satellite measurements of nitrogen dioxide: current and former capabilities *

Satellite platform	Instrument	Operational dates	Approx. spatial resolution	Temporal resolution
ERS-2	GOME	1995 - 2011	40 km	Daily
Envisat	SCIAMACHY	2002 - 2012	30 x 60 km	Daily
Aura	OMI	2004 - 2020	13 x 24 km	Daily
MetOp-A	IASI	2006 - 2021	12 km	Twice daily
MetOp-B	IASI	2012 - 2024	12 km	Twice daily
MetOp-C	IASI	2018 - 2025	12 km	Twice daily
MetOp-A	GOME-2	2006 - 2021	40 km	Daily
MetOp-B	GOME-2	2012 - 2024	40 km	Daily
MetOp-C	GOME-2	2018 - 2025	40 km	Daily
Sentinel-5P	TROPOMI	2018 - 2024	5.5 x 3.5km	Daily

Table 2.4   Satellite measurements of methane: current and former capabilities *

Satellite platform	Instrument	Operational dates	Approx. spatial resolution	Temporal resolution
Terra	MOPITT	2000 - 2020	22 km	Daily
Aqua	AIRS	2002 - 2020	50 km	Daily
Envisat	SCIAMACHY	2002 - 2012	30 x 60 km	Daily
MetOp-A	IASI	2006 - 2021	12 km	Twice daily
MetOp-B	IASI	2012 - 2024	12 km	Twice daily
MetOp-C	IASI	2018 - 2025	12 km	Twice daily
TANSO-FTS	GOSAT	2009 - 2020	10.5 km	Daily
TANSO-FTS/2	GOSAT-2	2018 - 2023	10.5 km	Daily
Suomi-NPP	CrIS	2011 - 2020	14 km	Twice daily
NOAA-20	CrIS	2017 - 2024	14 km	Twice daily
GHGSat	D (Claire)	2016 - N/A	50 m	Daily
Sentinel-5P	TROPOMI	2018 - 2024	7 x 5km	Daily

* A full timeline of satellite instruments measuring methane amount faction is available at [6].

2.5.3   Signal 'sharpening' techniques

Introduction

The use of techniques to 'sharpen' pollutant signals from satellite data is widespread. Techniques such as over sampling and supersampling can be used to enhance spatial resolution to the sub-pixel scale. Other techniques such as wind-rotation and conditional aggregation can be used to increase the intensity of the signal without substantially (if at all) affecting the spatial resolution. These two sets of techniques can be used in combination with each other.

All these techniques used gridded averaged data as their basis, which is the approach where each grid box is simply assigned the arithmetic mean of all measurements whose centres fall into the grid box.

An example of a practical realisation of a number of these techniques is the work of Clarisse *et al.* (2019), where oversampling, wind-rotated oversampling, wind-rotated oversampling and wind-adjusted supersampling were used to pinpoint ammonia point sources.

Techniques to enhance spatial resolution

- **Oversampling** exploits the changing ground footprint of satellite measurements. If the centre and field-of-view of each measurement is known, a smaller sub-grid can be defined and the value of each grid box in this sub-grid can be defined as the average value of all overlapping measurements. In this

---

[4] https://www.wmo-sat.info/oscar/gapanalyses?variable=105
[5] https://www.wmo-sat.info/oscar/gapanalyses?variable=106
[6] https://www.wmo-sat.info/oscar/gapanalyses?variable=23

work, we applied oversampling in the nitrogen dioxide case study (Section 5) and the methane case study (Section 6).

- **Supersampling** is a computational data fitting technique used in other imaging fields that was first applied to satellite air pollutant data in Clarisse *et al.* (2019) – this paper should be referred to for full details. Supersampling is in theory able to provide data at very high spatial resolution, but care must be taken not to over-fit the data, thereby introducing artificial structure.

Techniques to enhance signal strength

- **Wind-rotation:** Each measurement is rotated around a presumed point source along the direction of the wind at the point source. This technique therefore aligns all measurements as if the prevailing wind was from a constant direction. Wind rotation was not used in any of the case studies in this work, but further details are available in Clarisse *et al.* (2019).

- **Wind-directional / wind-speed conditional aggregation** uses measurements when the wind direction (or wind direction *and* wind direction) meets specified criteria - all other measurements are not included in the averaging process. In the ammonia case study (Section 4) and methane case study (Section 6) in this work, we used a simple wind directional conditional aggregation approach based on Lamb weather types (which classify the synoptic meteorology over the UK). The NO_2 case study (Section 5) used hourly wind data around the source of interest to investigate signals from point sources using first wind-directional conditional aggregation, then wind-directional and wind-speed conditional aggregation.

- **Aggregation of measurements from overpasses with (near-)homogenous coverage around the source.** This technique, which was used in the methane case study (Section 6) in this report, uses only measurements from a satellite overpass with a homogenous (or near-homogenous) coverage around the source of interest, usually when these is no (or little) cloud coverage. This can help distinguish between the emissions of interest and artefacts in the data. In the methane case study, we used coverage criteria of > 70% or > 90% over the study area.

- **Other conditional aggregation approaches** may also be defined and implemented, for example by aggregating measurements where:
  - Wider dispersion conditions (*i.e.* not simply wind direction and speed) enhance the emissions from a source. Dispersion modelling can be employed to identify such scenarios.
  - The wind direction means that upwind air impingent on a source has low concentrations of the pollutant of interest, and pollution from the source disperses into an area that has otherwise low concentrations of the pollutant.
  - The activity of the source(s) under study results in high levels of emissions, for example when a power station is operating at full capacity. Detailed knowledge of the operating patterns of the source is required to implement this technique.

These techniques can be used most successfully when a large number of measurements are available. For current satellite instruments with a maximum of two overpasses per day, a long dataset is therefore likely to be needed.

2.6 Future satellite air pollutant and greenhouse gas capabilities

2.6.1 Introduction

Planned future launches of instruments on sun-synchronous or polar orbiting satellites will complement existing air quality and greenhouse gas capabilities by either extending the lifetime of measurements from the same (or similar) instruments already in orbit and/or by providing incremental improvements in sensitivity or spatial resolution. The spatial resolution of future instruments on sun-synchronous or polar orbiting satellites will however still be in the order of a few km, and the temporal resolution will still be no more than two measurement per day.

Two other classes of satellites that offer a potential step-change in capability to measure air pollutants and greenhouse gases are:

- Geostationary satellites. Instruments on geostationary satellites can provide more frequent observations (for example hourly), but do not offer an improvement in spatial resolution over similar instruments on polar orbiting or sun-synchronous satellites.

- Miniaturised satellites[7] / constellation of satellites. Instruments on miniaturised satellites can offer unparalleled spatial resolution, down to a few tens of metres, but the spatial coverage of miniaturised satellites is usually very limited. Constellations of miniaturised satellites are therefore needed to provide broader, perhaps country-scale coverage.

The following sections discuss future geostationary and miniaturised / constellation satellite capabilities for measuring air pollutants and greenhouses gases. High-altitude platform stations are also mentioned briefly.

2.6.2 Geostationary satellites

Three geostationary satellites with instruments to measure air pollutants will be launched planned for the early 2020s. The approximate spatial coverage of each of these instruments are shown in shown in Figure 2.1.

---

[7] In this report, the term 'miniaturised satellite' is used as a generic term to describe any satellite smaller than those launched by major space agencies containing traditional instruments as payloads. Other terms such as 'medium satellite', 'mini (or small) satellite', 'micro satellite', 'nano satellite', 'pico satellite' and 'femto satellite' are sometimes used to describe satellites of different (decreasing) mass ranges.
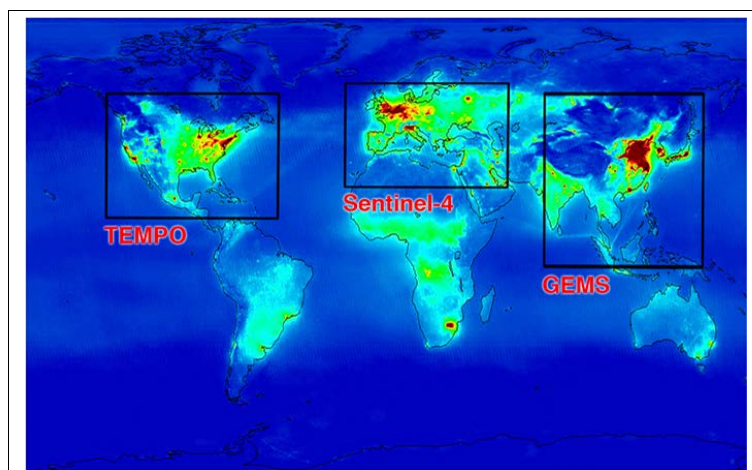
Figure 2.1 Spatial coverage of the TEMPO, Sentinel-4 and GEMS instruments (on geostationary satellites). *Image courtesy of Andreas Richter (University of Bremen) and Jhoon Kim (Yonsei University)*

Further information on each of these three instruments is provided below. The main L2 products for all instruments are O_3, NO_2, SO_2, formaldehyde and aerosols – see the references below for full information of all products)

- The **ESA Sentinel-4** instrument (European Space Agency 2020b) will be launched on the MTG-S1 satellite in 2023 and the MTG-S2 satellite in 2031. The instrument will have a spatial coverage of Europe and parts of North Africa, a spatial resolution of approximately 4 km x 4 km and an hourly temporal resolution.

- The **NASA** (National Aeronautics and Space Administration) **TEMPO** (Tropospheric Emissions: Monitoring of Pollution) instrument (Tropospheric Emissions: Monitoring of Pollution 2020) is planned to be launched on a SpaceX Falcon 9 launch vehicle in 2022. The instrument will have a spatial coverage of North America, a spatial resolution of 2.1 x 4.5 km and an hourly temporal resolution.

- The **KARI** (Korea Aerospace Research Institute) **GEMS** (Geostationary Environment Monitoring Spectrometer) instrument (Kim *et al.* 2020) was launched on the Geostationary Korea Multi Purpose Satellite-2B (GEO-KOMPSAT-2B) satellite in February 2020. The instrument has a spatial coverage of East Asia, a spatial resolution of 5 km x 5 km (over Korea) and an hourly temporal resolution.

2.6.3   Miniaturised satellites and constellations of satellites

Miniaturised satellites have the capability to provide very high spatial resolution measurements of greenhouses gases and air pollutants, but measurements are typically restricted to a relatively small area of the Earth's surface. Constellations of these satellites can however increase this spatial coverage.

Capabilities for measuring greenhouses gases with miniaturised satellites are more advanced than those for air pollutants, with GHGSat currently providing the state-of-the-art capability.

The GHGSat-D - Claire satellite (GHGSat 2020a) was launched in 2016 and measures methane. It has already been used in a number of studies measuring industrial emissions of methane in the US and Middle East: some examples of this are given in the methane case study of this report (Section 6). The instrument has a spatial resolution of 50 m, and is often used in conjunction with a lower spatial resolution instrument such as TROPOMI: the lower resolution instrument can be used to detect the approximate location of large methane emissions and GHGSat-D can then be employed to pinpoint these emissions.

The first of a next generation of GHGSat instruments: GHGSat-C1 - Iris (GHGSat 2020b) was launched in September 2020. The second, GHGSat-C2 - Hugo is planned to be launched in December 2020. These instruments, which will provide an improved spatial resolution of 25 m and a field of view of 12 km x 12 km, are planned to be part of a constellation of 10 satellites operating by 2022. Although GHGSat are a commercial operation, they have recently signed an agreement with ESA to make 5% of data from the GHGSat-C1 – Iris instrument freely available (European Space Agency 2020c).

Other future miniaturised satellites with the capability to measure methane with a high spatial resolution are:

- The Environmental Defense Fund (EDF) MethaneSAT satellite (MethaneSAT 2020). Due to launch in 2022, MethaneSat is a push-broom instrument[8] able to measure methane with a spatial resolution of 1 km x 1 km and a field-of-view of 200 km.

- The ESA Copernicus Carbon Dioxide Monitoring (CO2M) constellation of three satellites (European Space Agency 2020d); (note that these are *not* miniaturised satellites), which with measure CO_2 with a spatial resolution of 2 km x 2 km. A methane product will also be available from CO2M.

- The Bluefield and PlanetLab companies are also developing methane monitoring capabilities (Scientific American 2019), but full details are not currently publicly available.

Miniaturised and satellite capabilities for measuring air pollutants are less advanced, although proposals for a constellation of air quality monitoring sensors have been previously developed by the UV Satellite Data and Science Group (UVSat) at IUP, University of Bremen and ThalesAlenia Space.

2.6.4   High altitude platform stations

Although strictly outside the satellite scope of this report, high-altitude platform stations (HAPS) are worthy of a brief mention in this report. HAPS are typically aeroplanes and balloons operating at altitudes of around 20,000 m and have the advantage over satellites that they do not operate in a fixed orbit, thereby allowing measurements to be focused on area of interest. Their lower altitude also means that measurements with low spatial resolution may be possible.

Several companies and research groups (*e.g.* Airbus and University of Leicester) are actively investigating the use of HAPS for measuring air pollutants and greenhouse gases. Detail of the Airbus Zephyr HAPS can be found at Airbus (2020).

---

[8] Push-broom (or along-track) instruments use a line of detectors arranged perpendicular to the flight direction of the satellite .Measurements are taken one line at a time, with all of the pixels in a line being measured simultaneously

2.6.5 Future satellite capabilities for measuring ammonia, nitrogen dioxide and methane

Table 2.5, Table 2.6 and Table 2.7 outline selected future satellite instruments that will be able to measure the three gases studied in the case studies presented later in this report (ammonia, nitrogen dioxide and methane). When viewing these tables, it should be noted that:

- The stated spatial resolution is the best available 'pixel size' (before any application of over sampling techniques) and does not necessarily represent the spatial resolution available over the UK for some or all measurements.

- The stated temporal resolution indicates the approximate measurement frequency over the UK.

- N/A indicates that the information was not be able to be found from public resources at the time of writing.

- Full (non-abbreviated) names of the satellite platforms and instruments can be found in the list of abbreviations at the end of this report.

- More detailed information about these instruments is available through the WMO OSCAR and CEOS / ESA Earth Observation Handbook databases, or websites dedicated to the instruments.

Table 2.5   Satellite measurements of ammonia: future capabilities. *Instruments on geostationary satellites are shown in italics.*

Satellite platform	Instrument	Operational dates	Approx. spatial resolution	Temporal resolution
JPSS-2	CrIS	2022 - 2029	14 km	Twice daily
JPSS-3	CrIS	2026 - 2033	14 km	Twice daily
JPSS-4	CrIS	2031 - 2038	14 km	Twice daily
MetOp-SG-A1	IASI-NG	2023 - 2030	12 km	Twice daily
MetOp-SG-A2	IASI-NG	2030 - 2037	12 km	Twice daily
MetOp-SG-A3	IASI-NG	2037 - 2044	12 km	Twice daily
MTG-S1	*IRS**	*2023 - 2031*	*4 km*	*Hourly*
MTG-S2	*IRS**	*2031 - 2039*	*4 km*	*Hourly*

* The IRS instruments on the MTG-S satellites has relatively poor spectral resolution which may be an issue in obtaining ammonia lines

Table 2.6   Satellite measurements of nitrogen dioxide: future capabilities. *Instruments on geostationary satellites are shown in italics.**

Satellite platform	Instrument	Operational dates	Approx. spatial resolution	Temporal resolution
MetOp-SG-A1	IASI-NG	2023 - 2030	12 km	Twice daily
MetOp-SG-A2	IASI-NG	2030 - 2037	12 km	Twice daily
MetOp-SG-A3	IASI-NG	2037 - 2044	12 km	Twice daily
MTG-S1	*Sentinel-4*	*2023 - 2031*	*4 km*	*Hourly*
MTG-S2	*Sentinel-4*	*2030 - 2038*	*4 km*	*Hourly*
MTG-S1	*IRS*	*2023 - 2031*	*8 km*	*Hourly*
MTG-S2	*IRS*	*2031 - 2039*	*8 km*	*Hourly*
MetOp-SG-A1	Sentinel-5	2023 - 2030	7 km	Daily
MetOp-SG-A2	Sentinel-5	2030 - 2037	7 km	Daily
MetOp-SG-A3	Sentinel-5	2037 - 2044	7 km	Daily
CO2M-1 Sentinel-7A	Name TBC	2025 - N/A	2 km	Every 3 days
CO2M-2 Sentinel-7B	Name TBC	2025 - N/A	2 km	Every 3 days

* A full timeline of satellite instruments measuring NO_2 amount faction is available at [4]; a full timeline of satellite instruments measuring total column NO_2 is available at [5].

Table 2.7   Satellite measurements of methane: future capabilities. *Instruments on geostationary satellites are shown in italics.**

Satellite platform	Instrument	Operational dates	Approx. spatial resolution	Temporal resolution
MetOp-SG-A1	IASI-NG	2023 - 2030	12 km	Twice daily
MetOp-SG-A2	IASI-NG	2030 - 2037	12 km	Twice daily
MetOp-SG-A3	IASI-NG	2037 - 2044	12 km	Twice daily
MetOp-SG-A1	Sentinel-5	2023 - 2030	7 km	Daily
MetOp-SG-A2	Sentinel-5	2030 - 2037	7 km	Daily
MetOp-SG-A3	Sentinel-5	2037 - 2044	7 km	Daily
MTG-S1	*IRS*	*2023 - 2031*	*8 km*	*Hourly*
MTG-S2	*IRS*	*2031 - 2039*	*8 km*	*Hourly*
GHGSat	C1 - Iris	2020 - N/A	25 m	N/A
GHGSat	C2 - Hugo	2020 - N/A	25 m	N/A
CO2M-1 Sentinel-7A	Name TBC	2025 - N/A	2 km	Every 3 days
CO2M-2 Sentinel-7B	Name TBC	2025 - N/A	2 km	Every 3 days

* A full timeline of satellite-based instruments measuring methane amount faction is available at [6].

2.7   Current uptake of satellite air pollutant and greenhouse gas measurements by UK Government Departments and Bodies

2.7.1   The Environment Agency

Satellite measurements of air quality or greenhouse gases are not used currently used within the Environment Agency for regulatory activities. Work has however been undertaken during 2020 to explore the possibility of using satellite air quality data in the Environment Agency's future activities, and the case studies described later in this

report give a fuller understanding of the challenges of processing and analysing such data.

The Environment Agency does however have interests in using satellite measurements or images for other applications, for example it is currently delivering, or providing potential end-user input into projects that are:

- Detecting the location of bare soil locations vulnerable to erosion

- Detecting the locations and extent of flooding

- Measuring chlorophyll concentrations in water

2.7.2   Other UK Government bodies

A Defra-funded project is investigating how consistent spatial and temporal observations from satellites can validate emissions measurements and reduce uncertainty in the spatial distribution of emissions data in the UK National Atmospheric Emissions Inventory (NAEI) (Department for Business, Energy & Industrial Strategy 2020b). Focussing on validating emissions inventories for NO_2, NH_3 and $PM_{2.5}$, the project is led by the National Centre for Earth Observation and is being delivered through University of Leeds, University of Leicester and STFC-RAL Space. Preliminary results were reported in a poster by Chipperfield *et al.* (2019).

No other UK government bodies or agencies are current utilising satellite measurements of air quality, although there is a significant interest in this emerging field. The Environmental Protection Agency (Ireland) are however currently working with the Central Statistics Office in Ireland to map tropospheric NO_2 measurements from TROPOMI (Linehan 2020).

The potential use of satellite or other remote sensing measurements of air quality is however highlighted as worthy as further investigation or implementation in Highways England's 'Our strategy to improve air quality' (Highways England 2017) and the 2019 review of the Clean Air for Scotland Strategy (Scottish Government 2019).

A flavour of other environmental applications of Earth observation data by other UK Government Departments and bodies are given below. Other applications are currently in development.

- Producing the annual Crop Map of England (CROME) using Sentinel-1 radar and Sentinel-2 optical satellite images.

- Mapping habitat land cover use.

- Detecting the location, timing and extent of wildfires / moorland burning.

- Mapping and monitoring natural capital habitats and ecological services.

- Detecting the patterns and densities of shipping vessels.

2.8 Use of Earth observation measurements for air quality and greenhouse gas applications

2.8.1 Air quality

Selected studies that have used satellite data for air quality applications are summarised below. Due to the extensive nature of research activity in this field, it should be noted that this not intended to be an exhaustive list – it is more to give a flavour of UK-focussed activities, or activities delivered by UK-based research groups.

- Identifying trends in UK air quality between 2005 and 2015, specifically trends in tropospheric column NO_2 and AOD over London, Manchester, Birmingham and the Drax power station (Yorkshire). The study uses data from OMI (Ozone Monitoring Instrument) for NO_2 and the MODIS (Moderate Resolution Imaging Spectroradiometer) instrument for AOD (Pope *et al.* 2018).

- Determine tropospheric column NO_2 levels around three Yorkshire power stations under high and low wind speed conditions using data from OMI (Pope and Provod 2016a).

- Identify increases in particulate matter around Bonfire Night at several locations in the UK between 2011 and 2015 using AOD data from the MODIS instrument (Pope *et al.* 2016b).

- Determining UK-scale NO_2 variations in tropospheric column NO_2 under different meteorological conditions (based on Lamb weather types) using data from OMI (Pope *et al.* 2014).

- Measuring tropospheric column NO_2 at 0.025 x 0.025° resolution (approx. 2-3 km x 2-3 km) over the UK in summer 2018 using data from TROPOMI and comparing these to tropospheric column NO_2 measurements from OMI for the period 2005-2015 and emissions data from the NAEI (Pope *et al.* 2019).

- Determining trends in NO_2 and NH_3 in London, Birmingham, Delhi and Kanpur (2005-2018) using data from OMI and IASI respectively, and trends in AOD in London (2009-2018) and Birmingham (2009-2017) using data from the MODIS instrument (Vohra *et al.* 2020).

- Identifying changes in NO_2 during the first month of the Covid-19 'lockdown' measures introduced by the UK Government in March 2020 (National Centre for Earth Observation 2020).

- Assessing the number and speed of road vehicles using the World View-2 and World View-3 satellites to provide new emissions data for non-exhaust emissions in emissions inventories (Sheehan *et al.* 2019).

2.8.2 Greenhouse gases

Studies using satellite instruments to measure greenhouse gases specifically over the UK are rare, in part because of the low sensitivity of these measurements over the UK and the lack of large methane emissions. There are however many papers in the literature that utilise satellite measurements of methane and CO_2 on a global or regional scale. Noting again that this is not intended to give an exhaustive list of these studies, instead to just provide a flavour, these include:

- Estimating annual methane emissions using data from the SCIAMACHY (Scanning Imaging Absorption Spectrometer for Atmospheric Chartography)

and GOSAT (Greenhouse Gases Observing Satellite) instruments (Buchwitz *et al.* 2017).

- Determining regional fluxes of CH_4 and CO_2 using data from the GOSAT instrument (Feng *et al.* 2017).

- Determining total global, United States and North American methane emissions (Turner *et al.* 2015) and total Indian methane emissions (Ganesan *et al.* 2017) using data from the GOSAT instrument and other non-satellite sources.

- Producing global height-resolved methane retrievals using data from the IASI instrument (Siddans *et al.* 2017).

Palmer *et al.* (2018) notes that satellite measurements are likely to play an increasing future role in validating UK greenhouse gas emissions.

2.9 Uncertainty and quality assurance

2.9.1 Uncertainty

The air pollutant and greenhouse gas geophysical parameters in L2 products are typically provided with uncertainties, although the metrological robustness of these uncertainties is likely to vary from product-to-product. Details of the method used to derive these uncertainties should be available in the literature accompanying each product. Contributing factors to the uncertainty on the L2 products include uncertainties from: spectral fitting, conversion from slant column density to vertical column density, and corrections from ground-based validation measurements.

The magnitude of the uncertainty can vary significantly for different L2 products from the same instrument. For example, for TROPOMI, the relative errors associated with the L2 total column methane product are typically 1.5% (bias) and 1% (random), whereas for SO_2, the relative bias error is 30-50%.

The determination of uncertainties for L3 products is even more complex as the uncertainty structure of the L2 products needs to be determined in order for the uncertainties to be appropriately propagated to L3 products.

Work is underway to provide a robust underpinning metrological framework for satellite measurement. For example, the National Physical Laboratory are currently working to develop a robust uncertainty approach for ozone total column retrievals from the SCIAMACY and GOME (Global Ozone Monitoring Experiment) instruments.

2.9.2 Quality assurance

Some brief information about the traceability, calibration and validation of satellite greenhouse gas and air quality products is given in this section.

Traceability

As air quality and greenhouse gas products are derived from a number of data sources and parameters including 'raw' satellite data, ancillary data (*e.g.* cloud retrievals and

slant column densities) and reference data (*e.g.* spectral calibration data), the traceability chain back to SI units is highly complex.

The QA4ECV (Quality Assurance for Essential Climate Variables) project (Quality Assurance for Essential Climate Variables 2020a) studied the traceability and other quality assurance aspects of satellite products of essential climate variables (ECVs) and is a detailed source of information on the matter. For example, detailed and interactive traceability chains for three atmospheric products (formaldehyde, NO_2 and CO) have been produced (Quality Assurance for Essential Climate Variables 2020b).

Calibration and validation

The spectrometers on satellite instruments are calibrated in the appropriate radiometric regions with data from spectroscopic databases. Calibration typically take place pre-launch and then in-flight using black bodies.

Satellite measurements of air pollutants and greenhouse gases are validated against either ground-based measurements or aircraft-based measurement of vertical profiles. As an example, methane measurements from TROPOMI are validated against FTIR instruments that form part of the NDACC (Network for the Detection of Atmospheric Composition Change) and TCCON (Total Carbon Column Observing Network) networks. Any required corrections from these validation measurements are incorporated into the algorithm producing the L2 product. Full details on the calibration and validation activities for TROPOMI are available (European Space Agency 2020g).

2.10   Use of satellite data with data from other sources

As mentioned in Section 2.4, satellite measurements of air pollutants and greenhouse gases currently have a number of constraints if used in isolation, most obviously their limited temporal and spatial resolution.

Combining satellite data with data from other sources such as ground-based monitors (*e.g.* monitors comprising the UK ambient air quality-monitoring networks managed by the Environment Agency), sensors, emissions inventories, metrological data and modelling is however potentially a much more powerful approach - the complementary strengths of these can produce a powerful tool for the end-user. The combination of data from satellite instruments with data from other sources has not been investigated in this work described in this report: the three case studies used data *only* from satellite instruments.

It is however worthwhile to mention products which do combine data from satellite instruments with data from other sources.

The Copernicus Atmospheric Monitoring Service (CAMS) (Copernicus Atmospheric Monitoring Service 2020a) provides real-time and 5-day air quality forecast data free-of-charge to end-users using input data from satellites, ground-based observation stations, aircraft, ships and balloons in combination with an ensemble model. Details of the satellite observations used by CAMS are given at Copernicus Atmospheric Monitoring Service (2020b); the pollutants and greenhouse gases for which satellite data are used by CAMS are O_3, CO, NO_2, SO_2, AOD, CH_4 and CO_2. Full details of the datasets available in CAMS data catalogue are given at Copernicus Atmospheric Monitoring Service (2020c).

An advanced UK commercial application of combining satellite and other air quality data is the EarthSense MappAir® product (EarthSense 2020). This uses computation fluid dynamics to combine data from satellites, emissions inventories, traffic, weather, sensors and reference analysers to produce high spatial resolution (up to 10 m) three-day forecast maps of NO_2, O_3, SO_2, $PM_{2.5}$ and PM_{10}. Historic datasets are also available. Similar products may be available from other companies.

3 Case studies: Introduction and overview

3.1 Introduction

This section outlines and provides the rationale for three proof-of-concept case studies. The case studies investigated whether data from current satellite instruments were able to provide evidence of air pollution or greenhouse gases from regulated processes, and what further developments (if any) would be required before satellite measurements can provide evidence to support regulation. The results of the case studies are presented and discussed in Section 4, 5 and 6

We were fully aware that the 'next generation' of satellite instruments promise significant improvements in temporal resolution, spatial resolution and sensitivity. These case studies were however an exercise in investigating the capabilities of *current* satellite instruments. This enabled us to, for example: understand the background to these future improvements; prepare refined analysis methods ready for use with these improved data, and to build awareness and skills for future applications. The three case studies were an exercise in investigating the capabilities of current satellites, for these purposes. In particular, they enabled the Environment Agency to develop data processing methods, including signal sharpening techniques (see Section 2.5.3) such as oversampling that could be adapted in the future for application to this next-generation satellite data.

3.2 Overview

The three case studies are summarised in Table 3.1.

Table 3.1   Case studies delivered in this work

Case study	Target	Question(s)	Instrument [satellite]	Delivered by
A	Ammonia	1. Can monthly, seasonal or annual variations in ammonia over the UK be identified? 2. Can areas of the UK with recent large increases in measured ammonia be identified? 3. Can IASI ammonia data be used in regulatory activities?	IASI [MetOp-A]	Environment Agency (Geomatics Team)
B	Nitrogen dioxide	1. Can above-background NO_2 emissions from large regulated sources in the UK be identified? 2. Can directional plumes of NO_2 be from these sources be observed and quantified 3. Can TROPOMI NO_2 data be used in regulatory activities?	TROPOMI [Sentinel-5P]	University of Leeds / National Centre for Earth Observation (NCEO)
C	Methane	1. Can emissions of methane from landfills be observed? 2. Can TROPOMI methane data be used in regulatory activities?	TROPOMI [Sentinel-5P]	Environment Agency (Geomatics Team) with University of Leicester / NCEO[1]

In order to maximise the chances of success, the case studies were defined by identifying potentially high signal-to-background situations associated with emissions from Environment Agency regulated sources. For example, for nitrogen dioxide and methane, we investigated situations where the 'foreground' signal due to relevant source emissions was thought to be relatively distinct, and prominent relative to 'background' air that contained low levels of the pollutant.

Some further detail on each of the case studies is provided below:

- The **ammonia case study** did not try to resolve ammonia from individual agricultural sites, because of the relatively coarse spatial resolution of the satellite data (oversampling was not used in this case study) and because individual UK sites are not large emitters of ammonia. Instead, composite ammonia signals from groups of regulated sites at a district scale were investigated, because such district signals were considered large enough to be resolved. As part of this case study, Lamb weather types were used as a signal sharpening technique that collated and aggregated satellite data into different wind-direction sectors.

- The **NO$_2$ case study** investigated whether plumes containing emissions from industrial complexes or other large regulated sources could be identified. The amounts of NO$_2$ measured in the local area over and around these sources were expected to be above outlying background levels. This case study used oversampling, wind-directional conditional aggregation, and wind-directional and wind-speed conditional aggregation as signal sharpening techniques.

- The **methane case study** also investigated whether signals containing emissions from site-scale regulated sources could be identified. The amounts of methane measured in the local area over and around these sources were also expected to be above outlying background levels. This case study also used Lamb weather types as a wind-conditional aggregation signal 'sharpening' technique. The aggregation of measurements from overpasses with near-homogenous coverage around the source (see Section 2.5.3) was also investigated.

In the process of defining the three case studies, several other possible case studies were considered. Examples of these include the measurement of SO$_2$ and NO$_2$ emissions from shipping in UK waters (which was not taken forwarded because shipping is not a regulated activity) and particulate matter upwind / downwind of a large steel works (which was not taken forward because of resource constraints).

4 Case study A: Ammonia / IASI

4.1 Introduction

4.1.1 Background

Ammonia, either directly or as ammonium compounds, can cause significant long-term damage to sensitive habitats through the process of nitrogen deposition. On average between 2016 and 2018, 58% of sensitive habitats in the UK had more nitrogen deposition than they could effectively cope with (Rowe *et al.* 2020). Ammonia also can be converted into fine particulate matter by reacting with nitrogen oxides and sulphur dioxide and can therefore indirectly contribute to significant human health impacts such as cardiovascular and respiratory diseases (Department for Environment, Food & Rural Affairs 2019).

Ammonia is emitted predominantly from agricultural activities such as the storage and spreading of manures, slurries and fertilisers, and from animal waste produced in intensive agriculture facilities. In 2018, 87% of all UK ammonia emissions were from agriculture (Department for Environment, Food & Rural Affairs 2020c). Compared to the other pollutants targeted by the Clean Air Strategy (Department for Environment, Food & Rural Affairs 2019), ammonia emissions have fallen relatively little over the last few decades, decreasing by only 13% between 1990 and 2018. In fact, emissions of ammonia have risen by 2% during the period 2015 and 2018 (Department for Environment, Food & Rural Affairs 2020c).

The National Emissions Ceilings Directive (NECD) (Council of the European Communities, 2016) sets EU emissions reductions targets for five major pollutants. For the UK, this includes a requirement to reduce ammonia emissions against the 2005 baseline of 288 kt by 8% by 2020 (*i.e.* to 265 kt) and 16% by 2030 (*i.e.* to 242 kt). By 2018 (the latest year for which data are available), ammonia emissions in the UK were 276 kt (Department for Environment, Food & Rural Affairs 2020c), so were still higher than the 2020 target.

To address this, the Clean Air Strategy sets out several planned regulatory measures to reduce ammonia emissions. These measures are primarily focussed on emissions from the farming industry, and are:

- Introducing rules on specific ammonia emission reduction practices. For example, it requires the spreading of slurries and digestate to be performed using low-emission spreading equipment by 2025, the covering of slurry and digestate stores (or the use of slurry bags), and ensuring that the levels of protein in livestock diets are well matched to nutritional needs.

- Regulating to minimise pollution from organic and inorganic fertiliser use. In 2016, fertiliser application accounted for 23% of UK agricultural ammonia emissions (Department for Environment, Food & Rural Affairs 2019).

- Extending environmental permitting to dairy and intensive beef farms by 2020. As specified in the Industrial Emissions Directive (Council of the European Communities 2010), only pig and poultry farms over the specified sizes of 40,000 poultry, 2,000 pigs or 750 sows are currently regulated. In 2016, pig and poultry farming accounted for 22% of UK agricultural ammonia emissions,

significantly less than the 48% of agricultural ammonia emissions resulting from currently unregulated dairy and beef cattle farming (Department for Environment, Food & Rural Affairs 2019).

The nature of UK livestock farming has changed in recent years, with a large increase in the amount of intensive farming activity. Data held by the Environment Agency show that between 2010 and 2019, the number of permitted farms more than doubled from 648 to 1,302.

Using poultry farming as an example to demonstrate the recent increase in the number of livestock farmed in the UK, poultry numbers increased by 19% over the decade to June 2018: from 159 million in June 2009 to 188 million in June 2018 (Department for Environment, Food & Rural Affairs 2020g). The increases in poultry farming has been concentrated particular parts of the UK. For example, the number of heads of poultry in Powys in Wales increased by 185% over the period 2008 – 2018 (Welsh Government 2019) and the number of poultry in Northern Ireland increased by 54% over the period June 2008 – June 2018 (Department of Agriculture, Environment and Rural Affairs 2020).

The Environment Agency regulates emissions of pollutants to air (and water and land) from sources in England, including from farms of sufficient size to be within scope of the Industrial Emissions Directive. The Environment Agency is required to use permitting and enforcement tools to ensure that sites do not specifically contribute to exceedances of the UK's Air Quality Standards. Satellite measurements of ammonia and other air pollutants are currently not used by the Environment Agency when assessing permit applications.

The formation of district-scale 'clusters' of intensive farms in some areas of the UK provides a challenge to regulators in terms of understanding the relative contribution of each farm to the critical threshold for ammonia in the district. It is also not straightforward to manage the permitting process for new installations in districts that already have significant number of intensive farms, particularly those districts where the critical threshold for ammonia has already been exceeded and/or where there is a need to consider the combined impacts from several nearby farms.

4.1.2 Ground-based measurements of ammonia

This section provides a summary of ground-based methods for the measurement of ammonia, so as to provide background to the work presented in Section 4.3.1 where satellite measurements of ammonia are compared to measurements taken by the ammonia monitoring network. It also provides general context regarding other approaches for the measurement of ammonia.

Ammonia measurements for regulatory purposes in the UK are performed by the ammonia monitoring network, which is part of the UK Eutrophying & Acidifying Network (UKEAP) (Department for Environment, Food & Rural Affairs 2020h). At the time of writing, there are currently 95 sites in the network. Further details of the network, and of the samplers used are given in Tang *et al.* (2018). In summary, two main types of sampling systems are used: active diffusion denuder 'DELTA' (denuder for long-term atmospheric) samplers and passive 'ALPHA' (adapted low-cost passive high absorption) samplers. The two sampling systems are validated against each other on an ongoing basis at 12 of the networks sites, and are described below:

- Active DELTA samplers (UK Centre for Ecology & Hydrology 2020a) are at the time of writing used at 59 network sites and collect both gaseous and particulate ammonia for periods of approximately one month. Each DELTA sampler, which requires a power supply and pump to operate, consist of four denuders and three filters / membranes to allow a range of species to be

sampled. Gaseous ammonia is captured on a citric acid coated denuder and particulate ammonia is captured on an acid coated filter. Samples are extracted using water and analysed using colorimetry (although particulate ammonia is measured at one network site using ammonia flow injection analysis). DELTA samplers are used to provide the main spatial and temporal patterns of ammonia across the UK. The systems can also be extended to sample acid gases and aerosols,

- Passive ALPHA samplers (UK Centre for Ecology & Hydrology 2020b) are used at 49 network sites, including 12 sites where DELTA samplers are also operational (to provide ongoing validation of both methods). Gaseous (not particulate) ammonia is captured on a citric-acid-coated filter, which is extracted using water and analysed using ammonia flow injection analysis with conductivity detection. ALPHA samplers, which do not require a power supply to operate, are used to assess regional and local scale patterns and changes in ammonia concentrations.

A wide range of other methods and analysers are available for the analysis of ammonia in ambient air. These include, but are not limited to: cavity ring down spectroscopy, photoacoustic spectroscopy, off-axis integrated cavity output spectroscopy, laser dispersion spectroscopy, laser infrared spectrometry, differential optical absorption spectroscopy, photoacoustic quantum cascade laser spectroscopy and ion chromatography.

The ground-based measurement methods described above do not by themselves provide any directional information, *i.e.* information on the ammonia concentration in the air sampled when the wind comes from a specific direction. Such information is invaluable when assessing the relative contribution of the total measured ammonia concentration from each source within a cluster. Directional information may be estimated by the use of modelling techniques with local emissions and meteorological data, but a more direct approach is to use a directional sampling device such as the directional passive air sampler (DPAS) described in Solera García *et al.* (2017), which contains a carousel of 12 channels, each of which sample the prevailing air from one of twelve 30° wind directions. The DPAS can house ALPHA samplers (described above) or mini annular denuder (MANDE) flux samplers. MANDE samplers consist of two coaxial borosilicate glass tubes coated on the inside with citric acid and are analysed using the same method as described above for the ALPHA samplers.

4.1.3 Aims

This case study investigated whether existing satellite measurements of ammonia could be a useful addition to the 'toolbox' of existing techniques briefly described above. Specifically, we investigated whether data from the Infrared Atmospheric Sounder Interferometer (IASI) instrument on the EUMETSAT (European Organisation for the Exploitation of Meteorological Satellites) MetOp-A (Meteorological Operational Satellite Programme-A) satellite could be used to address the following questions:

- Can monthly, seasonal or annual variations in ammonia over the UK be identified?

- Can areas of the UK with recent large increases in measured ammonia be identified?

- Can IASI ammonia data be used in regulatory activities?

By using data from the IASI instrument in this case study, we investigated the potential application and limitations of currently-available ammonia satellite data, thereby trialling

and piloting methods that may be used with future generations of instruments, for example, any ammonia instruments on future geostationary satellites.

As described in more detail in Section 2.4, satellite measurements of ammonia have several potential advantages over ground-based measurements, most importantly that a complete dataset is available for the whole of the UK over the lifetime of the satellite instrument. However, measurements of ammonia are only possible during daylight hours and when there is little or no cloud cover, as they rely on reflected infrared radiation. They are also highly dependent on the thermal contrast between the land surface and the near-surface air – see Clarisse *et al.* (2010) for a detailed discussion of this - and are therefore relatively insensitive over the UK, especially at specific times of the day *(e.g.* evening) and times of the year *(e.g.* winter) . As described in Section 4.2.2, for this reason we only used the morning (09:30) rather than the evening (21:30) IASI measurement in order to use the more sensitive of the two daily measurements.

A number of publications have used ammonia measurements from the IASI instrument to identify long-term trends in ammonia on global scales *(e.g.* Van (Damme *et al.* 2014a) and regional scales *(e.g.* Van Damme *et al.* 2014b). More recently, and of relevance to this UK-focussed study, Vohra (2020) used IASI data to determine long-term trends in ammonia and other pollutants at London and Birmingham (both UK), and Delhi and Kampur (both India) - the UK IASI ammonia measurements were compared to ground-based ammonia measurements at three UK locations (Auchencorth Moss, Harwell and Chilbolton). The work we present in Section 4.3.1 of this report is to our knowledge, the first time IASI and ground-based measurements of ammonia on a UK-wide scale have been compared.

The IASI instrument has also been used to derive ammonia emissions in tropical biomass burning regions (Whitburn *et al.* 2015), and to identify ammonia emissions from industrial and agricultural point sources (Van Damme *et al.* 2018, Dammers *et al.* 2019 and Clarisse *et al.* 2019). These latter two studies used sophisticated signal sharpening techniques such as oversampling, wind-rotational oversampling, super-sampling and wind-adjusted super-sampling. These techniques were not employed in the proof-of-concept case study reported here, although a more simple conditional aggregation approach using Lamb weather types was tested (see Section 4.3.3).

It is also important to emphasise that the ammonia point sources identified by Van Damme *et al.* (2018) and Dammers *et al.* (2019) were much larger and more spatially concentrated than those found in the UK, and that the sensitivity of the IASI measurements is higher in such low latitudes than it is in the UK. In Section 4.3.2 of this report we therefore did not try to resolve individual ammonia sources from, for example, intensive agriculture sites – the size of grid box we employed (0.25° x 0.25°) without the use of oversampling or super-sampling also precluded this. Instead we investigated whether changes in measured ammonia at could be observed at larger local scales *i.e.* combinations of signals from a number of sources in a district corresponding to about one, or a few, grid box(es).

4.2   Method

4.2.1   IASI instrument and Level 2 ammonia product

The IASI instrument (European Organisation for Meteorological Satellites 2020) is on board three EUMETSAT MetOp satellites: MetOp-A, MetOp-B and MetOp-C. Data from the IASI instrument on the MetOp-A satellite, which was launched in October 2006, was used in this case study.

The IASI instrument is a passive remote-sensing instrument operating in downward viewing geometry that measures the infrared radiation emitted by the Earth and its atmosphere in the spectral range of 645 - 2,760 cm^{-1}. It has an observational swath width of 2000 km and an on-ground pixel footprint of approximately 12 km x 12 km (circular) at the nadir, increasing to 20 km x 39 km (elliptical) and the outermost viewing angle of 48°. The instrument passes over the UK twice per day with approximate local overpass times of 09:30 and 21:30. Full details of the IASI instrument can be found in Clerbaux *et al.* (2009).

In this work, we used pre-release v3R (reanalysed) of the IASI L2 ammonia product, kindly provided by Martin Van Damme and colleagues at Université Libre de Bruxelles. The product covered the 11-year period 2008-2018, and the data files contained the following information for each individual measurement: time of measurement, angle of observation, percentage cloud coverage, total column ammonia (in molecules.cm^{-2}), error, latitude, longitude and vertical fitting profile used (Aeris 2020a).

The reanalysed versions of the ammonia products differ from the standard version of the products in that they use temperature profiles from ECMWF (European Centre For Medium-Range Weather Forecasts) ERA5 meteorological data (European Centre For Medium-Range Weather Forecasts 2020) in their production. The standard products instead use temperature profiles taken from instruments on the same satellite as the IASI instrument.

The pre-release v3R of the IASI ammonia product used here is the next iteration of v2 of the IASI ammonia neural network retrieval algorithm described in detail by Van Damme *et al.* (2017). v2.2R of the ammonia product, which can be downloaded free of charge from the Aeris IASI data portal (Aeris 2020b), has been used to produce results in a number of publications, *e.g.* Dammers *et al.* (2019). The v3R product incorporates a new correction protocol to account for a declining trend of ammonia values over remote locations, but uses the same general approach as v2.2R of the product in which an artificial neural network is used to link the hyperspectral range index with a set of parameters which represent the atmospheric state to derive total column ammonia (in molecules.cm^{-2}), At the time of publication of this report, a paper describing v3R of the product is being prepared. Once this is published, v3R of the product will subsequently be made available on the Aeris IASI data portal.

Although the ammonia product used is in theory available for the whole of the period 2008-2018, data coverage is incomplete as satellite instruments have data collection outages due to periods of calibration, anomalies, moon intrusions, sensor updates, satellite manoeuvres, and maintenance. For the IASI ammonia product, these events resulted in 52 days of missing data during the 11 year period. Significantly more extensive data loss was caused by the cloud filtering applied, which removed all measurements where the cloud coverage over the area corresponding to the pixel in questions is greater than 10%.

4.2.2   Data processing methodology

The ammonia products (in NetCDF4 file format) were processed using python code developed in-house, and read into the ArcGIS software (Esri, United States) used by the Environment Agency.

Each measurement was assigned to a grid covering the UK, Ireland and surrounding waters. The grid comprised 3,600 grid boxes each 0.25° x 0.25° in size (which corresponds to approximately 27 km x 16 km over the centre of the UK). Measurements were assigned to the grid box corresponding to the centre of the

observation, and no attempt was made to determine or utilise the pixel size of each measurement.

As discussed above, of the two measurements per day over the UK, only the morning (09:30 local time) measurements were used when producing the results presented and discussed in Section 4.3 due to their greater sensitivity over the evening measurements (21:30 local time) because of the larger temperature difference between the surface and boundary layer and the higher prevalence of measurements taken in daylight hours. L3 products were produced using the unweighted median (rather than the mean) of all the data in each grid box. It should also be noted that the uncertainty of each measurement has not been used when producing any of the results reported in this report. Negative total column ammonia values (in units of molecules.cm^{-2}) were not removed from the dataset as these are artefacts of unconstrained retrieval approach based on a neural network (Whitburn *et al.* 2016) and theoretically allow an average background value at zero to be obtained over remote areas.

In this work, we have not converted the total column ammonia results (in units of molecules.cm^{-2}) to near-surface concentrations (in units of, for example, µg.m^{-3}). Although near-surface concentrations would be far more useful to compare with ground-based ammonia measurements, the method needed to achieve this (Liu *et al.* 2019), which requires the ammonia satellite retrievals to be combined with modelled vertical profiles of ammonia, is complex, and was beyond the scope of this exploratory and proof-of-concept case study. It should also be noted that the uncertainty in each measurement was not used when producing any of the results reported in this report.

4.2.3   Ammonia monitoring network data

Details of the ammonia monitoring network are given in Section 4.1.2. For the comparison of IASI data and emissions inventory data in Section 4.3.2, we downloaded all ammonia monitoring network data from all monitoring sites for the period 2008-2018. A total of 11,318 individual measurements from 111 monitoring sites were used, but not all monitoring sites were operational for the whole period studied. Data from both ALPHA and DELTA samplers were used – the sampling period for both was typically one month. For monitoring sites where both samplers were employed, only data from the DELTA samplers were used in this case study.

For simplicity, each measurement was assigned to the month which corresponded to the mid-point of its sampling period. This approach was considered to be adequate for this exploratory analysis, because differences from the mid-point would tend to cancel out due to the large volume of data used- any resulting bias would be negiligable . Monthly mean concentrations of ammonia measured from each network site were then determined by weighting each individual measurement by the number of days over which it was taken.

4.2.4   Ammonia emissions data

The NAEI (Department for Business, Energy & Industrial Strategy 2020b) estimates annual UK emissions of pollutants through collecting and analysing information from a wide range of sources. Emissions data for Ireland are published by the Environmental Protection Agency in Ireland (Environmental Protection Agency 2020).

For the comparison of IASI data and emissions inventory data in Section 4.3.2, total annual ammonia emissions data for each of the years 2008-2018 were downloaded for the UK as whole, Ireland, England, Scotland, Wales and Northern Ireland.

4.2.5　Lamb weather types

To explore whether spatial patters of ammonia could be identified when measurements obtained under similar wind conditions were combined (Section 4.3.1), we used Lamb weather types (Jones *et al.* 2013) as a tool to classify the synoptic meteorology over the UK for each day in 2017. Lamb weather type data was obtained from the Climate Research Unit website (University of East Anglia 2020).

Lamb weather categories are defined for different conditions of synoptic-scale wind over the UK and Ireland. The weather of each day is assigned to a category, so that daily satellite records could be allocated to different categories based the category defined for each day. The categories used for this study covered 8 main directions (45° sectors) and two circulation types (cyclonic and anticyclonic), , which provided a relatively simple approach for comparing aggregate ammonia signals between different wind-direction regimes. Average wind speeds vary between different wind directions (*e.g.* westerly wind speeds are typically higher then easterly wind speeds), so the differences in ammonia signals between categories were affected by differences in wind speed as well as by differences in wind direction.

4.3　Results and discussions

4.3.1　Annual, seasonal and monthly temporal variations of ammonia in the UK

The 2008-2018 IASI ammonia dataset was processed to investigate whether any annual, seasonal or monthly variations of measured ammonia over the UK could be identified. The following datasets were produced, and are each presented and discussed in turn below:

- **Annual:** Annual average datasets and maps were produced for each of the 11 years covered by the IASI L2 ammonia product (*i.e.* 2008 to 2018).

- **Seasonal:** The entire 11-year dataset was used to produce four seasonal-average datasets and maps, each therefore containing 44 months of data. Specifically there were:

    o *Spring*: all measurements between March and May (2008-2018)

    o *Summer*: all measurements between June and August (2008-2018)

    o *Autumn*: all measurements between September and November (2008-2018)

    o *Winter*: all measurements between December and February (2008-2018)

- **Monthly:** The entire 11-year dataset was used to produce an average dataset and map for each calendar month (12 in total), so that each map contained 11 months' worth of data. For example:

- *January*: all measurements in the months of January (2008-2018)

- *February*: all measurements in the months of February (2008-2018)

- *March:* all measurements in the months of March (2008-2018)

- *Etc.*

The results from each of these datasets are shown in Figure 4.1 to Figure 4.3. Each figure shows the median total column ammonia in each grid box over UK and Ireland (and surrounding waters), plotted on the same colour scale.

When considering these data, it is very important to note that apparent differences and variations in total column ammonia between plots may be artefacts of differences in the number of measurements available for each plot. For example, the annual plots are necessarily biased towards times of year when there were more data available *e.g.* summer seasons with less cloud. Such biases could potentially be corrected by applying conditional normalisation to account for differences in temporal occupancy *i.e.* data availability - this is discussed further later in this section.
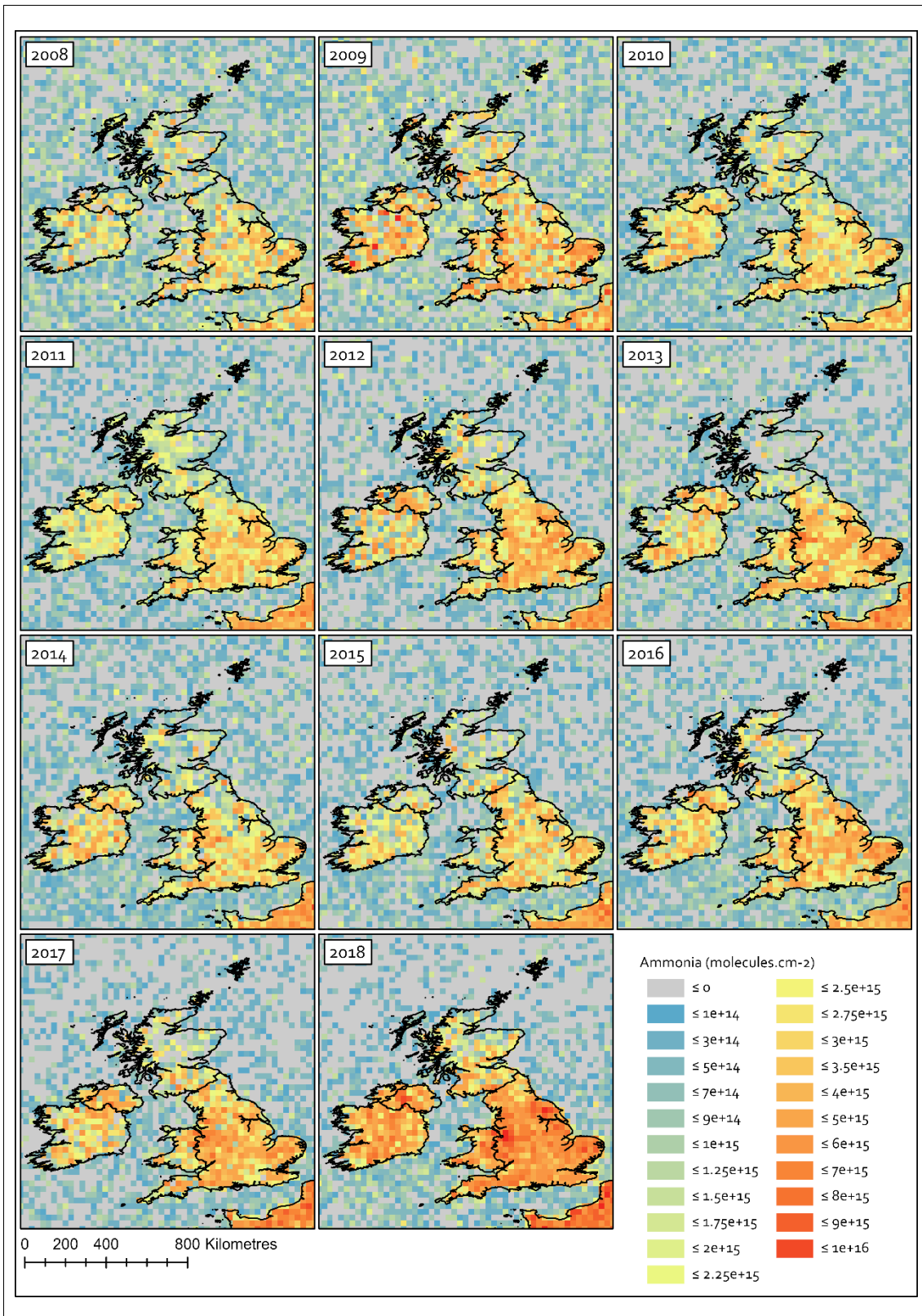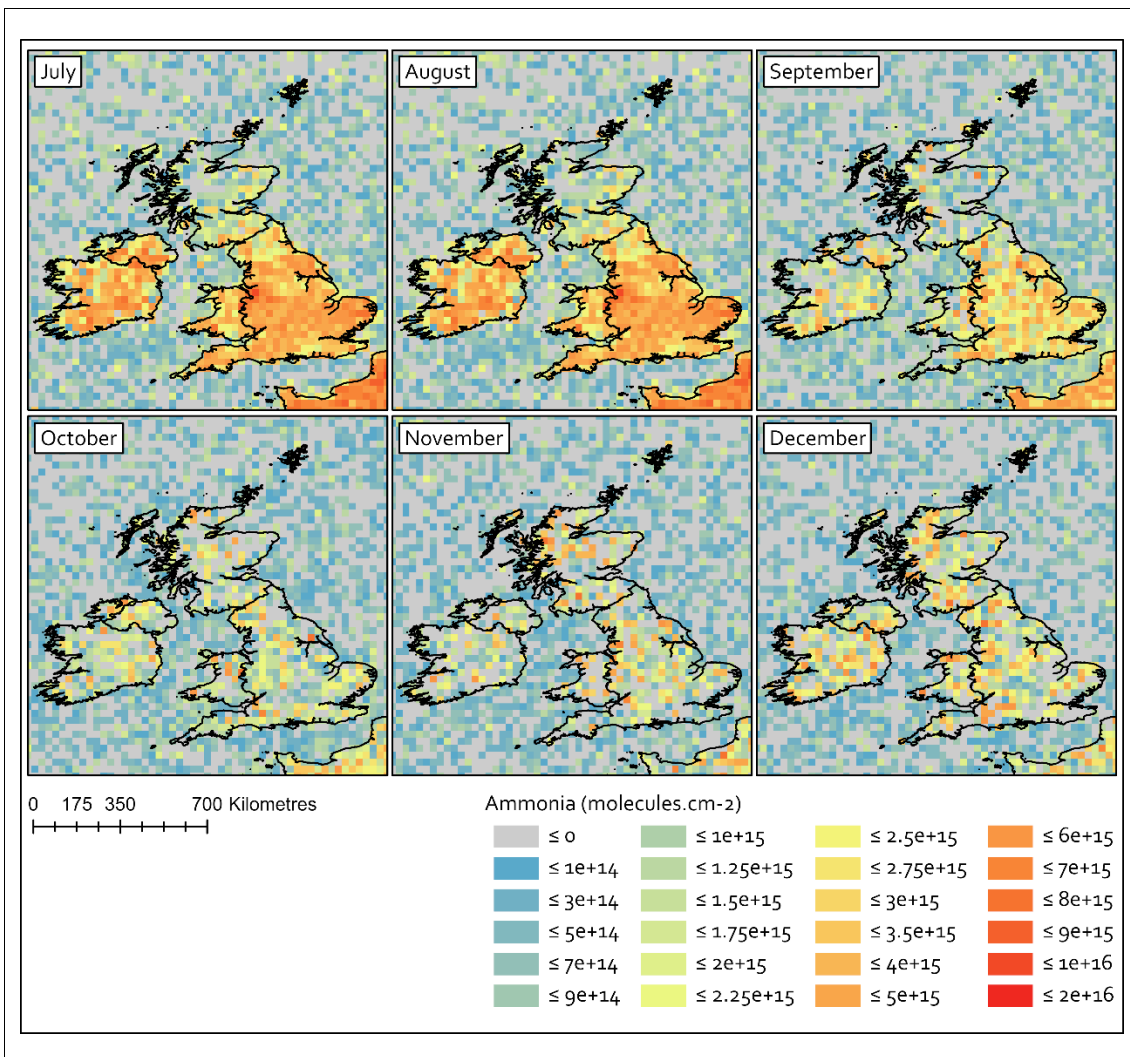
Figure 4.1 Median total column ammonia (in molecules.cm^{-2}) in each grid box over the UK, Ireland and surrounding waters for each of the years 2008-2018. See legend for colour scale.
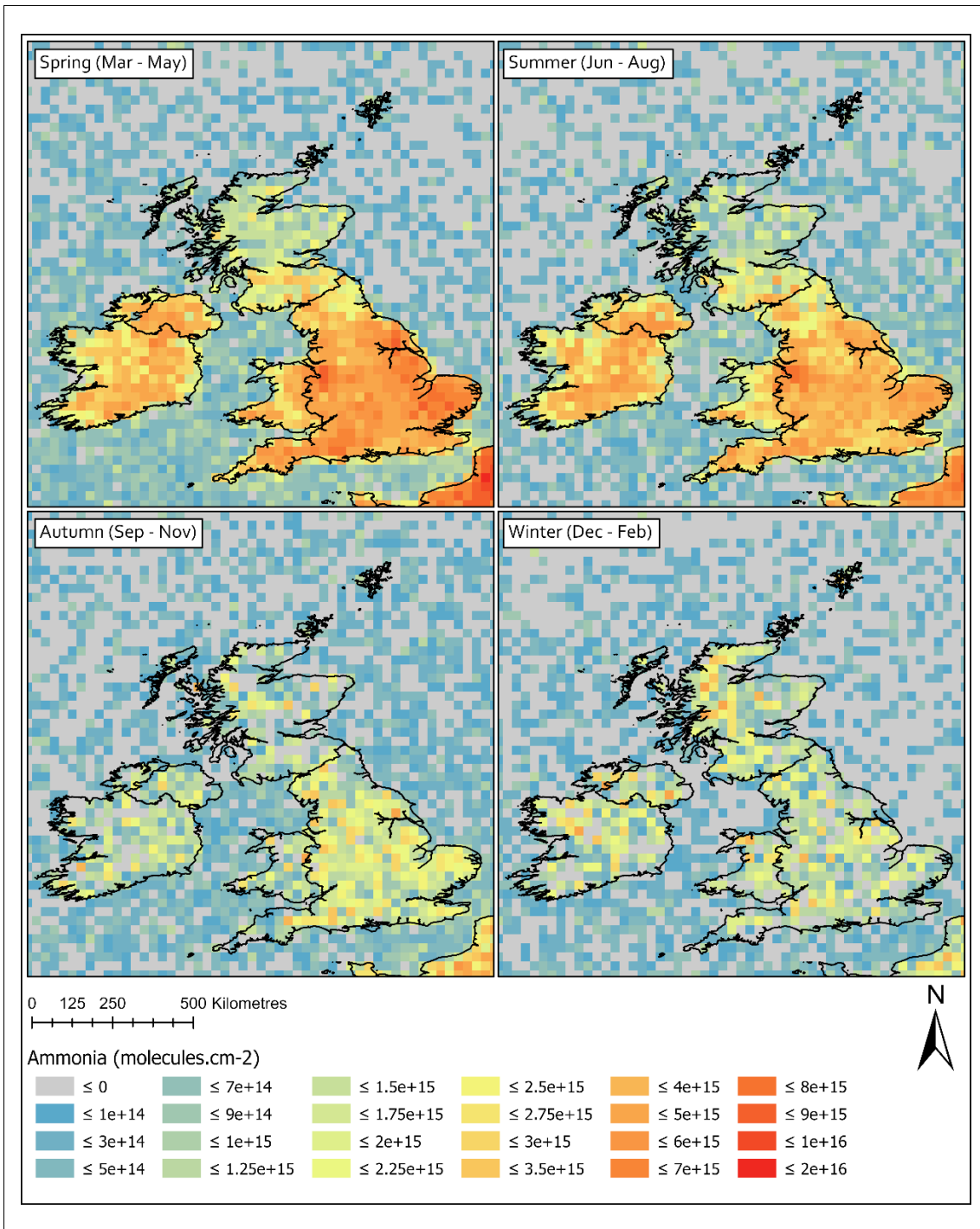
Figure 4.2 Median total column ammonia (in molecules.cm^{-2}) in each grid box over the UK, Ireland and surrounding waters for each of the four meteorological seasons (using all data from 2008-2018). See legend for colour scale.
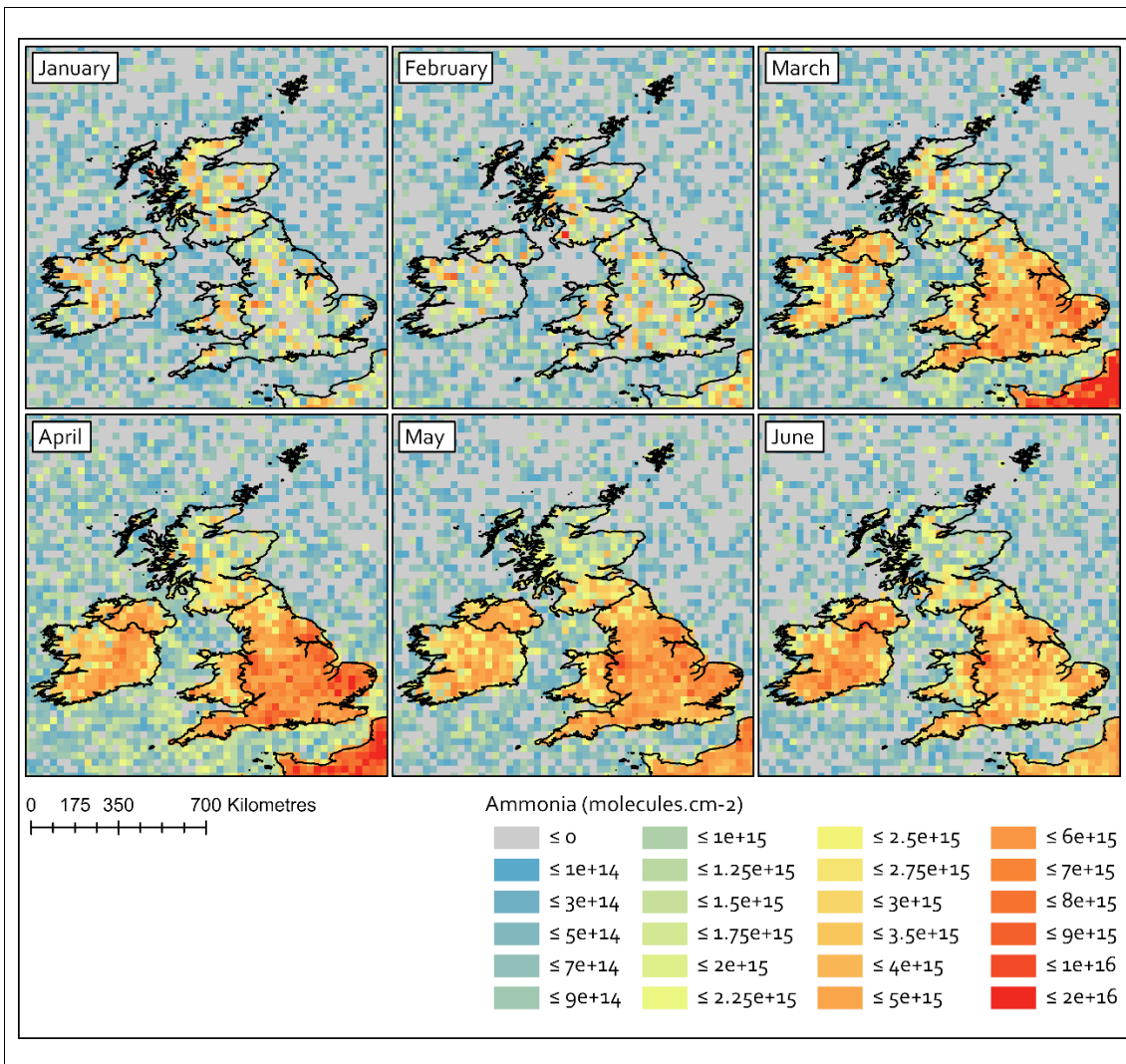
Figure 4.3 Median total column ammonia (in molecules.cm^{-2}) in each grid box over the UK, Ireland and surrounding waters for each of the months January to June (using all data from 2008-2018). See legend for colour scale.
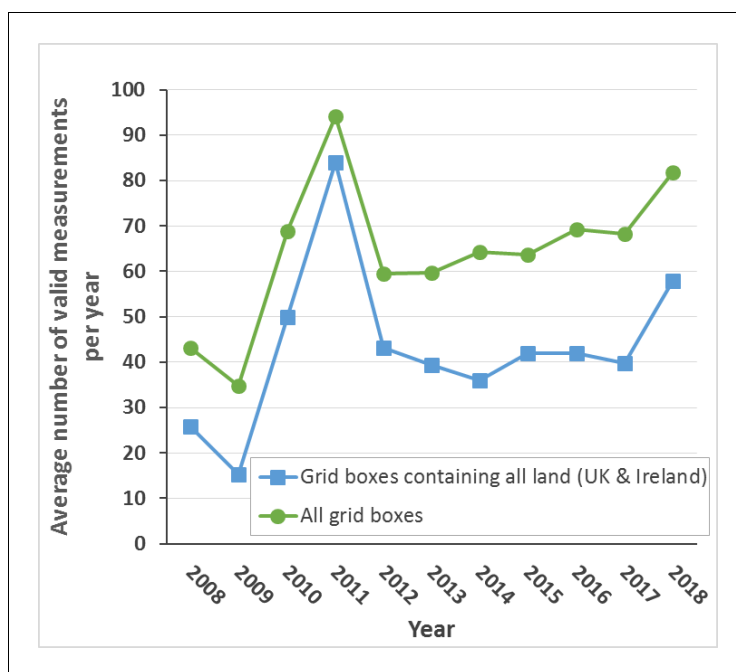
Figure 4.4 Median total column ammonia (in molecules.cm⁻²) in each grid box over the UK, Ireland and surrounding waters for each of the months July to December (using all data from 2008-2018). See legend for colour scale.

Annual temporal variations

Considering first the annual results shown in Figure 4.1, by observation, the years exhibiting the highest values of total column ammonia appear to be 2018, 2017 and 2009. There is no obvious long-term trend of measured total column ammonia over the 11-year period studied, certainty none that matches the trend in ammonia emissions reported by the NAEI (Department for Business, Energy and Industrial Strategy 2020b), which have shown slight year-on-year increased between 2008 and 2017 (typically by < 2% per year), except for three years where there were small decreases from the previous year: 2012 (a 1.3% decrease from 2011), 2013 (a 1.4% decrease from 2012) and 2018 (a 0.5% decrease from 2017).

This lack of any coherent trend in the annual total column ammonia measured over the UK measured is likely to be because of the limited and sparse number of valid measurements[9] that comprise each annual average value: the average number of valid measurements per grid box for each year is shown in Figure 4.5. Taking the 11-year period as a whole, the average number of valid measurements per grid box is 64 per year for all grid boxes (*i.e.* 18% of the possible maximum of 365 measurements per year or 43 per year (12% of the possible maximum) if only UK and Ireland grid boxes comprised entirely of land (including internal waterways and bodies of water) are considered. (Note that grid boxes containing sea or other bodies of water will typically have lower ammonia emissions than grid boxes comprising entirely of land.)
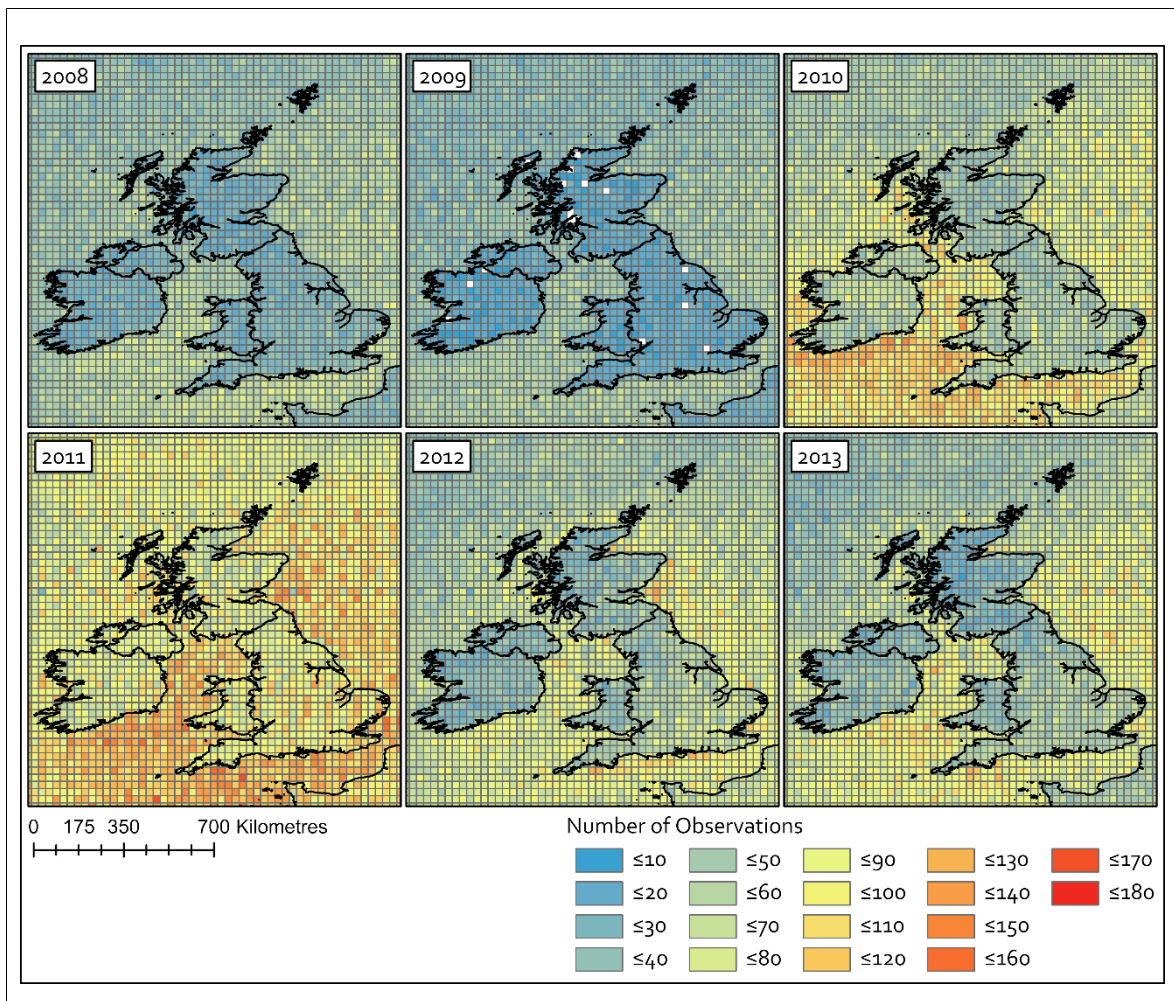

Figure 4.5 Average number of valid measurements per grid box used to generate the annual median total column ammonia data. Green line / circles indicate the average number of valid measurements for all 3,600 grid boxes; blue line / squares indicates the average number of valid measurements for those UK and Ireland grid boxes comprised entirely of land (including inland waterways and bodies of water).

---

[9] As described in Section 4.2.1, in this we use the term 'valid measurement' to indicate a remaining measurement after data collection outages and the application of this cloud filtering

The relatively small amount of data can cause biases in the annual datasets if the available data are not distributed throughout the year in a consistent fashion, for example if there are differences and variations in the data from month to month. For example, Figure 4.2 shows that measured ammonia concentrations are significantly higher over the UK in Spring and Summer than in Autumn and Winter, so any year with a large proportion of its valid measurements in the Spring and Summer months would see its annual average being positively biased. An intra-annual bias may also result from the changes in sensitivity of the measurement throughout the year due to differences between the land surface and the near-surface air varying throughout the year. This issue could potentially be addressed by applying conditional normalisation to account for differences in temporal occupancy, but this was out-of-scope for this case study.

To show the distribution of valid data points across the study area, the number of valid measurements for each of the 3,600 grid boxes for each year are shown in Figure 4.6 and Figure 4.7.

Figure 4.6 Number of valid measurements per grid box for each of the years 2008-2013. See legend for colour scale; white grid boxes indicate no valid measurements
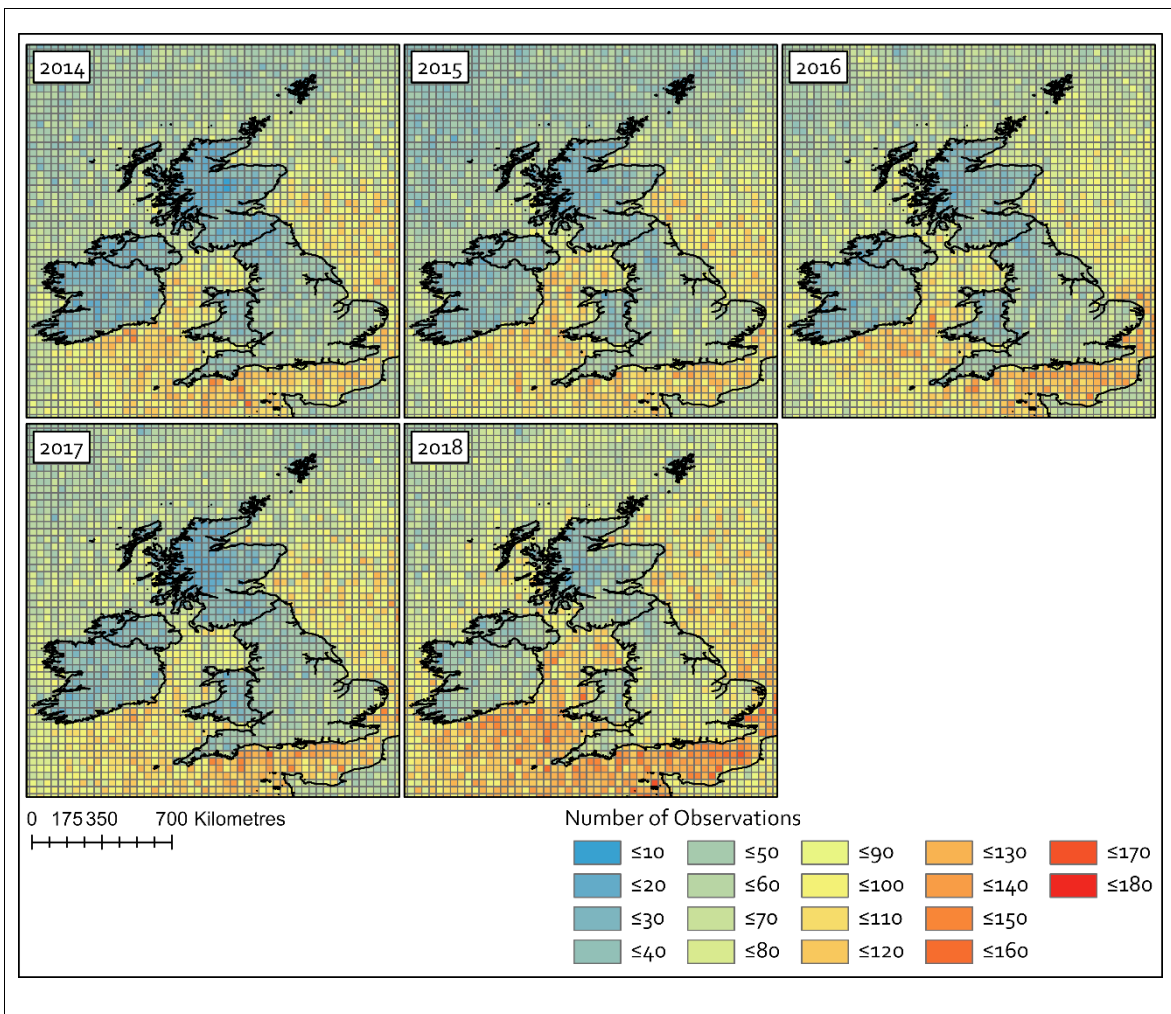
Figure 4.7 Number of valid measurements per grid box for each of the years 2004-2018. See legend for colour scale.

In addition to indicating the small number of valid measurements per year, the images in Figure 4.6 and Figure 4.7 show that in general the number of valid measurements across the UK and Ireland increases as one moves in a south-easterly direction. This is likely to be because south-easterly regions of UK have fewer overcast days per year. The small number of valid measurements in north-westerly regions is a potential barrier for the use of IASI data in regulatory activities, although this will be addressed to some extent if ammonia measurements are available from instruments on future geostationary satellites which perform measurements at a much higher frequency.

A second clear observation is that the number of valid measurements per year over sea is greater than that over land. This is a result of the different 'land profile' and 'sea profile' neural network retrieval algorithms used to produce the total column ammonia data over land and sea regions (Van Damme *et al.* 2017). For the 'land profile', the peak in the vertical ammonia profile is at the surface whereas for the 'sea profile', it is at a higher altitude (approximately 1.4 km). The 'sea profile' therefore favours higher thermal contrast and results in a higher number of valid measurements.

Returning to the median total column ammonia maps in Figure 4.1, these also show a relatively high level of grid box-to-grid box noise, *i.e.* the difference in median total column ammonia in adjacent grid boxes is often large. Although some of this effect may be real, a contributory factor is likely to that adjacent grid boxes often contain significantly different numbers of valid measurements. Another possible cause may be

that we have used unweighted (rather than inversely weighted with uncertainty) median values with no outlier removal methods, meaning that any outlying data and/or data with large uncertainties may be skewing the datasets.

Seasonal temporal variations

Figure 4.2 shows median total column ammonia over the area studied for each meteorological season over the whole of the 11-year period from 2008-2018. For clarity, this means that, for example, the Spring plot is the median of all measurements taken in March-May 2008, March-May 2009, March-May 2010, March-May 2011, March-May 2012, March-May 2013, March-May 2014, March-May 2015, March-May 2016, March-May 2017 and March-May 2018. Similarly, the Summer plot comprises all data recorded in June, July and August, the Autumn plot all data in September, October and November, and the Winter plot all data in December, January and February.

These seasonal data clearly display much more obvious variations that the annual data, with a well-defined peak in measured total column ammonia in Spring, and the lowest values being recorded in the Winter. The seasons where the maximum and minimum total column ammonia are observed are those with the highest and least amount of agricultural activity in the UK. It is suggested that these clearer variations in the seasonal data are a result of the smaller extent of the differences in ammonia emissions across the time period in question (three months rather than a year): an incomplete dataset will therefore bias the average (either low or high) to a much lesser extent. The clearer variations may also be an effect of the larger number of measurements comprising each seasonal average plot (see Figure 4.8) compared to the smaller number of measurements in annual average plots.
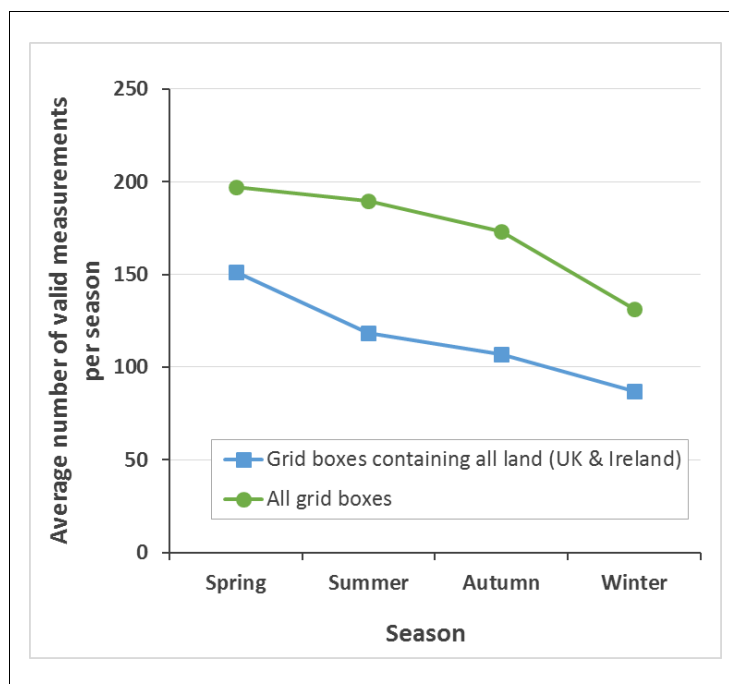
Figure 4.8 Average number of valid measurements per grid box used to generate the seasonal median total column ammonia data. See the caption for Figure 4.5 for further details

The observation that the largest number of valid measurements occurs during Spring is likely to be because the thermal contrast between land and air temperatures in Spring is greater than at other times of the year, and the prevalence of clear skies during that period of the year.

The relatively high level of grid box-to-grid box noise observed in the annual dataset also appears to be present in this seasonal dataset. This may again in part be due to differences in numbers of valid measurements in adjacent grid boxes and/or the use of unweighted (rather than weighted) median values without an outlier removal procedure. Plots of the number of valid measurements per grid box are shown in Figure 4.8, and images showing the number of valid measurements per grid box for each month are shown in Figure 4.9.
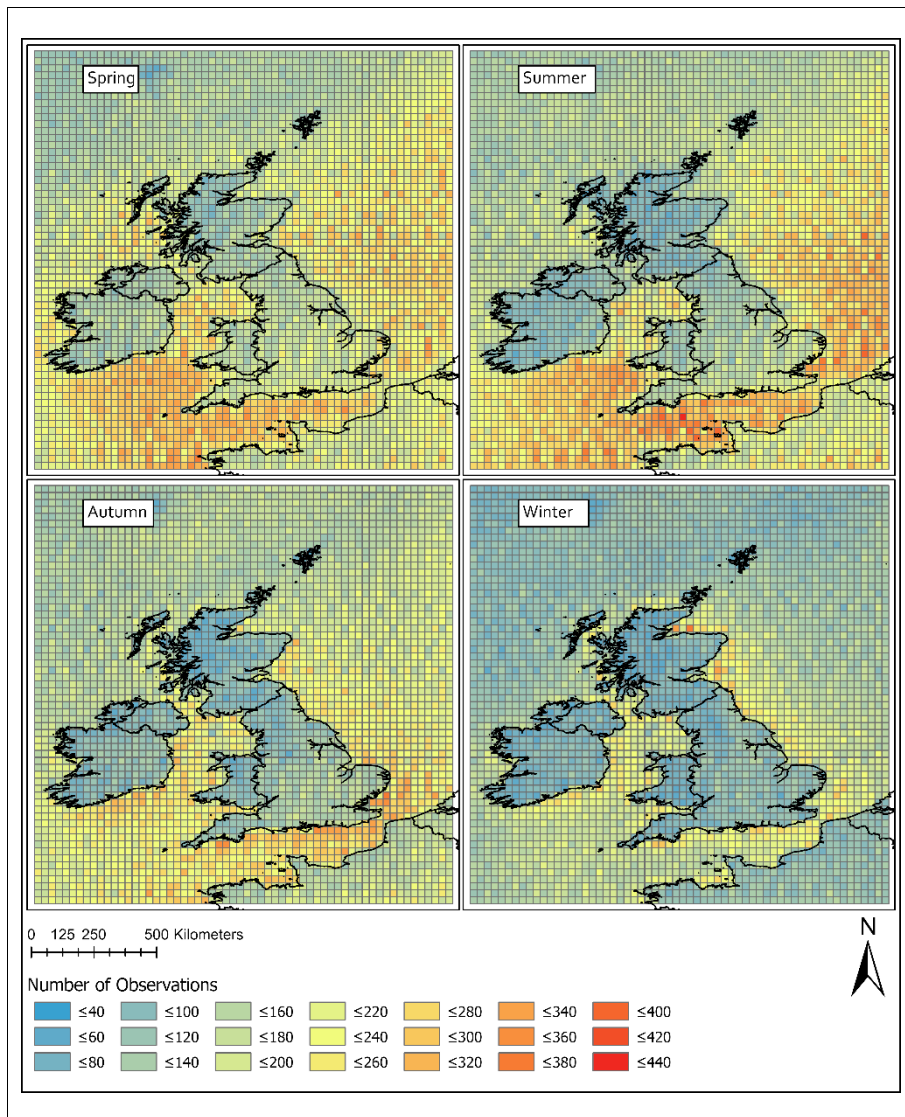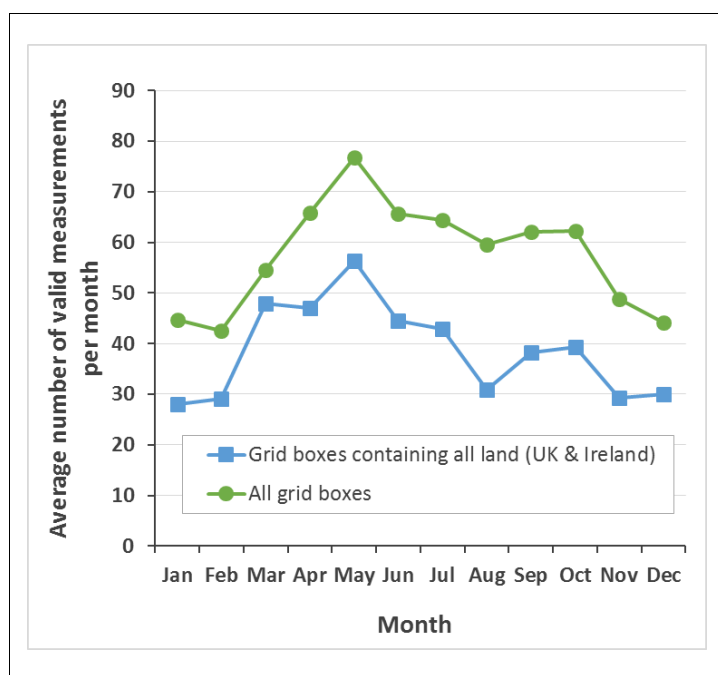

Figure 4.9 Number of valid measurements per grid box for each season. See legend for colour scale.

*Monthly temporal variations*

Figure 4.3 and Figure 4.4 show the median total column ammonia over the UK, Ireland and surrounding waters for each calendar month over the whole of the 11-year period from 2008 – 2018. For clarity, this means that, for example, the 'January' plot shows the median of all measurements taken in January 2008, January 2009, January 2010, January 2011, January 2012, January 2013, January 2014, January 2015, January 2016, January 2017 and January 2018.

As with the seasonal data, these monthly results display much clearer variations than the annual data, with a clear peak in measured total column ammonia around April and May, and the lowest values being recorded in the winter. These months align well with the times of the highest and lowest amount of agricultural activity in the UK.
The high level of grid box-to-grid box noise observed in the annual and seasonal datasets are also present here – possible reasons for this are discussed above. For completeness, the average number of measurements per grid box used to calculate the median total column ammonia plots are shown in Figure 4.10, and images showing the number of valid measurements per grid box for each month are shown in Figure 4.11and Figure 4.12.

Figure 4.10 Average number of valid measurements per grid box used to generate the monthly median total column ammonia data. See the caption for Figure 4.5 for further details
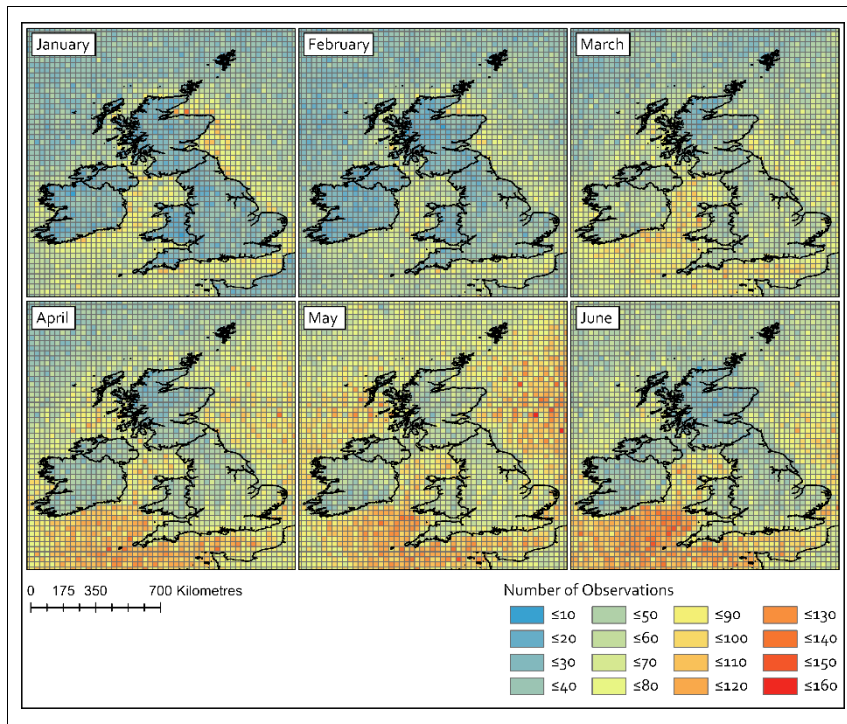
Figure 4.11 Number of valid measurements per grid box for calendar months from January to June. See legend for colour scale.
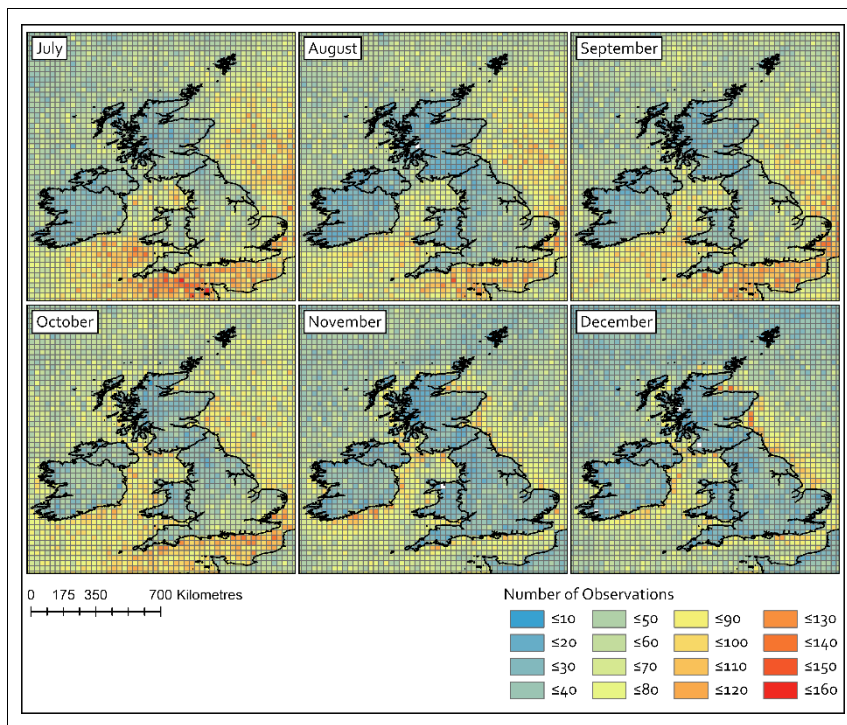

Figure 4.12 Number of valid measurements per grid box for calendar months from July to December. See legend for colour scale.

Comparison of monthly, seasonal and annual data against data from the UK ammonia monitoring network

To investigate whether the seasonal and monthly variations observed in the IASI satellite data were real effects, we performed a comparison of these results against data from the UK ammonia monitoring network. Details of the network including the samplers used and the duration of sampling are given in Section 4.1.2 and Section 4.2.3.

Monthly, seasonal and annual UK mean ammonia concentrations for the UK ammonia monitoring network were calculated by taking a simple mean from all monthly concentrations obtained from all monitoring sites. (For those sites where ALPHA and DELTA samplers were both employed at any time from 2008-2018, only data from DELTA samplers were used for the whole period.) These calculated means were not intended to reflect 'all-UK' average ammonia concentrations as the network monitoring sites are not distributed evenly across the UK in terms of geographical location, nor do they representatively sample areas of differing ammonia concentrations. This approach, which aggregates a large number of data points from a large number of monitoring sites does however give reasonable first-order feel of ammonia concentrations in ambient air over the whole of the UK.

Average UK total column ammonia from the IASI instrument was determined from additional processing of the data used to generate Figure 4.1 to Figure 4.4. The grid boxes comprising more than 50% UK land (including inland waterways and bodies of water) were selected, and a UK mean total column ammonia was calculated using a simple mean and assuming that all negative results were equal to zero. The results of this analysis are shown in Figure 4.13.
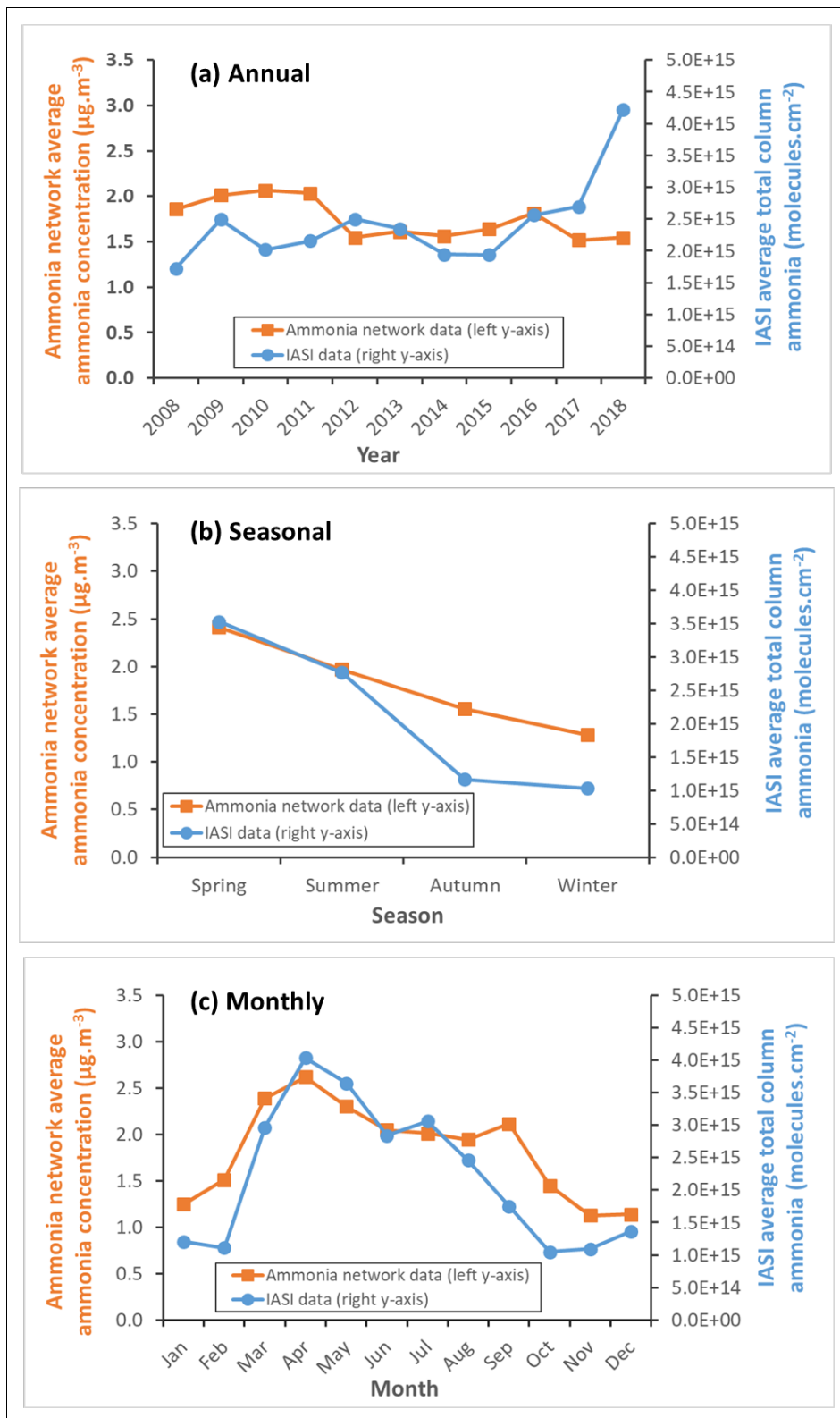
Figure 4.13 Average UK ammonia concentrations calculated from ammonia monitoring network data (orange, squares) and average UK total column ammonia calculated from IASI (blue, circles) plotted as: (a) annual averages, (b) seasonal averages and (c) monthly averages. For the ammonia network dataset, only data from DELTA samplers were used for those sites where ALPHA and DELTA samplers were both employed. For the IASI dataset, grid boxes containing > 50% UK land were used

Figure 4.14 shows the data in Figure 4.13 for all network sites replotted after being normalised to the mean of each dataset. For example, for Figure 4.14 (a) (the annual dataset), each of the 11 annual averages has been normalised to the mean of these 11 values. The same approach has been taken for the IASI data (using the 11 averages calculated from grid boxes containing > 50% UK land).
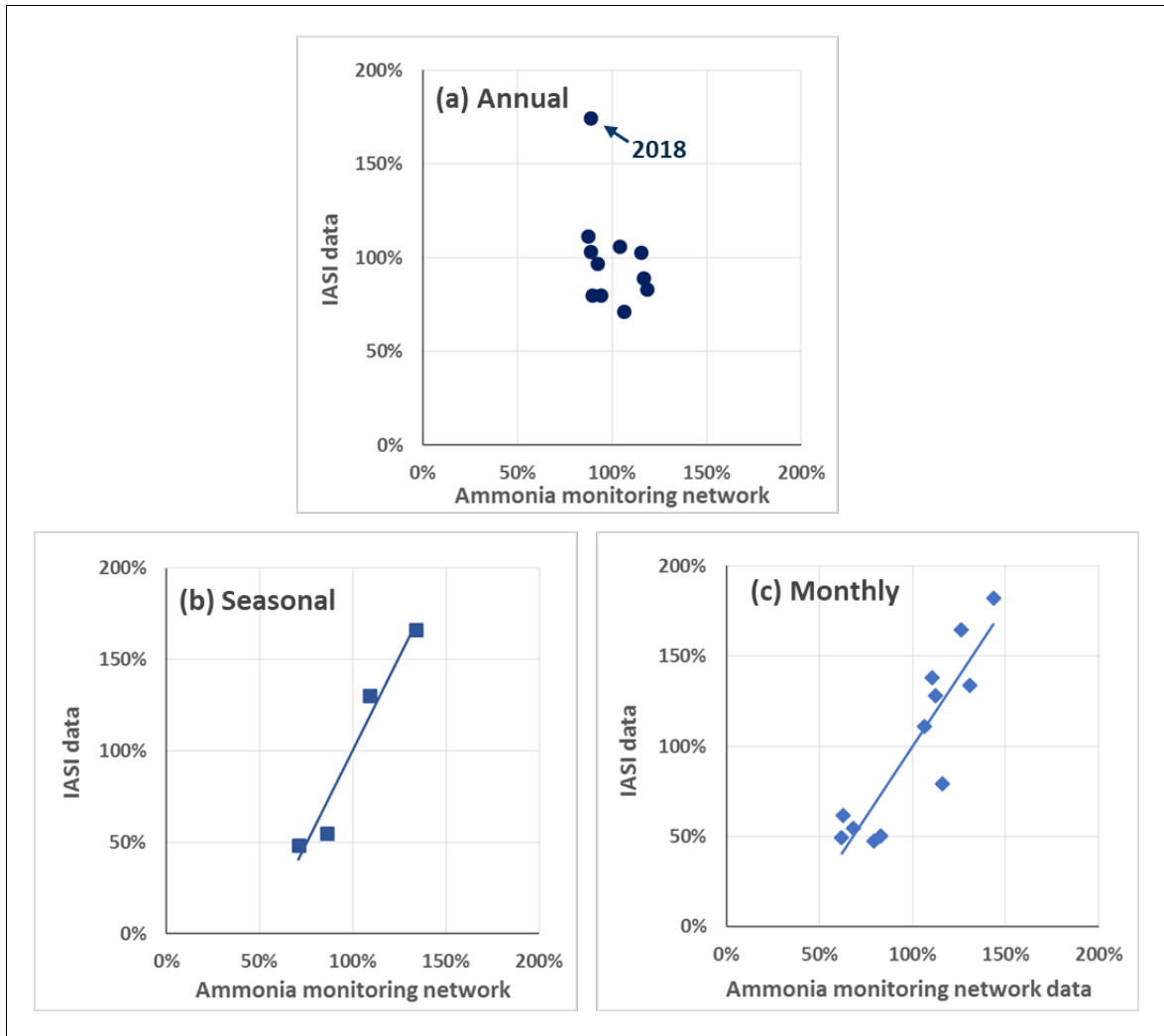
Figure 4.14 Data from Figure 4.13 replotted normalised to the mean value for each dataset plotted for (a) the 11 annual averages, (b) the four seasonal averages, (c) the 12 monthly averages. Data from all samplers have been used for the 'ammonia monitoring network' data, and data from grid boxes containing > 50% UK used for the 'IASI' data

The data in Figure 4.14 (a) show that the two datasets (ammonia monitoring network and IASI) do not show the same variations in annual average ammonia values from year-to-year. If the variations had been the same, then the points would form a 45° diagonal straight line, with the length of the line indicating the extent of the range of the annual averages.

The level of agreement between the two sets of data is reflected by the amount of scatter in the data: exact agreement would be reflected by all points lying perfectly on

the line, or at (100%, 100%) if there were no variations from year-to-year. The extent of the scatter on the data in Figure 4.14 (a) therefore reflect a weak level of agreement between the two datasets. The outlier at (98%, 175%) is the point representing 2018 which, as can be seen from Figure 4.13 (a) and (b) reports an annual average IASI total column ammonia value that is significantly higher than that from any other year.

Figure 4.14 (b) and (c) show strong seasonal and monthly variations. The seasonal data in Figure 4.14 (b) show a good linear correlation and little scatter from the line of best fit (R^2 = 0.96). This indicates that there is a strong seasonal variation (indicated by the length of the line) with good agreement between the datasets (indicated by the low amount of scatter from the line). The monthly data in Figure 4.14 (c) show strong monthly variations, but slightly more scatter from the line of best fit (R^2 = 0.83) – the latter is likely to be an artefact of the smaller number of data points in each monthly dataset compared to the seasonal datasets.

In both cases, the gradient of the straight line is not unity and the range of the network data on the x-axis (approximately 70% to 135%) is approximately half that of the IASI data on the y-axis (approximately 45% to 170%). The reasons for this are not clear, although it may also be indicative of the satellite measurements being biased towards clear-sky conditions, where measurements occur when ammonia evaporation from the surface is enhanced by the higher temperatures on sunny days.

These results therefore show that, despite there being a large number of underlying assumptions when producing the average values from both the IASI and ammonia monitoring network data, the IASI instrument can be used to identify temporal variations in UK ammonia concentrations provided that the time period covered by dataset is selected appropriately. The good agreements demonstrated between the IASI and ammonia monitoring network data also go some way in validating the IASI results by comparison with robust ground-based measurements of ammonia.

4.3.2   Identification of spatial patters in ammonia concentrations over parts of the UK

Can areas with above-UK average changes in ammonia be identified?

We investigated whether areas of the UK with relatively large increases in measured ammonia concentrations could be identified from IASI data over the period 2008-2018. At a first-order estimation, increases in measured ammonia in any areas should correspond to increases in ammonia emissions from, for example, an increase in intensive farming activity.

We combined the IASI annual median data into six-year means (assuming that all negative results were equal to zero) in order to identify whether changes between six-year means such as 2008-2013 and 2013-2018 could be identified. Six-year means were used to reduce the amount of noise in the data, and partially to address the fact that each annual dataset was non-equivalent in terms of the number of measurements and their spread throughout the year).

For each six-year dataset, we evaluated a spatial mean of all the total column ammonia values that were measured for grid boxes that were entirely land-based. Each value was then expressed as a percentage of this land-based mean and re-plotted to give a 'percentage of mean' map. We then subtracted the maps for each 6-year period (i.e. 2013-18 minus 2008-2013) to give a map of the change in the 'percentage of mean' for

total column ammonia over UK. The resulting map is shown in Figure 4.15 and only covers grid-boxes that were entirely land-based.
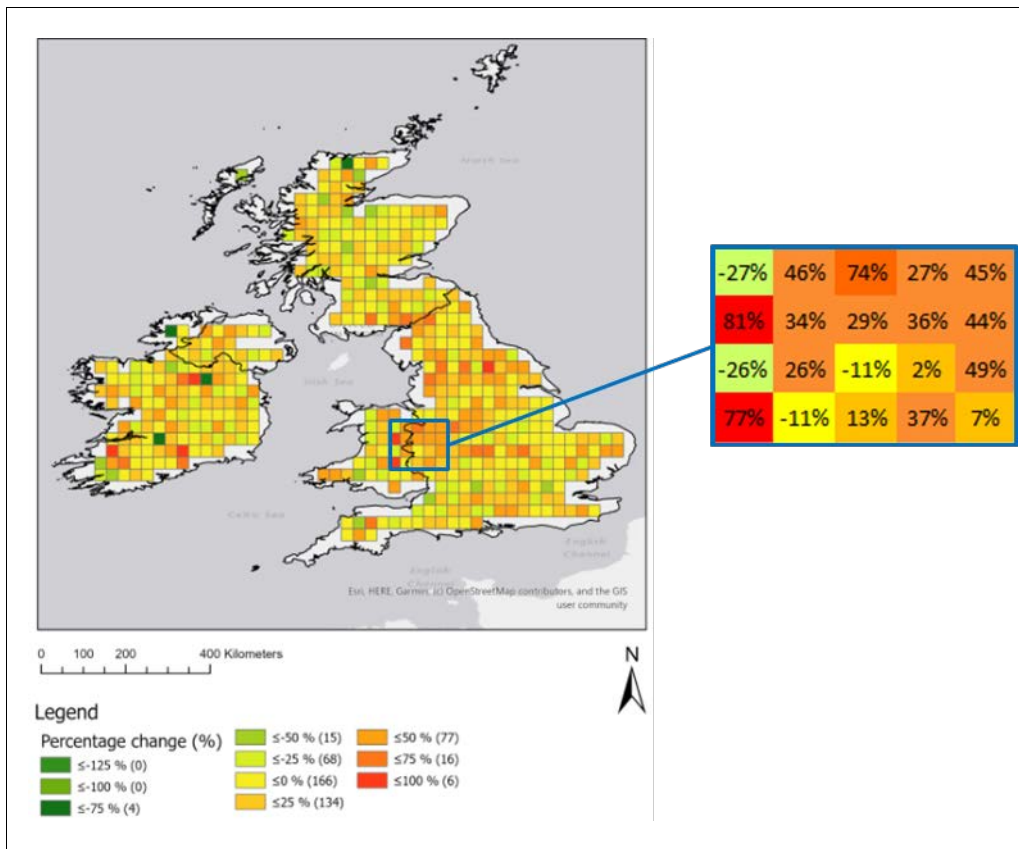
Figure 4.15 Change in mean total column ammonia for the six year period 2013-2018 compared to the period 2008-2013 relative to the UK (land) average change over the same period. The blue box indicates the magnitude of the increase for those grid boxes which sit wholly within Powys (in Wales) and Cheshire and Shropshire (in England)

Although the data in Figure 4.15 displays some grid box-to-grid box noise (some of which may be real), the grid boxes that sit wholly within Powys, Cheshire and Shropshire shown by the blue box in the insert exhibit a relatively large increase over the period 2008-2013 to 2013-2018. The average change in total column ammonia in these 15 grid boxes is of 28% more than the UK (land) average increase over the same period.

Over a period of six years, these 15 grid boxes have therefore become relatively more prominent compared to the UK average, which could indicate they had a disproportionate increase in poultry and ammonia emissions. The four grid boxes in the left hand column of the insert in Figure 4.15 sit wholly within Powys and show an average increase in total column ammonia of 26% more than the UK (land) average increase. During the same period, the number of poultry in the whole of Powys increased by 60% which is 48% above the whole-UK increase of 12%. Although the area covered by these four grid boxes and the area of the whole of Powys are not exactly the same, and transport of ammonia is not considered. It is however interesting to note that these two relative increases above the UK average (26% and 48%) are of a similar order. This indicates that satellite measurements of ammonia do have some

potential in identifying areas of the UK with relatively large increases in ammonia emissions

These same four 0.25° x 0.25° grid boxes (which in total cover a latitude range of 52.00° N to 53.00° N and a longitude range of 3.25° E to 3.50° E) also display an distinctive pattern of alternating 'hot' (red) and 'cold' (green) grid boxes that broadly matches the geography of Powys. Specifically, the two red grid boxes that indicate large increases in measured ammonia coincide approximately with lowland areas of Powys, where the amount of intensive poultry farming had likely increased over the period studied. Similarly, the two green boxes that indicate decreases in measured ammonia coincide approximately with mountainous areas where there would be relatively little increase in intensive agricultural activities over the same period. The match between higher/lower ammonia measurements and geographical areas with higher/lower potential for additional intensive agriculture, suggests that the satellite measurements distinguished patterns of ammonia and agriculture change at district-scales of a few tens of kilometres.

Comparison of measured national-scale changes in measured ammonia against emission inventory data

We also investigated whether changes in total column ammonia measured by the IASI instrument were reflected in national-scale changes in ammonia emissions in the NAEI. Ammonia NAEI emissions data are available on a 5 km x 5 km grid, but interrogating the data at this spatial resolution was beyond the scope of this project, so the results presented here only look at the total emissions from the UK and Ireland as a whole, and each of the five constituent countries (England, Scotland, Wales, Northern Ireland and Ireland). Six-year averages of IASI data were again used, and changes between the periods 2008-2013 to 2013-2018 studied. The results from this are compared against changes in ammonia emissions as reported by the NAEI for the same period inTable 4.1. It should be noted that modelling of the transport of ammonia emissions has not been considered in this case study.

Table 4.1   Relative changes in ammonia emissions (from the NAEI) and measured total column ammonia (from IASI data) between the periods 2008-13 and 2013-2018. Note the caveats in the footnotes in the table

Area	Change in ammonia emissions (2013-2018) vs (2008-2013) using NAEI data	IASI measured change in measured total column ammonia[1] (2013-2018) vs (2008-2013)
UK and Ireland	+ 5%	+ 19%
England	+ 5% [1]	+ 23%
Scotland	+ 1% [1]	- 1%
Wales	+ 8% [1]	+ 22%
Northern Ireland	+ 11% [1]	+ 20%
Ireland	+ 5% [1]	+ 13%

[1] Calculated using grid boxes containing all land only. Grid boxes were assigned to whichever country comprised > 50% of the grid box.

For all areas investigated except Scotland, the IASI-measured change in total column ammonia measured from the period 2008-2013 to 2013-2018 is higher than the change in emissions determined from NAEI data over the same period. These differences are

likely to be within the uncertainty of the measurement: although the uncertainty of the IASI measurements have not been considered in this case study, the uncertainty in the NAEI data by itself is high. For example, in the 2017 ammonia emissions data has a stated relative uncertainty of 46% (Richmond *et al.* 2017).

It should also be emphasised that a much more extensive project using satellite data to validate NAEI emissions data was in progress at the time of writing of this report/ (Chipperfield *et al.* 2019). For ammonia, this project compares measurements from the CrIS (Cross-track Infrared Sounder) instrument on the Suomi NPP (National Polar-orbiting Partnership) satellite to ammonia concentrations derived from NAEI emissions and the GEOS-Chem model.

4.3.3   Use of wind-directional conditional aggregation

To explore whether spatial patters of ammonia could be identified when measurements obtained under similar wind conditions were combined *(i.e.* wind-conditional aggregation), we took the simple approach of using Lamb weather types with IASI data from 2017 (only).

Lamb weather types (Jones *et al.* 2013) were used as a tool to classify the synoptic meteorology over the UK for each day in 2017, and each IASI measurement aggregated into groups representing each of the eight Lamb weather type directions (northerly, north-easterly, easterly, south-easterly, southerly, south-westerly, westerly and north-westerly), and each of the anticyclonic and cyclonic weather types, *i.e.* 10 groups in total.

The results of this analysis were generally inconclusive, but maps of the average total column ammonia for each of the 10 groups of Lamb weather types described above are shown in Figure 4.16. The difficulty in drawing any conclusions from these results is in a large part due to the small number of measurements comprising each aggregated dataset. Even for the weather-type group containing the most measurements (anticyclonic), the majority of grid boxes in the UK contain fewer than 15 measurements. The least populous group (north-easterly) comprises no more than a single measurement in almost all UK grid boxes. It is therefore likely that more conclusive results would have been obtained if this whole 2008-2018 dataset had been used.

The data is Figure 4.16 is not however without its interesting features. For example, the highest average total column ammonia values are observed for the south-easterly wind direction Lamb weather type group. This wind direction most commonly brings warm air to the UK in the summer month, so is likely to coincide with periods of high ammonia concentrations.

It is also important point to note that different Lamb weather types will have different average wind speeds: this then affects the measured amount of ammonia. For example, south-westerly winds typically are of higher speeds than the easterly winds, so south-westerly winds, so are likely to result in lower ammonia concentrations nearer to the original source of the ammonia as a result of the higher level of dilution. These wind speed differences therefore complicate the comparison of ammonia measured using different Lamb weather types.

We therefore recommend that any future work explores the use of meteorological conditional-aggregation in more detail, for example by using use more specific and local meteorological data (e.g. ERA5 data), aggregating for different wind directions *and* wind speeds, and employing a wind-rotational averaging approach.
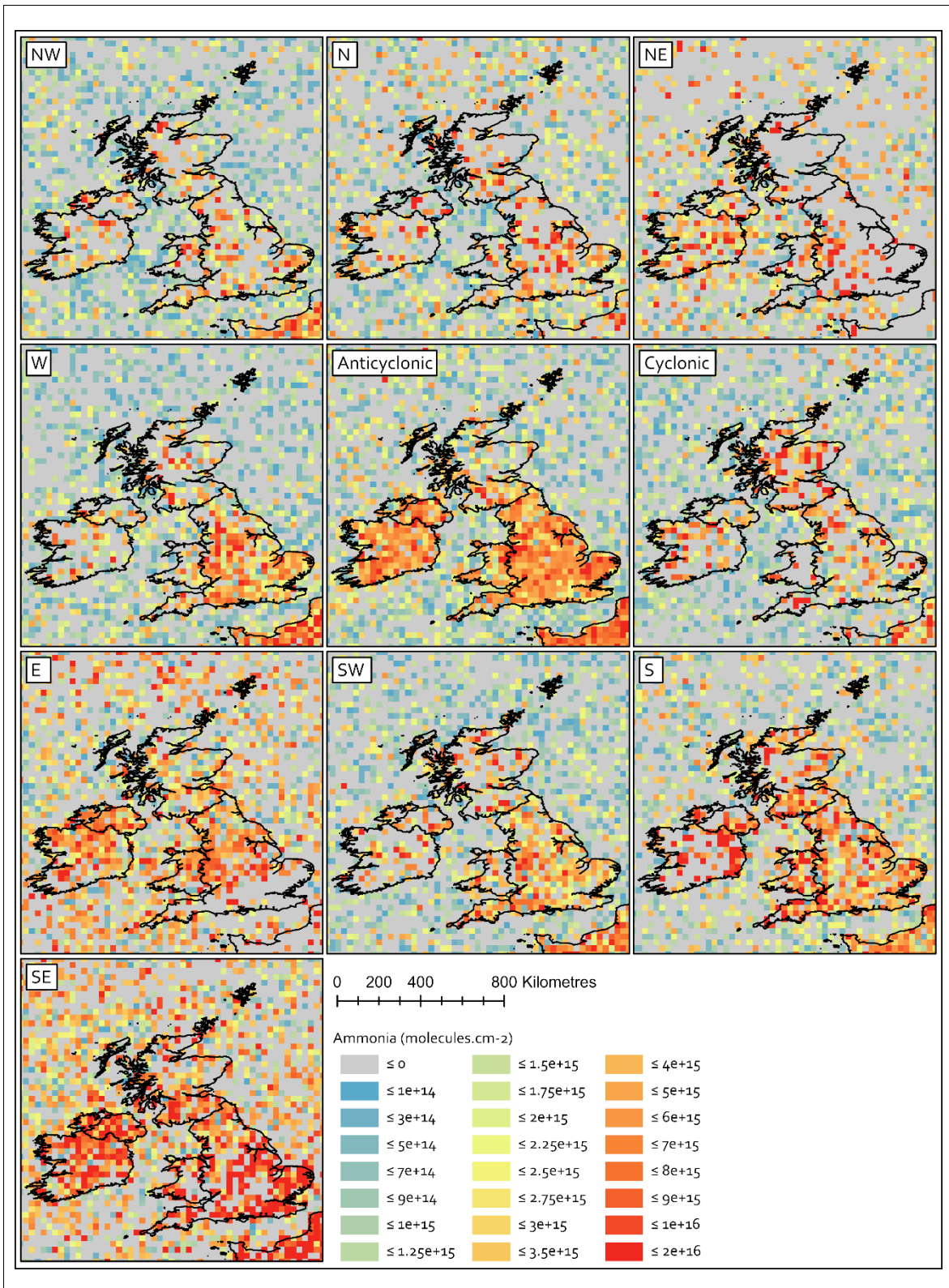
Figure 4.16 Median total column ammonia (in molecules.cm^{-2}) in each grid box over the UK, Ireland and surrounding waters for each Lamb weather type group (indicated on each image). See legend for colour scale.

4.4 Conclusions and suggestions for future work

4.4.1 Conclusions

A new capability at the Environment Agency has been developed to process and interpret L2 ammonia products from the IASI instrument on MetOp satellites. This capability has been used to investigate whether:

- Annual, seasonal or monthly temporal tends in ammonia over the UK can be identified

- Areas of the UK with recent large increases in measured ammonia can be identified

- IASI ammonia data be used in regulatory activities

We have found the IASI instrument can be used to identify temporal variations in total column ammonia over the UK provided that the time period covered by dataset is selected appropriately. Specifically, seasonal and monthly temporal variations can clearly be observed. The identification of the much more subtle annual variations (which vary by only a few percent each year) does not however appear possible using the method applied here.

We have also shown that the seasonal and monthly variations in IASI-measured ammonia can also be observed in data from the UK ammonia monitoring network. This comparison with the ground-based reference method for ammonia also goes some way in validating the IASI results.

An investigation of whether satellite data can be used to detect changes in spatial patterns of measured ammonia in small areas of the UK, for example where there have been recent large increases in intensive agriculture was also performed. This found some evidence of above-UK average increases in counties such as Powys (Wales) and Cheshire and Shropshire (England) when long-term changes and multi-year averages are considered. All these areas of the UK have experienced recent significant increases in intensive farming activity. In Powys, the increases in measured ammonia appear to be focussed in lowland areas of the county, which is likely a result of increased intensive agricultural activity being focussed in these areas.

When investigating spatial patterns of ammonia in larger areas of the UK & Ireland, specifically the five constituent countries of England, Scotland, Wales, Northern Ireland and Ireland, we found a long-term increase in measured total column ammonia for all countries except Scotland (where the change is very slightly negative). These results are in line with emissions inventory data for all countries, which shows increases in ammonia emissions over the same period; the differences between the IASI results and emissions data are within the uncertainties of the emissions data.

A brief investigation that used Lamb weather types to perform wind-directional conditional aggregation for one year of data (2017), did not reveal any firm conclusions. However, evidence of higher average total column ammonia was observed for the south-easterly wind direction Lamb weather type group. This wind direction most commonly brings warm air to the UK in the summer months, so is likely to coincide with periods of high ammonia concentrations. It is however likely that more conclusive results would have been obtained if this whole 2008-2018 dataset had been used in the study. We recommend the use of more sophisticated signal sharpening and meteorological conditional aggregation techniques (see below) in future work.

Despite the positive findings from the case study, it appears unlikely that *current* satellite measurements of ammonia can play a day-to-day role in the regulatory compliance activities of the Environment Agency. This is because:

- The data are currently too coarse in terms of spatial resolution

- The temporal resolution of valid measurements is too sparse

- Satellite measurements of ammonia over the UK are not sufficiently sensitive (particularly in north-western regions)

- There is a lack of sufficiently large ammonia point sources in the UK

- Further work is needed to convert measurements of total column ammonia (in molecules.cm^{-2}) to more useful ground-level concentrations (in μg.m^{-3}).

Data from the IASI instrument has however been used to identify ammonia point sources outside the UK (Clarisse *et al.* 2019 and Van Damme *et al.* 2018), but these sources are larger and less dispersed than those in the UK, and the sensitivity of the measurement is higher. Methods to 'sharpen' or 'tune' the ammonia signal to obtain sub-pixel resolution, for example the use of oversampling and super-sampling (with wind rotation) have also been used by other studies; however, they were not employed in this case study, so are recommended for further investigation. These methods have the potential to be particularly powerful when used in combination with meteorological conditional aggregation techniques such as wind-directional and wind-speed conditional aggregation, and wind-rotational sampling.

In the future, ammonia measurements may become available from instruments on geostationary satellites. For example, the IRS (Infrared Sounder) instrument, which will be launched (with the Sentinel-4 instrument) in 2023 on the MTG-S satellite, could potentially provide ammonia data at hourly intervals. However, the IRS instrument has lower spectral resolution than the IASI instrument, so obtaining ammonia retrievals may be challenging. If measurements from geostationary satellites are available, the combination of the resulting higher frequency measurements with the use of 'signal sharpening' techniques is likely to significantly increase the applicability of satellite measurements of ammonia to UK regulatory activities. The use of IASI or future ammonia satellite data in combination with other data sources (*e.g.* ground-based instruments and sensors) also has exciting potential.

4.4.2   Suggestions for future work

Some suggestions for further work to explore the applicability of ammonia measurements to regulated activity are:

- The use of state-of-the-art 'signal sharpening' techniques. For example:

  o Using oversampling or super-sampling to allow smaller areas of the UK to be interrogated than the 0.25° x 0.25° grid boxes used here.

  o Using meteorological conditional aggregation, for example by using more specific and local meteorological data (*e.g.* ERA5 data), aggregating for different wind directions *and* wind speeds, and employing wind-rotational averaging.

- Further investigation of the apparent variations in the IASI annual average data by using conditional normalisation to account for differences in temporal occupancy.

- Employing a method to convert total column ammonia to ground-level concentrations.

- Determining the uncertainty of the processed L3 data.

- Investigating ammonia data from new polar-orbiting and sun-synchronous satellite instruments. For example, the IASI-NG (Infrared Atmospheric Sounded Interferometer - New Generation) instrument on the MetOp-SG (Meteorological Operational Satellite Programme – Second Generation) series of satellites due to be launched from 2023 has higher spectral resolution and lower radiometric noise than the current IASI instrument.

- When available, using ammonia data from instruments on geostationary satellites. The IRS (Infrared Sounder) instrument which will be launched (with the Sentinel-4 instrument) in 2023 on the MTG-S satellite could potentially provide ammonia data at hourly intervals. However, the IRS instrument has lower spectral resolution than the IASI instrument, so obtaining ammonia retrievals may be an issue.

5 Case study B: Nitrogen dioxide / TROPOMI

5.1 Introduction

5.1.1 Background

Nitrogen dioxide (NO_2) and nitric oxide (NO) are usually referred to as nitrogen oxides (NO_x). Short-term exposure to NO_x can trigger inflammation of airways; longer-term exposure increases susceptibility to respiratory allergens or infections as well as being linked to an array of heart and lung conditions which reduce life expectancy and quality of life (Department for Environment, Food & Rural Affairs 2019). NO_x can also react with other pollutants to form tropospheric ozone and fine particulates which are harmful to health, and, as nitrogen deposition, is capable of altering soil chemistry and harming the biodiversity of sensitive habitats. The major UK sources of NO_2 are road transport (34%), energy generation (22%) and domestic / industrial combustion (19%) (Department for Environment, Food & Rural Affairs 2019). The Environment Agency regulates a number of industrial processes that emit NO_x into the atmosphere,

The NECD (Council of the European Communities, 2016) set EU emissions reductions targets for five major pollutants. For the UK, this includes a requirement to reduce NO_x emissions by 55% compared with the 2005 baseline (of 1727 kt) by 2020 (*i.e.* to 771 kt), and by 73% by 2030 (*i.e.* to 463 kt). By 2018 (the latest year for which data is available), NO_x emissions in the UK had fallen to 823 kt (Department for Environment, Food & Rural Affairs 2020d).

Although annual mean concentrations of NO_2 have also decreased over the last two decades, for example by an average of 1.0 µg.m^{-3} each year between 2006 and 2019 at urban background sites (Department for Environment, Food & Rural Affairs 2020i), the annual mean NO_2 limit value of 40 µg.m^{-3} is still exceeded in the majority of UK urban areas (Department for Environment, Food & Rural Affairs 2020j). Exposure to high levels of NO_2 therefore remains a priority health issue in the UK and contributes to the estimated 40,000 excess deaths per year from exposure to outdoor air pollution (Royal College of Physicians 2016). Details of the steps being taken by the UK Government to further reduce roadside NO_2 concentrations can be found in Department for Environment, Food & Rural Affairs and Department for Transport (2017). The Clean Air Strategy (Department for Environment, Food & Rural Affairs 2019) goes further and sets out the UK Government's future strategy for emissions reduction.

5.1.2 Ground-based measurements of nitrogen oxides

In the UK, the following national networks take continuous ground-based measurements of NO_x and NO_2 (Department for Environment, Food & Rural Affairs 2020j). Full details of each of the networks can be found on the UK-AIR website (Department for Environment, Food & Rural Affairs 2020a).

- The Automatic Urban and Rural Network (AURN). Measurements of NO_2 are performed at approximately 160 monitoring sites using the chemiluminescence analysis method (European Committee for Standardization 2012) specified by

the European Air Quality Directive (Council of the European Communities 2008).

- The UK Eutrophying and Acidifying Pollutants (UKEAP) NO_2 network, which takes diffusion tube measurements of NO_2 at 24 rural monitoring sites; analysis is performed by spectrophotometry.

- The European Monitoring and Evaluation Programme (EMEP) network, which measures NO_x at two sites: Auchencorth Moss in Scotland and Chilbolton in England.

- The UK urban NO_2 network (UUNN), which has measured NO_2 at approximately 180 roadside locations using Palmes-type diffusion tubes since January 2020.

Other regional or sector-specific scale measurements are carried out on behalf of local authorities, (*e.g.* the London Air Quality Network (LAQN)), seaport authorities, the Highways Agency and other organisations.

Other methods available to measure oxides of nitrogen include electrochemical sensors, tuneable diode laser absorption spectroscopy, photoacoustic spectroscopy, Fourier transform infrared spectroscopy and cavity-enhanced methods (*e.g.* cavity ring-down spectroscopy, cavity attenuated phase shift spectroscopy, optical feedback cavity enhanced absorption spectroscopy and integrated cavity output spectroscopy), and directional passive air sampling. These measurement methods can provide useful data in many circumstances for a range of applications, however formal equivalence with the reference chemiluminescence method has not yet been demonstrated.

5.1.3   Aims

The work in this case study investigated whether satellite measurements of NO_2 could be a useful addition to existing tools to monitor NO_2 from regulated sources[10]. As described in more detail in Section 2.4, satellite measurements of NO_2 air pollution in general have a number of advantages over ground-based measurements, including being able to perform measurements where ground-based measurements do not exist. By measuring integrated columns of air through the atmosphere rather than surface concentrations, satellite measurements are also more representative of widespread pollution through inclusion of complex meteorology and strong surface emission gradients (Pope *et al.* 2019). Satellite observations, given their wide spatial coverage, may provide an opportunity to monitor emissions at regional or national scales and to detect changes over time.

Several recent studies have successfully employed satellite measurements of NO_2. Amongst these, Beirle *et al.* (2011, 2019) used data from the Ozone Monitoring Instrument (OMI) on the NASA Aura satellite and data from the TROPOMI instrument on the Sentinel-5P satellite to pinpoint NO_2 emissions over Riyadh, Saudi Arabia. Similarly, Pope *et al.* (2019) utilised data from OMI and TROPOMI to assess levels of NO_2 pollution on a UK-wide scale. Pope *et al.* (2018) made use of OMI data to observe changes in UK NO_2 pollution hotspots, and Pope and Provod (2016a) used OMI data to

---

[10] It should be noted that not all the NO_2 emissions from the investigated point sources are from regulated processes – it is likely there will be other NO_2 emissions from non-regulated sources on the same industrial complex. It is however expected that a significant proportion of the NO_2 emissions do originate from regulated processes, so the use of the phrase 'regulated sources' throughout this report is reasonable and appropriate.

determine tropospheric column NO_2 levels around three Yorkshire power stations under high and low wind speed conditions.

Prior to this work, no study had specifically investigated regulated NO_2 sources using TROPOMI data combined with conditional aggregation by wind direction, or by both wind speed and wind direction. This work therefore presents a novel analysis of TROPOMI data, and increases understanding of whether TROPOMI NO_2 data can be used for regulatory purposes in the UK.

When commencing this work, we were aware of a number of potential drawbacks of using TROPOMI to measure NO_2. For example, measurements from TROPOMI are of tropospheric column NO_2, not surface or near-surface concentrations (which would be more useful for assessing compliance and regulation). TROPOMI also only takes one measurement of the UK each day at its local overpass time of approximately 13:30. Also, the uncertainty of the measurements is very difficult to quantify, and typically larger than the uncertainties for ground-based measurements.

This case study aimed to use the Sentinel-5P TROPOMI instrument to address the following questions:

- Can TROPOMI identify above-background NO_2 emissions from large regulated sources in the UK?

- Can directional plumes of NO_2 be from these sources be observed and quantified under specific wind-directional or wind-directional and wind-speed conditions?

- Can TROPOMI NO_2 data be used in regulatory activities?

5.2   Method

5.2.1   NAEI emissions data

2017 NO_x emissions data (in map and point source form) were downloaded from the NAEI (Department for Business, Energy & Industrial Strategy 2020c). These were the most recent data available at the time of this case study. Although emissions from some of the point sources are likely to have changed since 2017, we only used the NAEI data to give a feel for which large point sources were potentially worthy of investigation.

NAEI NO_x point source data was downloaded and sorted in descending order of NO_x emissions. Offshore sites were excluded as these are not regulated by the Environment Agency. The 10 remaining largest emitters were investigated further – see Section 5.3.1. Note that the downloaded NAEI point source data contained Ordnance Survey coordinates for each point source. The British Geological Survey coordinate converter (British Geological Survey 2020) was utilised to convert coordinates into latitude and longitude.

5.2.2   TROPOMI instrument and Level 2 nitrogen dioxide product

ESA launched the TROPOMI (European Space Agency 2020h) on board the Sentinel-5P precursor (Sentinel-5P) satellite (European Space Agency 2020a) in October 2017 as part of the Copernicus programme. The Sentinel-5P mission objectives are to

globally monitor air quality, climate and the ozone layer between 2017 and 2023. Sentinel-5P was launched into a sun-synchronous polar orbit with a local time of approximately 13:30.

TROPOMI has a nadir-viewing spectral range of 270 - 500 nm (ultraviolet-visible, UV–vis), 675 - 775 nm (near-infrared, NIR) and 2305 - 2385 nm (short wave-infrared, SWIR). TROPOMI has an unparalleled nadir horizontal spatial resolution of 3.5 km × 7.0 km for UV-NIR bands (used for NO_2 measurements) and 7.0 km x 7.0 km for SWIR bands.

We obtained TROPOMI tropospheric column nitrogen dioxide ($TCNO_2$) data (TM5-MP-DOMINO vn1.0) from the Royal Netherlands Meteorological Institute (Tropospheric Emission Monitoring Internet Service 2019; Royal Netherlands Meteorological Institute 2019). TROPOMI completed spherical observations to commission the instrument and ground processing systems for the first six months in orbit, so the operational phase of the instrument commenced in February 2018. This case study utilised a 27 month $TCNO_2$ dataset period between 01.02.2018 and 30.04.2020.

Data collection outages however mean that data coverage within this 27 month study period are incomplete: periods of instrument outages, calibration, sensor updates, satellite manoeuvres and maintenance lessen the number of days of usable data. Further data losses occur when quality filters are applied to the data at the processing stage (see Section 5.2.5).

5.2.3   Wind data

ERA5 data (European Centre for Medium-Range Weather Forecasts 2020) was used in this case study to account for meteorological conditions impacting NO_2 concentration observations. For the purpose of this case study, the data used covered the same 27 month period (01.02.2018 - 30.04.2020) as the TROPOMI data. We used wind data at the 850 hPa pressure level, corresponding to approximately 1.5km above sea level. 850 hPa winds were chosen as near-surface winds will be subject to boundary layer processes (turbulence) not in line with the general flow and mid-upper tropospheric winds (*e.g.* 500 hPa) will be above the primarily bulk of the tropospheric NO_2 loading (*i.e.* in the boundary layer).

5.2.4   Computing system

This processed NO_2 data was read into an Interactive Data Language (IDL) programme on the HPC (high performance computing) Lytham CentOS Linux release 7.6.1810 (Core) 2x Intel® Xeon® Central Processing Unit (CPU) E5-2687W v3 @ 3.10 GHz with 20 cores (40 threads) total. The HPC had 352 GB memory, and a further 917 GB memory accessible in the /scratch disk space.

5.2.5   Data processing methodology

TROPOMI NO_2 products were processed using IDL code developed in-house and previously validated (Pope *et al.* 2018). The following quality filters were applied:

- 0 - 0.2 (20%) geometric cloud fraction

- Quality Assurance (QA) value > 0.5 to account for cloud cover, surface albedo, presence of snow-ice, saturation and geometry

- Missing Data Index (MDI) > 10^{36} to filter out 'bad' pixels

- NO_2 product > 0 to filter out negative or null values

The TROPOMI data record used in this case study was between 01.02.2018 and 30.04.2020, giving a time coverage of 27 months. The data were mapped onto a 10° x 10° grid (8.0° W - 2.0° E longitude; 50.0° N - 60.0° N latitude) with grid boxes 0.025° x 0.025° in size, each corresponding to an average surface area of approximately 5 km^2. Each TROPOMI pixel therefore covered an area equivalent to approximately 5 of these grid boxes.

We employed the oversampling method used in Pope (2019) where satellite pixels are spliced and mapped onto this higher (0.025° x 0.025°) resolution grid. This is a more sophisticated approach than the method of using only the centre of the pixel position to map the measurement onto a grid. Our oversampling method used both the central and corner positions of the satellite pixel to splice the pixel into sub-pixels which were mapped onto the higher resolution grid, thereby retaining much more information and yielding higher quality spatial patterns.

When calculating mean $TCNO_2$ values, an unweighted average was used. The use of an inverse-weighted averaging approach would have meant that pixels with smaller uncertainties would have been weighted more heavily when determining the mean. However, large $TCNO_2$ values retrieved by TROPOMI will inherently have larger absolute uncertainties, and retrievals with lower $TCNO_2$ values will have smaller absolute uncertainties – although they will be less sensitive to $TCNO_2$ (*i.e.* there is less NO_2 for the satellite to observe). Relative uncertainties may therefore be a more appropriate method for weighting $TCNO_2$ data when averaging in future studies.

In addition to investigating the full 27 month period, we also investigated whether NO_2 signals could be determined over shorter timescales: periods of 24 months, 12 months, six months and three months were typically investigated. No attempt was made to convert $TCNO_2$ to ground-based NO_2 concentrations or emissions during the course of this work.

5.2.6   Use of conditional aggregation

Overview

This case study comprised of three different stages

1. Use of no conditional aggregation (*i.e.* use of all measurements)

2. Use of wind-directional conditional aggregation

3. Use of wind-directional and wind-speed conditional aggregation

The experimental details of each of these three stages are described below:

Stage 1: No conditional aggregation (i.e. use of all measurements)

In stage 1 of the case study, mean $TCNO_2$ (in mol.m^{-2}) were first determined for the whole of the UK, Ireland and surrounding waters with no filtering based on wind speed or wind direction. Larger scale maps with stretched colour scales were also produced to identify of potential NO_2 signals around the point sources investigated.

Stage 2: Wind-directional conditional aggregation

For the wind directional conditional aggregation work (stage 2 of the case study), we aggregated the wind data in the following eight 45° wind-directional categories:

- **SW**: 22.50° – 67.49°

- **W:** 67.50° – 112. 49°

- **NW:** 112.50° – 157.49°

- **N:** 157.50° – 202.49°

- **NE:** 202.50° – 247.49°

- **E:** 247.50° – 292.49°

- **SE:** 292.50° – 337.49°

- **SW:** 337.50° – 359.99° and 0.00° – 22.49°

For each measurement, we determined the wind direction in radians and then converted this angle to degrees. The average wind directions over the area of study were plotted as arrows superimposed over the mean $TCNO_2$ data.

Wind-directional conditionally aggregated mean $TCNO_2$ plots were first produced for the whole of the UK, Ireland and surrounding waters for a range of time periods between 27 months and one day to validate that the code was running correctly. Once this was confirmed, wind-directional conditionally aggregated mean $TCNO_2$ plots were then produced for the point sources of interest for a range of time periods between 27 months and three months.

Stage 3: Wind-directional and wind-speed conditional aggregation

For the wind-directional and wind-speed conditional aggregation work (stage 3 of the case study), we defined the following four wind speeds intervals to be used in conjunction with the eight wind-directional categories defined above:

- 0 - 2.5 m.s^{-1}

- 2.5 - 5.0 m.s^{-1}

- 5.0 - 7.5 m.s^{-1}

- 7.5 - 10.0 m.s^{-1}

For each point source of interest, we produced $TCNO_2$ plots for each combination of the eight wind directions and four wind speeds (*i.e.* 32 combinations in total). Each resulting mean $TCNO_2$ plot was accompanied by a plot showing the number of TROPOMI observations corresponding to each mean $TCNO_2$ determination.

Wind-directional and wind-speed conditionally aggregated plots were produced for the full 27 month period only. Data for shorter time periods were not produced due to the very limited number of valid measurements that would have comprised each of these datasets.

5.3 Results and discussion

5.3.1 Selection of point sources

The 2017 NO_x emissions map (Figure 5.1) and corresponding point source data were downloaded from NAEI. 2017 was the most recent data available at the time of the case study. Table 5.1 shows the top largest 10 onshore UK point sources selected for further investigation. We used a UK-wide approach, rather than specifically focussing on those point sources in England which are regulated by the Environment Agency.
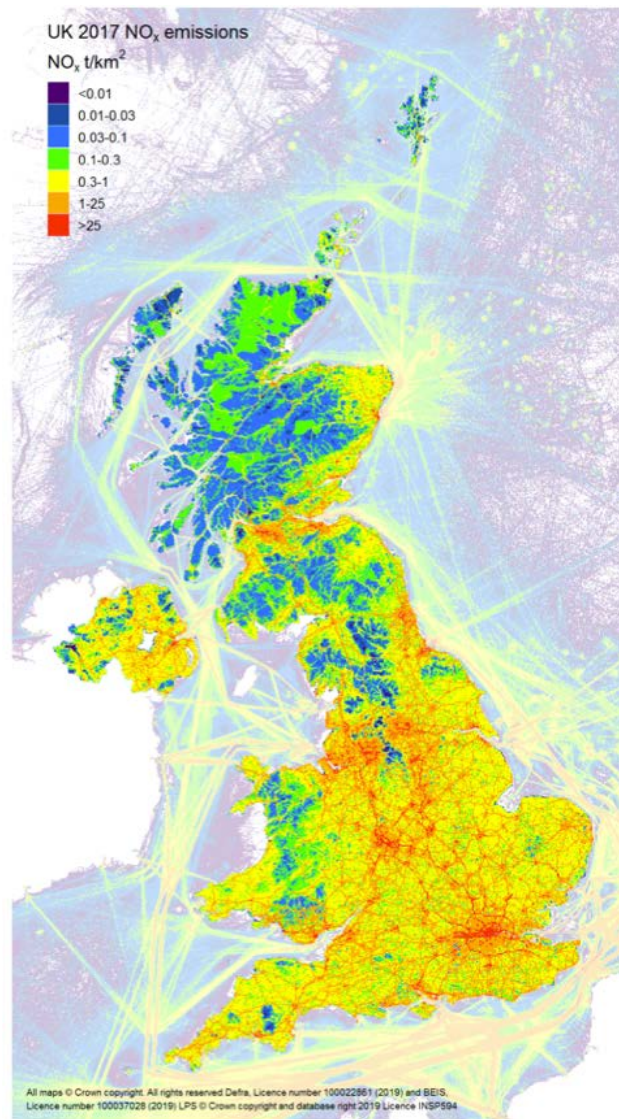

Figure 5.1. UK total NO_x emissions in 2017 (colour scale is < 0.01 to > 25 tonnes.km^{-2}) Image downloaded from the National Atmospheric Emissions Inventory website.

Table 5.1 Largest 10 UK NO$_x$ point sources in 2017 (in descending emissions order) excluding offshore point sources. Note that all stated 'Operators' were correct as of 2017.

Site	Latitude	Longitude	Country	Operator	NO$_x$ emissions (tonnes)
Drax power station	53.73244	-0.99041	England	Drax Power Ltd	15656
Aberthaw B power station	51.38917	-3.39975	Wales	RWE Generation UK plc	6255
Scunthorpe steel works	53.58124	-0.62002	England	Longs Steel UK Limited	5305
Cottam power station	53.30339	-0.78149	England	EDF Energy (Thermal Generation) Ltd	5200
Port Talbot steel works	51.56495	-3.76728	Wales	Tata Steel UK Limited	4968
Grangemouth refinery	56.00690	-3.69589	Scotland	Petroineos Manufacturing Scotland Ltd	2946
West Burton power station	53.36072	-0.81154	England	EDF Energy (Thermal Generation) Ltd	2630
Pembroke refinery	51.68669	-5.02783	Wales	Valero Energy Limited	2611
South Killingholme refinery	53.63168	-0.24406	England	Phillips 66 Limited	2515
Saltend power station	53.73552	-0.24444	England	Saltend Cogeneration Company Ltd	2317

These 10 point sources were plotted on a simplified UK map (Figure 5.2) to enable their locations to be compared with the NAEI 2017 NO$_x$ emissions map. This allowed us to assess which of the point sources were isolated and not downwind of other large NOx sources, and therefore most promising to investigate.
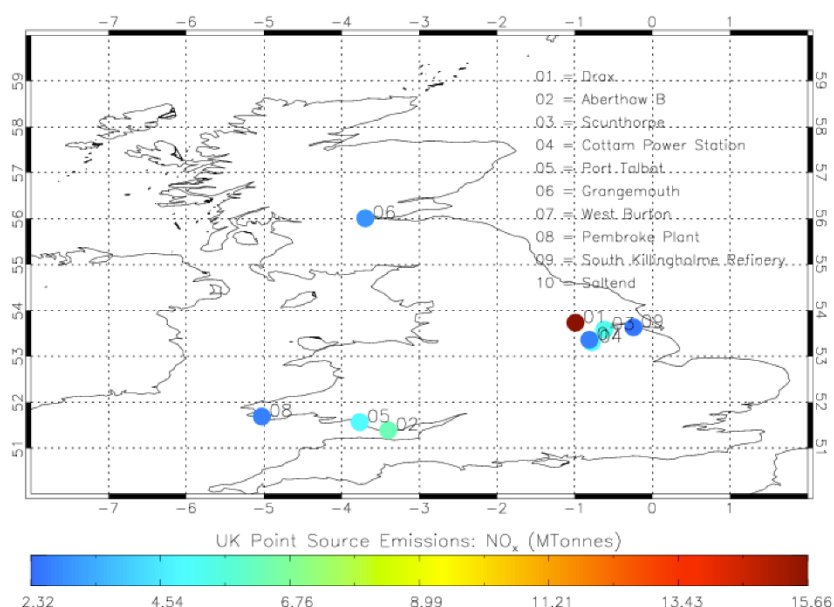

Figure 5.2. Map showing the ten onshore NO$_x$ point sources investigated in this case study. The scale emissions from each point source is indicated by the colour of the point; extent of colour scale is 2.32 – 15.66 Mt.

## 5.3.2 Stage 1: No conditional aggregation (*i.e.* use of all measurements)

We first produced mean $TCNO_2$ maps for the whole of the UK, Ireland and surrounding waters with labels identifying the 10 point sources in Table 5.1. $TCNO_2$ maps were created for a number of different time periods between 24 months and one month to demonstrate how the $TCNO_2$ signals change over various timescales. Figure 5.3 shows the $TCNO_2$ plot for a 24-month period; equivalent plots for shorter time periods are not shown in this report for the sake of simplicity.
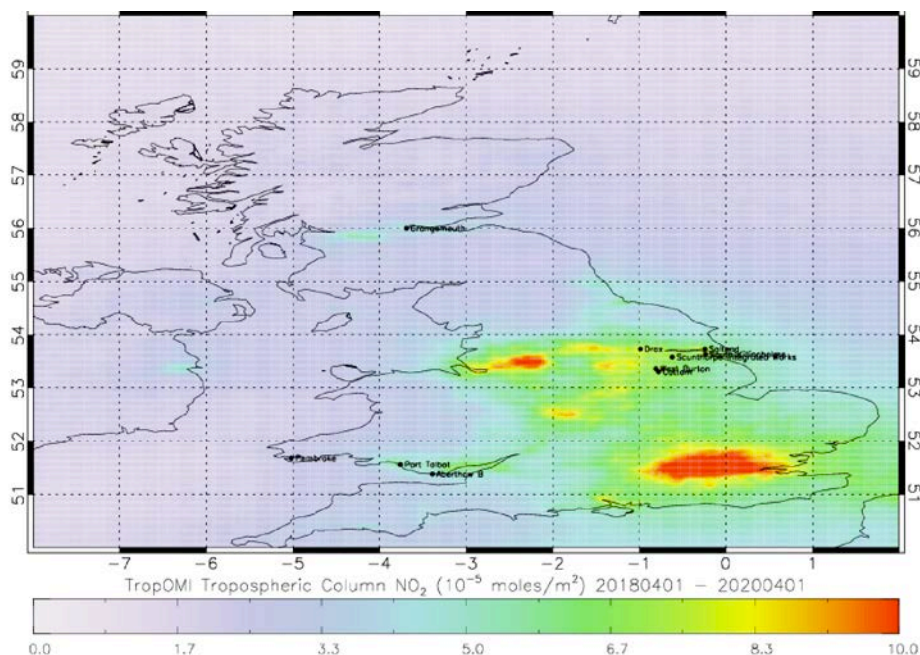
Figure 5.3. Mean $TCNO_2$ (in mol.m^{-2}) over the UK for the 24 month period 01.04.2018 - 01.04.2020. Extent of colour scale is 0 - 10x10^{-5} mol.m^{-2}. The text labels indicate the point sources investigated in this case study (see Figure 5.2).

Initial inspection of the data in Figure 5.3 showed the presence of NO_2 signals around seven of the 10 point sources: Port Talbot steel works, Aberthaw B power station (both South Wales), Grangemouth refinery (mid-Scotland), Drax power station, Saltend power station, Scunthorpe steel works and South Killingholme refinery (all Yorkshire / Lincolnshire). Larger scale mean $TCNO_2$ maps for these three regions are shown in Figure 5.4.
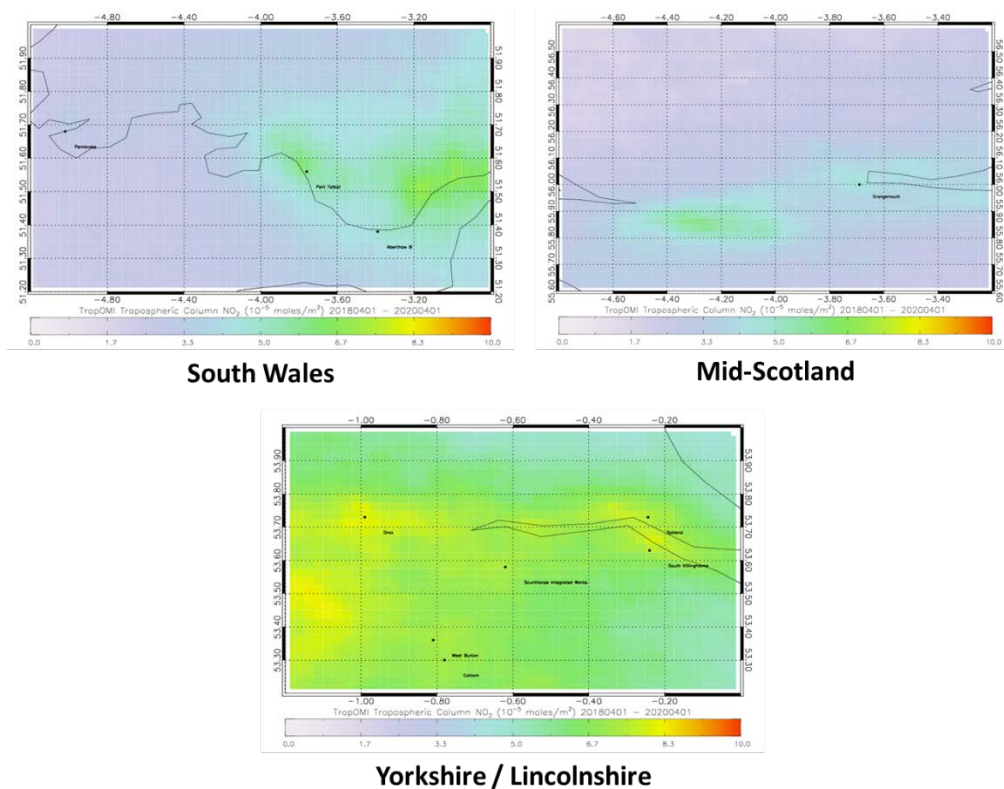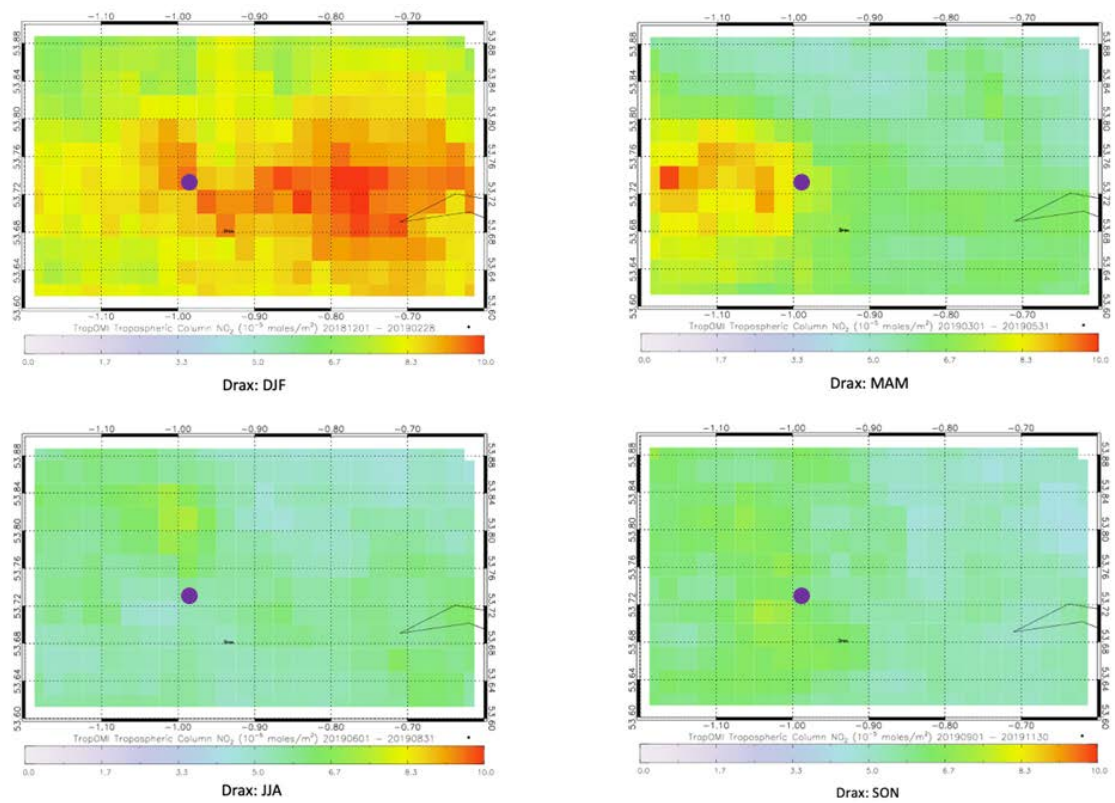
Figure 5.4. Mean TCNO$_2$ (in mol.m^{-2}) over the three areas of the UK approximately corresponding to mid-Scotland, Yorkshire/Lincolnshire and South Wales (as indicated below each image) for the 24 month period 01.04.2018 - 01.04.2020. Extent of colour scales are 0 - 10x10^{-5} mol.m^{-2}. The black dots indicate the point sources investigated in this case study (see Figure 5.2). The dashed gridlines indicate graduations of 0.1° latitude and 0.2° longitude.

At this point, Saltend power station and South Killingholme refinery were not selected for further study as it is was thought likely that a large proportion of the TCNO$_2$ signal at these point sources signal originated from other large industrial sources of NO$_2$ (e.g. two oil refineries), shipping in the River Humber and the Humber Estuary, and from the city of Hull.

Two of the other sources, Aberthaw B power station and Scunthorpe steel works were also deemed to be unworthy of further investigation as the TCNO$_2$ signals around these point sources were relatively indistinct. We therefore focussed the case study on the three remaining point sources: Drax power station, Grangemouth refinery and Port Talbot steel works. For simplicity, in the remainder of this report, these three sources are referred to as, respectively, 'Drax', 'Grangemouth' and 'Port Talbot'.

Shorter timescale mean TCNO$_2$ plots were then produced for these three sources for three month periods corresponding to each meteorological season: DJF = Winter (December, January & February); MAM = Spring (March, April & May); JJA = Summer (June, July & August); SON = Autumn (September, October & November) to determine whether a smaller quantity of data was still able to identify enhanced levels of TCNO$_2$ around these sources. These plots are shown in Figure 5.5 to Figure 5.7.

Figure 5.5. Seasonal (three month) mean TCNO$_2$ (in mol.m^{-2}) over the area around the Drax point source (identified by the purple circles) for the period 01.12.2018 - 30.11.2019. Extent of colour scales are 0 - 10x10^{-5} mol.m^{-2}. Top left (DJF) = Winter; top right (MAM) = Spring; bottom left (JJA) = Summer; bottom right (SON) = Autumn. The dashed gridlines indicate graduations of 0.04° latitude and 0.10° longitude.
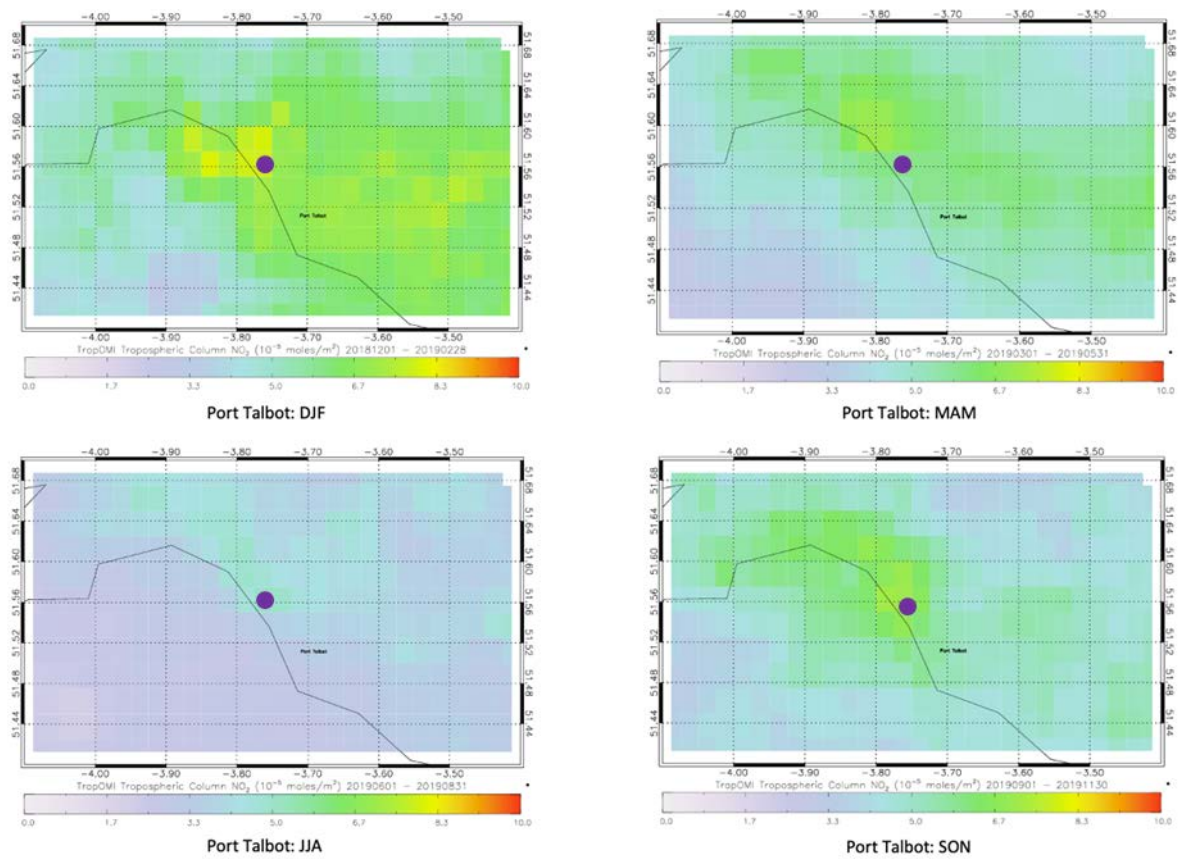
Figure 5.6. Seasonal (three month) mean TCNO₂ (in mol.m⁻²) over the area around the Port Talbot point source (identified by the purple circles) for the period 01.12.2018 - 30.11.2019. Extent of colour scales are 0 - 10x10⁻⁵ mol.m⁻². Top left (DJF) = Winter; top right (MAM) = Spring; bottom left (JJA) = Summer; bottom right (SON) = Autumn. The dashed gridlines indicate graduations of 0.04° latitude and 0.10° longitude.
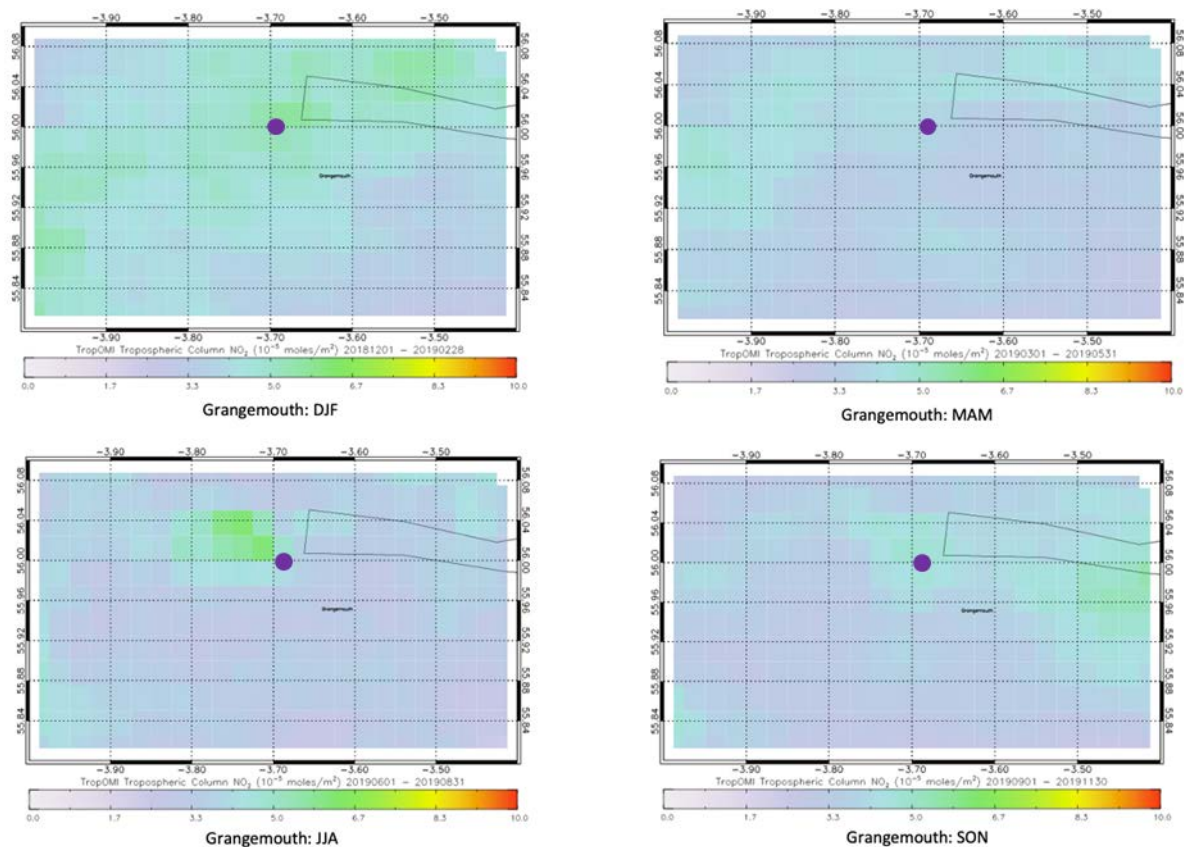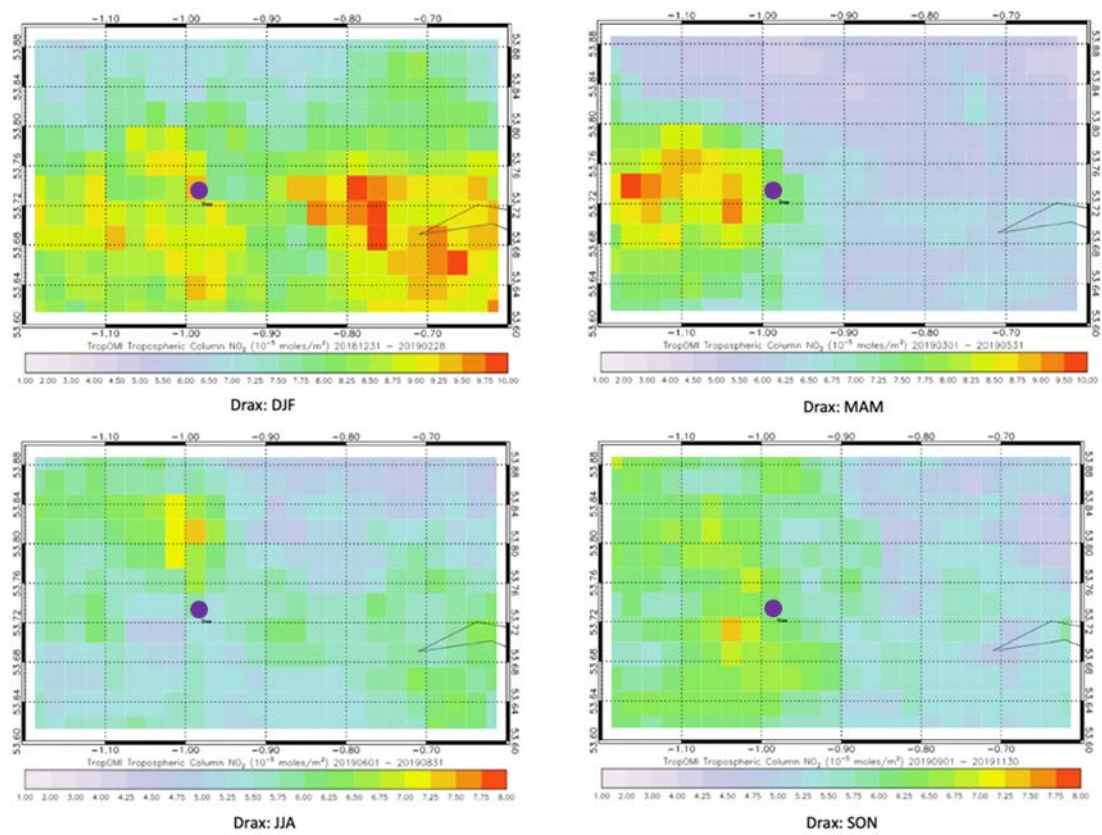
Figure 5.7. Seasonal (three month) mean TCNO$_2$ (in mol.m^{-2}) over the area around the Grangemouth point source (identified by the purple circles) for the period 01.12.2018 - 30.11.2019. Extent of colour scales are 0 - 10x10^{-5} mol.m^{-2}. Top left (DJF) = Winter; top right (MAM) = Spring; bottom left (JJA) = Summer; bottom right (SON) = Autumn. The dashed gridlines indicate graduations of 0.04° latitude and 0.10° longitude.

Figure 5.5 to Figure 5.7 all show some evidence of enhanced TCNO$_2$ signals around all three sources for all three month periods, although the signals around Grangemouth (Figure 5.7) are weaker than those around Drax (Figure 5.5) or Port Talbot (Figure 5.6). The Drax DJF and MAM seasonal plots in Figure 5.5 show the strongest signals, although it is difficult to ascertain what proportion of this enhanced TCNO$_2$ signal originates from Drax itself and is not a result of NO$_2$ emissions from Drax mixing with emissions from other nearby sources. The weakest signals appear to be for Port Talbot JJA, Grangemouth MAM and Grangemouth SON.

Figure 5.5 to Figure 5.7 were re-plotted using a stretched colour scale to allow better visual identification of the signals above background levels: see Figure 5.8 to Figure 5.10. All three sources now display a more distinguishable TCNO$_2$ signal for each three month period. In general, the TCNO$_2$ signals are higher at Drax than at Port Talbot than at Grangemouth (which is in line with the relative size of NO$_x$ emissions from these sources), although the Port Talbot signals are perhaps clearest above background due to there being fewer nearby large NO$_2$ sources that at Drax.

We have therefore demonstrated that above-background levels of TCNO$_2$ can be identified around all three sources when only three months of data is used. Use of all valid data over these three month periods does not however reveal any clear directional plumes for any of the sources as the data was recorded under a range of wind directions and speeds – it is therefore very likely that any plumes would be

'smeared out'. To investigate this further, Step 2 of the case study, described in Section 5.3.3, investigated the use of wind-directional conditional aggregation.

Figure 5.8. Seasonal (three month) mean TCNO₂ (in mol.m⁻²) over the area around the Drax point source (identified by the purple circles) for the period 01.12.2018 - 30.11.2019 with a stretched colour scale (extent of colour scales are 1x10⁻⁵ – 8x10⁻⁵ mol.m⁻²). Top left (DJF) = Winter; top right (MAM) = Spring; bottom left (JJA) =Summer; bottom right (SON) = Autumn. The dashed gridlines indicate graduations of 0.04° latitude and 0.10° longitude.
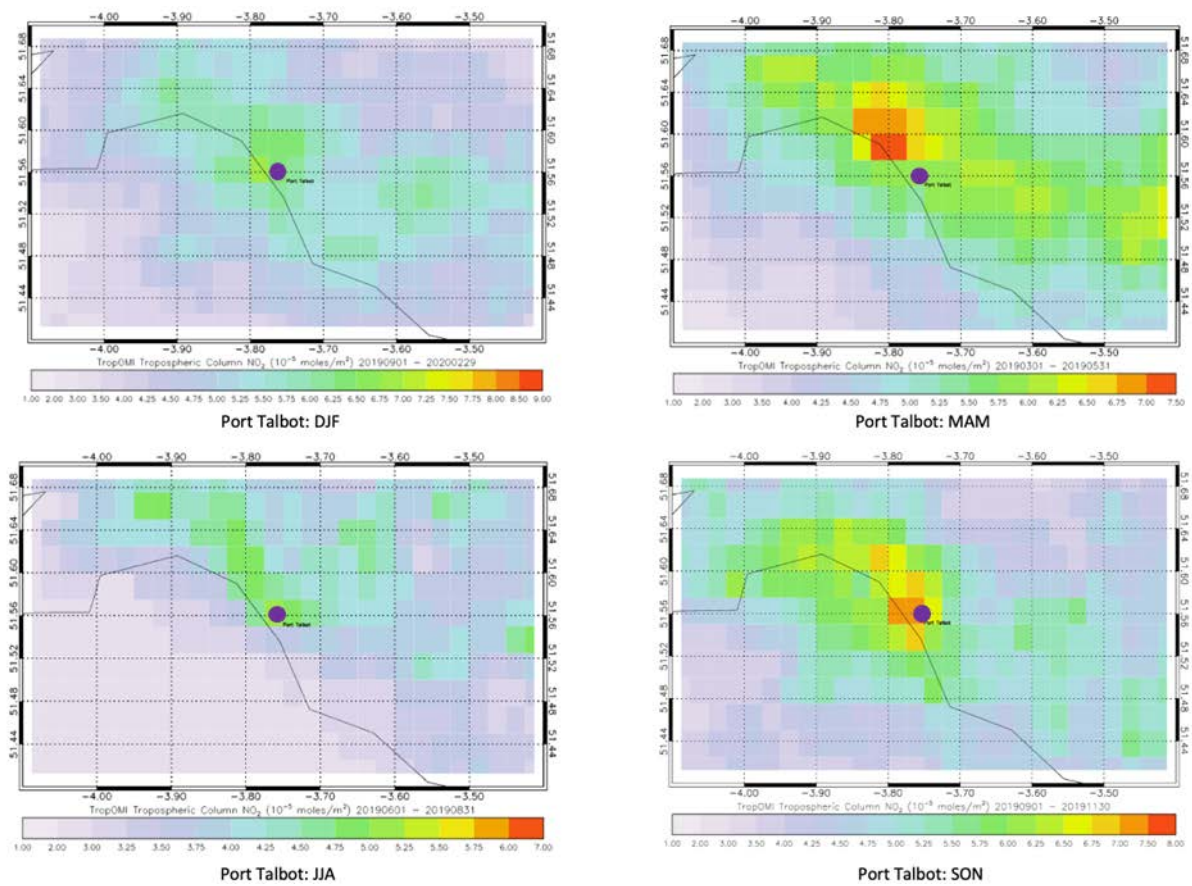
Figure 5.9. Seasonal (three month) mean TCNO$_2$ (in mol.m^{-2}) over the area around the Port Talbot point source (identified by the purple circles) for the period 01.12.2018 - 30.11.2019 with a stretched colour scale (extent of colour scales are 1x10^{-5} - 9.0x10^{-5}, 7.5x10^{-5}, 7.0x10^{-5} and 8.0x10^{-5} mol.m^{-2}). Top left (DJF) = Winter; top right (MAM) = Spring; bottom left (JJA) =Summer; bottom right (SON) = Autumn. The dashed gridlines indicate graduations of 0.04° latitude and 0.10° longitude.
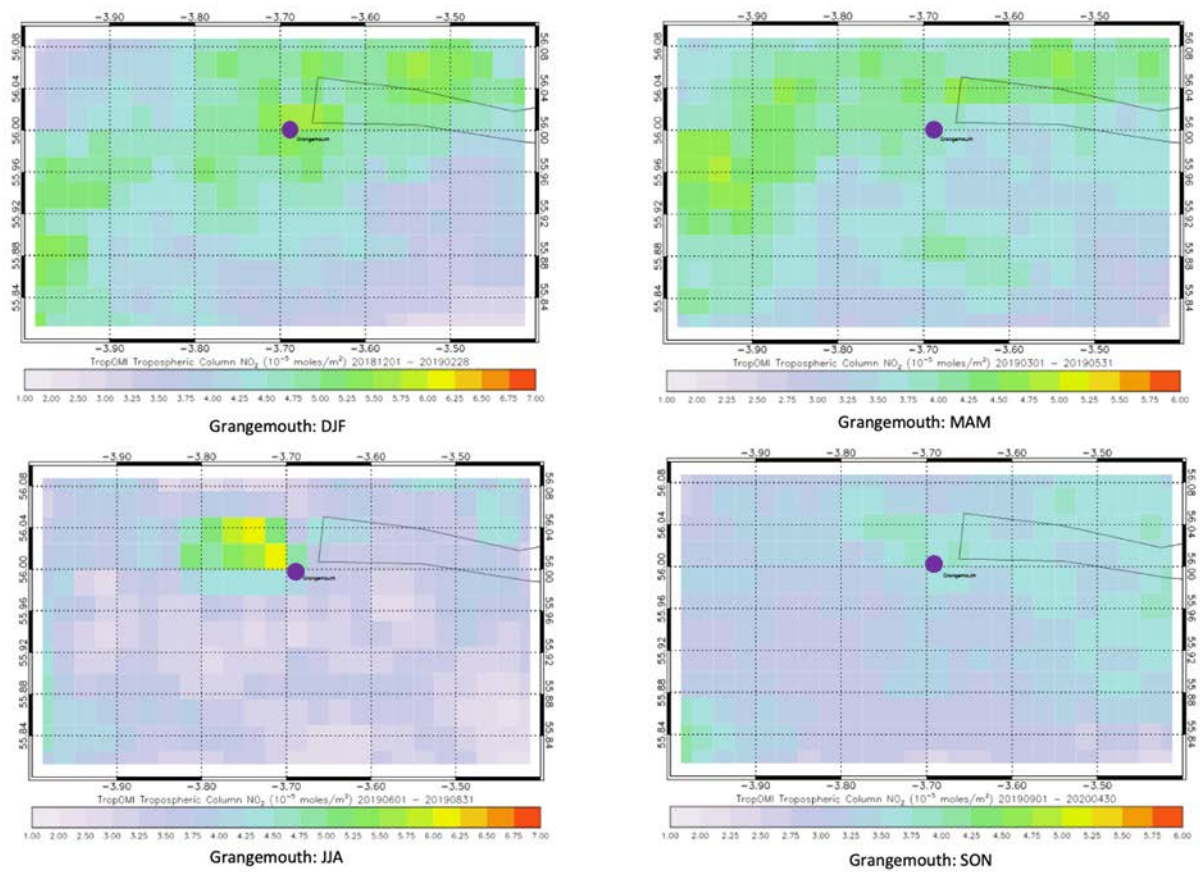
Figure 5.10. Seasonal (three month) mean TCNO$_2$ (in mol.m^{-2}) over the area around the Grangemouth point source (identified by the purple circles) for the period 01.12.2018 - 30.11.2019 with a stretched colour scale (extent of colour scales are 1x10^{-5} - 7.0x10^{-5}, 6.0x10^{-5}, 7.0x10^{-5} and 6.0x10^{-5} mol.m^{-2}). Top left (DJF) = Winter; top right (MAM) = Spring; bottom left (JJA) =Summer; bottom right (SON) = Autumn. The dashed gridlines indicate graduations of 0.04° latitude and 0.10° longitude.

5.3.3 Stage 2: Wind-directional conditional aggregation

Overview

Wind-directional conditionally aggregated $TCNO_2$ plots for each of the three point sources of interest using the ERA5 wind data. To investigate the timescale over which emissions of NO_2 might be seen, plots were generated for the whole 27 month period, and also for the shorter time periods of 12 months, six months and three months. For the three month datasets, plots for each metrological season were generated.

For ease of reference, the wind-directional conditionally aggregated plots are summarised in Table 5.2. Plots for Port Talbot and Grangemouth for time periods of less than 27 months were also produced but are omitted from this report for the sake of simplicity.

Table 5.2 Summary of wind-directional conditionally aggregated figures

Time period	Wind directions	Figure (Drax)	Figure (Port Talbot)	Figure (Grangemouth)
27 months	All	Figure 5.11	Figure 5.18	Figure 5.19
12 months	All	Figure 5.12	Not shown	Not shown
6 months	All	Figure 5.13	Not shown	Not shown
3 months (DJF)	All	Figure 5.14	Not shown	Not shown
3 months (MAM)	All	Figure 5.15	Not shown	Not shown
3 months (JJA)	All	Figure 5.16	Not shown	Not shown
3 months (SON)	All	Figure 5.17	Not shown	Not shown

Drax: 27 month period

Figure 5.11 shows clear and large NO_2 plumes from Drax for S, SW and W wind directions over the 27 month period. However, the location of Leeds, other conurbations and the Eggborough and Ferrybridge power stations to the west and south-west of Drax means that it is difficult to assess the amount of the NO_2 plume that originated from the Drax power station itself. An intense plume is also visible for SE wind directions.

Equally clear, but less intense, plumes from Drax are also seen for the other four wind directions (N, NE, E and NW). The N, NE and NW wind directional plots are of particular interest as winds from these directions come from North Yorkshire which is an area with relatively little emission of NO_2. The incoming concentration of NO_2 is therefore low, and most of the observed plume will likely originate from Drax. The E wind directional plot shows a plume that is also likely to contain NO_2 emissions from Hull, the large point sources of Saltend power station and South Killingholme refinery (see Table 5.1) and shipping in the Humber Estuary.

Port Talbot: 27 month period

The Port Talbot plots (Figure 5.18) show less obvious evidence of NO_2 plumes than the Drax plots. Plumes are however visible in the NE, E and SE wind directional plots, but these are likely to also contain upwind NO_2 emissions from Cardiff. There is some

evidence of less intense NO_2 plumes in the other five Port Talbot wind-directional plots, but it is difficult to identify these plumes with any certainty.

Grangemouth: 27 month period

The Grangemouth plots (Figure 5.19) display the weakest evidence of any NO_2 plumes. Instead, an area of elevated $TCNO_2$ appears to run in an east-to-west direction from just west of Grangemouth to the Firth of Forth. In some of the Grangemouth plots, for example for the S wind direction, there appears to be an area of high $TCNO_2$ to the west of Grangemouth , but the southerly wind direction implies that this is likely to be a result of NO_2 emissions from of Falkirk, Stenhousemuir and the town of Grangemouth rather than the Grangemouth refinery.

Drax: 12 month period

The reminder of this section focusses on the shorter time periods produces for Drax only (as the Drax source displays the strongest evidence of NO_2 plumes). These plots are shown in Figure 5.11 to Figure 5.17. Use of a 12 month time period (Figure 5.12) gives a similar picture to the 27 month plots: the largest intensity plumes are observed for SE, S, SW and W wind directions, with clearer (but less intense) plumes observed from the NE, E, NW and N wind directions.

Drax: 6 month period

The six month plots (Figure **5.13**) show a broadly similar pattern to the 12 month plots, although the smaller number of measurements comprising each plot means that some differences to the longer time period plots begin to be observed. Most strikingly, the N wind directional plot shows high $TCNO_2$ levels around Drax and York, whereas very low levels of $TCNO_2$ are observed in the NW wind directional plot. Interestingly, the elevated levels of $TCNO_2$ in, for example, the N wind directional plot are more centred over the sources rather than elongated plumes, which is likely to indicate the presence of low wind speeds when these measurements were taken. The white area on the NW plots indicates where no valid measurements were recorded over the six month time period.

Drax: 3-month period

When we move to a three month time period (Figure 5.14 to Figure 5.17 for each meteorological season), greater differences from the longer time series plots are shown, which is again mainly a result of the small number of valid measurement contributing to each plot – the white patches on these three month plots (indicating no valid measurements) are much more prevalent than on the six month plots.

The DJF plots (Figure 5.14) do however show some evidence of above-background plumes of NO_2 from Drax from W and NW directions, but these are likely to contain some contribution from urban areas – further interrogation of the wind speed data would be useful to deconvolute these. In contrast, the MAM plots (Figure 5.14) show some evidence of plumes from Drax from N, E and SE wind directions.

The JJA plots (Figure 5.16) show a surprising lack of valid measurements in the W, NW and N wind directional plots for summer months which indicates that the prevailing wind during this three month period was from predominantly from S, SE, E and NE directions. Clear NO_2 plumes from Drax are difficult to observe for this period, which may be because of a reduced level of operation of the power station in the summer due

to the increased contribution from renewable energy sources. Some evidence of plumes can however be seen in the plots for S, SW and NE wind directions. A number of the SON plots (Figure 5.17) also have sparse data coverage, with any clear NO_2 plumes from Drax difficult to determine.

Drax: comparison of periods

We have therefore found some evidence of wind-directionally aggregated plumes of NO_2 from Drax for all time periods studied. These plumes are clearly visible from all wind directions when 27 or 12 months of data are used. For a six month period, the plumes from some wind directions become less distinct, the plots show some differences to those from longer time periods, and the low number of measurements begins to become an issue for some wind directions. For the three month datasets, fewer obvious plumes are observed and a number of the plots have areas where no observations were recorded – most commonly the N, NE and NW plots which correspond to the least prevalent prevailing wind conditions over the UK.

The results of this part of the case study therefore suggest that six months of wind-directional conditionally aggregated data are in general required to visually identify plumes of NO_2 from Drax (the largest UK NO_2 point source); fewer plumes are identified when using only three months of data is used, and sparsity of data then becomes a significant issue. It should however be noted that we have not explored every possible six month time period over the lifetime of TROPOMI, and the amount of data needed to identify plumes is likely to vary as the operation of (and therefore emissions from) the Drax power station and metrological conditions change over time.

Port Talbot & Grangemouth: comparison of periods

For the Port Talbot point source, some evidence of NO_2 plumes also can be observed (for some wind directions) when using 27 months, 12 months and six months of data. Where three months of data are used (these results are not shown in this report), clear plumes are much less common, and issues are encountered with low numbers of valid measurements, or indeed no valid measurements at all. Investigation of the Grangemouth point source revealed very little evidence of NO_2 plumes for any wind direction, even when the whole 27 month dataset was used.

We then investigated the use of wind-directional and wind-speed conditional aggregation to attempt to tease out more distinct plumes of NO_2. The results of these studies are described in the next sub-section.
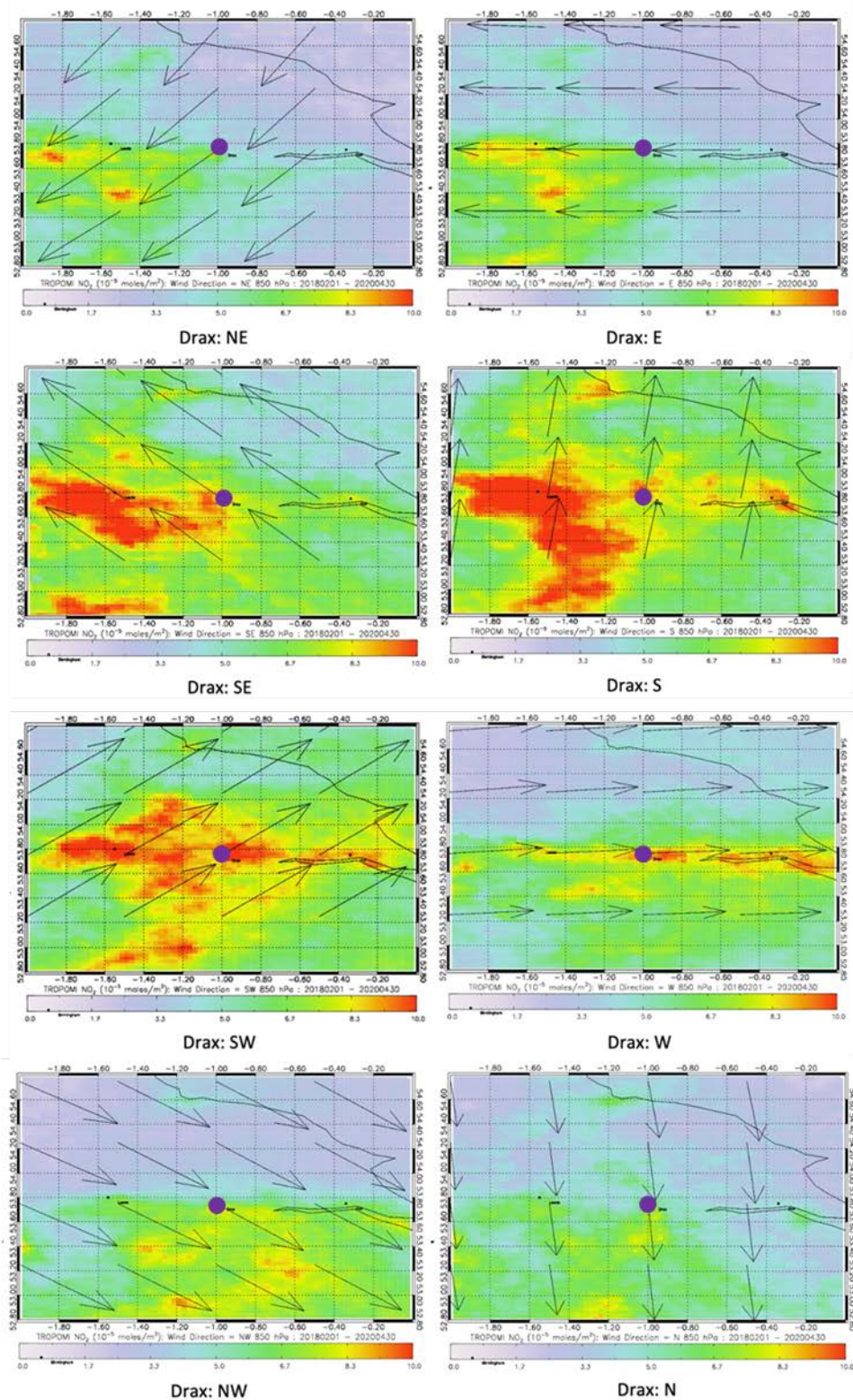
Figure 5.11. Mean TCNO$_2$ (in mol.m^{-2}) over the area around the Drax point source (identified by the purple circles) for the 27 month period 01.02.2018 - 30.04.2020 using *wind-directional conditional averaging*. Extent of colour scales are 0 - 10x10^{-5} mol.m^{-2}; wind direction category indicated beneath each image. The dashed gridlines indicate graduations of 0.2° latitude and 0.2° longitude.
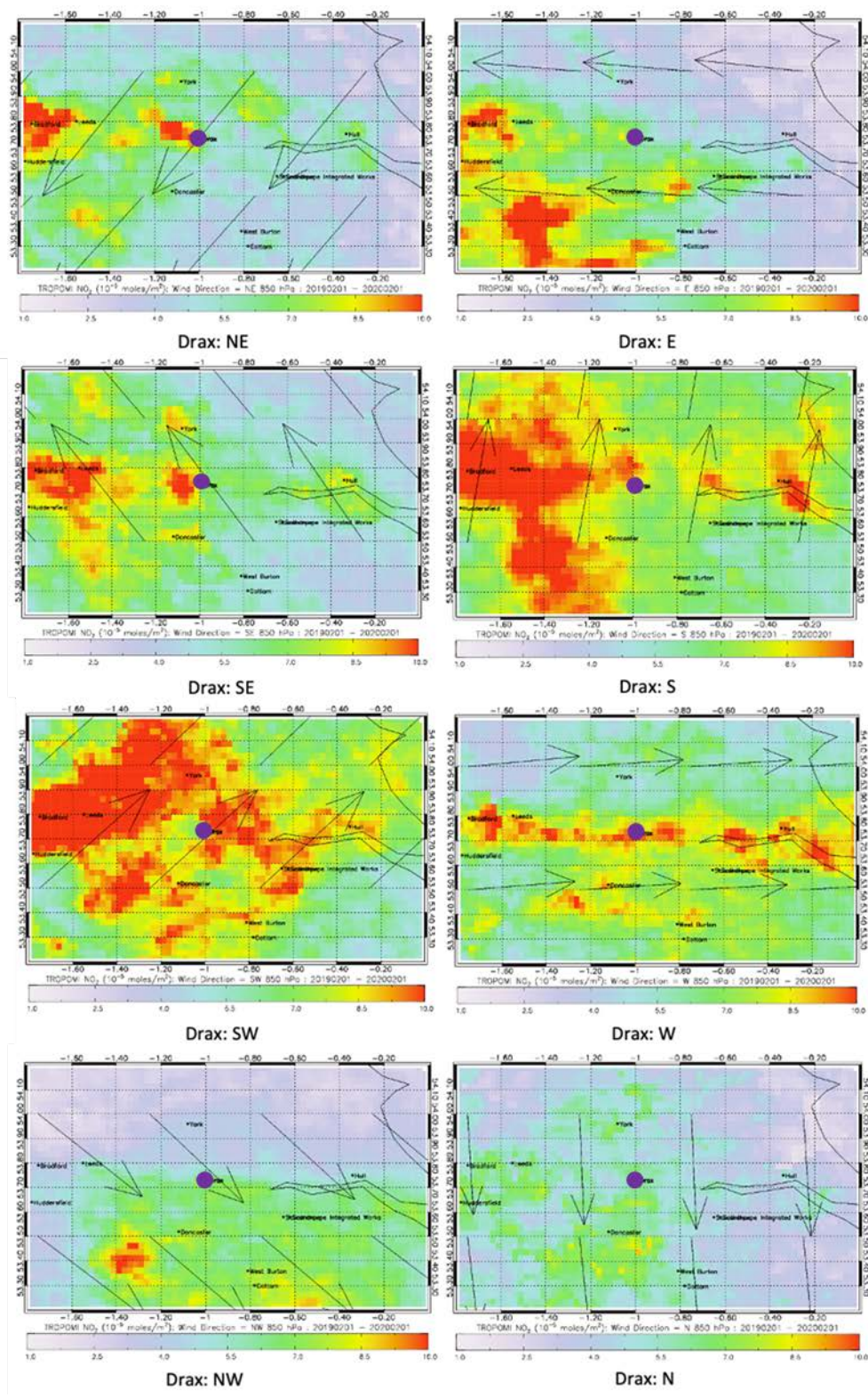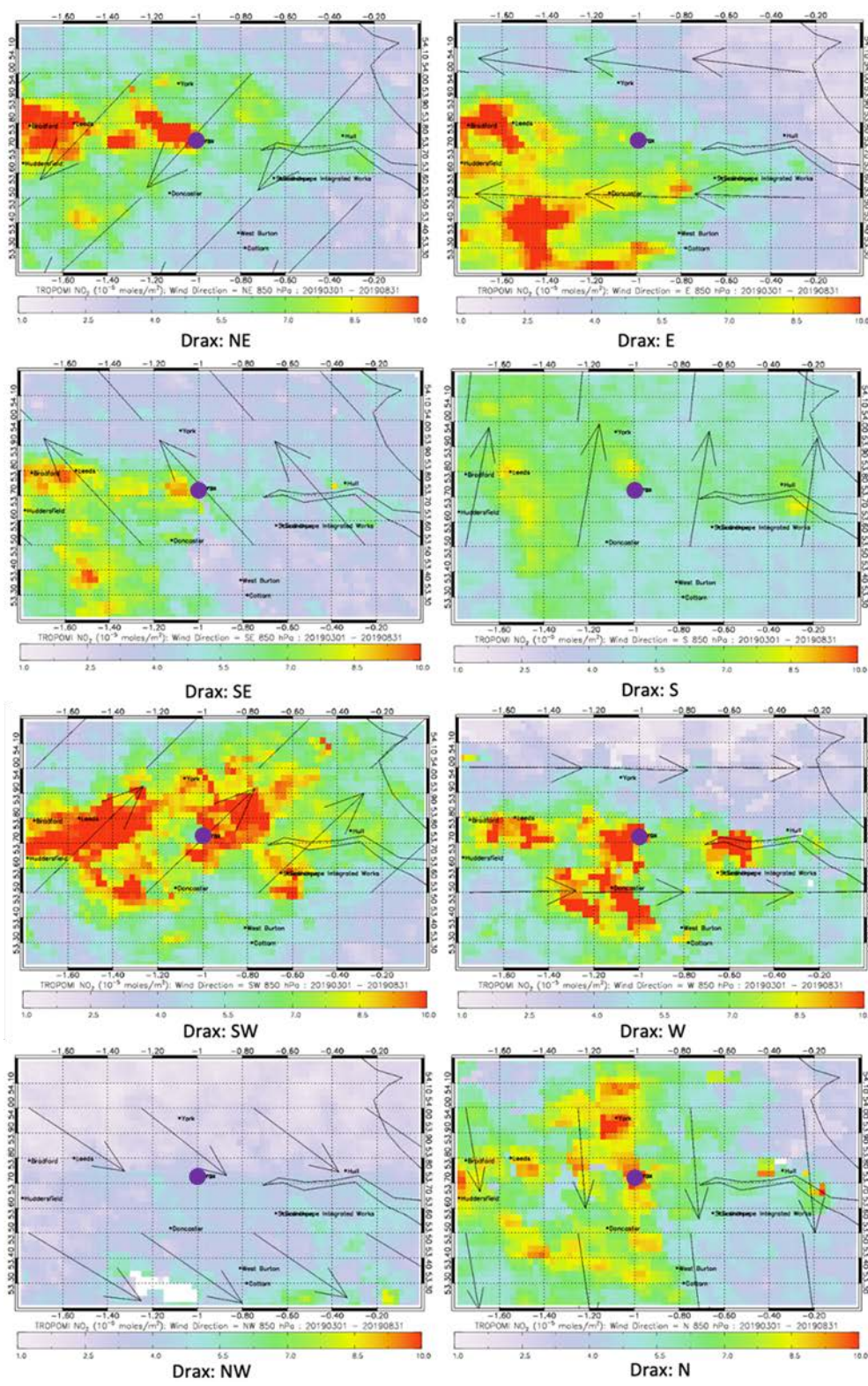
Figure 5.12. As Figure 5.11, but for the 12 month period 01.02.2019 - 01.02.2020. Extent of colour scales are 1x10⁻⁵ - 10x10⁻⁵ mol.m⁻²; wind direction category indicated beneath each image. The dashed gridlines indicate graduations of 0.1° latitude and 0.2° longitude.

Figure 5.13. As Figure 5.11, but for the six month period 01.03.2019 - 31.08.2019. Extent of colour scales are 1x10⁻⁵ - 10x10⁻⁵ mol.m⁻²; wind direction category indicated beneath each image. The dashed gridlines indicate graduations of 0.1° latitude and 0.2° longitude.
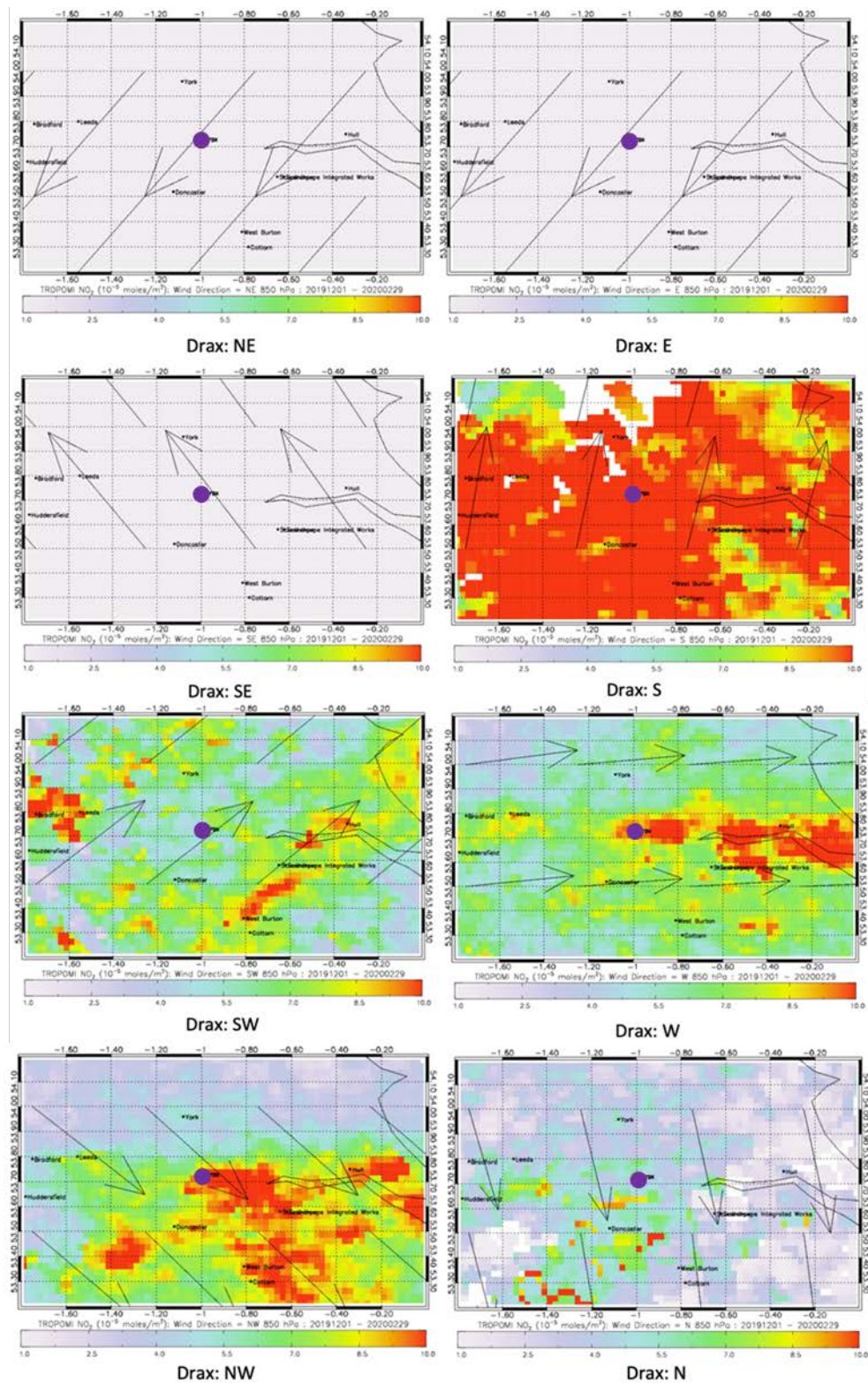
Figure 5.14. As Figure 5.11, but for the three month period of Winter (DJF) 2018-2019 (01.12.2018 - 29.02.2019). Extent of colour scales are 1x10⁻⁵ - 10x10⁻⁵ mol.m⁻²; wind direction category indicated beneath each image. The dashed gridlines indicate graduations of 0.1° latitude and 0.2° longitude.
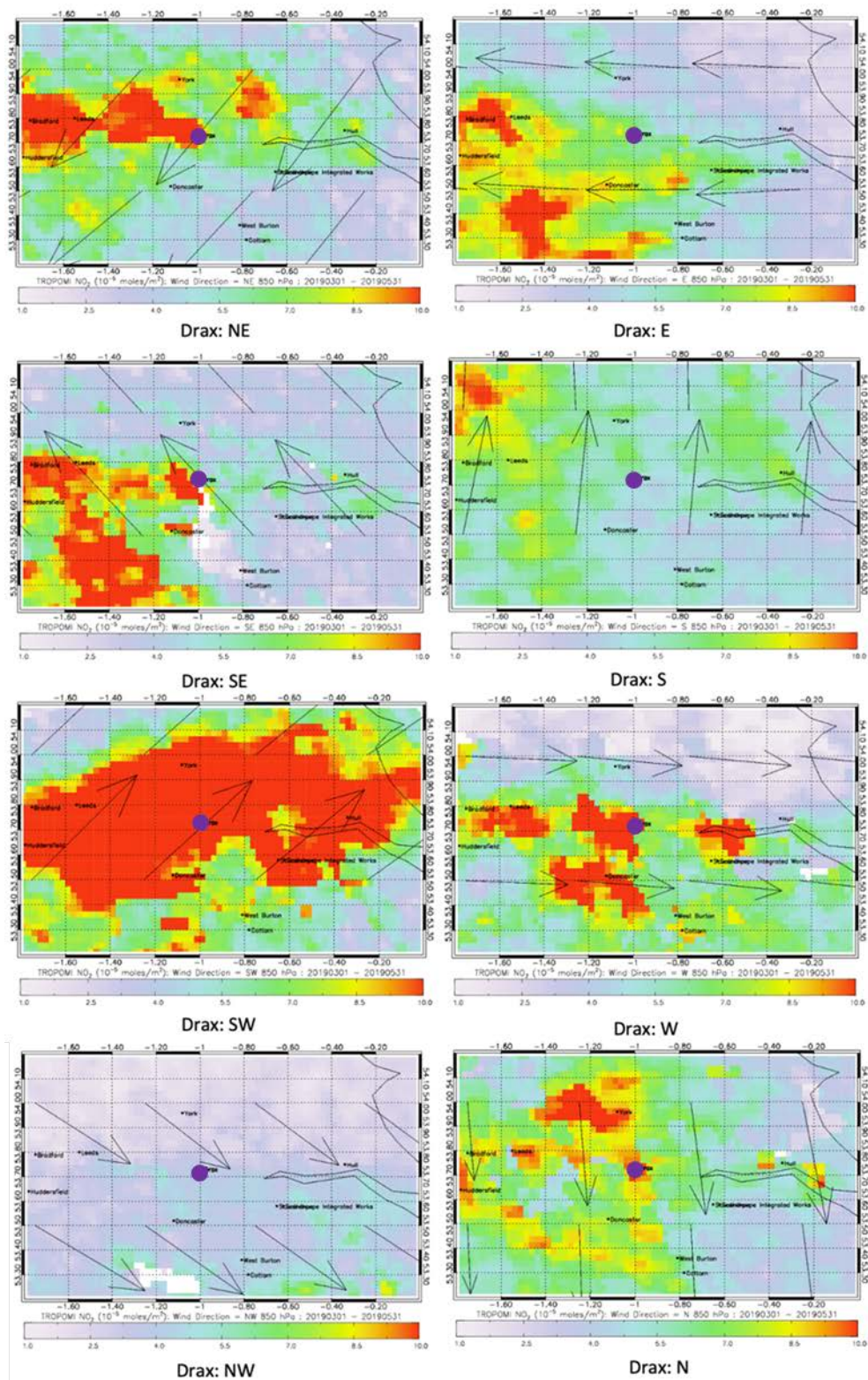
Figure 5.15. As Figure 5.11, but for the three month period of Spring (MAM) 2019 (01.03.2019 - 31.05.2019). Extent of colour scales are 1×10^{-5} - 10×10^{-5} mol.m^{-2}; wind direction category indicated beneath each image. The dashed gridlines indicate graduations of 0.1° latitude and 0.2° longitude.
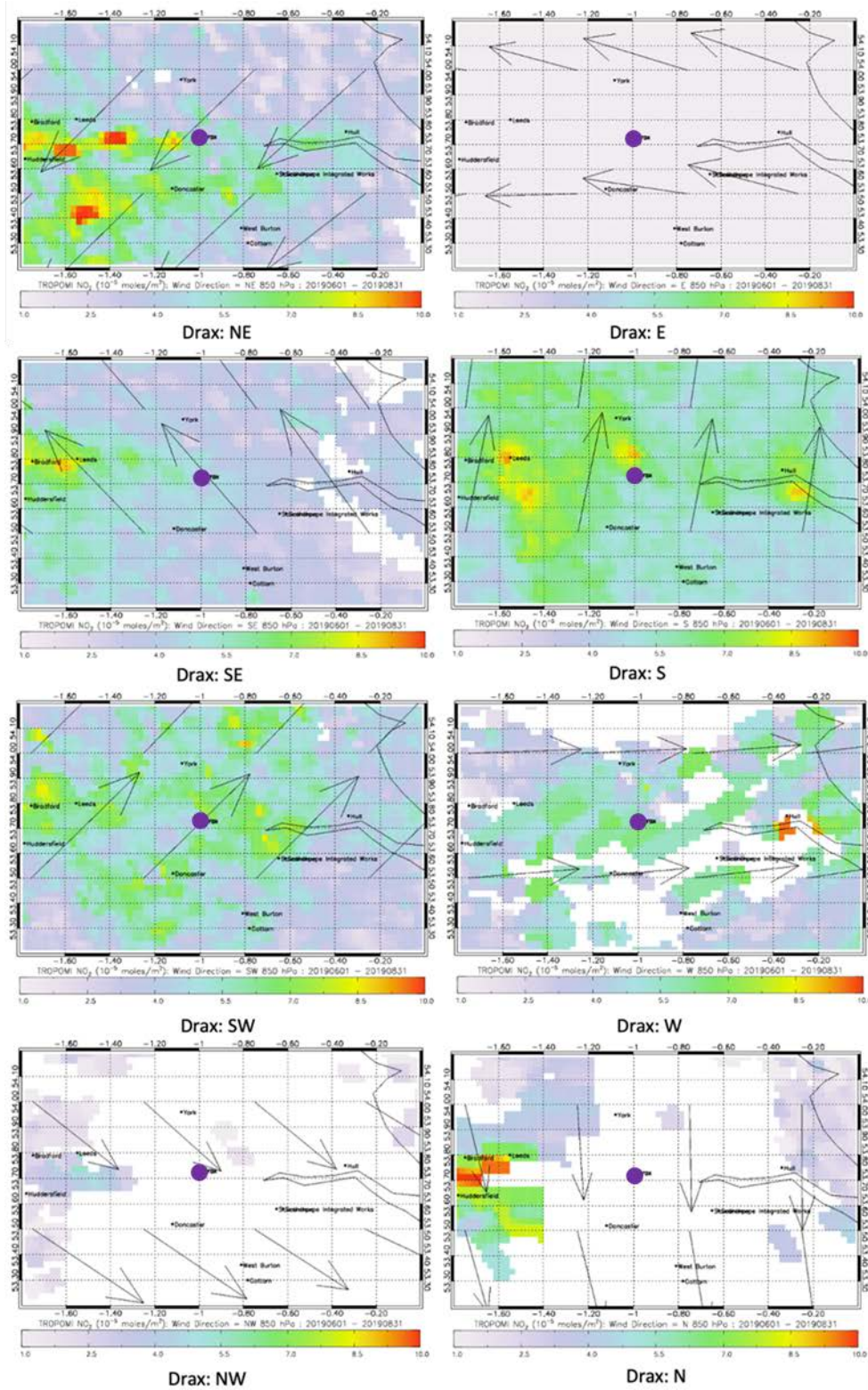
Figure 5.16. As Figure 5.11, but for the three month period of Summer (JJA) 2019 (01.06.2019 - 31.08.2019). Extent of colour scales are 1.0×10^{-5} - 10×10^{-5} mol.m^{-2}; wind direction category indicated beneath each image. The dashed gridlines indicate graduations of 0.1° latitude and 0.2° longitude.
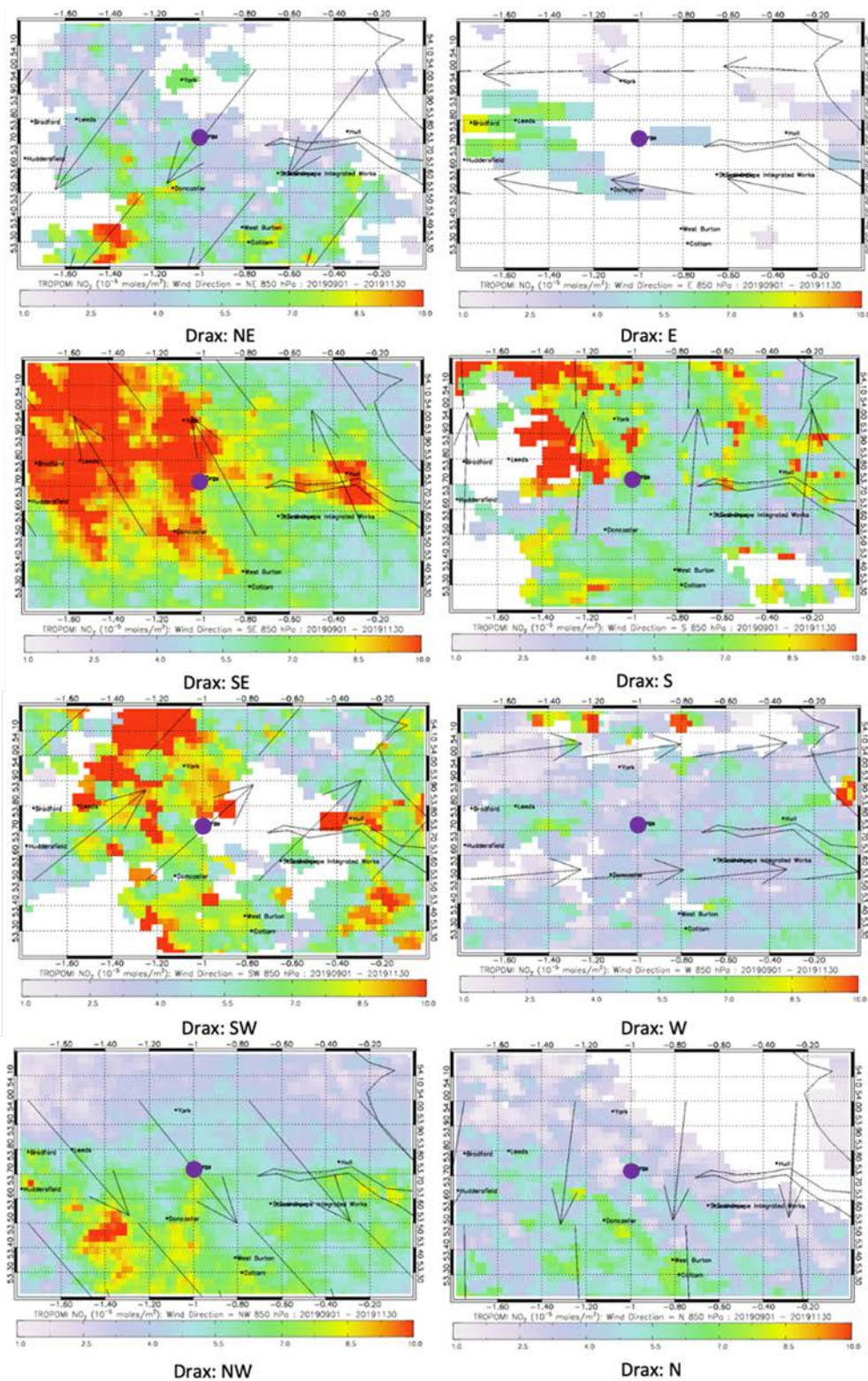
Figure 5.17. As Figure 5.11, but for the **three month** period of Autumn (SON) 2019 (01.09.2019 - 30.11.2019). Extent of colour scales are 1.0×10^{-5} - 10×10^{-5} mol.m^{-2}; wind direction category indicated beneath each image. The dashed gridlines indicate graduations of 0.1° latitude and 0.2° longitude.

Figure 5.18. Mean TCNO₂ (in mol.m⁻²) over the area around the Port Talbot point source (identified by the purple circles) for the 27 month period 01.02.2018 - 30.04.2020 using _wind-directional conditional averaging_. Extent of colour scales are 0 - 10x10⁻⁵ mol.m⁻²; wind direction category indicated beneath each image. The dashed gridlines indicate graduations of 0.2° latitude and 0.2° longitude.

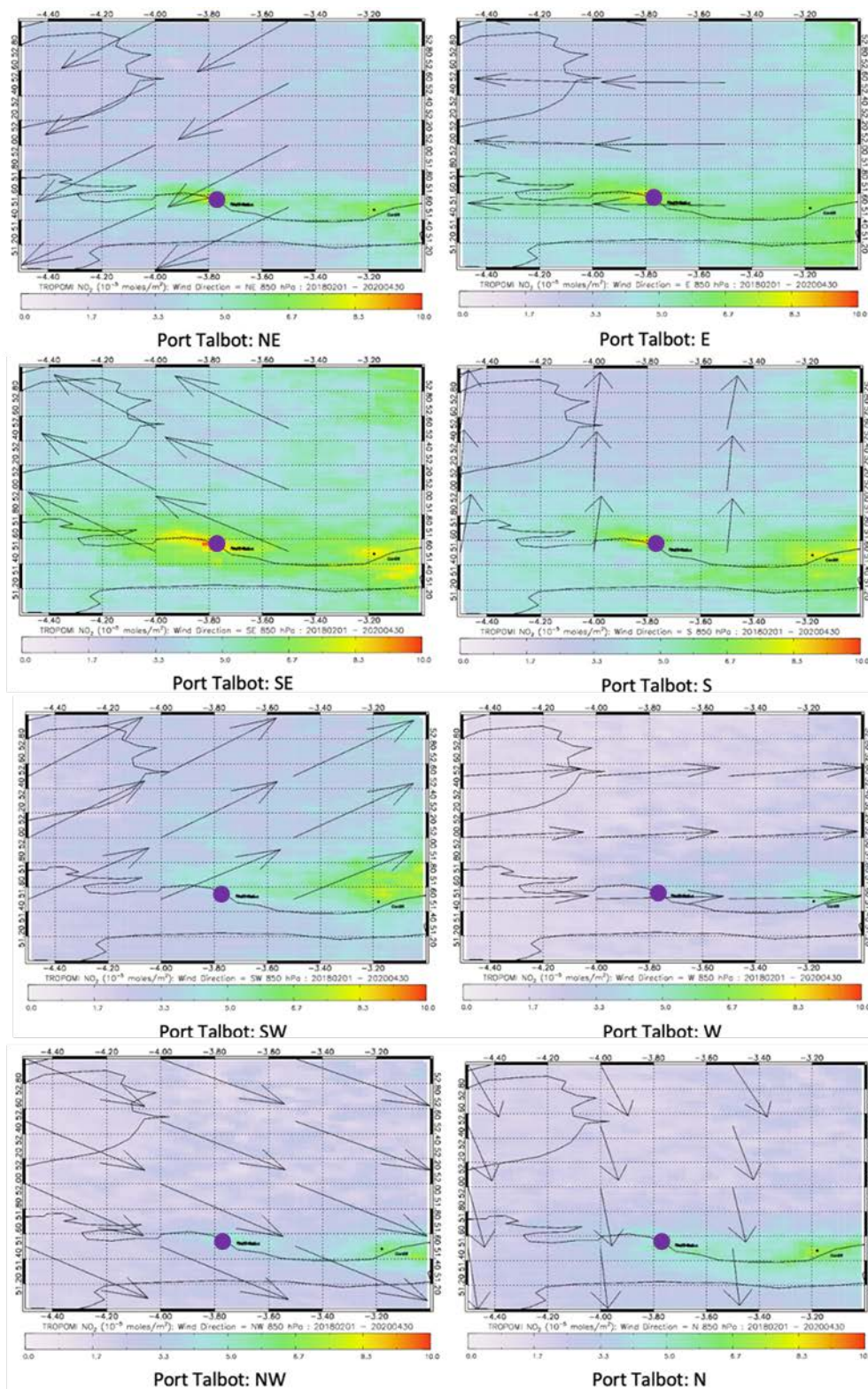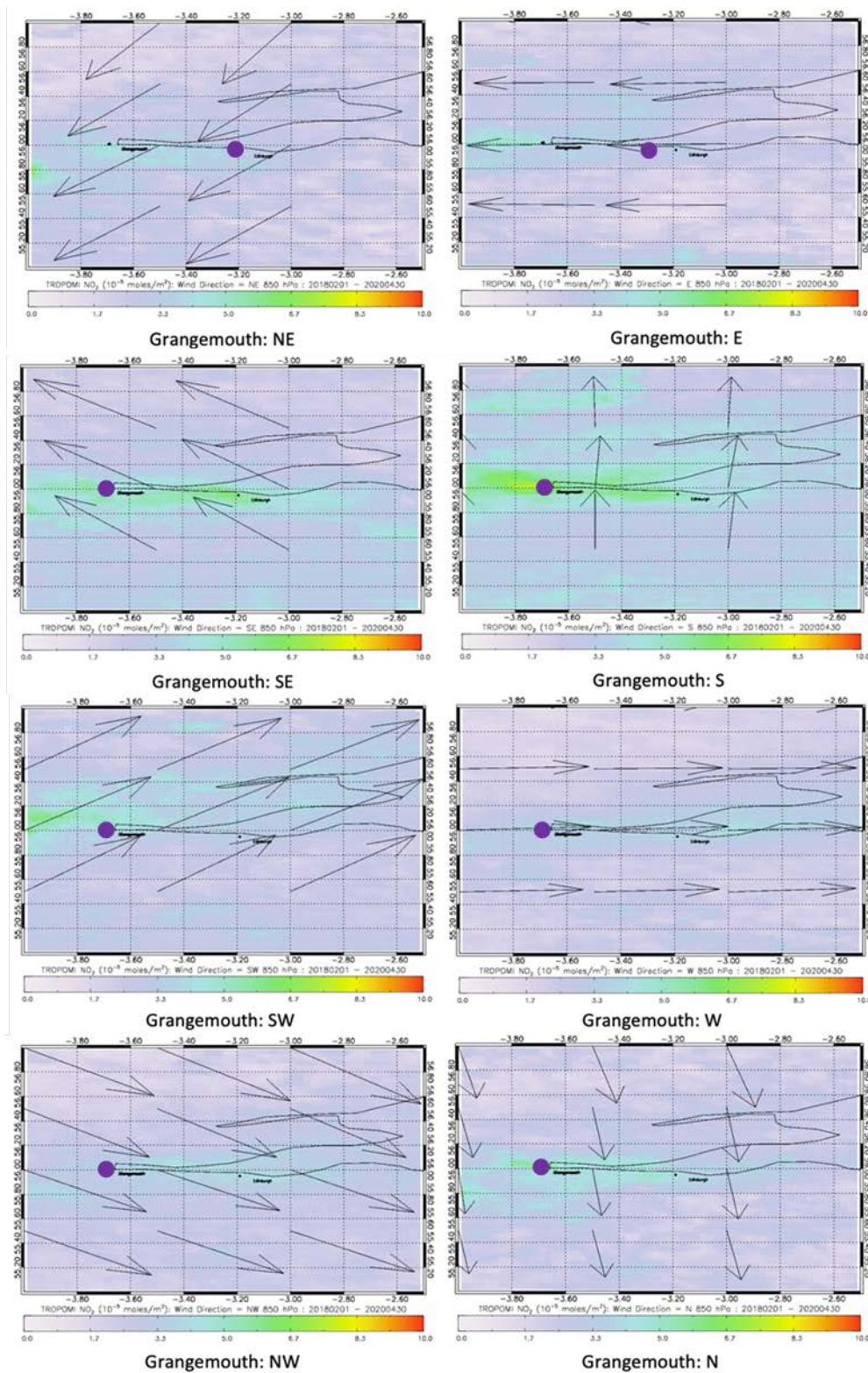**Figure 5.19. Mean TCNO₂ (in mol.m⁻²) over the area around the Grangemouth source (identified by the purple circles) for the 27 month period 01.02.2018 - 30.04.2020 using *wind-directional conditional averaging*. Extent of colour scales are 0 - 10x10⁻⁵ mol.m⁻²; wind direction category indicated beneath each image. The dashed gridlines indicate graduations of 0.2° latitude and 0.2° longitude.**

5.3.4 Stage 3: Wind-directional and wind-speed conditional aggregation

Visual investigation of plumes

For this wind-directional and wind-speed conditional aggregation part of this case study, we used the whole 27 month dataset, as use of shorter time periods of data would have resulted in a very small number of valid measurements in each of the 32 plots (four wind speed categories at each of eight wind direction categories - see Section 5.2.6).

Mean $TCNO_2$ wind-directional and wind-speed conditional aggregation plots were produced for each of the three point sources, accompanied by plots showing the number of valid observations used to produce these. For ease of reference, the wind-directional conditionally aggregated plots are detailed in Table 5.3. The plots for Drax are shown in this report; equivalent plots were also produced for Port Talbot and Grangemouth, but are omitted from this report for the sake of simplicity.

Table 5.3 Summary of wind-directional and wind-speed conditionally aggregated figures. All figures are show the area around the Drax point source and use 27 months of TROPOMI data

		Wind speed / $m.s^{-1}$			
		0 - 2.5	2.5 – 5.0	5.0 – 7.5	7.5 – 10.0
Wind directions	NE & E	Figure 5.20	Figure 5.24	Figure 5.28	Figure 5.32
	SE & S	Figure 5.21	Figure 5.25	Figure 5.29	Figure 5.33
	SW & W	Figure 5.22	Figure 5.26	Figure 5.30	Figure 5.34
	NW & N	Figure 5.23	Figure 5.27	Figure 5.31	Figure 5.35

Focussing this discussion on the largest source (Drax), using TROPOMI measurements taken when the wind speed was between 0 - 2.5 $m.s^{-1}$ (Figure 5.20 to Figure 5.23) does not reveal any clear plumes emerging from the source and aligned with the direction of the prevailing wind. The small number of measurements comprising each plot is noticeable here, and should be borne in mind during the remainder of this discussion – the number of observations are shown in the bottom row in each Figure. The average number of valid measurements in the study area around each point source (including Port Talbot and Grangemouth for information) for each wind direction are shown in Table 5.4, and for each wind speed category in Table 5.5. Considering that the dataset used encompasses 27 months, it is clear that only a very small fraction of these (potentially 820) measurements comprise each plot.

Table 5.4   Average number of valid measurements in the study area around each point source for each wind direction category using 27 months of TROPOMI data

Wind direction category	Drax	Port Talbot	Grangemouth
NE	4.50	3.25	2.25
E	3.50	5.87	1.58
SE	3.18	4.30	3.00
S	3.05	5.50	3.68
SW	4.08	5.18	1.50
W	5.00	4.25	5.18
NW	6.82	3.20	4.58
N	2.25	3.88	3.25

Table 5.5   Average number of valid measurements in the study area around each point source for each wind speed category using 27 months of TROPOMI data

Wind speed category / m.s^{-1}	Drax	Port Talbot	Grangemouth
0 - 2.5	1.56	3.06	1.96
2.5 - 5.0	5.34	4.71	4.62
5.0 - 7.5	4.62	5.47	3.00
7.5 - 10.0	4.66	4.46	2.91

The plots for wind speeds of 2.5 - 5.0 m.s^{-1} (Figure 5.24 to Figure 5.27) show NO$_2$ plumes from Drax for most wind directions, with the plots for NW, N and E wind directions showing the clearest plumes that are most distinct from other large sources of NO$_2$. Plumes may also be visible for S, SW and W wind directions although these are at least partially obscured by plume of NO$_2$ from urban conurbations.

For wind speeds of 5.0 - 7.5 m.s^{-1} (Figure 5.28 to Figure 5.31), the plot for the N wind direction contains no valid measurements. Distinct plumes do seem to be visible from Drax for NE and E wind directions, and perhaps also for the other five wind directions for which measurements were recorded (SE, S, SW, W and NW), although the relatively high levels of TCNO$_2$ across the majority of the plot area means any plumes are less distinct.

Finally, for wind speeds of 7.5 - 10.0 m.s^{-1} (Figure 5.32 to Figure 5.35), clear NO$_2$ plumes are again visible for N, NE and E wind directions; the elongated nature of the NE and E plumes is likely to be an artefact of these higher wind speeds.

Use of wind-directional and wind-speed conditional aggregation around the Drax point source has therefore, despite the small number of valid measurements, revealed plumes (or potential plumes) of NO$_2$ for most wind directions for three of the wind speed categories investigated: 2.5 - 5.0 m.s^{-1}, 5.0 - 7.5 m.s^{-1} and 7.5 – 10.0 m.s^{-1}. Clear plumes cannot however be identified for the 0 - 2.5 m.s^{-1} wind category.

It is interesting to note that some of these plots (e.g. the E wind plot of Figure 5.32) show an area of relatively low TCNO$_2$ next to the point source, then a TCNO$_2$ 'hotspot' a few kilometres downwind of the point source. This is consistent with Drax power station being a tall stack source where the NO$_2$ plume is aloft for a few kilometres before it is discernible by TROPOMI.

The equivalent results for the other two point sources, Port Talbot and Grangemouth are not shown in this report. However, for both of these sources, the findings are of a similar nature to those for Drax: namely that plumes of NO_2 from the sources cannot definitely be identified for any wind direction when using the 0 - 2.5 m.s^{-1} wind category. For the other three wind categories (2.5 - 5.0 m.s^{-1}, 5.0 - 7.5 m.s^{-1} and 7.5 - 10.0 m.s^{-1}), plumes of NO_2 are however observable from some wind directions, more so from Port Talbot than Grangemouth, which is unsurprising given the relative size of emissions from these two sources.

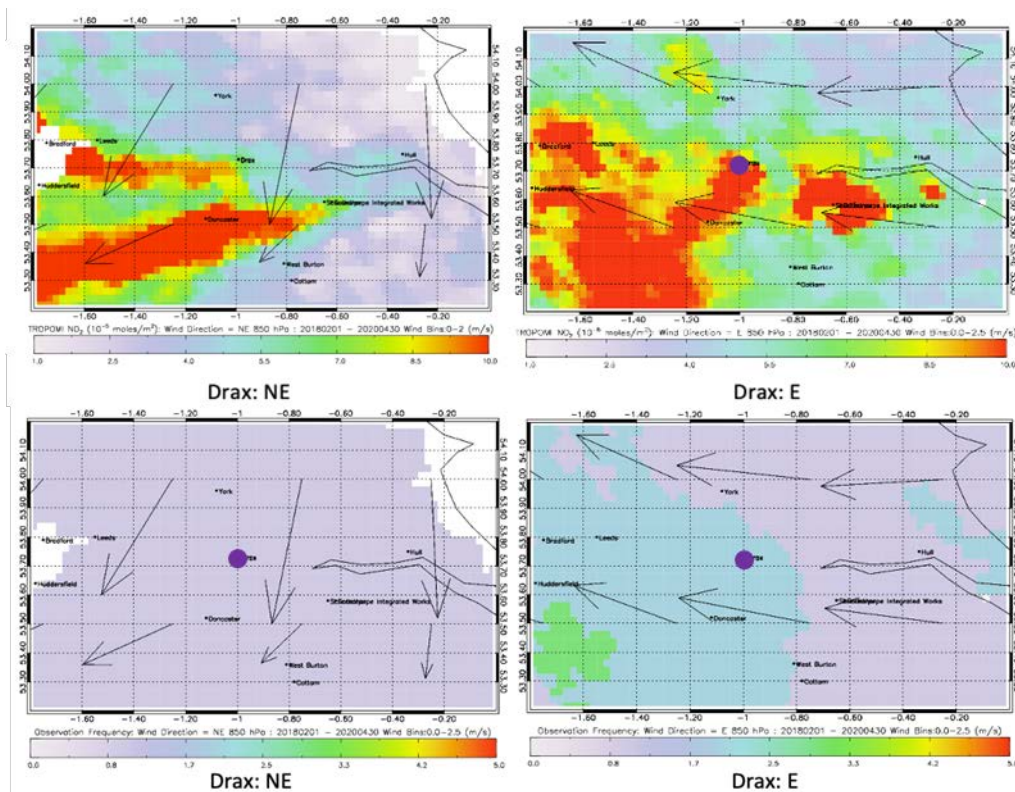A brief investigation to attempt to derive the emissions contributing to these plumes was then carried out.

Figure 5.20. Top row: Mean TCNO$_2$ (in mol.m^{-2}) over the area around the Drax point source (identified by the purple circles) for the 27 month period 01.02.2018 - 30.04.2020 using *wind-directional and wind-speed conditional averaging* (wind direction categories NE & E indicated beneath each image, wind speed category 0 - 2.5 m.s^{-1}). Extent of colour scales are 1x10^{-5} - 10x10^{-5} mol.m^{-2}; mean wind direction is indicated by the arrows. Bottom row: number of observations (extent of colour scale is 0 - 5). The dashed gridlines indicate graduations of 0.1° latitude and 0.2° longitude.

Figure 5.21. As Figure 5.20, but with wind direction categories SE & S indicated beneath each image, wind speed category 0 - 2.5 m.s^{-1}. Extent of top colour scale is 1x10^{-5} - 10x10^{-5} mol.m^{-2}; mean wind direction is indicated by the arrows. Extent of bottom colour scale is 0 - 5 observations.
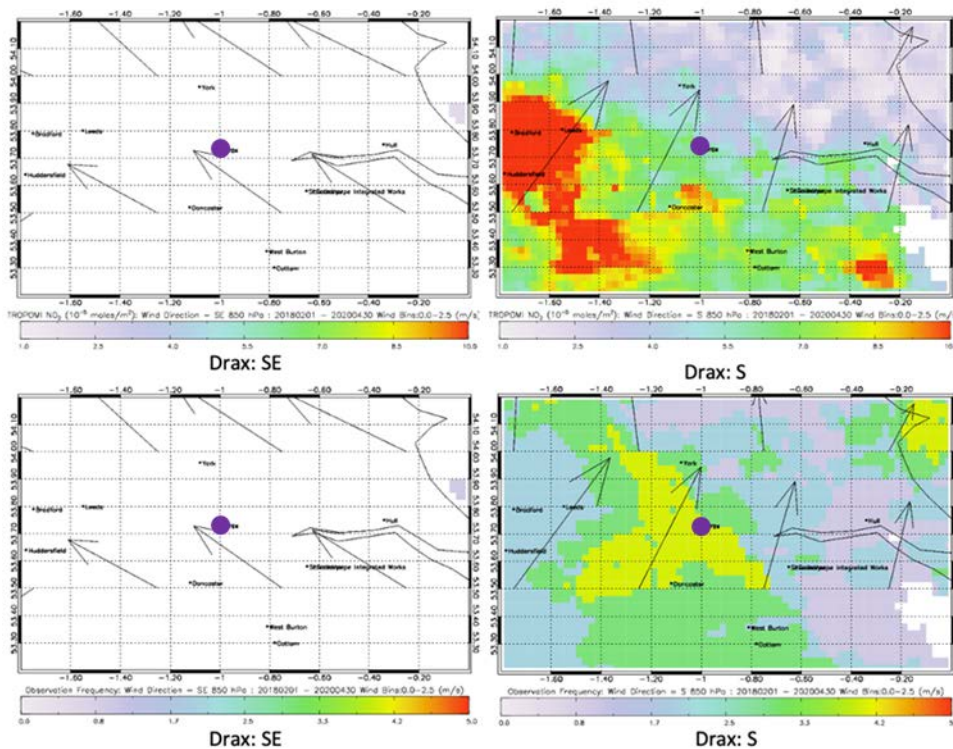

Figure 5.22. As Figure 5.20, but with wind direction categories SW & W indicated beneath each image, wind speed category 0 - 2.5 m.s^{-1}. Extent of top colour scale is 1x10^{-5} - 10x10^{-5} mol.m^{-2}; mean wind direction is indicated by the arrows. Extent of bottom colour scale is 0 - 5 observations.
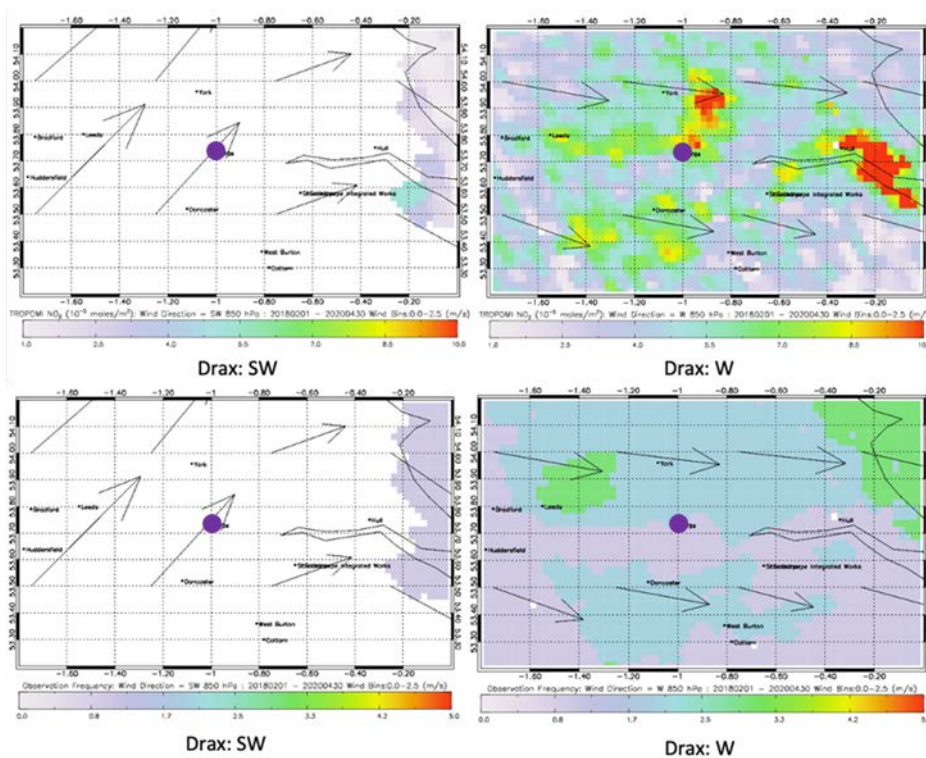
Figure 5.23. As Figure 5.20, but with wind direction categories NW & N indicated beneath each image, wind speed category 0 - 2.5 m.s⁻¹. Extent of top colour scale is 1x10⁻⁵ - 10x10⁻⁵ mol.m⁻²; mean wind direction is indicated by the arrows. Extent of bottom colour scale is 0 - 5 observations.

Figure 5.24. As Figure 5.20, but with wind direction categories NE & E indicated beneath each image, wind speed category 2.5 - 5.0 m.s⁻¹. Extent of top colour scale is 1x10⁻⁵ - 10x10⁻⁵ mol.m⁻²; mean wind direction is indicated by the arrows. Extent of bottom colour scale is 0 - 15 observations.

Figure 5.25. As Figure 5.20, but with wind direction categories SE & S indicated beneath each image, wind speed category 2.5 - 5.0 m.s^{-1}. Extent of top colour scale is 1x10^{-5} - 10x10^{-5} mol.m^{-2}; mean wind direction is indicated by the arrows. Extent of bottom colour scale is 0 - 15 observations.
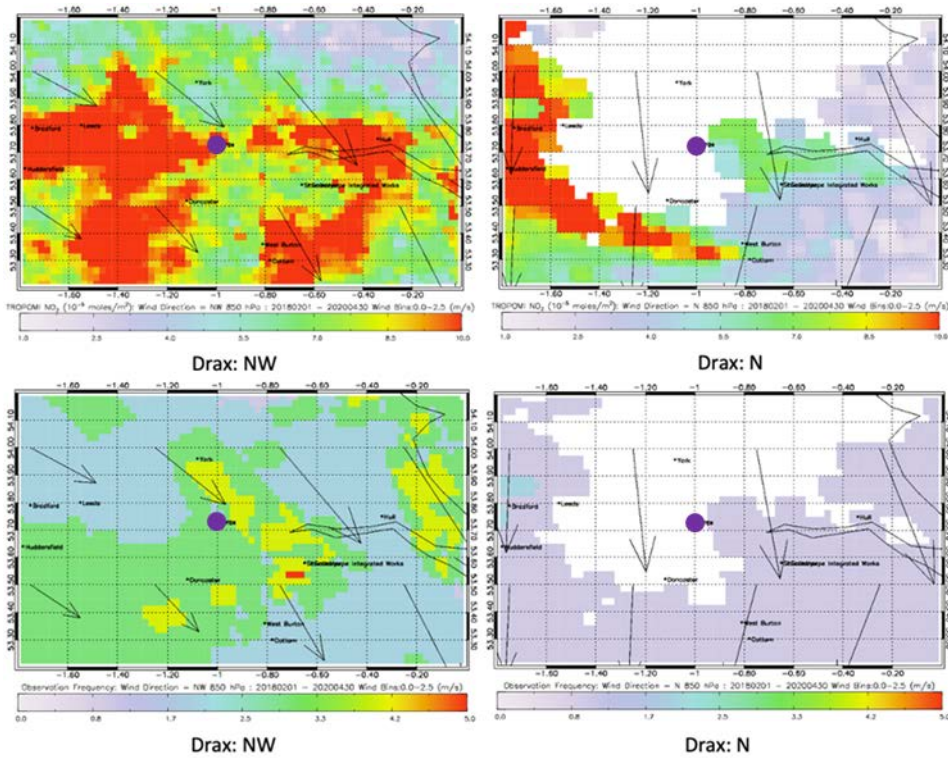

Figure 5.26. As Figure 5.20, but with wind direction categories SW & W indicated beneath each image, wind speed category 2.5 - 5.0 m.s^{-1}. Extent of top colour scale is 1x10^{-5} - 10x10^{-5} mol.m^{-2}; mean wind direction is indicated by the arrows. Extent of bottom colour scale is 0 - 15 observations.
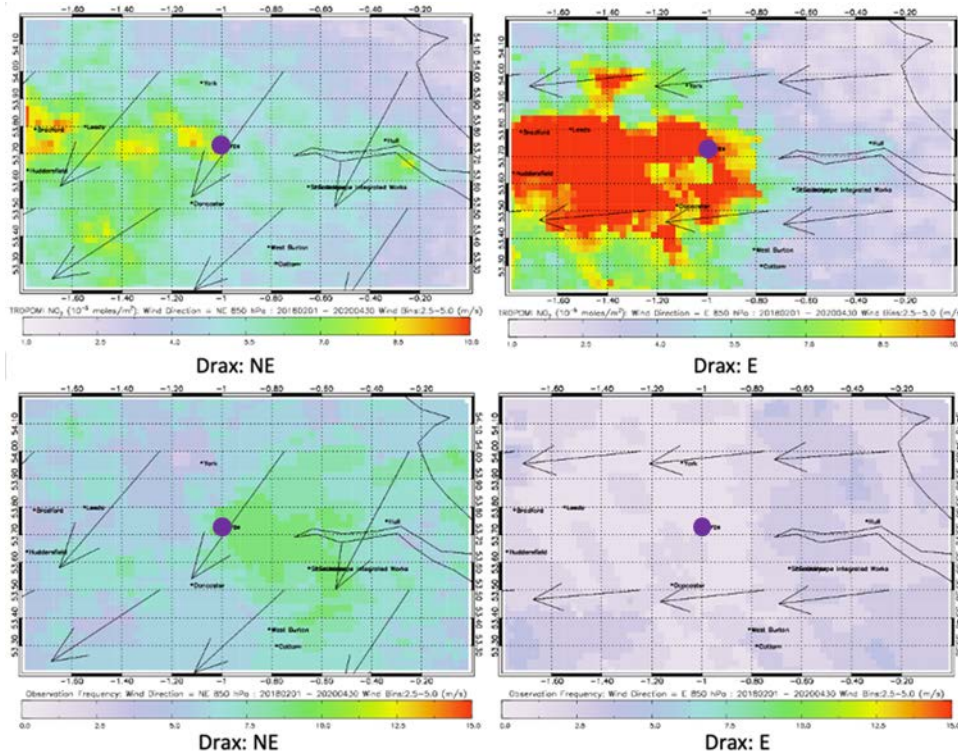
Figure 5.27. As Figure 5.20, but with wind direction categories NW & N indicated beneath each image, wind speed category 2.5 - 5.0 m.s^{-1}. Extent of top colour scale is 1x10^{-5} - 10x10^{-5} mol.m^{-2}; mean wind direction is indicated by the arrows. Extent of bottom colour scale is 0 - 15 observations.

Figure 5.28. As Figure 5.20, but with wind direction categories NE & E indicated beneath each image, wind speed category 5.0 - 7.5 m.s^{-1}. Extent of top colour scale is 1x10^{-5} - 10x10^{-5} mol.m^{-2}; mean wind direction is indicated by the arrows. Extent of bottom colour scale is 0 - 12 observations.
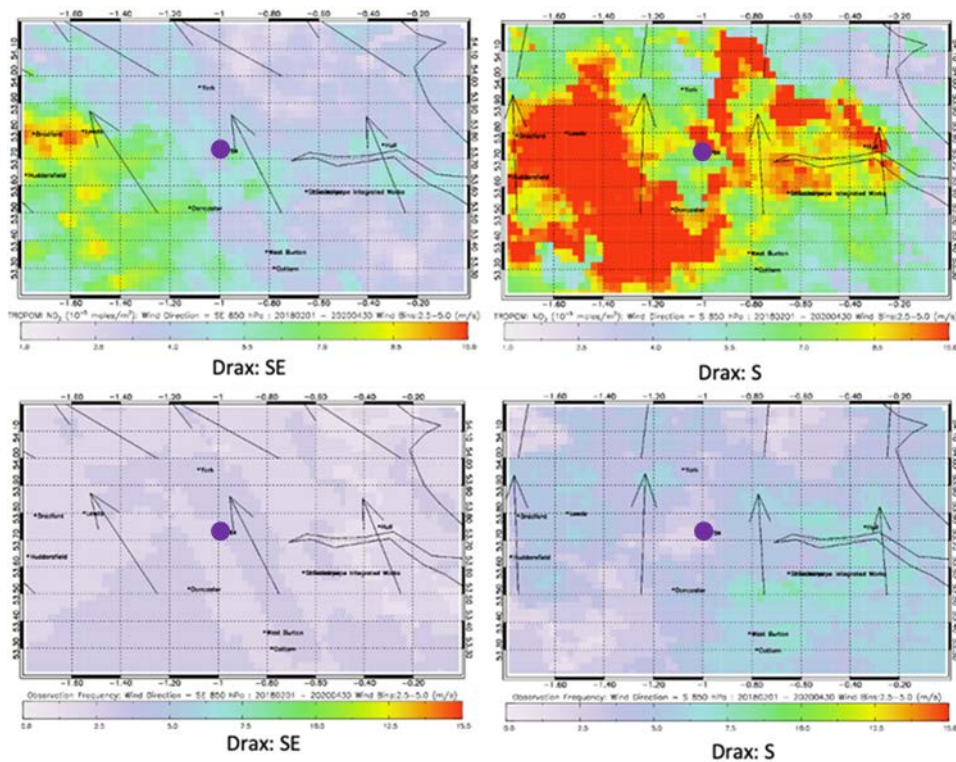
Figure 5.29. As Figure 5.20, but with wind direction categories SE & S indicated beneath each image, wind speed category 5.0 - 7.5 m.s^{-1}. Extent of top colour scale is 1x10^{-5} - 10x10^{-5} mol.m^{-2}; mean wind direction is indicated by the arrows. Extent of bottom colour scale is 0 - 12 observations.
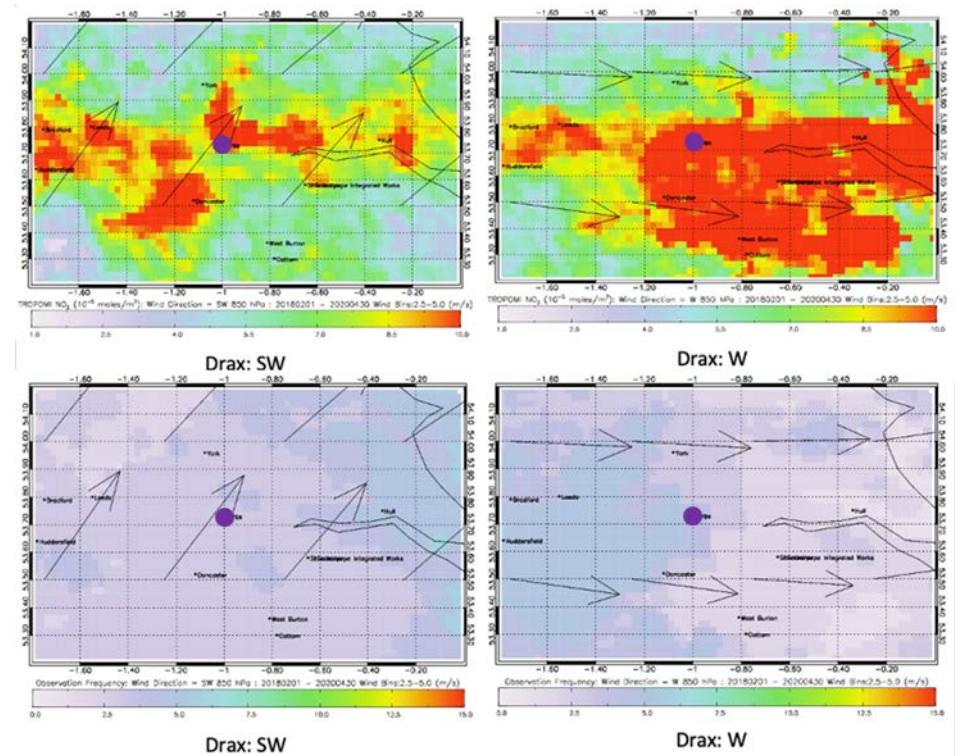

Figure 5.30. As Figure 5.20, but with wind direction categories SW & W indicated beneath each image, wind speed category 5.0 - 7.5 m.s^{-1}. Extent of top colour scale is 1x10^{-5} - 10x10^{-5} mol.m^{-2}; mean wind direction is indicated by the arrows. Extent of bottom colour scale is 0 - 12 observations.

Figure 5.31. As Figure 5.20, but with wind direction categories NW & N indicated beneath each image, wind speed category 5.0 - 7.5 m.s⁻¹. Extent of top colour scale is 1x10⁻⁵ - 10x10⁻⁵ mol.m⁻². ; mean wind direction is indicated by the arrows. Extent of bottom colour scale is 0 - 12 observations.
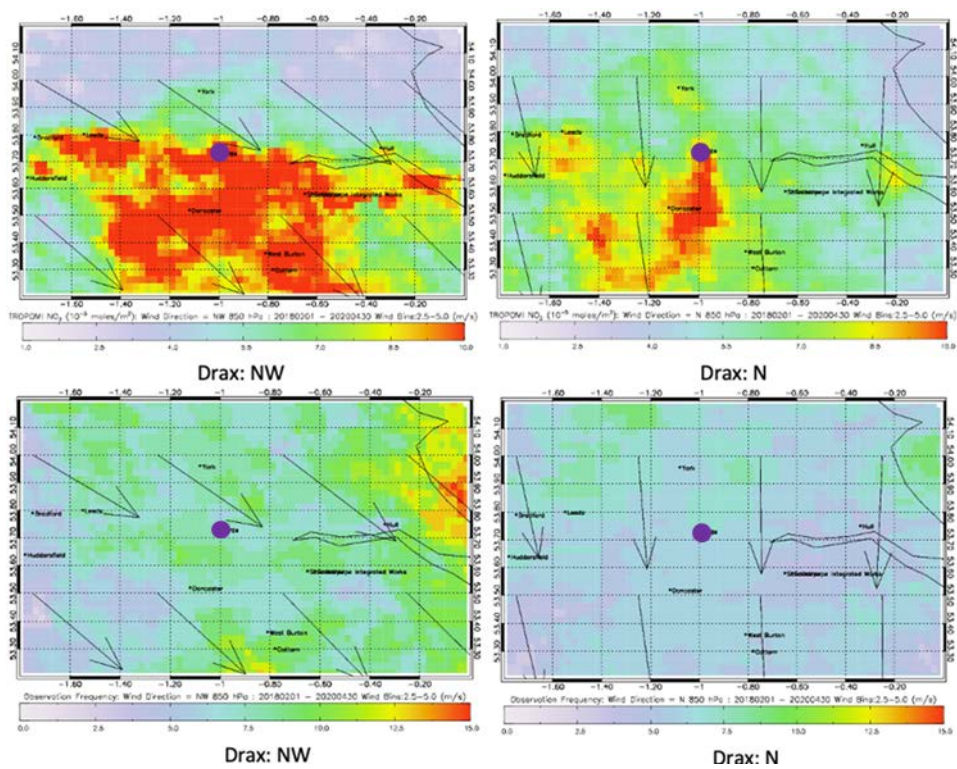

Figure 5.32. As Figure 5.20, but with wind direction categories NE & E indicated beneath each image, wind speed category 7.5 - 10.0 m.s⁻¹. Extent of top colour scale is 1x10⁻⁵ - 10x10⁻⁵ mol.m⁻². ; mean wind direction is indicated by the arrows. Extent of bottom colour scale is 0 - 10 observations.

Figure 5.33. As Figure 5.20, but with wind direction categories SE & S indicated beneath each image, wind speed category 7.5 - 10.0 m.s^{-1}. Extent of top colour scale is 1x10^{-5} - 10x10^{-5} mol.m^{-2}; mean wind direction is indicated by the arrows. Extent of bottom colour scale is 0 - 10 observations.
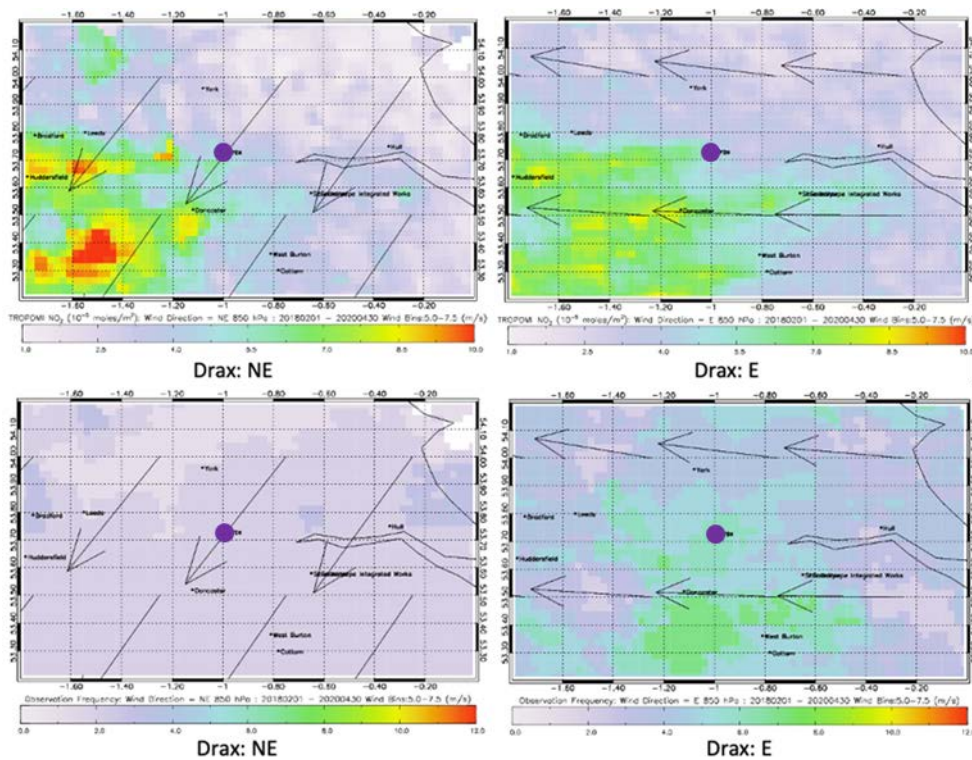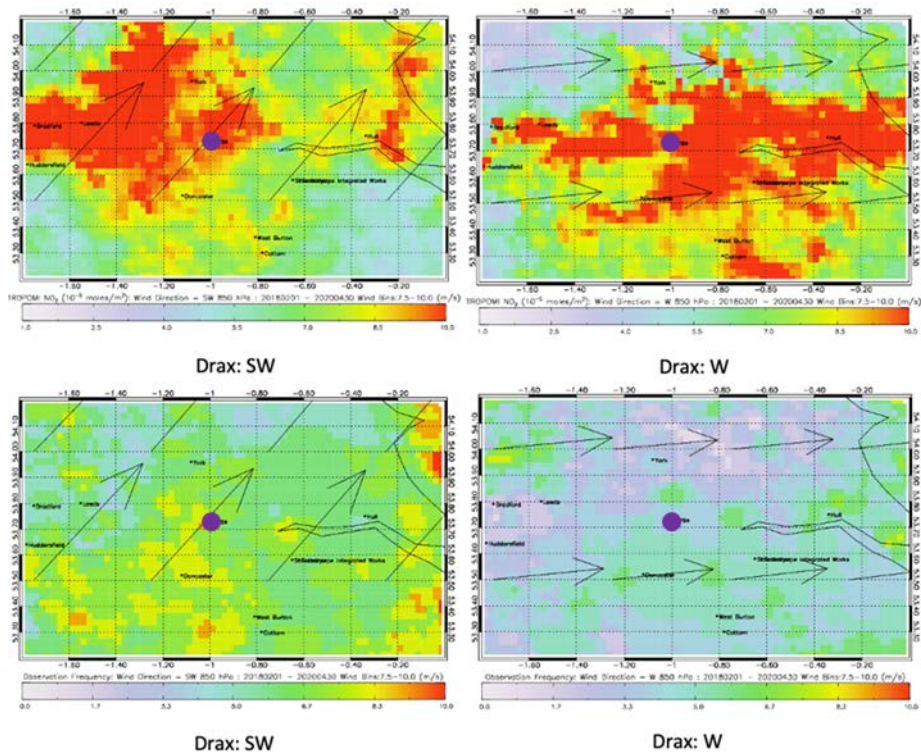

Figure 5.34. As Figure 5.20, but with wind direction categories SW & W indicated beneath each image, wind speed category 7.5 - 10.0 m.s^{-1}. Extent of top colour scale is 1x10^{-5} - 10x10^{-5} mol.m^{-2}; mean wind direction is indicated by the arrows. Extent of bottom colour scale is 0 - 10 observations.

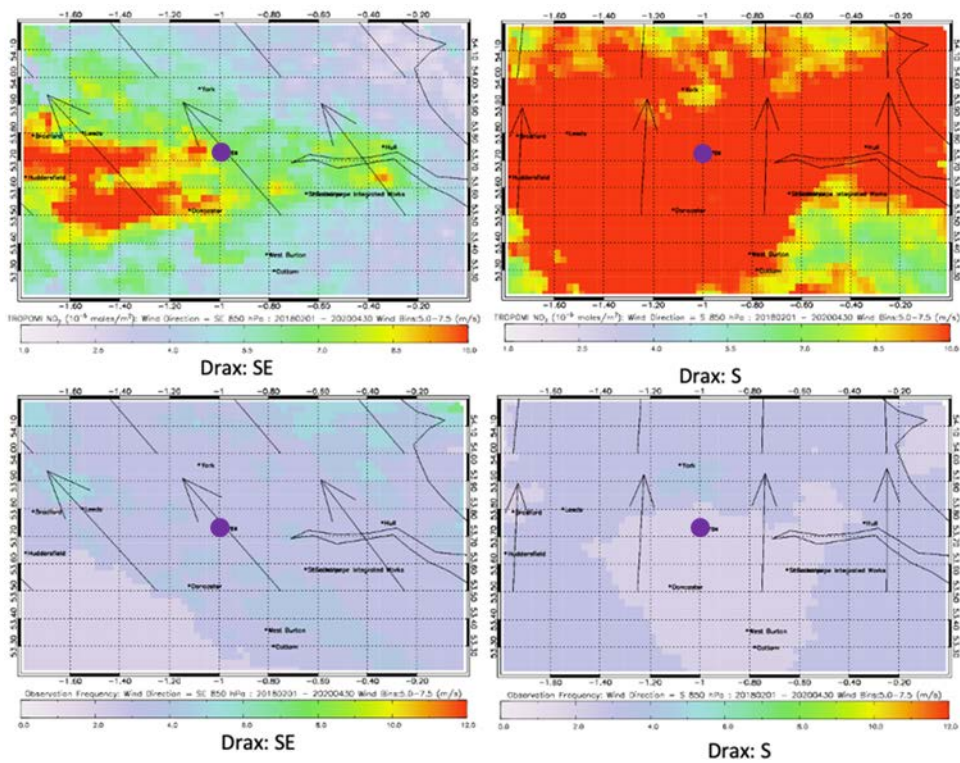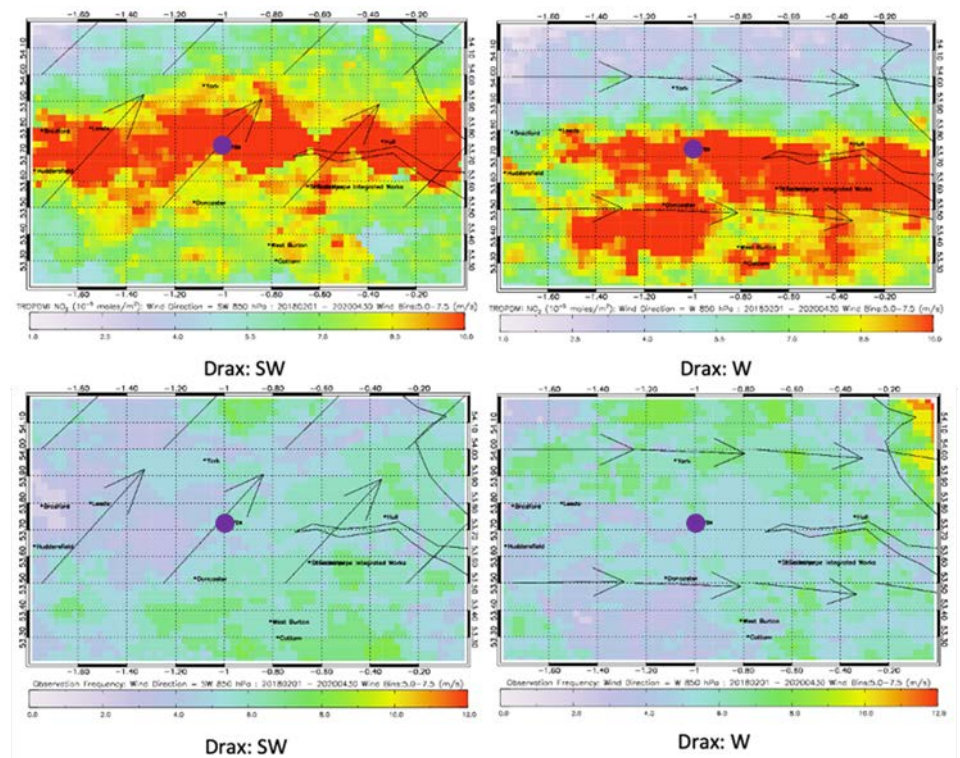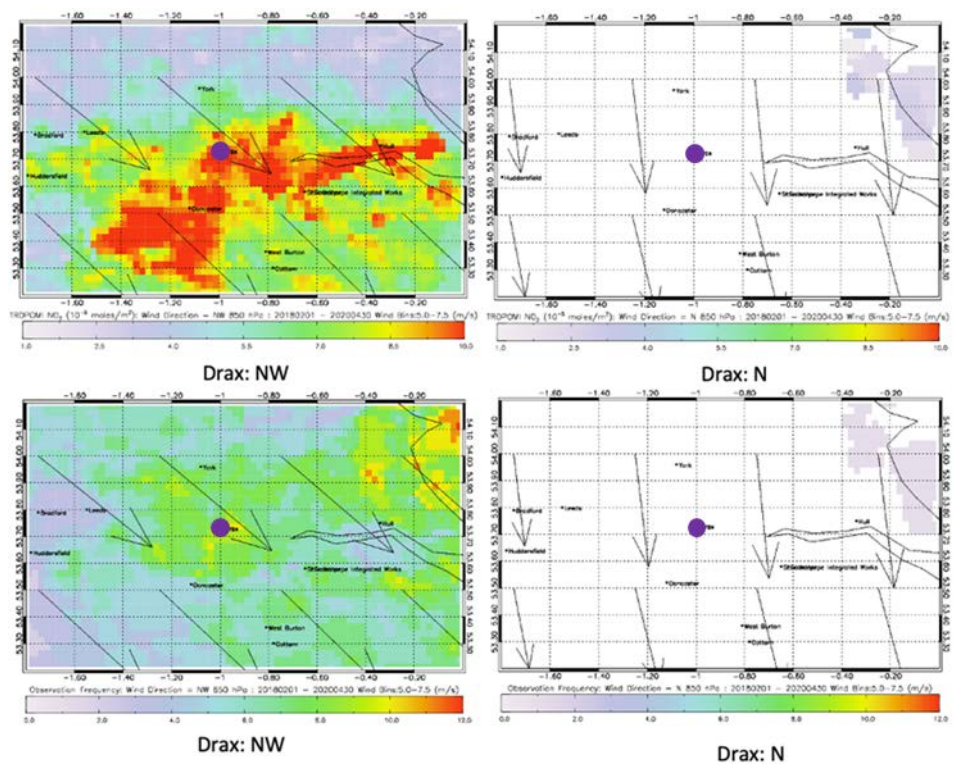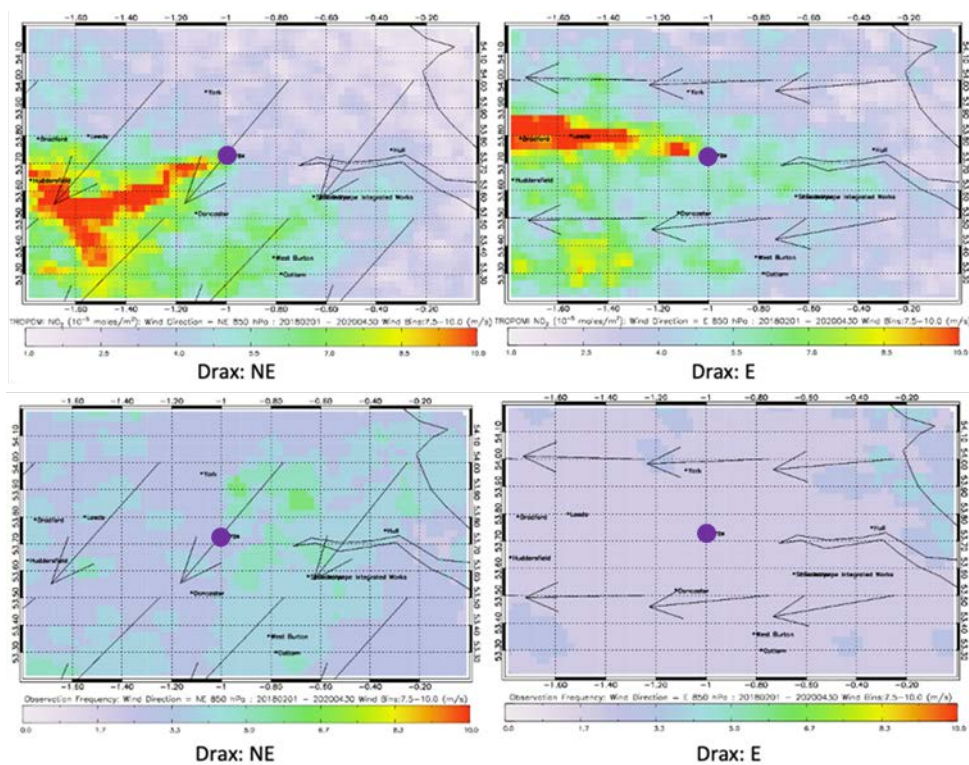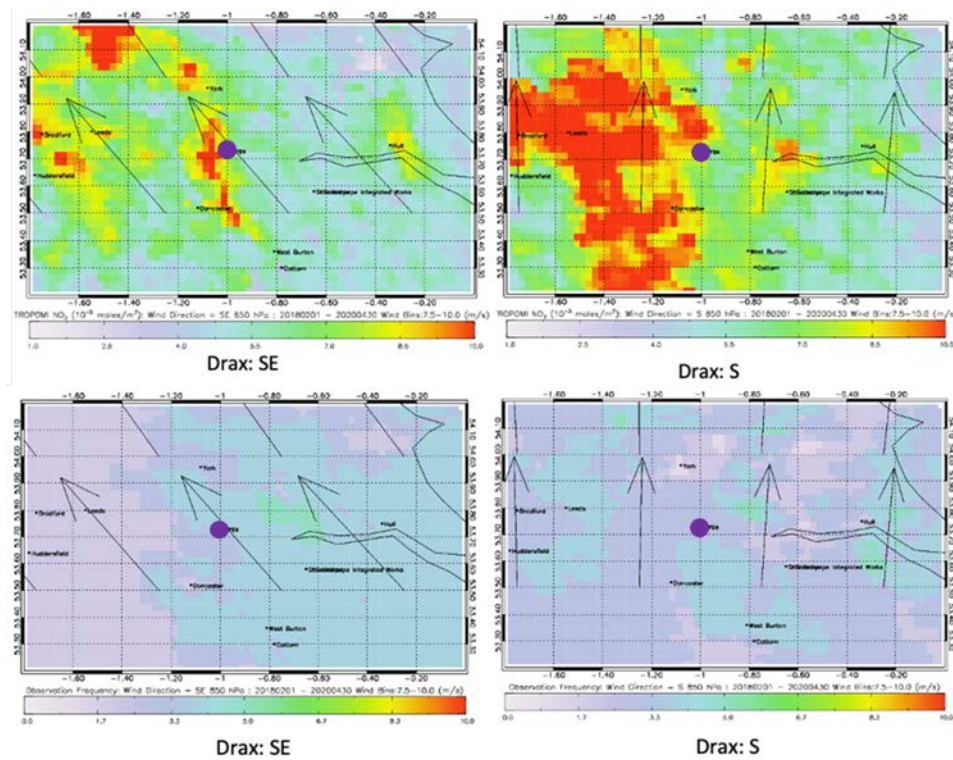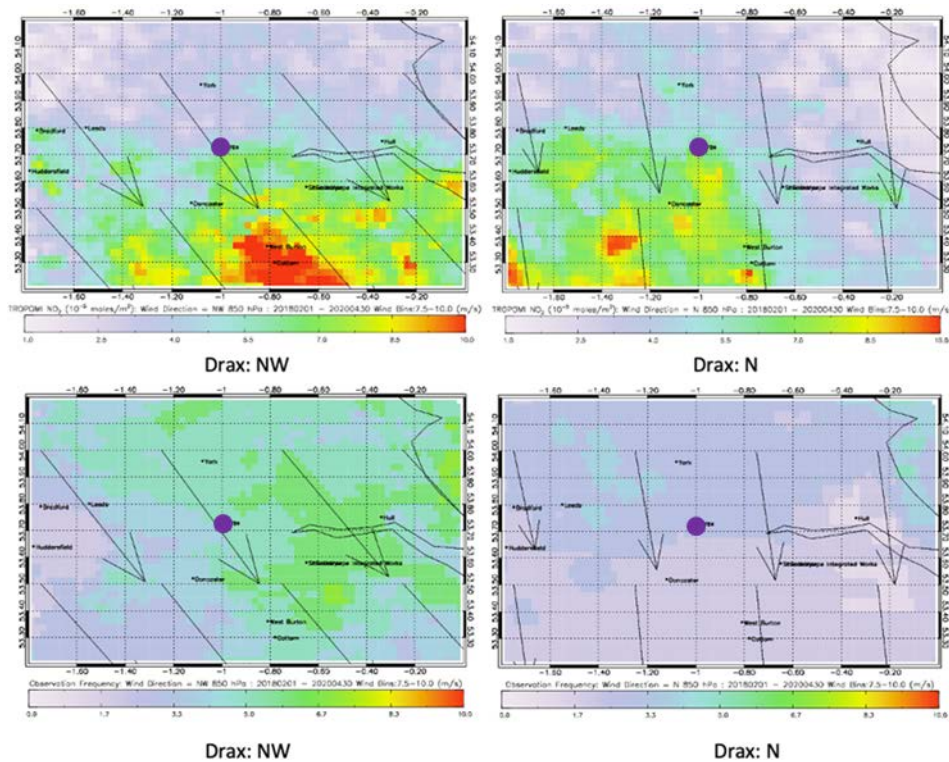**Figure 5.35. As Figure 5.20, but with wind direction categories NW & N indicated beneath each image, wind speed category 7.5 - 10.0 m.s^{-1}. Extent of top colour scale is 1x10^{-5} - 10x10^{-5} mol.m^{-2}; mean wind direction is indicated by the arrows. Extent of bottom colour scale is 0 - 10 observations.**

Quantification of plumes: derivation of emissions

Previous studies (*e.g.* Beirle *et al.* 2011) have used satellite observations to derive top-down emission estimates of NO$_x$. While the full non-linear Gaussian approach used by Beirle *et al.* (2011) could not be developed for use in the case study due to time restrictions, a simpler approach was however utilised in this work.

By taking a cross-section of the plume under certain wind directions (*i.e.* aligning the cross-section along the wind direction downwind of the source) and comparing against the background, it should be possible to quantify the amount of excess NO$_2$ attributable to the source of interest. This is in theory achievable for all wind directions as long as there is sufficient satellite data to obtain a realistic downwind NO$_2$ profile, but for simplicity we focused on the N, E, S and W wind directions – this did not require the production of new code to rotate the grid to align with the wind direction.

We determined the average downwind TCNO$_2$ profile and summed this from the source to the background level to obtain the excess NO$_2$ burden (in mol.m^{-2}). The aggregated mass of NO$_2$ was then multiplied by the width of the source and the distance downwind taken to reach background levels (giving the excess NO$_2$ burden in moles). Using knowledge of the average wind speed, it should then have been be possible to derive an emissions profile if the lateral transport of NO$_2$ out of the cross-section and chemical losses were also to be accounted for.

In this work, tests were performed on plumes from Drax. It was however found that even for this largest point source, the lack of a clear downwind plume cross-section meant that the application of this method was ultimately unsuccessful.

This method has however been successfully applied to UK NO_2 TROPOMI data to determining the NO_2 emissions flux from London over a 14 month period under westerly wind conditions. (Kelly, 2019). In the future, with a longer TROPOMI time-series, a cleaner downwind NO_2 plume from Drax or other large NO_2 point sources may be more distinguishable, enabling an emissions flux to be derived.

Potential validation of Environment Agency modelling tools

Although this report has focussed on source detection, satellite observations of air pollution also have the potential to evaluate air quality models and tools. For instance, the Met Office run the Air Quality in Unified Model (AQUM) to provide Defra with national air quality forecasts. As this regional atmospheric chemistry model represents the full atmosphere, satellite observations have previously been used to evaluate the performance of the model for simulating specific pollutants. Pope *et al.* (2015) used OMI $TCNO_2$ measurements to identify wintertime positive biases in the model, which were later linked to missing N_2O_5 heterogeneous chemistry (*i.e.* an NO_x sink) in the model.

As the Environment Agency use air quality models with some vertical information, satellite observations could therefore potentially be utilised to evaluate the output. For instance, the Environment Agency use ADMS (Atmospheric Dispersion Modelling System) and AERMOD to model plumes from point sources, and satellite $TCNO_2$ measurements could potentially be used to quantify the large-scale spatial structure of the plumes from NO_2 sources. Secondly, using the assumption that the plume represents the dominant NO_2 source in the column, validation of the absolute quantities might be possible by comparing the satellite tropospheric column measurements with the sub-columns generated from the plume model. Though such comparisons would require certain assumptions and careful development, this is potentially a topic for future consideration when utilising satellite data for monitoring purposes.

5.4   Conclusions and suggestions for future work

5.4.1   Conclusions

We have investigated whether measurements of NO_2 from TROPOMI can be used to identify large regulated sources of NO_2 emissions in the UK.

Specifically, we have addressed the following questions:

- Can TROPOMI identify above-background NO_2 emissions from large regulated sources in the UK?

- Can directional plumes of NO_2 be from these sources be observed and quantified under specific wind-directional or wind-directional and wind-speed conditions?

- Can TROPOMI NO_2 data be used in regulatory activities?

Using data from the first 27 months of TROPOMI measurements, we focussed on identifying emissions from three of the largest NO_x point sources in the UK: Drax (Yorkshire, England), Port Talbot (South Wales) and Grangemouth (Central Scotland).

To investigate the first of the above questions, stage 1 of the case study used the whole dataset (without any conditional aggregation) and subsets of different time periods. Clear above-background $TCNO_2$ signals were observed around all three sources when using all 27 months of TROPOMI data. In fact, elevated $TCNO_2$ signals could also be observed using some (but not all) three month seasonal datasets. Little evidence of elevated $TCNO_2$ signals was seen for time periods shorter than three months.

The relative strength of the $TCNO_2$ signals from each source was found to correspond to the size order of their NO_x emissions, i.e. Drax > Port Talbot > Grangemouth. The Port Talbot $TCNO_2$ signals were however clearest above background due to there being fewer nearby large NO_2 sources in the region around Port Talbot than in the region around Drax. These datasets did not however reveal any clear directional NO_2 'plumes' for any of the point sources.

We then investigated the second of the above questions. Evidence of NO_2 plumes were found in stage 2 of the case study, where we employed wind-directional conditional aggregation. It was found that six months of wind-directional conditionally aggregated data were in general required to visually identify plumes of NO_2 from Drax (the largest UK NO_2 point source). Fewer plumes were identified when using only three months of data as the sparsity of data (*i.e.* the low number of valid observations) became a significant issue. For the Port Talbot point source, some evidence of NO_2 plumes could also be observed from some wind directions when using six months of data; when three months of data were used, distinct plumes were much less common category. Investigation of the Grangemouth point source revealed very little evidence of NO_2 plumes for any wind direction, even when 27 months of data was used.

Stage 3 of the case study used wind-directional and wind-speed conditional aggregation. Despite the relative small number of valid measurements in each dataset, plumes (or potential plumes) of NO_2 from Drax were observed for most wind directions for three of the wind speed categories investigated: 2.5 - 5.0 $m.s^{-1}$, 5.0 - 7.5 $m.s^{-1}$ and 7.5 - 10.0 $m.s^{-1}$. Distinct plumes were not however be identified when using the 0 - 2.5 $m.s^{-1}$ wind speed category. Similar results were obtained for Port Talbot and, to a lesser extent Grangemouth, where fewest plumes were observed. A brief investigation to attempt to derive the emissions contributing to the plumes from Drax was carried out but was unsuccessful due to the lack of a clear downwind plume cross-section.

In summary, and with reference to the stated aims of the case study (see Section 5.1.3), we have found that TROPOMI is able to identify above-background NO_2 emissions from major industrial sources in the UK, and that these emissions can be identified using as little as three months of TROPOMI data. Plumes of NO_2 were observed from the largest sources under specific wind-directional or wind-directional and wind-speed conditions, but in this brief case study we have not been able to quantify the NO_2 emissions contributing to these plumes.

Although we have observed plumes of NO_2 from large sources, a number of issues currently prevent TROPOMI data alone being used in the Environment Agency's regulatory activities, most importantly the sparse time coverage of the dataset: less than one measurement per day is typically recorded over the UK when data losses caused by *e.g.* cloud cover are taken into account. The planned launch of the geostationary Sentinel-4 instrument in 2023 will however provide hourly measurements of NO_2 over the UK and therefore a step-change in potential applicability (despite the pixel size of UK Sentinel-4 NO_2 measurements being larger than that of TROPOMI measurements). There is also real potential for using TROPOMI and future satellite

data in combination with other data sources (e.g. ground-based instruments and sensors) to strengthen the Environment Agency's regulatory toolkit in the future.

5.4.2   Suggestions for future work

The limited timescale of this case study meant that we were unable to explore a number of opportunities to potentially fine-tune the method to increase the probability of observing clear plumes and signals of NO_2. These include:

- Exploring different date ranges when using shorter time series of data (*e.g.* all, rather than selected, periods of six months and three month) to fully investigate seasonal and annual variations.

- Using wind data taking at altitudes closer to the levels at which plumes disperse

- Using different combinations of wind speeds (for example all winds above 2.5 m.s^{-1}) to potentially enhance the observed plumes.

- Using wind-directional rotation to 'sharpen' the NO_2 plumes.

- Establishing and implementing more complex methods to derive the NO_2 emissions resulting in the observed plumes, for example those used by Beirle *et al.* (2011, 2019).

Measurements of $TCNO_2$ from TROPOMI may also be used to validate air quality models used by the Environment Agency to model plumes of NO_2 from point sources (see Section 5.3.4). Similarly, atmospheric dispersion models could be used to optimise the selection of satellite data, and to facilitate subsequent interpretation of that data e.g. interpretation in terms of source emission rates.

6　Case study C: Methane / TROPOMI

6.1　Introduction

6.1.1　Background

Climate change is one of the greatest threats to people and the environment. It is having, and will continue to have, far-reaching effects on economies and societies, and major impacts on habitats and species. Anthropogenic emissions of greenhouse gases are the main contributor to climate change.

The UK has domestic targets for reducing greenhouse gases under the Climate Change Act 2008 (Legislation 2008), which initially committed the UK to a reduction in greenhouse gas emissions to at least a 1990 baseline by 2050. The Act was subsequently amended in 2019 to a 'net zero' target (*i.e.* a 100% reduction in its net emissions from the baseline) by 2050. In the UK, emissions of the basket of the seven greenhouses gases covered by the Kyoto Protocol (carbon dioxide, methane, nitrous oxide, hydrofluorocarbons, perfluorocarbons, sulphur hexafluoride and nitrogen trifluoride) fell from 43% between 1990 and 2018 to an estimated 452 $MtCO_2e$ (Department for Business, Energy & Industrial Strategy 2020a).

This report focusses on the measurement of methane, which has a global warming potential around 28 times greater than carbon dioxide on a 100-year timescale (Myhre *et al*. 2013) so even small decreases in methane can have significant benefits in terms of its contribution to climate change.

Total methane emissions in the UK in 2018 were 51.5 MtCO2e, 49% of which were emitted from agricultural process. Waste management activities were the next largest source of methane at 37%, with landfills specifically being responsible for 28% of UK methane emissions (Department for Business, Energy & Industrial Strategy 2020a). Emissions of methane from landfills have decreased by 77% in the last 20 years and by 56% in the last 10 years. This decrease has been largely a result of the introduction of the Landfill Tax and the Landfill Directive (Council of the European Communities 1999; Environment Agency 2010a), which have diverted biodegradable waste away from landfill and has led to a reduction in the number of operational sites.

6.1.2　Regulation and measurement of methane emissions from landfills

In 2018, landfills contributed 28% of all UK methane emissions (Department for Business, Energy & Industrial Strategy 2020a): 14.4 $MtCO_2e$ of methane was emitted from landfills, equivalent to 3.2% of all UK greenhouse gas emissions (calculated on a $MtCO_2e$ basis). The Environment Agency regulates landfill methane emissions through environmental permitting requirements on landfill gas management systems (Environment Agency 2014). The standards for landfill gas management systems are set out in Environment Agency guidance (Environment Agency 2004) and in an Industry Code of Practice for the management of landfill gas (Environmental Services Association 2020).

Reporting of emissions from landfills is based on the MELMod landfill gas generation model (Eunomia Research & Consulting 2011) using input parameters such as the

amount and composition of waste going to landfill, rather than measurement of the total (flux of) methane emissions from the landfill sites. The current Environment Agency guidance on surface emissions (Environment Agency 2010b) relates to measurements of methane in flux containers, but the small spatial coverage of these measurements is likely to result in errors in the determined total flux due to inhomogeneity in emissions across the landfill (Börjesson *et al.* 2000).

Candidate methods for more accurate measurement of methane flux include:

- Eddy covariance, which determines the exchange rate of methane within the soil to at or above landfill soils using a micrometeorological approach (Schroth *et al.* 2012). The accuracy of eddy covariance-derived fluxes can be however limited by the complex topography often found at landfill sites, which can perturb flow characteristics.

- DIAL (differential absorption lidar) (Innocenti *et al.* 2017), which determines emissions fluxes by scanning a laser beam through the atmosphere to build up a methane concentration map, and combining this with measurements of the wind speed and direction.

- Tracer gas dispersion techniques (Mønster *et al.* 2015), where a tracer gas such as nitrous oxide or acetylene is released at a landfill and the ratio of methane and tracer gas measured simultaneously, for example using Fourier transform infrared spectroscopy or cavity-ring down spectroscopy. The methane emission rate is then calculated using knowledge of the release rate of the tracer gas.

- Combining *in situ* FTIR spectroscopy measurements downwind of a landfill with computational fluid dynamics modelling (Sonderfeld *et al.* 2017).

- Aerial measurement techniques using unmanned aerial system (UAS), which take measurements of the concentration of methane through and outside of the downwind plume using a sampling tube connected to a ground-based greenhouse gas analyser (or inferred from a UAS-mounted CO_2 sensor). These measurements are then interpolated to give a methane cross section and integrated and combined with wind vectors to determine the methane flux (Allen *et al.* 2019).

6.1.3 Measurement of methane emissions by satellite instruments

Atmospheric methane can be measured by satellite instruments by observing methane absorption bands in the SWIR spectral range at 1.6 and 2.3 μm of reflected and backscattered sunlight. Sunlight in the SWIR is impacted by gaseous absorption and scattering by aerosol particles which will impact the light path. If not corrected for, this light-path modification will introduce large biases in the retrieved methane columns. As these measurements depend on sunlight being reflected from the Earth's surface, these passive remote sensing methods cannot be performed when there is cloud cover.

So-called full-physics retrieval approaches attempt to model the radiative impact of aerosol scattering using information on atmospheric aerosols extracted from a near-infrared O_2 band (*e.g.* Boesch *et al.* 2011). To avoid biases from uncertainties in the treatment of aerosols and thin clouds, strict filtering is applied to remove scenes with moderate to high aerosol loadings. An alternative method is the so-called 'CO$_2$ proxy method' which use spectrally-close CH_4 and CO_2 absorption bands so that aerosol effects cancel out in the retrieved CH_4:CO_2 ratio. The methane column is then obtained

by combining the ratio with modeled CO_2 (Parker *et al.* 2015). This method results in enhanced coverage compared to full-physics methods, specifically polluted areas. In contrast to the full-physics method where aerosols are the main reason for retrieval biases, it is primarily uncertainties in modeled CO_2 that can introduce biases in the retrieved proxy methane columns.

Satellite methane column data has been available since 2002 from the SCIAMACHY instrument on the Envisat (Environmental Satellite) satellite, which was followed by the first dedicated greenhouse gas sensor GOSAT launched in 2009. These satellites have allowed the creation of a long-term, climate dataset on the global distribution of methane that informs on sources and sink on sub-continental scale. This SCIAMACHY and GOSAT data record forms one of the fundamental ECV datasets of the ESA Greenhouse Gas Climate Change Initiative GHG-CCI and Copernicus C3S programs (Buchwitz *et al.* 2015).

The global nature of methane, combined with its importance as a greenhouse gas has led to a series of science investigations into global methane cycle and budget (e.g. Bloom *et al.* 2010, Pandey *et al.* 2017; Parker *et al.* 2018 and Ganesan *et al.* 2019).

It has also been demonstrated that satellite methane columns can provide information on methane emissions on a country and sub-country scale. For example, GOSAT data has been used to estimate methane emissions for India (Ganesan *et al.* 2017) and North America (Turner *et al.* 2015). Methane hotspot emissions from localised sources has also been investigated (Buchwitz *et al.* 2017 and Sheng *et al.* 2018) but SCIAMACHY and GOSAT have limited capabilities due to their coarse coverage, so that significant averaging is required.

The launch of Sentinel-5P satellite in 2017 with its TROPOMI instrument represents a step-change in methane monitoring from space, because it combines daily global coverage with high spatial resolution. This is particularly the case for point sources so that, for example, TROPOMI has already successfully been used to observe a range of sources including a gas well blowout in Ohio (Pandey *et al.* 2019), methane leakage from gas and oil petroleum production (de Gouw *et al.* 2020 and Schneising *et al.* 2020).

GHGSat, is a commercial satellite mission that is dedicated to methane point source detection with a spatial resolution of tens of metres over a target area of about 12 km x 12 km. It was first launched in 2006, and a second generation Iris (GHGSat-C1) instrument was launched in 2020. There are a number of successful plume detections from GHGSat, and GHGSat has been used in tandem with TROPOMI to identify and diagnose plumes from oil and gas operations (Varon *et al.* 2019) and more recently from landfills in Argentina and Pakistan (Maasakkers *et al.* 2020). GHGSat has also joined the ESA third party program and 5% of its data will be made available free of charge via ESA (European Space Agency 2020c). Future satellites such as EDF MethaneSat, Bluefield and Copernicus CO2M will further enhance the capabilities for monitoring methane plumes from space.

6.1.4   Aims and risks

This case study aimed to develop a capability at the Environment Agency to process TROPOMI L2 methane products to L3 products and use this to investigate whether:

- Emissions of methane from UK landfills could be observed (using oversampling and/or time-averaging if required)

- TROPOMI methane data be used in regulatory activities

At the commencement of the case study, we were fully aware that there was a real risk that TROPOMI would not be able to detect any emissions of methane from large sources in the UK & Ireland due to:

- The relative low methane emission from major sources in the UK & Ireland compared to other locations in the world. In 2017 (the latest year for which data is available), the largest methane source in UK & Ireland was the Calvert landfill site in Buckinghamshire, England, with emissions of 10.3 kt.y^{-1} (or 1,276 kg.h^{-1}) (European Pollutant Release and Transfer Register 2020). For comparison, the study by Varon *et al.* (2019) used TROPOMI and GHGSat-D satellite measurements to identify a methane release of 87.6 - 377 kt.y^{-1} (in >50% of observations), from a gas compressor station in Turkmenistan *i.e.* approximately eight to 37 times the emissions from the Calvert landfill site.

- The relatively low sensitivity of methane measurements from TROPOMI over the UK & Ireland.

- The relative low amount of valid data from TROPOMI in the UK & Ireland compared to other locations in the world due to the relatively high frequency of days with cloud cover.

However, we proceeded with the case study, as this gave a good overall balance of risk with the (lower risk) ammonia and nitrogen dioxide case studies. In addition, even if TROPOMI was not able to detect any emissions of methane from large sources, a significant amount of knowledge about methane products and their processing would be gained. This knowledge could then be applied to new and future satellite instruments for measuring methane, for example the Copernicus CO2M constellation of satellites, GHGSat-D and GHGSat-Claire satellites, the EDF MethaneSat satellite and Bluefield micro-satellites.

6.2　Method

6.2.1　The Sentinel-5P satellite and TROPOMI instrument

Information about the Sentinel-5P satellite and TROPOMI are provided in Section 5.2.2.

6.2.2　Data products

Dissemination of the official TROPOMI products produced by ESA is via the Copernicus Open Access Hub (European Space Agency 2020e). In addition to the official (operational) ESA products, third-party research products exist for a number of TROPOMI L2 geophysical parameters. For methane, other key L2 products are from:

- SRON (Netherlands Institute for Space Research), the same group who provided the algorithm for the current ESA operational product. The SRON development products are of high quality as they are improved versions of the operational product, and offer an insight into future operational products (Lorente *et al.* 2020).

- IUP (Institute of Environmental Physics, University of Bremen), the L2 data generated by this group was produced thorough the ESA Greenhouse Gas Climate Change Initiative (GHG-CCI). This dataset uses a different algorithm and also includes measurements over the ocean in areas of sun glint (Schneising *et al.* 2019).

While these datasets offer credible alternatives to the ESA operational product, their maintenance is not guaranteed to be continued in the same manner as the ESA product. Also, at the time of writing of this report (October 2020), the current version (14.14) of the SRON product was only available until March 2020 while the IUP product was available until December 2019. Additionally, documentation and user support for these other products is not as extensive as for the official ESA product.

This case study used the official ESA product, as the contingency and timeliness of this product release fulfilled the needs of this investigation and of any future studies that the Environment Agency might conduct with TROPOMI data products. A comparison of results from all three datasets is however shown in Figure 6.1 for reference, where we have verified results from the ESA operational product with those from the SRON and IUP products.
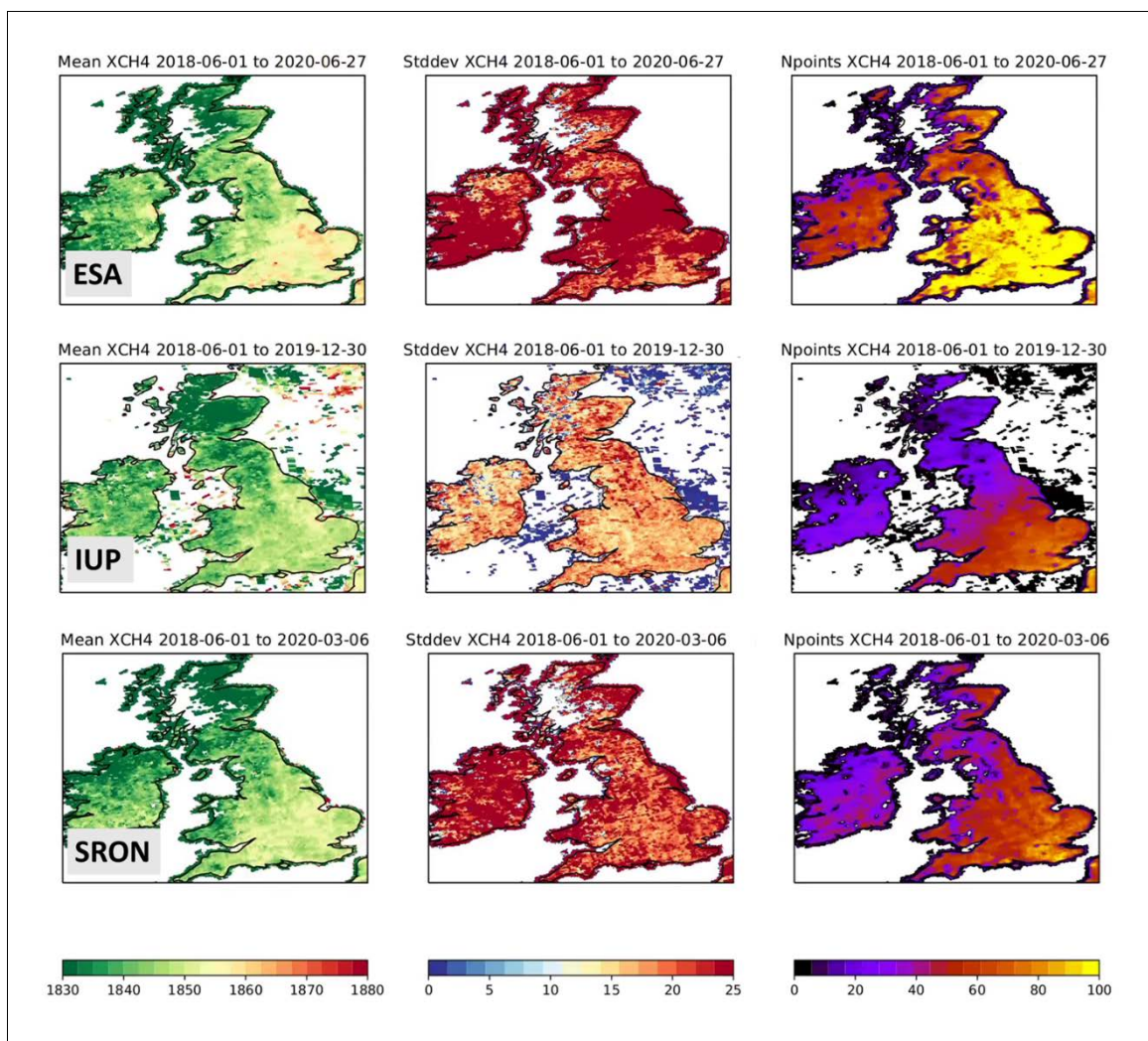
Figure 6.1 Comparative maps of TROPOMI column average amount fraction generated from three different L2 products (ESA, IUP and SRON) using the all data available between the period 01.06.2018 and 27.07.2020 (date based on ESA operation product on CEDA). Note only the operational ESA product spans the whole date range, the IUP product was only available to 31.12.2019 and the SRON L2 product to 06.03.2020. The left-hand column shows the average methane amount fractions in ppb averaged over the whole time series for each product, with the corresponding standard deviation shown in the middle column. The total number of TROPOMI pixels included in each plot is shown in the right-hand column.

6.2.3 Study area

Figure 6.2 displays the extent of the study area used in this case study. The area covers the whole of the UK and Ireland. The North-west coast of France is also included in this bounding box although in the final analysis this area was removed. The black square shown in Figure 6.2 was used as an input into an application programming interface (API) to define the geographical search extent for data products.
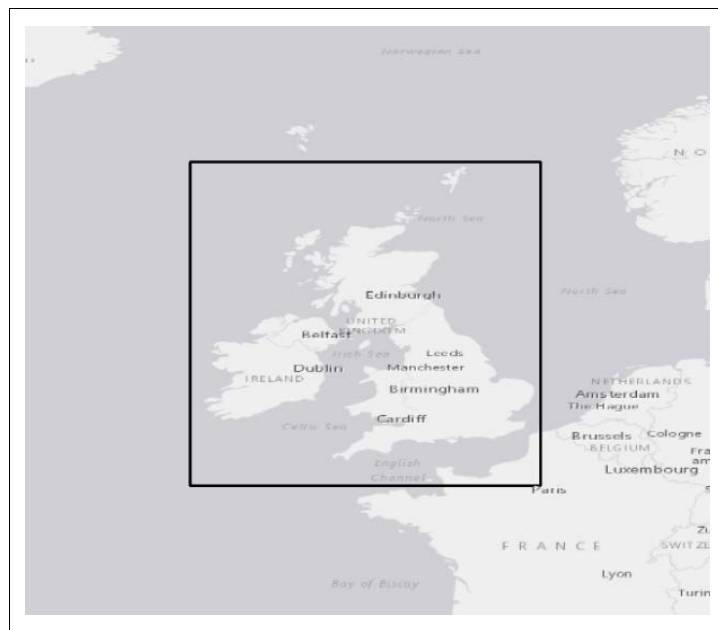
Figure 6.2 Extent of the study area.

6.2.4 Computer specification and environment settings

Data processing was first attempted using a standard Environment Agency Geomatics workstation (Intel Xeon E5-2680 @ 2.70 GHz – 8 cores, NVIDIA Quadro 4000 – 2GB DDR5), which was found to lack sufficient processing power. A higher specification workstation was then used with the specification below:

- CPU: Intel Xeon W-2295 @ 3.00 GHz (18 cores, 36 threads
- RAM (random access memory): 32 Gb

- GPU (graphics processing unit): NVIDIA Quadro RTX 5000 (16Gb GDDR6)

- Memory: Samsung SSD 860 Evo 2Tb

- Operating system: Windows 10

This workstation easily processed the TROPOMI products from L2 (at swath resolution to L3 (averaged and mapped onto a regular grid) and also completed other geo-processing tasks within ArcGIS Pro considerably faster than the standard Environment Agency Geomatics workstation. It is therefore recommended that a workstation of similar specification is used for any future work with TROPOMI data

The main Python packages used in this case study were:

- Packages installed within the python environment distributed with ArcGIS Pro 2.6

- Sentinelsat[11]

- HARP & Science [&] Technology[12]

.

6.2.5   Dataset processing methodology

Downloading TROPOMI Level 2 products

TROPOMI L2 methane products were downloaded by the Environment Agency directly from the Sentinel-5P pre-operational data access page on the Copernicus Open Access Hub (European Space Agency 2020e)[13]. Larger amounts of data were downloaded from the Copernicus Open Access API Hub[14] using the python package Sentinelsat.

All methane products which intersected the study area were downloaded for the period 04.05.2018 (the first date when TROPOMI data was available) to 30.06.2020, a total of 3,093 L2 methane files in NetCDF format.

Processing Level 2 products to Level 3 products

The ESA L2 TROPOMI data products are provided without a fixed spatial grid[15] - the pixels within the product are on an along-track grid defined by the pointing of the instrument. This makes the comparison, or combination, of multiple scenes very difficult as the exactly repeating overpasses only occur once every 16 days due to the sun-synchronous orbit of the satellite. This issue can be overcome through processing the datasets to a L3 data product where the geophysical variables are mapped onto a regularly defined spatial grid.

---

[11] https://sentinelsat.readthedocs.io/en/stable/install.html
[12] https://stcorp.github.io/harp/doc/html/install.html
[13] TROPOMI (and other EO) data products are also available at the CEDA resource (Centre for Environmental Data Analysis 2020).
[14] https://scihub.copernicus.eu/apihub/
[15] Note that ESA are planning to provide L2 products with a fixed grid in the future, but the timescales for these being available is uncertain. The availability of such products would eliminate the section of the pre-processing required to convert the data to analysis-ready level.

The HARP toolbox was used to process ESA L2 methane products into a L3 gridded product. HARP is a python library developed by Science [&] Technology Corporation to process a range of atmospheric Earth Observation datasets[16]. This library is recommended by the Research and User Support (RUS) branch of Copernicus (European Space Agency 2020h), which provide online training webinars focusing on how to use this Python library. A grid with a resolution of 0.01° x 0.01° (approximately 1 x 1 km over the area of interest (AOI)) was used in this case study.

The L2 methane products contain two versions of the main product: total column methane and total column methane bias corrected. In this case study we used the bias corrected version of the product as this corrects a bias which otherwise would result in increased methane amount fractions in areas with relatively low albedo and decreased methane amount fractions in areas with high albedo (Netherlands Institute for Space Research 2019).

We also applied data quality (QA) filters (Royal Netherlands Meteorological Institute 2017) when processing L2 products. We found that use of a QA > 0.5 filter (as recommended by ESA) removed a significant amount of the data over the study area, especially over coastal regions. We therefore proceeded by producing two sets of L3 products, one using a QA > 0.3 filter (to ensure full land coverage over the study area) and one using a QA > 0.5 (filter as recommended by ESA). The output L3 products were in the WGS (World Geodetic System) 84 coordinate system and output as NetCDF files.

Conversion of NetCDF files to TIFF images

To further analyse the L3 products, the data needed to be in a raster image format to be read into the geoprocessing tools (raster calculator) of ArcGIS Pro. This process involved generating a raster layer from the NetCDF file using the 'Make NetCDF Raster Layer' tool from the multidimensional geoprocessing toolbox. The resultant raster layer was then exported to a TIFF (tagged image file format) using the 'Copy Raster' tool from the Raster Dataset toolset. The workflow was automated to process the L3 datasets (both QA > 0.3 and QA > 0.5)

Producing average methane amount fractions

To calculate the average methane amount fractions from all valid measurements across the study period (04.05.2018 to 30.06.2020) the data was first transformed so that it could be processed within ArcGIS Pro.

The TIFFs produced for the L3 products were converted into a point shapefile. Here, the centre point of each pixel within the raster was converted to a point and attributed with the methane value of the pixel. This was performed using the 'Raster to Point' geoprocessing tool from the Conversion toolbox. Attributes such as the date of the measurement were also added to the points.

The point shapefile datasets (*e.g.* QA > 0.3 and QA > 0.5) were then merged into a singular point dataset using the 'Merge' tool from the 'Data Management Tools' geoprocessing toolbox. The resultant product was a singular file for each dataset that contained all valid measurements across the entire study period. This dataset was then spatially joined to the 0.01° x 0.01° grid (a replica of the one used in the L3 processing was created in ArcGIS as a polygon shapefile) using 'mean' as the join rule to derive an average value for each grid cell. The unweighted mean was calculated - it should also be noted that the uncertainty of each measurement was not used when producing

---

[16] http://stcorp.github.io/harp/doc/html/index.html#

any of the results reported in this report. Finally, data over north-west France were removed from the L3 product.

Use of Lamb weather types

A brief exploration of whether spatial patters of methane could be identified when measurements obtained under similar wind conditions were combined (i.e. wind-conditional aggregation), was undertaken. Further information about Lamb weather types is given in Section 4.2.5

6.3   Results and discussions

6.3.1   Quality assurance of Environment Agency Level 3 products

NCEO (University of Leicester) carried out an independent validation of methane L3 data products produced by the Environment Agency

TROPOMI data from the time period 01.06.18 – 30.06.20 was initially chosen for this exercise. A comparison of the L3 products produced by each organisation revealed some differences around the edges of pixels and at coastal areas. These artefacts were determined to be respectively due to (1) minor differences in the gridding methods used the Environment Agency and NCEO (the approach used by NCEO resulted in slightly smaller grid boxes those produced by the Environment Agency), and (2) the use of slightly different versions of the L2 methane product.

Despite this, the overall agreement between the Environment Agency and NCEO result was however still good: 0.76% of grid boxes showed absolute differences of > 30 ppb, which is approximately the level of bias in each ESA L2 product.

To further investigate the difference around coastal areas, L3 products were then generated from a more limited set of L2 products covering a period of one week: 01.06.20 – 07.06.20. Both the Environment Agency and NCEO downloaded these files afresh to create a new archive, in order to negate any issues that may be caused by using differing data versions. The results from this comparison are shown in map form in Figure 6.3 and in histogram form in Figure 6.4.
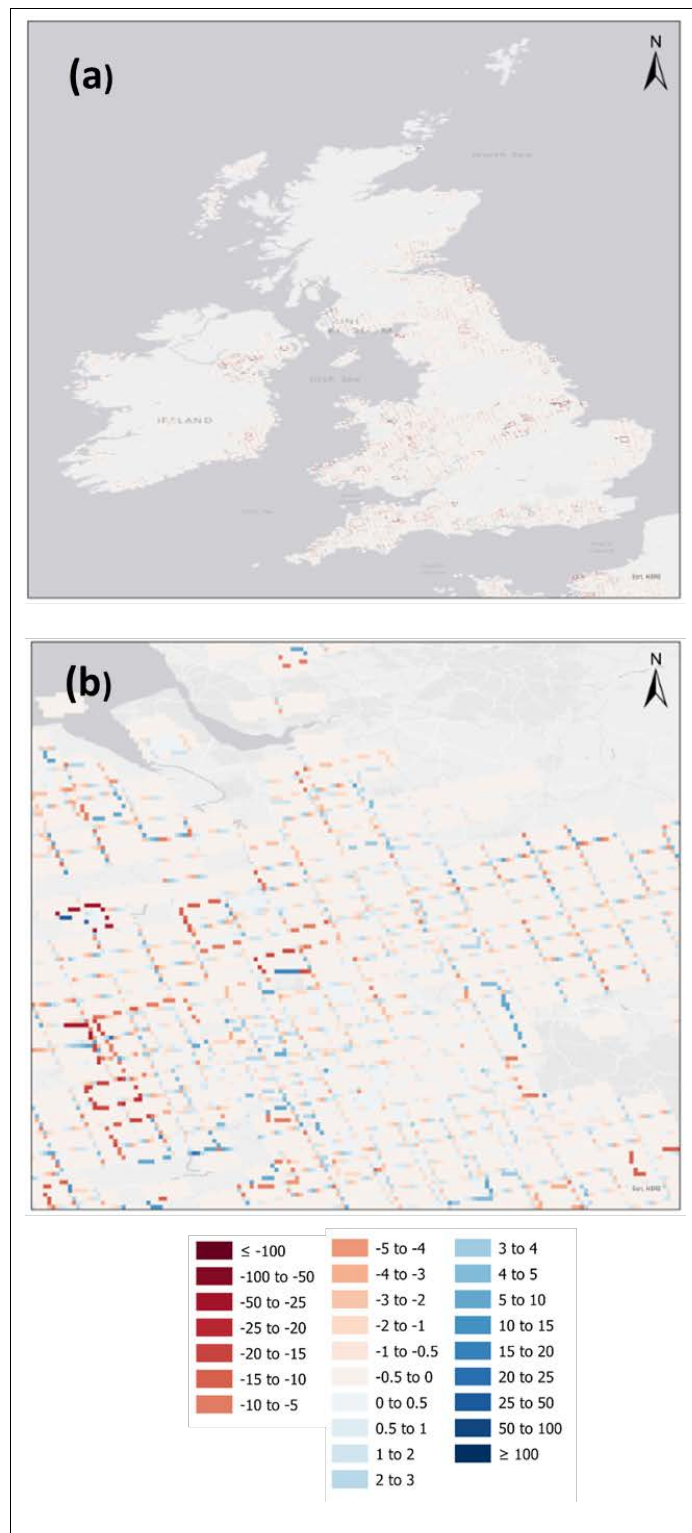
Figure 6.3 (a) Differences in methane column amount fractions (in parts-per-billion) determined over the UK & Ireland by the Environment Agency and NCEO. Data generated using v1.3 of the bias-corrected ESA L2 TROPOMI methane product for the period 01.06.20 – 07.06.20 with an oversampled grid box size of 0.01° x 0.01° and a QA > 0.3 filter. The same coastline mask was applied to both the Environment Agency and NCEO datasets. (b) shows an expansion of the area covering the West Midlands of England, Northern England and north and west Wales.
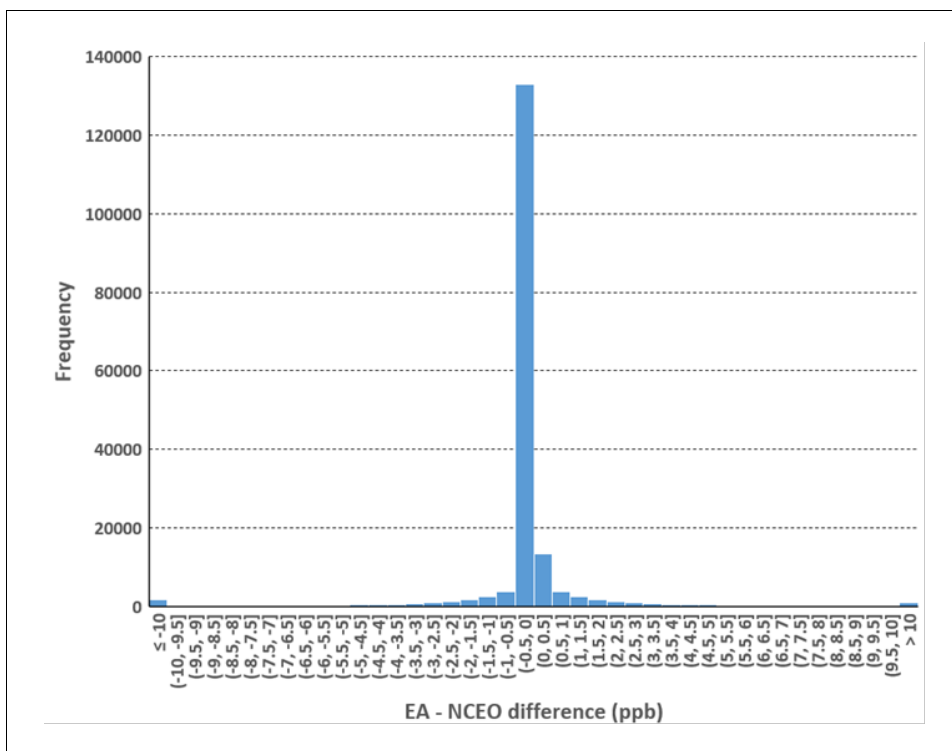
Figure 6.4 Data in Figure 6.3 (a) plotted in histogram form.

The differences in coastal areas are not present in Figure 6.3, confirming that these differences originally resulted from non-identical versions of the ESA product being used.

An excellent agreement between the Environment Agency and NCEO results was therefore now observed, with only 0.12% of grid boxes showing absolute differences of > 30 ppb, which is approximately the level of the bias in each ESA L2 product (1.5% relative).

This confirms that the capability developed at the Environment Agency during this case study can replicate L3 products produced by NCEO to an appropriate extent, meaning that the capability is suitable for continued use and future further development.

6.3.2 UK & Ireland column methane amount fractions

Average column average dry air methane amount fractions (hereafter referred to as column methane amount fractions) were first determined for the whole of the UK & Ireland using all available TROPOMI data. These are shown in map form in Figure 6.5 (a) and (b), using all measurements with QA values > 0.3 and QA values > 0.5 being presented for comparison. The following observations can be made:

- Higher average mean column methane amount fractions are produced when using QA > 0.5 compared to when using QA > 0.3. This may be an effect of the cloud masking applied, meaning that only the QA > 0.5 data might truly be seeing the surface

- A pattern in increasing mean column methane amount fractions towards the south-east of England is present. This pattern, which is not reflected by emissions data in the National Atmospheric Emissions Inventory (Department for Business, Energy & Industrial Strategy 2020b) may be an artefact of seasonal sampling bias (there are many more valid measurements in the south easterly regions compared to north westerly regions) and/or biases in the ESA product used. It may also be an effect of the typically lower wind speeds in the south-east of the UK, which would likely result in higher column methane amount fractions

- Some land areas of the UK have measured mean column methane amount fractions that are clearly lower that the surrounding areas, for example Thetford Forest (East Anglia), New Forest (Hampshire) and part of the South Downs. This effect is likely to be due to the albedo bias correction used in v2.1.2 of the ESA methane product needing further refinement: Figure 6.1 shows that this effect is not observed in the IUP and SRON products.

- Coastal areas typically report lower mean column methane amount fractions than inland areas (QA > 0.3) or have no valid measurements (QA > 0.5) This is due to the variability in terrain/surface types, and pixels containing water surfaces which appear very dark in the shortwave infrared (low signal).

- Large areas of the west of Scotland have no valid measurements over the entire 26 month period even when using the QA > 0.3 filter. This indicates that TROPOMI is unlikely to be a useful tool to measure methane at these northerly latitudes.

Figure 6.5 (c) and (d) show the number of valid measurements used to produce the mean column amount fractions for the 26-month period studied, and clearly show the significant losses of data due to filtering and other effects, for example instrument maintenance and outages. Figure 6.6 shows the same data in histogram format.

For the QA > 0.3 dataset, the maximum number of valid measurements in any grid box was 169 (23% of theoretical available data assuming a single measurement per day) and the mean number of valid measurements was 67 (9.1%). For the QA > 0.5 dataset, the number of valid measurements is even smaller: a maximum of 76 (10%) and a mean of 20 (2.7%). Because of these very small numbers of valid measurements, drawing any firm conclusions from the calculated annual mean column amount fraction is likely to be very difficult as the valid measurements are likely to sample a non-representative sub-section of the calendar year.

Following this initial generation of UK & Ireland data, it was decided to use a QA > 0.3 filter for the remainder of the investigation. Although this approach introduces some lower quality data than using a QA > 0.5 filter, it results in a more comprehensive spatial coverage over the UK.
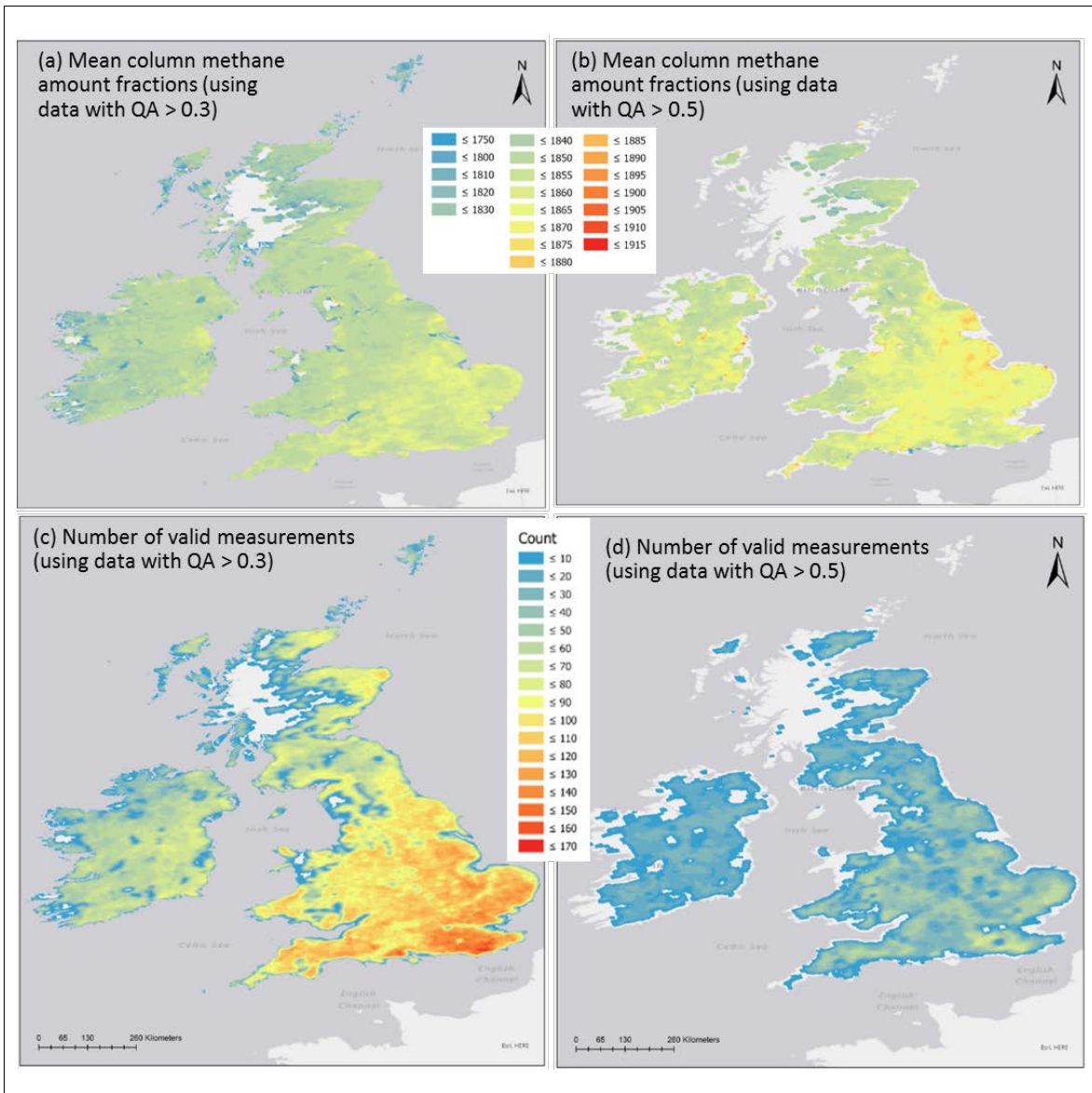
Figure 6.5 (a) and (b) show mean methane column amount fractions (in parts-per-billion) over the UK & Ireland using v2.1.2 of the bias-corrected ESA L2 TROPOMI methane product for the period 04.05.18 – 30.06.20 using an oversampled grid size of 0.01° x 0.01° and the QA filter indicated by the caption. (c) and (d) show the number of valid measurements used to compile the mean column amount fractions (using the same criteria as (a) and (b)).
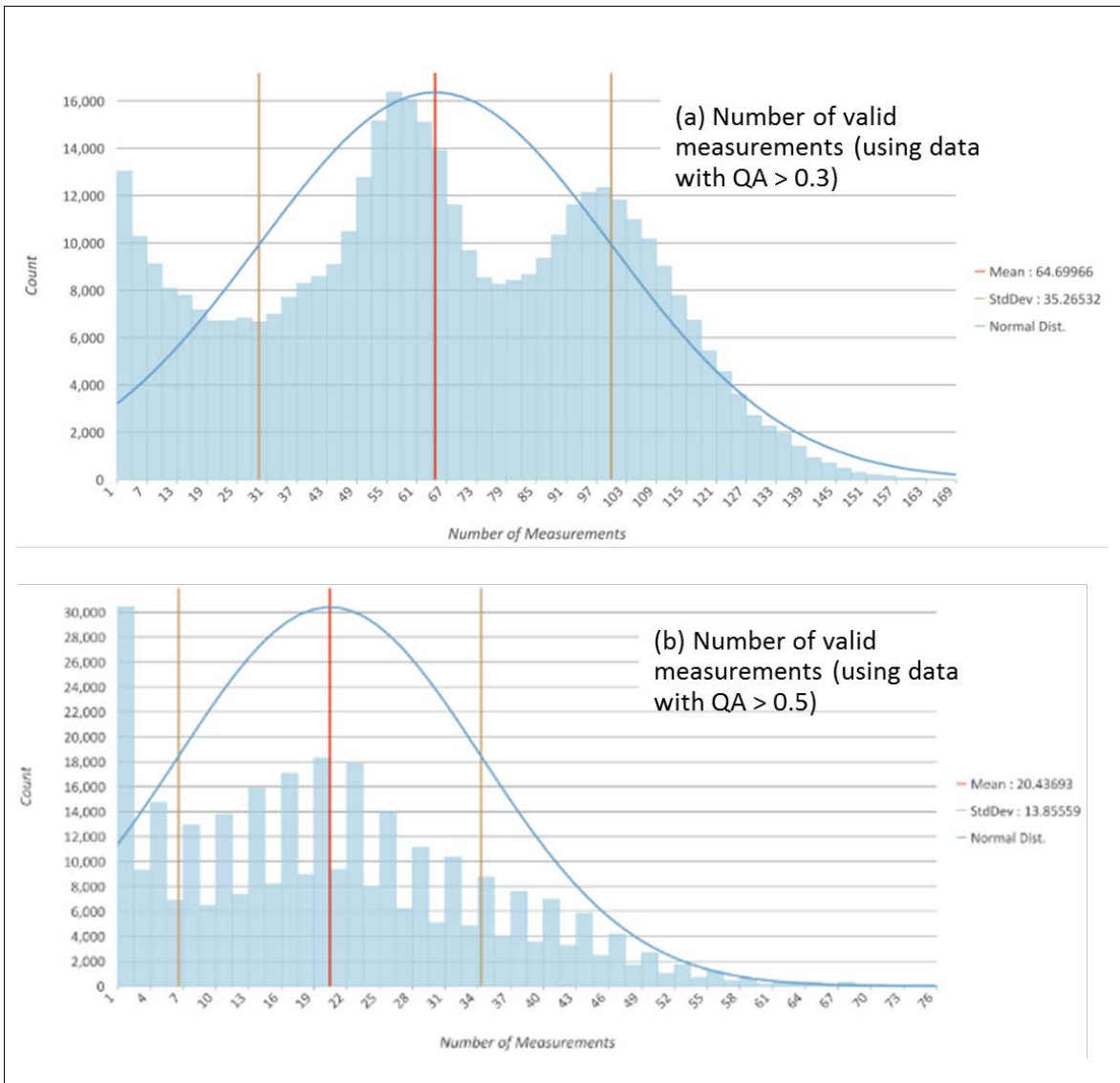
Figure 6.6 Data in Figure 6.5 (c) and (d) plotted as histograms. The x-axis shows the number of valid measurements in a grid box; the y-axis shows the number of grid boxes contaning that number of valid measurements.

Seasonal mean methane column amount fractions over the UK and Ireland were also determined using the meteorological seasons of Spring (March - May), Summer (June - August), Autumn (September - November) and Winter (December - February). The resulting four seasonal average maps are shown in Figure 6.7.
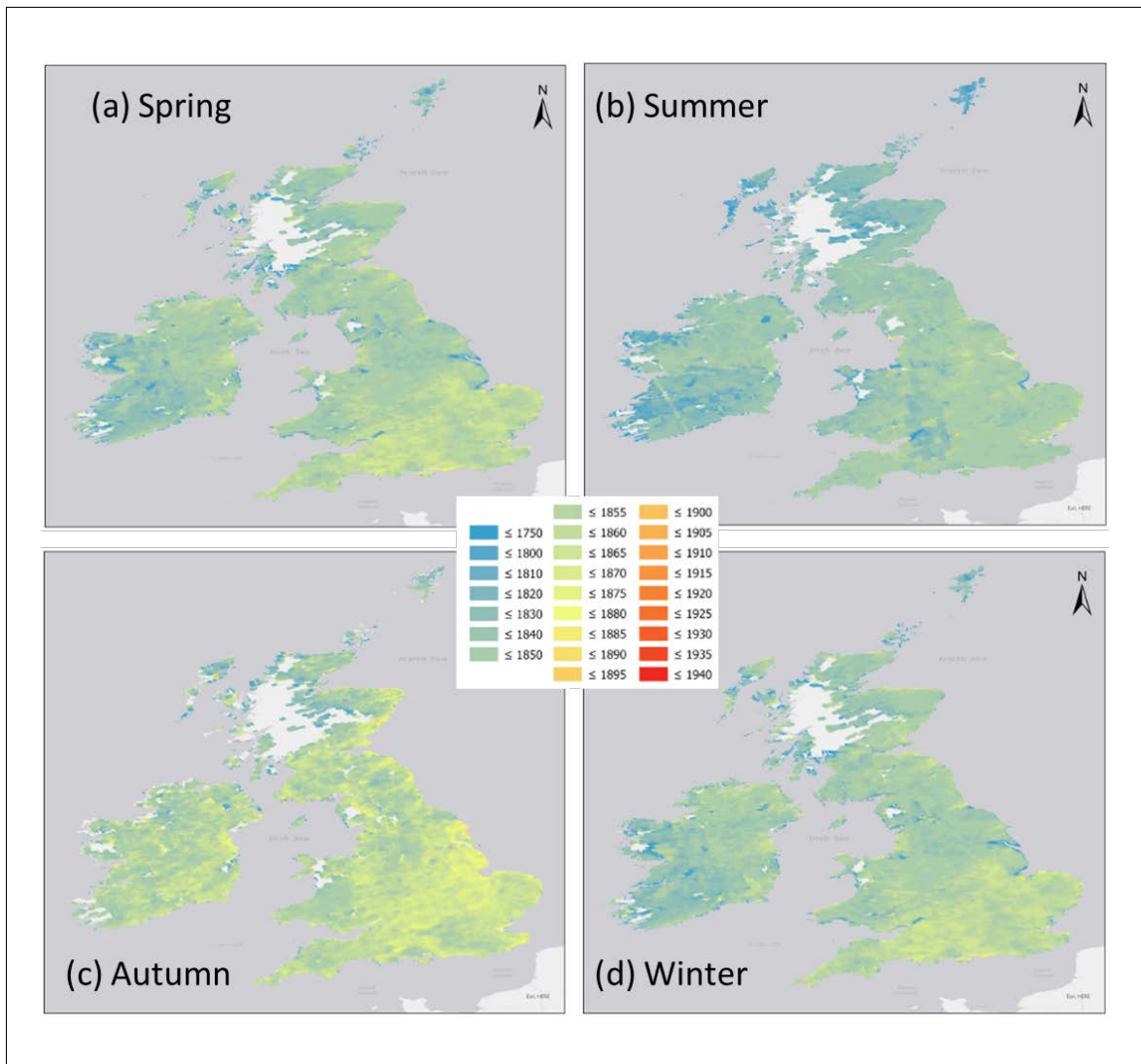

Figure 6.7. Mean seasonal methane column amount fractions (in in ppb over the UK & Ireland using v2.1.2 of the bias-corrected ESA L2 TROPOMI methane product for the period 04.05.18 – 30.06.20 using an oversampled grid size of 0.01° x 0.01° and a QA > 0.3 filter. Results shown for the meteorological seasons of (a) Spring, (b) Summer, (c) Autumn and (d) Winter.

By visual inspection of Figure 6.7, the highest methane column amount fractions over the UK are in Autumn (followed closely by Winter), and the lowest in the Summer. The observation of low methane column amount fractions in the Summer in line with data obtained from the Mace Head background monitoring sites, where the lowest average methane amount fractions are also recorded in the Summer. (It should however be note that at Mace Head, the average methane amount fractions recorded in Spring, Autumn are Winter are broadly similar to each other).

124

6.3.3   Investigation of large sources of methane

Selection of sources to investigate

For the purposes of this case study, we used a UK & Ireland-wide approach, rather than focussing on those sources in England which are regulated by the Environment Agency. Details of the largest methane emitters in UK & Ireland were obtained from the European Pollutant and Transfer Register (E-PRTR) (European Pollutant and Transfer Register 2020) and the NAEI (Department for Business, Energy & Industrial Strategy 2020b) for 2017, the most recent year for which data was available at the time. It should be noted that NAEI contains data for very few landfills sites, as the NAEI treats these as area sources, not point sources, so all landfill data used were taken from the E-PRTR. Pre-publication data for 2018 for Ireland only were obtained directly from the Environmental Protection Agency (Ireland).

The largest 10 sources of methane in UK are shown in Table 6.1, along with the largest methane source for Northern Ireland and Ireland (which are ranked 11th and 14th respectively in the UK & Ireland). As mentioned in Section 6.1.4, even the largest methane source in the UK & Ireland emits a relatively small amount of methane compared to sources found elsewhere in the world.

Table 6.1   The largest 10 sources of methane in the UK with the largest sources in Ireland (rank 11) and Northern Ireland (rank 14). Data for England, Scotland, Wales and Northern Ireland is for 2017; data for Ireland is for 2018.

UK & Ire rank	Site	Longitude	Latitude	Country	Methane emissions (kg.h^{-1})
1	Calvert landfill site	-1.0014	51.9159	England	1176
2	Welbeck landfill site	-1.4542	53.6940	England	946
3	Mucking landfill site	0.4292	51.5037	England	870
4	St. Fergus area[1]	-1.8410	57.579	Scotland	583
5	Bryn Pica landfill site	-3.4366	51.7379	Wales	538
6	Arpley landfill site	-2.6432	53.3718	England	433
7	Skelton Grange landfill site	-1.4508	53.7678	England	425
8	Brogborough landfill site	-0.5855	52.0481	England	392
9	Pitsea landfill site	0.5057	51.5560	England	353
10	Drax power station	-0.9904	53.7324	England	349
11	Kinsale Road landfill site	-8.4608	51.8781	Ireland	346
14	Mullaghglass landfill site	-6.0722	54.5550	N. Ireland	328

[1] Incorporates a number of point sources in the NAEI in close proximity in the St. Fergus area of Scotland.

The results presented in the remainder of this section focus on three landfill sites, the Calvert landfill site (rank 1 in Table 6.1) and the Welbeck and Skelton Grange landfill sites (rank 2 and rank 7 respectively) – these latter two landfill sites are in very close geographical proximity, These landfill sites were selected to develop and test the data processing method uses with the intention of applying these to other large methane sources if successful.

Use of TROPOMI to instigate methane emissions from landfill sites

Our investigations of large sources of methane have focussed on the largest to emitters in Table 6.1: Calvert and Welbeck landfill sites. The Skelton Grange landfill

site has also been included in some of the discussion below by nature of its close proximity to the Welbeck landfill site.

Figure 6.8 was produced using all valid measurements over the 26 month period from 04.05.18 - 30.06.20 and shows no obvious pattern of methane around the three landfill sites investiagted. To check that this was not an atefact of the colour scale selected, a 'stretched' colour scale was also applied – the results from this (which are not shown here) also provided no clear evidence of any enhanced methane column amount fractions around the landfill sites. A similarly non-conculsive result was obtained when QA > 0.5 data was used.
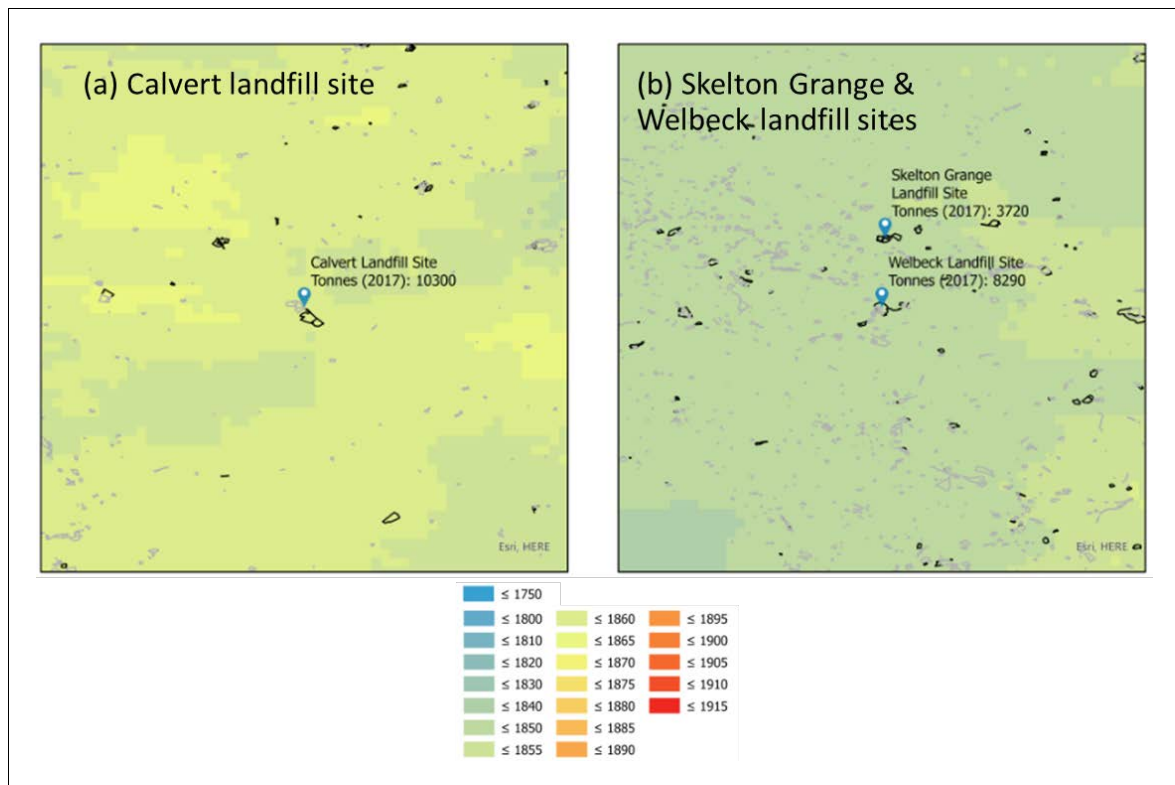
Figure 6.8 Mean methane column amount fractions (in ppb) over aread around (a) the Calvert landfill site, (b) the Skelton Grange and Welbeck landfil sites. Data generated using v2.1.2 of the bias-corrected ESA L2 TROPOMI methane product for the period 04.05.18 - 30.06.20 using an oversampled grid box size of 0.01° x 0.01° and a QA > 0.3 filter.

It was then investigated whether enhanced levels and/or plumes of methane could be identified around the Calvert landfill site when measurements obtained under similar wind conditions were combined (i.e. wind-conditional aggregation). Lamb weather were used to classify the synoptic meteorology over the UK for each day of TROPOMI observations. Each measurement was then aggregated into one of 10 groups representing each of the eight Lamb weather type directions (northerly, north-easterly, easterly, south-easterly, southerly, south-westerly, westerly and north-westerly), and the each of the anticyclonic and cyclonic weather types.

The mean methane column amount fractions determined for each Lamb weather type group are shown in Figure 6.9.

126
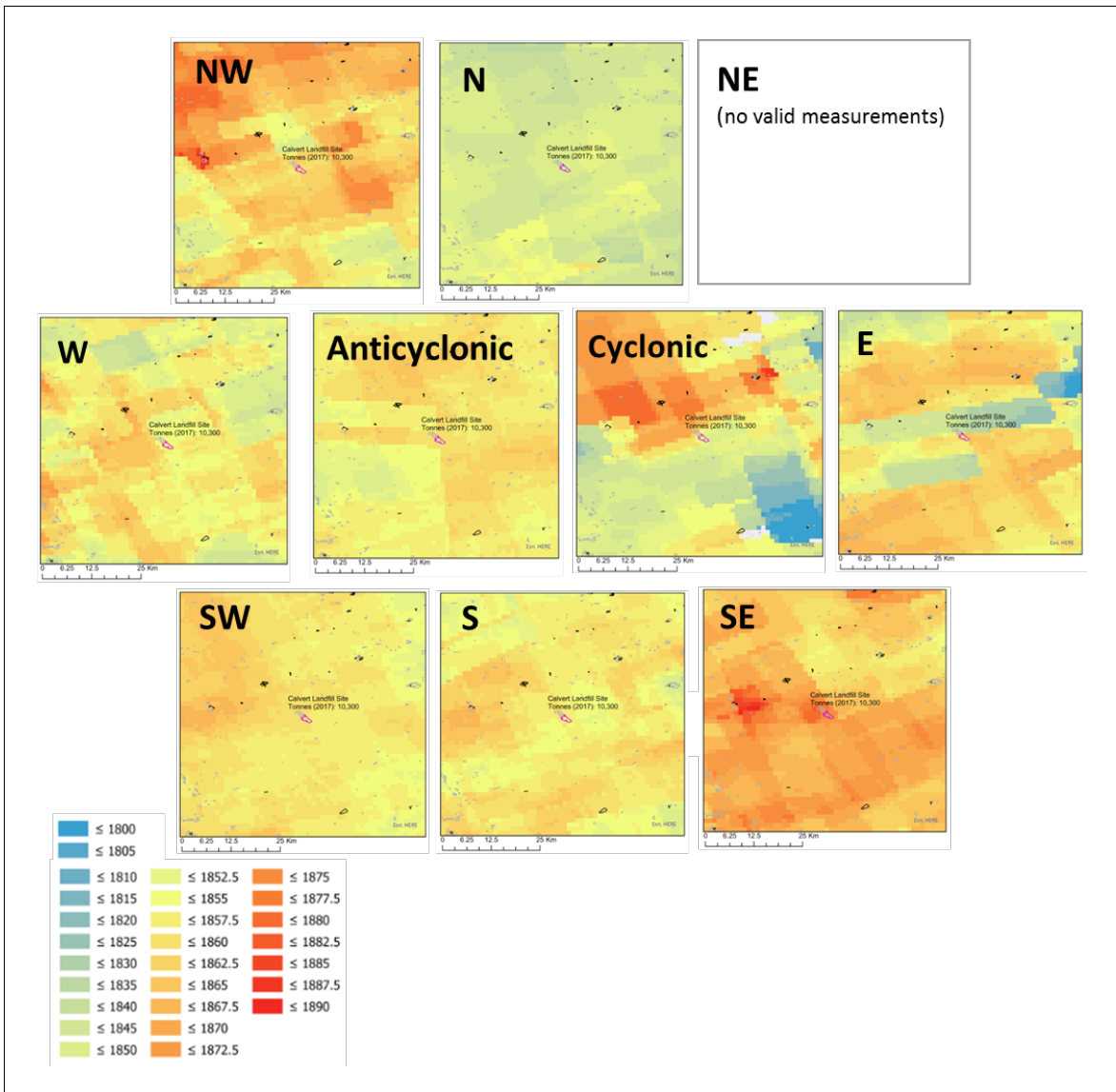
Figure 6.9 Mean methane column amount fractions (in ppb) over areas around the Calvert landfill site for each of the 10 Lamb weather type groups investiagted (stated in each image). Data generated using v2.1.2 of the bias-corrected ESA L2 TROPOMI methane product for the period 04.05.18 - 30.06.20 using an oversampled grid box size of 0.01° x 0.01° and a QA > 0.3 filter. No valid measurements were recorded for the NE Lamb weather type group.

Figure 6.9 also shows no clear methane enhancement or methane plumes around the landfill site. It is however worth emphasising that the number of measurements comprising each Lamb weather Type group is often small (hence the 'blocky' nature of some of the images) and even zero in the case of the NE Lamb Weather Type group). A more sophisticated approach for any future study would be to use the wind data directly associated with each measurement in the TROPOMI product.

The fact that any methane signal was not identified from the above studies above was not unexpected as methane enhancements related to the expected fluxes from UK landfills are small. Using the integrated mass enhancement approach as described in Varon *et al*. (2018), we can however estimate the expected methane anomalies for a given flux and wind speed. For a methane flux of 10 t.y^{-1} and a wind speed of 1.5 m.s^{-1}, we find an enhancement of 8 ppb (i.e. approximately 0.5 % above the background) for

a 7 km x 7 km ground pixel, which may be detectable from TROPOMI with further refinement to the method used. The results of some investigations to further refine the methane emission detection method are described below.

Refinements to the emissions detection method

The methods described up to this point average over the whole UK dataset or a subset selected based on prevailing wind classification. Another approach when studying smaller regions of interest is to only use overpasses which cover a significant fraction of the study area (e.g. > 70%). This approach provides a fairly homogenous coverage when averaging temporally (at the oversampled resolution), which can help distinguish between data artefacts and the surface emissions of interest. Here we focus purely on the Calvert landfill site, and in addition to filtering for overpass coverage, we also investigate other potential sources that can affect the calculated mean methane from TROPOMI.

We first looked at differences when considering Sentinel-5P swaths with 70% and 90% coverage of the study area. In addition to these filters, a correction based on surface altitude of 7 ppb.km^{-2} that takes into account the increasing influence of the stratosphere (Buchwitz *et al.* 2017) and the effect of averaging to a coarser 0.05° x 0.05° grid is also shown (Figure 6.10). The spatial averaging used here is a weighted mean approach where each 0.01° x 0.01° grid cell is given a weight based on the reciprocal of the total number of 0.01° x 0.01° grid cells within a TROPOMI pixel. At this point we also deviate from the ESA L2 operational product and instead used the SRON L2 research product covering the period 01.06.18 - 29.02.20. As previously mentioned, the SRON L2 research product is representative of the future ESA product releases: by making use of the potentially higher-performing product the results are more indicative of where future efforts by the Environment Agency will be needed.
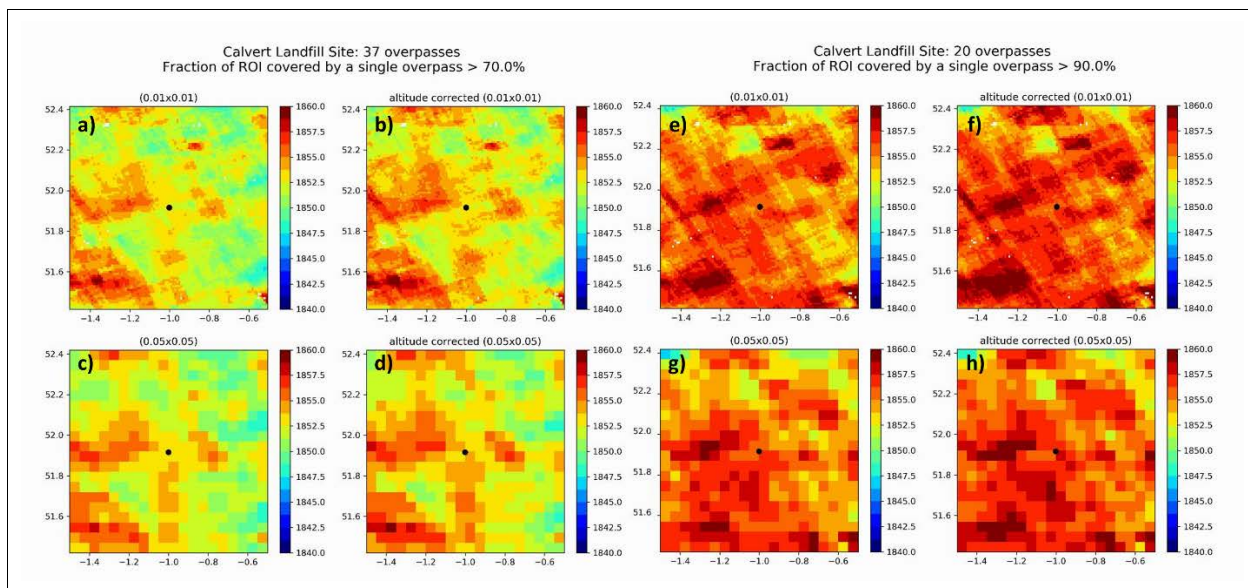
Figure 6.10 Spatial and temporal averaging over the Calvert landfill site using the SRON L2 product when the Sentinel-5P swath cover 70% or more (figures (a)-(d)) and 90% or more (figures (e)-(h)) of the study region. Data generated using v14.14 of the bias-corrected SRON L2 TROPOMI methane product for the period 01.06.18 - 29.02.20. A surface altitude bias is also applied to highlight any topography induced effects. The Calvert landfill site is indicated by a black circle in the centre of each figure.

The first noticeable consequence of this approach is that the number of overpasses drops dramatically, with only 37 files for > 70% coverage reducing to 20 files when this criterion is increased to > 90% coverage. This first step yields very different results especially in background concentrations, with higher values seen for the stricter coverage filter (Figure 6.10 (a) and (b) respectively). Observed structure in the averages is preserved when we average spatially as well as temporally using the weighted mean method onto a grid more representative of TROPOMI resolution (Figure 6.10 (c) and (g) respectively).

Application of the altitude bias correction indicates very little if no change relatively to the observed gradients across the study area (Figure 6.10 (b), (d), (f) and (h) respectively). We do however observe in all cases two distinct high regions to the west and south west of the landfill site. Other high spots occur but are not necessarily consistent across all cases. Therefore, to be able to attribute these high spots to emissions we need to look at individual overpasses themselves to determine whether we are confident that there are no further data artefacts that could be biasing what we observe. Due to the low number of overpasses for the > 90% threshold we default to the > 70% criteria as we progress and neglect the surface altitude correction.

Individual days with more than 70% data coverage were found to have striping patterns which were also identified in figures for larger areas (which are not shown here) and corrected for the TROPOMI CO product by Borsdorff *et al.* (2019). These patterns can be seen in Figure 6.11 where along-track pixels (visualised as 'columns' or north-to-south 'lines') present high values in contrast to their neighbouring along-track pixel for various days such as 08.01.2019, 28.01.2019, 25.02.2019, 19.04.2019 and 29.11.2019. The effect is more visible when saturating the colour scale (which are not shown here).
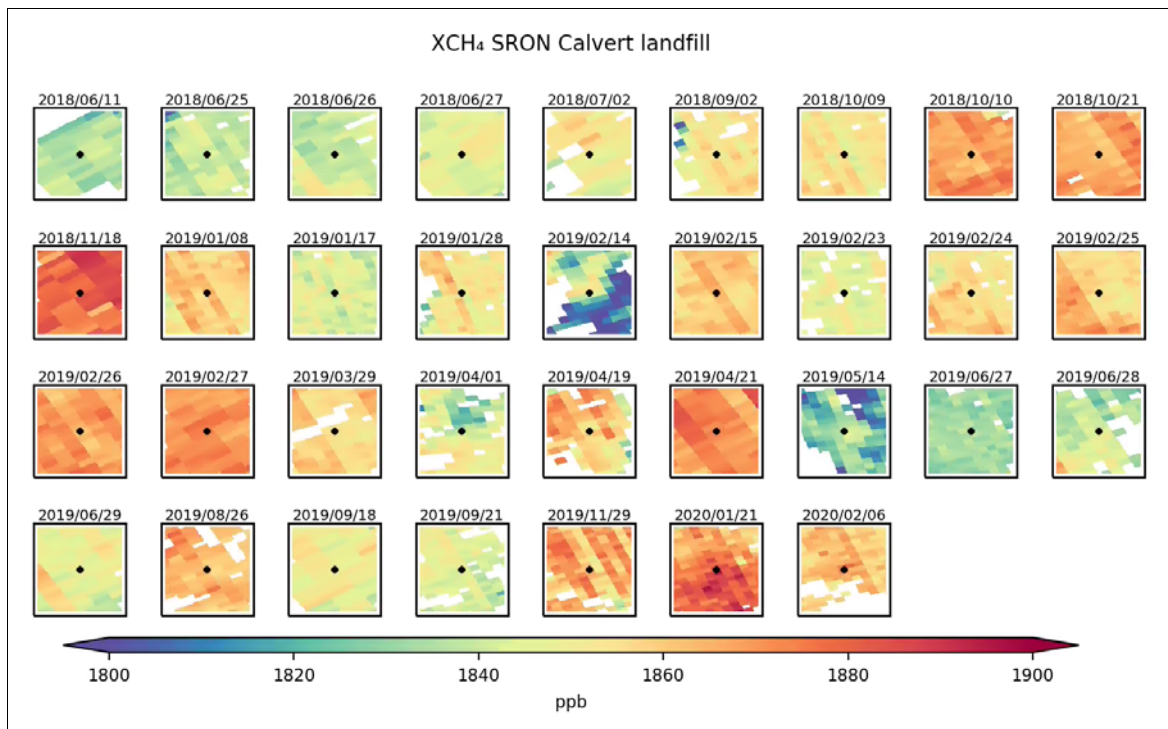
Figure 6.11 Methane column amount fractions (in parts-per-billion) for every day with more than 70% data coverage over the area around the Calvert landfill site, in a 100 by 100 km box. Data generated using v14.14 of the bias-corrected SRON L2 TROPOMI methane product for the period 01.06.18 - 29.02.20 using an oversampled grid box size of 0.01° x 0.01° and a QA ≥ 0.4 filter.

We applied a simple method to correct for the random bias introduced by the striping, which consisted of normalising each pixel along-track. Assuming an additive effect of the striping bias toward the mean for all the days, the normalisation was applied by taking the mean of the three top and three bottom pixels from every along-track 'line' and subtracting it from each pixel value on that 'line'.
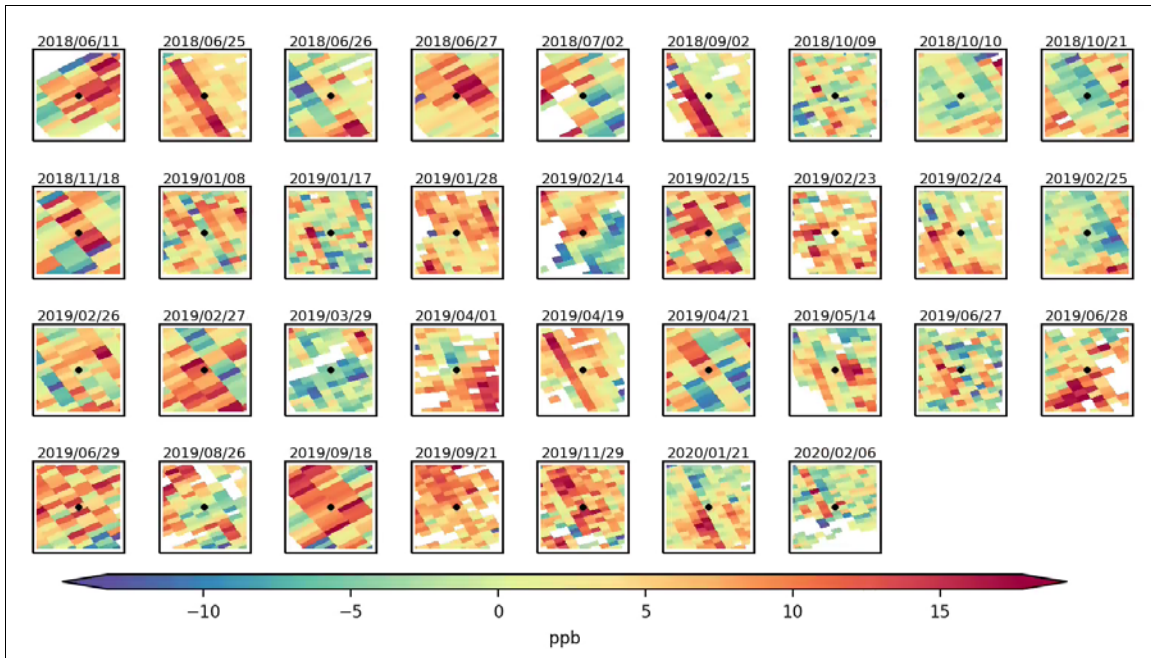
Figure 6.12 Along-track normalised data from Figure 6.11 shown as the difference (in parts-per-billion) to the mean of the three top and three bottom pixels for every along-track 'line', or enhancement.

Figure 6.12 shows that striping patterns remain present, especially in a feature present on 25.06.2018, 02.09.2018, 19.04.2019 and 21.01.2020. As this feature could be accumulating to cause the enhancement in the mean (see Figure 6.13), we removed those days in order to check if the enhancement remained (see Figure 6.14).
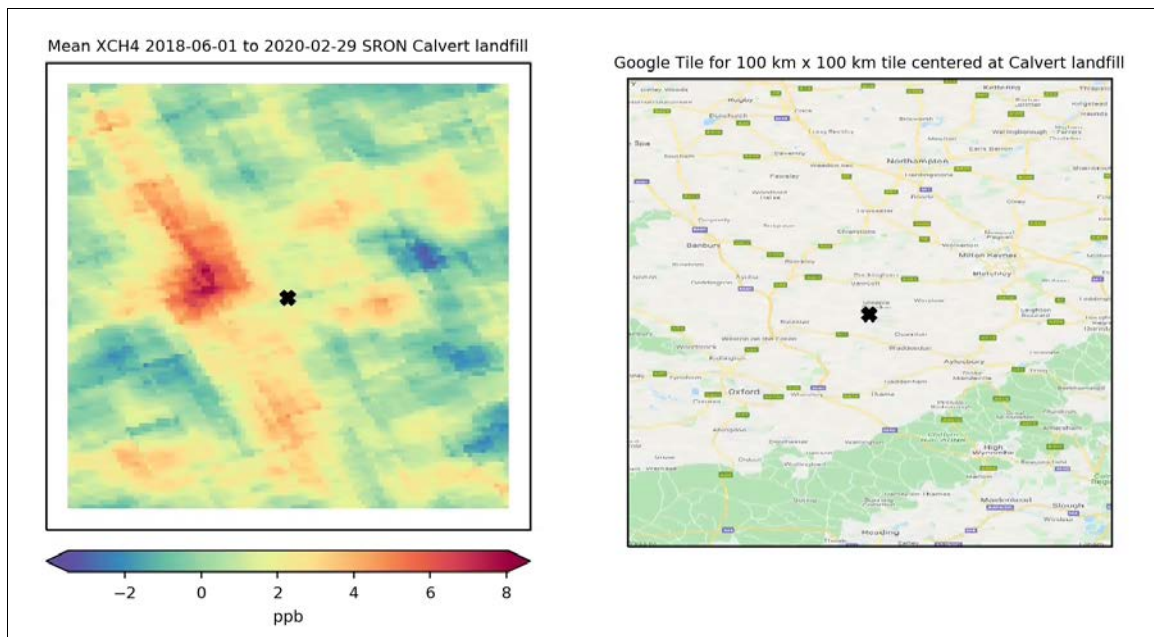
Figure 6.13 Mean methane column amount fractions (in parts-per-billion) calculated using data from days with more than 70% data coverage (see Figure 6.11) over the area around the Calvert landfill site, in a 100 by 100 km box. Data generated using v14.14 of the bias-corrected SRON L2 TROPOMI methane product for the period 01.06.18 - 29.02.20 using an oversampled grid box size of 0.01° x 0.01° and a QA ≥ 0.4 filter.
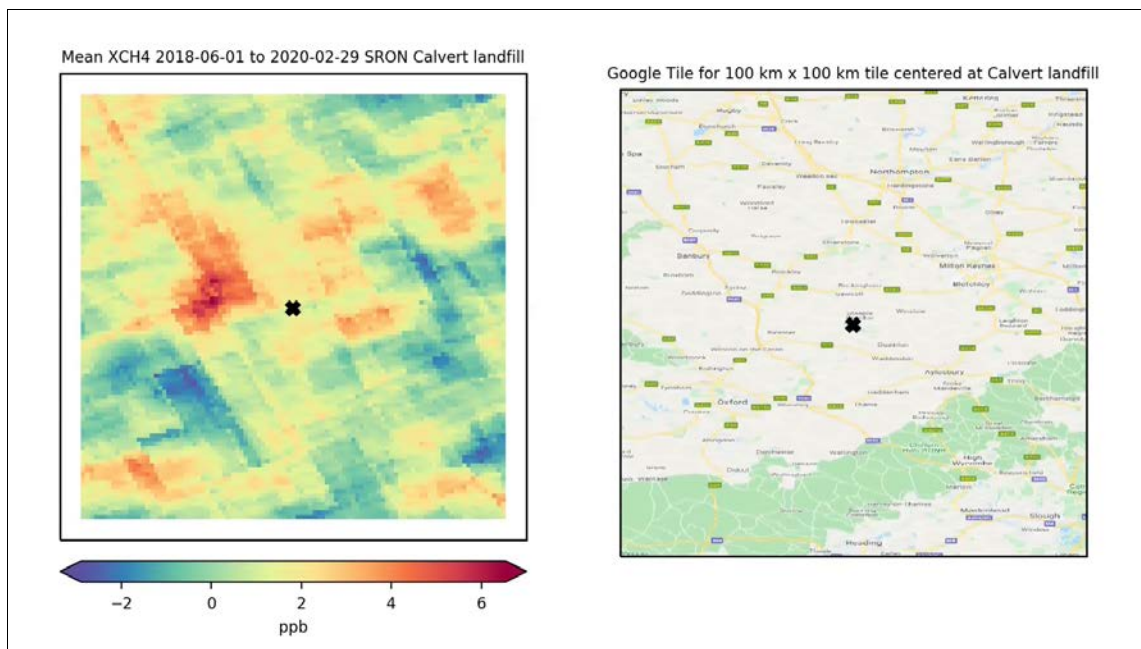
Figure 6.14 Mean methane column amount fraction difference to the mean of the three top and three bottom pixels for every along-track 'line', or enhancement (in parts-per-billion) calculated using data from days with more than 70% data coverage (see Figure 6.12) over the area around the Calvert landfill site, in a 100 by 100 km box. Data generated using v14.14 of the bias-corrected SRON L2 TROPOMI methane product for the period 01.06.18 - 29.02.20 using an oversampled grid box size of 0.01° x 0.01° and a QA ≥ 0.4 filter.

As can be seen in Figure 6.14, the enhancement remains after removing the days with a systematic striping even after attempting to remove the effect. However, it is around 2 ppb lower, suggesting that if this work is to be progressed further, a more robust de-striping method should be applied to avoid overestimations.

6.4 Conclusions and suggestions for future work

6.4.1 Conclusions

We have successfully developed a capability at the Environment Agency to download TROPOMI methane L2 products data and process these to L3 products. The L3 products produced by the Environment Agency show excellent agreement when compared with those produced by NCEO (University of Leicester). This new Environment Agency capability is therefore suitable for continued use and future development.

We investigated whether emissions of methane from UK landfill sites could be identified by the TROPOMI instrument. Landfill sites were chosen as the focus of this case study because individual landfills emit larger amounts of methane emissions than other (*e.g.* agricultural) individual methane sources.

Although emissions of methane from landfills have been observed by TROPOMI in other countries, work by the Environment Agency and NCEO in this short case study did not identify any methane emissions from even the UK landfills that emit the largest amount of methane (according to emissions inventories). This is primarily because methane sources in the UK (and other landfills in Europe) are small compared to those identified in publications using TROPOMI measurements. The coverage of valid measurements over the UK was also sparse due to cloud cover and (in part) low data quality, with some areas of Scotland recording no valid measurements over the 26 month period studied.

Satellite monitoring of methane has the potential to support regulatory activities by measuring landfill emissions but, when using the current ESA L2 methane product and the methods we have applied here, TROPOMI cannot be used to detect emissions from landfills in the UK. In Section 6.4.2, we present a number of suggestions for future work, including further development of the current product, which may be able to tease out a methane signal from landfills.

This case study has however provided valuable insight into the applicability and limitations of the current ESA methane product, for example, use of different versions of the product give results that can differ significantly. Further planned improvements to the product products is likely to increase the potential applicability of TROPOMI methane measurements to regulated activity

The experiences gained during the case study has also helped the Environment Agency significantly increase its knowledge of satellite measurements in general (and methane in particular), and specifically of handling TROPOMI data. These skills and the tools developed will be beneficial when working with future satellite capabilities more specifically designed for measurements of point sources of methane (*e.g.* Copernicus CO2M, GHGSat satellites, EDF MethaneSat and Bluefield). These have the potential to provide game-changing capabilities.

6.4.2   Suggestions for future work

Additional work that may increase the probability of measuring methane emissions from landfills using TROPOMI is:

- Using ground-based methane surveys to first establish what near-landfill methane signals are likely to be and under what weather situations they are most discernible. TROPOMI data targeting those situations could then be interrogated

- Implementation of the improved de-striping method already in use for the TROPOMI CO product.

- Use of a more sophisticated use of wind data to do wind-directional sampling, ideally using wind-rotational sampling.

- Use an image analysis or decluttering method to remove false features

It should also be noted that this case study has not considered any aspect of the uncertainty of the measurement, specifically the propagation of uncertainties from L2 product. This would improve the understanding of the potential applicability of these measurements but is highly complex and it would require a large research project to achieve this.

The capabilities of GHGSat satellites should also be investigated in more detail. Some data from GHGSat satellites which is available free-of-charge from ESA, and these data are likely to be more immediately applicable to regulatory activities.

7   Conclusions

This report details the findings of an exploratory Environment Agency project delivered in 2020 to investigate how satellite-based measurements of air pollutants and greenhouse gases might be applied to the Environment Agency's regulatory activities. The exploratory nature of the work means that the findings presented in this report are indicative rather than conclusive and definitive. Similarly, the conclusions and recommendations stated here for future work are based on expert judgement rather than a firm forecast of the use of satellite data in regulatory applications.

To understand whether data from current satellite instruments were able to provide evidence of air pollutant or greenhouse gas emissions or impacts due to regulated activity, we delivered three proof-of-concept case studies. These case studies, which are summarised in more detail in Section 3 investigated:

- Ammonia using the IASI instrument on the MetOp-A satellite

- Nitrogen dioxide using the TROPOMI instrument on the Sentinel-5P satellite

- Methane using the TROPOMI instrument on the Sentinel-5P satellite

In order to maximise the chances of success, the case studies were defined by identifying potentially high signal-to-background situations resulting from emissions from Environment Agency regulated sources.

The results of the case studies are presented in detail in Section 4, Section 5 and Section 6, where full conclusions and suggestions for further work are also provided. These are not reproduced in full here, but the key findings of each case study are summarised below:

In the ammonia / IASI case study, we identified clear monthly and seasonal variations in measured ammonia over the UK when data from an 11-year record were aggregated for each month and season. Variations in annual average concentrations from year to year were more subtle, and no long-term trend in annual-average ammonia could be identified over the 11-year record. The variable and relatively sparse temporal coverage of the IASI data contributed to the observed year-to-year variations in annual-average ammonia. We showed that the seasonal and monthly variations in ammonia measured by the IASI instrument can also be observed in data from the UK ammonia monitoring network. This comparison with the ground-based reference method for ammonia goes some way in validating the IASI data.

An investigation of whether IASI data can be used to detect changes in spatial patterns of measured ammonia in small areas of the UK, for example where there have been recent large increases in intensive agriculture, was also performed. This found evidence of above-UK average increases in areas such as Powys (Wales) and Cheshire and Shropshire (England) when long-term changes and multi-year averages are considered. All these areas have experienced recent significant increases in intensive farming activity. We also found some evidence that satellite data could identify differences in ammonia increases between lowland and upland districts in Powys – these were consistent with differences in the potential for locating intensive agriculture in such districts.

Data from current satellite instruments cannot however identify ammonia emissions from individual sites as the data is too sparse, the spatial resolution is too large and measurements over the UK are not sufficiently sensitive (there is a lack of large ammonia point sources in the UK). Outside the UK, there are larger and less disperse

point sources of ammonia that other groups have identified using IASI data with signal sharpening techniques.

In the nitrogen dioxide / TROPOMI case study, we found that TROPOMI data could be used to identify elevated levels of $TCNO_2$ around three large UK point source emitters of NO_x (Drax power station, Port Talbot Steel Works and Grangemouth refinery), even when averaging only three months of data. The relative strength of the $TCNO_2$ signals from each source was found to correspond to the size order of their NO_x emissions reported in emissions inventories, *i.e.* Drax > Port Talbot > Grangemouth.

Directional NO_2 plumes from Drax and Port Talbot could be identified using conditional aggregation based on wind direction. When using wind-speed and wind-direction conditional aggregation, directional NO_2 plumes from these point sources could be identified for most wind speed groups. Although this visual identification of plumes from these large sources was possible, a brief investigation to quantify the emissions contributing to the plumes was unsuccessful.

The methane / TROPOMI case study was not able to detect elevated levels or plumes of methane from UK landfills – the largest methane emissions from UK landfills are small compared to methane sources outside the UK that have been successfully detected by TROPOMI. The case study did however identify a data presentation issue (specifically the occurrence of 'stripes' in plotted data) in the ESA TROPOMI Level 2 product. It also significantly advanced the Environment Agency's tools, skills and knowledge, which will be beneficial for application to future satellites designed for methane point sources - these satellites are expected to be much more applicable to regulation.

In summary, although some evidence of regulated activity was found in the ammonia and nitrogen dioxide case studies, we determined that current satellite data for air-quality pollutants and greenhouse gases are not yet able to resolve individual sites routinely. However, this conclusion is limited to analysis of satellite data alone, *i.e.* not in combination with other data or modelling, so analyses that combine satellite and other data may be still effective at identifying individual site activities.

The 'next generation' of satellite instruments (including geostationary satellites, miniaturised satellites and constellation satellites) do however promise significant improvements in temporal resolution, spatial resolution and sensitivity, so that these instruments are much more likely to be applicable to regulation. Details of these future capabilities are given in Section 2.6, and in the 'Conclusions and suggestions for future work' sub-section of each case study.

The continued development of data products from current satellite instruments and techniques for their use will also increase the potential usefulness of data from current satellites to regulators. These include:

- The use and further development of 'signal-sharpening' techniques to enhance spatial resolution (*e.g.* oversampling and supersampling) and/or to enhance signal strength (*e.g.* wind-rotation and conditional aggregation techniques). These 'signal-sharpening' techniques are described in more in detail in Section 2.5.3.

- Improvements to existing Level 2 satellite products (*e.g.* improved bias correction).

- Better understanding of uncertainties and the more robust determination of uncertainties in Level 3 products.

The use of satellite data in combination with other data sources (*e.g.* ground-based instruments and sensors) also has significant potential. These additional sources of

data can also be used to provide quality assurance of satellite measurements. They can also be used, perhaps in combination with dispersion modelling to identify to optimise the selection, analysis and interpretation of satellite data - such analyses based on combined methods are recommended as a priority for future investigations.

These future developments mean that satellite measurements of air quality and greenhouse gases are soon likely to be applied to a wide range of outcomes including health, ecosystems, climate change and the path to net zero emissions. Some specific potential uses include:

- Validating emissions inventories

- Validating of models

- Improving ground-based monitoring. For example, optimising the location of monitors; enabling more intelligent 'in-filling' of gaps in monitoring, and providing a better interpretation of monitoring data (including better understanding of how representative ground-based data is of sites, districts, sectors and national-scale patterns).

- Underpinning international Protocols and Agreements through providing transboundary measurements

- Assessing source, area and sector compliance

- Determining the exposure of people and ecosystems

- Monitoring the effectiveness of air quality improvement activities (*e.g.* agricultural controls)

The use and availability of satellite air quality and greenhouse gas data continues to grow, with an expected major increase in the next 2-3 years arising from instruments on geostationary, miniaturised and constellation satellites. As a result of this, the Environment Agency and other government bodies can expect to be presented with satellite data from industry, campaign groups and members of the public. These stakeholders are likely to compare the new data with other evidence that the Environment Agency already uses to inform its decisions, such as data from emissions inventories and ground-based monitoring. These comparisons are likely to raise questions that the Environment Agency will want to answer, and for this purpose it will need to stay abreast of the ongoing developments satellite data and analysis methods.

The work in the project has enabled the Environment Agency to understand the current and future landscape of satellite measurements of air pollutants and greenhouse gases. It has also enabled data processing methods, including signal-sharpening techniques such as oversampling, to be developed - these could be further adapted to be applied to next-generation satellite data. It will therefore help the Environment Agency to be well positioned to understand, adopt and respond to future developments in this area.

References

AERIS (2020) *IASI ammonia product guide* [online]. Available at: https://iasi.aeris-data.fr/NH3_readme/ [Accessed 17 January 2021].

AIRBUS (2020) *Zephyr: Pioneering the Stratosphere* [online]. Available at: https://www.airbus.com/defence/uav/zephyr.html [Accessed 17 January 2021].

ALLEN, G., HOLLINGSWORTH, P., KABBABE, K., PITT, J., MEAD, M., ILLINGWORTH, S., ROBERTS, G., BOURN, M., SHALLCROSS, D. AND PERCIVAL, C. (2019) The development and trial of an unmanned aerial system for the measurement of methane flux from landfill and greenhouse gas emission hotspots. *Waste Management*, 87, 883–892. Available at: https://doi.org/10.1016/j.wasman.2017.12.024 [Accessed 17 January 2021].

BBC NEWS (2020) *Coronavirus: Lockdowns continue to suppress European pollution*, 27 March 2020 [online]. Available at: https://www.bbc.co.uk/news/science-environment-52065140 [Accessed 17 January 2021].

BEIRLE, S., BOERSMA, K. F., PLATT, U., LAWRENCE, M. G. AND WAGNER, T. (2011) Megacity emissions and lifetimes of nitrogen oxides probed from space, *Science*, 333(6050), 1737-1739. Available at: https://doi.org/10.1126/science.1207824 [Accessed 17 January 2021].

BEIRLE, S., BORGER, C., DÖRNER, S., LI, A., HU, Z., LIU, F., WANG, Y. AND WAGNER, T. (2019) Pinpointing nitrogen oxide emissions from space, *Science Advances,* 5(11), eaax9800. Available at: https://doi.org/10.1126/sciadv.aax9800 [Accessed 17 January 2021].

BLOOM, A.A., PALMER, P.I., FRASER, A., REAY, D.S. AND FRANKENBERG, C. (2010) Large-scale controls of methanogenesis inferred from methane and gravity Spaceborne Data, *Science*, 327 (5963), 322-325. Available at: https://doi.org/10.1126/science.1175176 [Accessed 17 January 2021].

BOERSMA, K. F., ESKES, H. J., RICHTER, A., DE SMEDT, I., LORENTE, A., BEIRLE, S., VAN GEFFEN, J. H. G. M., ZARA, M., PETERS, E., VAN ROOZENDAEL, M., WAGNER, T., MAASAAKERS, J. D., VAN SER A, R. J., NIGHTINGALE, J., DE RUDDER, A., IRIE, H., PINARDI, G., LAMBERT, J.-C., AND COMPERNOLLE, S. C. (2018) Improving algorithms and uncertainty estimates for satellite NO_2 retrievals: results from the quality assurance for the essential climate variables (QA4ECV) project, *Atmospheric Measurement Techniques*, 11, 6651–6678. Available at: https://doi.org/10.5194/amt-11-6651-2018 [Accessed 17 January 2021].

BOESCH, H., BAKER, D., CONNOR, B., CRISP, D. AND MILLER, C. (2011) Global characterization of CO_2 column retrievals from shortwave-infrared satellite observations of the Orbiting Carbon Observatory-2 Mission, *Remote Sens*ing, 3(2), 270-304. Available at: https://doi.org/10.3390/rs3020270 [Accessed 17 January 2021].

BORSDORFF, T., AAN DE BRUGH, J., SCHNEIDER, A., LORENTE, A., BIRK, M., WAGNER, G., KIVI, R., HASE, F., FEIST, D. G., SUSSMANN, R., RETTINGER, M., WUNCH, D., WARNEKE, T. AND LANDGRAF, J. (2019) Improving the TROPOMI CO data product: update of the spectroscopic database and destriping of single orbits, *Atmospheric Measurement Techniques,* 12, 5443–5455. Available at: https://doi.org/10.5194/amt-12-5443-2019 [Accessed 17 January 2021].

BÖRJESSON, G., DANIELSSON, A. AND SVENSSON, B. H. (2000) Methane fluxes from a Swedish landfill determined by geostatistical treatment of static chamber

measurements, *Environmental Science and Technology*, 34 (18), 4044–4050. Available at: https://doi.org/10.1021/es991350s [Accessed 17 January 2021].

BOURN, M., ROBINSON, R., INNOCENTI, F. AND SCHEUTZ, C. (2019) Regulating landfills using measured methane emissions: An English perspective, *Waste Management*, 87, 860-869. Available at: https://doi.org/10.1016/j.wasman.2018.06.032 [Accessed 17 January 2021].

BRITISH GEOLOGICAL SURVEY (2020) *Coordinate Convertor* [online]. Available at: https://www.bgs.ac.uk/data/webservices/convertForm.cfm [Accessed 17 January 2021].

BUCHWITZ, M., REUTER, M., SCHNEISING, O., BOESCH, H., GUERLET, S., DILS, B., ABEN, I., ARMANTE, R., BERGAMASCHI, P., BLUMENSTOCK, T., BOVENSMANN, H., BRUNNER, D., BUCHMANN, B., BURROWS, J. P., BUTZ, A., CHÉDIN, A., CHEVALLIER, F., CREVOISIER, C. D., DEUTSCHER, N. M., FRANKENBERG, C., HASE, F., HASEKAMP, O. P., HEYMANN, J., KAMINSKI, T., LAENG, A., LICHTENBERG, G., DE MAZIÈRE, M., NOËL, S., NOTHOLT, J., ORPHAL, J., POPP, C., PARKER, R., SCHOLZE, M., SUSSMANN, R., STILLER, G. P., WARNEKE, T., ZEHNER, C., BRIL, A., CRISP, D., GRIFFITH, D. W. T., KUZE, A., O'DELL, C., OSHCHEPKOV, S., SHERLOCK, V., SUTO, H., WENNBERG, P., WUNCH, D., YOKOTA, T. AND YOSHIDA, Y. (2015) The Greenhouse Gas Climate Change Initiative (GHG-CCI): Comparison and quality assessment of near-surface-sensitive satellite-derived global CO_2 and CH_4 data sets, *Remote Sensing of Environment*, 162, 344-362. Available at: https://doi.org/10.1016/j.rse.2013.04.024 [Accessed 17 January 2021].

BUCHWITZ, M., SCHNEISING, O., REUTER, M., HEYMANN, J., KRAUTWURST, S., BOVENSMANN, H., BURROWS, J. P., BOESCH, H., PARKER, R. J., SOMKUTI, P., DETMERS, R. G., HASEKAMP, O. P., ABEN, I., BUTZ, A., FRANKENBERG, C. AND TURNER, A. J. (2017) Satellite-derived methane hotspot emission estimates using a fast data-driven method, *Atmospheric Chemistry and Physics*, 17, 5751–5774. Available at: https://doi.org/10.5194/acp-17-5751-2017 [Accessed 17 January 2021].

CENTRE FOR ENVIRONMENTAL DATA ANALYSIS (2020), *Centre for Environmental Data Analysis* [online]. Available at: https://www.ceda.ac.uk [Accessed 17 January 2021]

CHIPPERFIELD, M., MARAIS, E., POPE, R., KERRIDGE, B., SIDDDANS, R., HARRISON, J., MONIZ, S. AND GHALAINEY, M. (2019) *Applying Earth Observation to Reduce Uncertainties in Emissions Inventories*, poster at the Air quality, past, present and future conference, November 2019, London, UK.

CLARISSE, L., SHEPHARD M. W., DENTENER, F., HURTMANS, D., CADY-PEREIRA, K., KARAGUILAN, F., HURTMANS, M., CLERBAUX, C. AND COHEUR, P.-F. (2010) Satellite monitoring of ammonia: a case study of the San Joaquin Valley, *Journal of Geophysical Research,* 115, D13302. Available at: https://doi.org/10.1029/2009JD013291 [Accessed 17 January 2021].

CLARISSE, L., CLERBAUX, C. AND COHEUR, P.-F. (2019) Tracking down global NH_3 point sources with wind-adjusted superresolution, *Atmospheric Measurement Techniques*, 12, 5457-5473. Available at: https://doi.org/10.5194/amt-12-5457-2019 [Accessed 17 January 2021].

CLERBAUX, C., BOYNARD, A., CLARISSE, L., GEORGE, M., HADJI-LAZARO, J., HERBIN, H., HURTMANS, D., POMMIER, M, RAZAVI, A., TURQUETY, S., WESPES, C AND COHEUR, P.-F. (2009) Monitoring of atmospheric composition using the thermal infrared IASI/MetOp sounder, *Atmospheric Chemistry and Physics*, 9, 6041–

6053. Available at: https://doi.org/10.5194/acp-9-6041-2009 [Accessed 17 January 2021].

COMMITTEE ON EARTH OBSERVATION SATELLITES (2020) *CEOS / ESA Earth Observation handbook.* Available at: http://database.eohandbook.com/ [Accessed 17 January 2021].

COPERNICUS ATMOSPHERIC MONITORING SERVICE (2020a) *Copernicus Atmospheric Monitoring Service* [online]. Available at: https://atmosphere.copernicus.eu/ [Accessed 17 January 2021].

COPERNICUS ATMOSPHERIC MONITORING SERVICE (2020b) *Copernicus Atmospheric Monitoring Service - Satellite Observations* [online]. Available at: https://atmosphere.copernicus.eu/satellite-observations [Accessed 17 January 2021].

COPERNICUS ATMOSPHERIC MONITORING SERVICE (2020c) *Copernicus Atmospheric Monitoring Service - Data* [online]. Available at: https://atmosphere.copernicus.eu/data [Accessed 17 January 2021].

COUNCIL OF THE EUROPEAN COMMUNITIES (1999) *Directive 1999/31/EC on the landfill of waste.* Available at: https://eur-lex.europa.eu/eli/dir/1999/31/oj [Accessed 17 January 2021].

COUNCIL OF THE EUROPEAN COMMUNITIES (2004) *Directive 2004/107/EC of the European Parliament and of the Council of 15 December 2004 relating to arsenic, cadmium, mercury, nickel and polycyclic aromatic hydrocarbons in ambient air.* Available at http://data.europa.eu/eli/dir/2004/107/oj [Accessed 17 January 2021].

COUNCIL OF THE EUROPEAN COMMUNITIES (2008) *Directive 2008/50/EC of the European Parliament and of the Council of 21 May 2008 on ambient air quality and cleaner air for Europe.* Available at: http://data.europa.eu/eli/dir/2008/50/oj [Accessed 17 January 2021].

COUNCIL OF THE EUROPEAN COMMUNITIES (2010) *Directive 2010/75/EU of the European Parliament and of the Council of 24 December 2010 on industrial emissions (integrated pollution prevention and control).* Available at: https://eur-lex.europa.eu/eli/dir/2010/75/oj [Accessed 17 January 2021].

COUNCIL OF THE EUROPEAN COMMUNITIES (2016) *Directive (EU) 2016/2284 of the European Parliament and of the Council of 14 December 2016 on the reduction of national emissions of certain atmospheric pollutants, amending Directive 2003/35/EC and repealing Directive 2001/81/EC.* Available at: http://data.europa.eu/eli/dir/2016/2284/oj [Accessed 17 January 2021].

DAMMERS, E., McLINDEN, C. A., GRIFFIN, D., SHEPHARD, M. W., VAN DER GRAAF, S. V., LUTSCH, R., SCHAAP, M., GAINAIRU-MATZ, Y., FIOLETIOV, V., VAN DAMME., M., WHITBURN, S., CLARISSE, L., CADY-PEREIRA, K., CLERBAUX, COHEUR P.-F. AND ERISMAN, J. W. (2019) NH_3 emissions from large point sources derived from CrIS and IASI satellite observations, *Atmospheric Chemistry and Physics*, 19, 12261-12293. Available at: https://doi.org/10.5194/acp-19-12261-2019 [Accessed 17 January 2021].

DE GOUW, J. A., PEPIJN VEEFKIND, J., ROOSENBRAND, E., DIX, B., LIN, J. C., LANDGRAF, J. AND LEVELT, P. F. (2020) Daily satellite observations of methane from oil and gas production regions in the United States, *Scientific Reports*, 10, 1379. Available at: https://doi.org/10.1038/s41598-020-57678-4 [Accessed 17 January 2021].

DEPARTMENT FOR BUSINESS, ENERGY & INDUSTRIAL STRATEGY (2017) *CRC Energy Efficiency Scheme* [online]. Available at:

https://www.gov.uk/government/collections/crc-energy-efficiency-scheme [Accessed 17 January 2021].

DEPARTMENT FOR BUSINESS, ENERGY & INDUSTRIAL STRATEGY (2019) *Energy Savings Opportunity Scheme (ESOS)* [online]. Available at: https://www.gov.uk/guidance/energy-savings-opportunity-scheme-esos [Accessed 17 January 2021].

DEPARTMENT FOR BUSINESS, ENERGY & INDUSTRIAL STRATEGY (2020a) *2018 UK Greenhouse Gas Emissions, Final figures* [online]. Available at: https://assets.publishing.service.gov.uk/government/uploads/system/uploads/attachment_data/file/862887/2018_Final_greenhouse_gas_emissions_statistical_release.pdf [Accessed 17 January 2021].

DEPARTMENT FOR BUSINESS, ENERGY & INDUSTRIAL STRATEGY (2020b) *National Atmospheric Emissions Inventory* [online]. Available at: https://naei.beis.gov.uk/ [Accessed 17 January 2021].

DEPARTMENT FOR BUSINESS, ENERGY & INDUSTRIAL STRATEGY (2020c) *National Atmospheric Emissions Inventory - Emissions Map Data for Nitrogen Oxides (NO_x expressed as NO_2) in 2017* [online]. Available at: https://naei.beis.gov.uk/data/map-uk-das?pollutant_id=6&emiss_maps_submit=naei-20200803130746 [Accessed 5 August 2020; note that the 2017 emissions data has since been superseded by the 2018 emissions data].

DEPARTMENT FOR ENVIRONMENT, FOOD & RURAL AFFAIRS (2007) *The Air Quality Strategy for England, Scotland, Wales and Northern Ireland* [online]. Available at: https://www.gov.uk/government/publications/the-air-quality-strategy-for-england-scotland-wales-and-northern-ireland-volume-1. [Accessed 17 January 2021].

DEPARTMENT FOR ENVIRONMENT, FOOD & RURAL AFFAIRS (2019) *Clean Air Strategy* [online]. Available at: https://assets.publishing.service.gov.uk/government/uploads/system/uploads/attachment_data/file/770715/clean-air-strategy-2019.pdf [Accessed 17 January 2021].

DEPARTMENT FOR ENVIRONMENT, FOOD & RURAL AFFAIRS (2020a) *UK-AIR - Monitoring Networks* [online]. Available at: https://uk-air.defra.gov.uk/networks/ [Accessed 17 January 2021].

DEPARTMENT FOR ENVIRONMENT, FOOD & RURAL AFFAIRS (2020b) *Emissions of air pollutants in the UK, 1970 to 2018 – Particulate matter (PM_{10} and $PM_{2.5}$)* [online]. Available at: https://www.gov.uk/government/publications/emissions-of-air-pollutants/emissions-of-air-pollutants-in-the-uk-1970-to-2018-particulate-matter-pm10-and-pm25 [Accessed 17 January 2021].

DEPARTMENT FOR ENVIRONMENT, FOOD & RURAL AFFAIRS (2020c) *Emissions of air pollutants in the UK, 1970 to 2018 – Ammonia (NH_3)* [online]. Available at: https://www.gov.uk/government/publications/emissions-of-air-pollutants/emissions-of-air-pollutants-in-the-uk-1970-to-2018-ammonia-nh3 [Accessed 17 January 2021].

DEPARTMENT FOR ENVIRONMENT, FOOD & RURAL AFFAIRS (2020d) *Emissions of air pollutants in the UK, 1970 to 2018 – Nitrogen oxides (NO_x)* [online]. Available at: https://www.gov.uk/government/publications/emissions-of-air-pollutants/annual-emissions-of-nitrogen-oxides-in-the-uk-1970-2018 [Accessed 17 January 2021].

DEPARTMENT FOR ENVIRONMENT, FOOD & RURAL AFFAIRS (2020e) *Emissions of air pollutants in the UK, 1970 to 2018 – Sulphur dioxide (SO_2)* [online]. Available at: https://www.gov.uk/government/publications/emissions-of-air-pollutants/emissions-of-air-pollutants-in-the-uk-1970-to-2018-sulphur-dioxide-so2 [Accessed 17 January 2021].

DEPARTMENT FOR ENVIRONMENT, FOOD & RURAL AFFAIRS (2020f) *Emissions of air pollutants in the UK, 1970 to 2018 – Non-methane volatile organic compounds (NMVOCs)* [online]. Available at: https://www.gov.uk/government/publications/emissions-of-air-pollutants/emissions-of-air-pollutants-in-the-uk-1970-to-2018-non-methane-volatile-organic-compounds-nmvocs [Accessed 17 January 2021].

DEPARTMENT FOR ENVIRONMENT, FOOD & RURAL AFFAIRS (2020g), *Livestock numbers in England and the UK* [online]. Available at: https://www.gov.uk/government/statistical-data-sets/structure-of-the-livestock-industry-in-england-at-december [Accessed 17 January 2021].

DEPARTMENT FOR ENVIRONMENT, FOOD & RURAL AFFAIRS (2020h), *UK-AIR Monitoring Networks; United Kingdom Eutrophying & Acidifying Network (UKEAP)* [online]. Available at: https://uk-air.defra.gov.uk/networks/network-info?view=ukeap [Accessed 17 January 2021].

DEPARTMENT FOR ENVIRONMENT, FOOD & RURAL AFFAIRS (2020i) *Concentrations of nitrogen dioxide* [online]. https://www.gov.uk/government/publications/air-quality-statistics/ntrogen-dioxide. [Accessed 17 January 2021].

DEPARTMENT FOR ENVIRONMENT, FOOD & RURAL AFFAIRS (2020j) *Air pollution in the UK 2019.* Available at: https://uk-air.defra.gov.uk/library/annualreport/viewonline?year=2019_issue_1 [Accessed 17 January 2021].

DEPARTMENT FOR ENVIRONMENT, FOOD & RURAL AFFAIRS and DEPARTMENT FOR TRANSPORT (2017) *UK Plan for Tackling Roadside Nitrogen Dioxide Concentrations: An Overview.* Available at: https://assets.publishing.service.gov.uk/government/uploads/system/uploads/attachment_data/file/633269/air-quality-plan-overview.pdf [Accessed 17 January 2021].

DEPARTMENT OF AGRICULTURE, ENVIRONMENT AND RURAL AFFAIRS (2020) *Poultry populations in Northern Ireland from 1981 to 2019* [online]. Available at:, https://www.daera-ni.gov.uk/publications/farm-animal-population-data [Accessed 17 January 2021].

EARTHSENSE (2020), *Products - MappAir®* [online]. Available at: www.earthsense.co.uk/mappair [Accessed 17 January 2021].

ENVIRONMENT AGENCY (2004) *LFTGN03: guidance on the management of landfill gas* [online]. Available at: https://assets.publishing.service.gov.uk/government/uploads/system/uploads/attachment_data/file/321606/LFTGN03.pdf [Accessed 17 January 2021]

ENVIRONMENT AGENCY (2010a) *Regulatory Guidance Series No. LFD 1: Understanding the Landfill Directive* [online]. Available at: https://assets.publishing.service.gov.uk/government/uploads/system/uploads/attachment_data/file/296536/LIT_8286_f89fa7.pdf [Accessed 17 January 2021]

ENVIRONMENT AGENCY (2010b) *Guidance on monitoring landfill gas surface emissions* [online]. Available at: https://assets.publishing.service.gov.uk/government/uploads/system/uploads/attachment_data/file/321614/LFTGN07.pdf [Accessed 17 January 2021]

ENVIRONMENT AGENCY (2014) *Environmental permitting: landfill sector technical guidance* [online]. Available at: https://www.gov.uk/government/collections/environmental-permitting-landfill-sector-technical-guidance [Accessed 17 January 2021]

ENVIRONMENT AGENCY (2018) *The state of the environment: air quality* [online]. Available at: https://assets.publishing.service.gov.uk/government/uploads/system/uploads/attachment_data/file/729820/State_of_the_environment_air_quality_report.pdf [Accessed 17 January 2021].

ENVIRONMENT AGENCY (2019) *Regulating for people, the environment and growth, 2018* [online]. Available at: https://assets.publishing.service.gov.uk/government/uploads/system/uploads/attachment_data/file/865277/Regulating_for_people_the_environment_and_growth_2018.pdf [Accessed 17 January 2021].

ENVIRONMENT AGENCY (2020) *Climate change agreements* [online]. Available at: https://www.gov.uk/guidance/climate-change-agreements--2 [Accessed 17 January 2021].

ENVIRONMENTAL PROTECTION AGENCY (2020) *Air Emissions* [online]. Available at: https://www.epa.ie/pubs/reports/air/airemissions/ [Accessed 17 January 2021].

ENVIRONMENTAL SERVICES ASSOCIATION (2020) *Landfill Industry Codes of Practice* [online]. Available at: http://www.esauk.org/what-we-do/raising-standards/guidance/landfill-guidance [Accessed 17 January 2021].

EUNOMIA RESEARCH & CONSULTING (2011) *Inventory Improvement Project – UK Landfill Methane Emissions Model: Final Report to Defra and DECC* [online]. Available at: http://sciencesearch.defra.gov.uk/Document.aspx?Document=9887_WR1124Finalreportincludingappendices.pdf [Accessed 17 January 2021].

EUROPEAN CENTRE FOR MEDIUM-RANGE WEATHER FORECASTS (2020) *ERA5 dataset* [online]. Available at: https://www.ecmwf.int/en/forecasts/datasets/reanalysis-datasets/era5 [Accessed 17 January 2021].

EUROPEAN COMMITTEE FOR STANDARDIZATION (2012) European Standard EN 14211:2012, *Ambient air quality - Standard method for the measurement of the concentration of nitrogen dioxide and nitrogen monoxide by chemiluminescence*

EUROPEAN COMMISION (2020) *EU Emissions Trading System* [online]. Available at: https://ec.europa.eu/clima/policies/ets_en [Accessed 17 January 2021].

EUROPEAN ORGANISATION FOR METEOROLOGICAL SATELLITES (2020) *IASI* [online]. Available at: https://www.eumetsat.int/website/home/Satellites/CurrentSatellites/Metop/MetopDesign/IASI/index.html [Accessed 17 January 2021].

EUROPEAN PARLIAMENT (2009) *Regulation (EC) No 1005/2009 of the European Parliament and of the Council of 16 October 2009 on substances that deplete the ozone layer.* Available at: http://data.europa.eu/eli/reg/2009/1005/oj [Accessed 17 January 2021].

EUROPEAN PARLIAMENT (2014) *Regulation (EU) No 517/2014 of the European Parliament and of the Council of 16 April 2014 on fluorinated gases and repealing Regulation (EC) No 842/2006.* Available at: http://data.europa.eu/eli/reg/2014/517/oj [Accessed 17 January 2021].

EUROPEAN POLLUTANT AND TRANSFER REGISTER (2020), Data obtained from the *E-PRTR Pollutant Releases database* [online]. Available at: https://prtr.eea.europa.eu/#/pollutantreleases [Accessed 17 January 2021]

EUROPEAN SPACE AGENCY (2020a) *Sentinel Online - Missions - Sentinel-5P* [online]. Available at: https://sentinel.esa.int/web/sentinel/missions/sentinel-5p [Accessed 17 January 2021].

EUROPEAN SPACE AGENCY (2020b) *Sentinel Online - Missions - Sentinel-4* [online]. Available at: https://sentinel.esa.int/web/sentinel/missions/sentinel-4 [Accessed 17 January 2021].

EUROPEAN SPACE AGENCY (2020c) *New Space satellite pinpoints industrial methane emissions* [online]. Available at: https://www.esa.int/Applications/Observing_the_Earth/Copernicus/Sentinel-5P/New_Space_satellite_pinpoints_industrial_methane_emissions [Accessed 17 January 2021].

EUROPEAN SPACE AGENCY (2020d) *Contract signed to build Europe's carbon dioxide monitoring mission* [online]. Available at: https://www.esa.int/Applications/Observing_the_Earth/Copernicus/Contract_signed_to_build_Europe_s_carbon_dioxide_monitoring_mission [Accessed 17 January 2021].

EUROPEAN SPACE AGENCY (2020e) *Technical Guides - Sentinel-5P TROPOMI - Cal/Val activities – overview* [online]. Available at: https://earth.esa.int/web/sentinel/technical-guides/sentinel-5p/calibration-validation-activities [Accessed 17 January 2021].

EUROPEAN SPACE AGENCY (2020f) *Instrument payload (TROPOMI)* [online]. Available at: https://sentinel.esa.int/web/sentinel/missions/sentinel-5p/instrumental-payload [Accessed 17 January 2021].

EUROPEAN SPACE AGENCY (2020g) *Copernicus Open Access Hub* [online]. Available at: https://scihub.copernicus.eu/ [Accessed 17 January 2021].

EUROPEAN SPACE AGENCY (2020h) *Research and User Support for Sentinel Core Products* [online]. Available at: https://rus-training.eu/ [Accessed 17 January 2021].

FENG, L., PALMER, P. I., BÖSCH, H., PARKER, R. J., WEBB, A. J., CORREIA, C. S. C., DEUTSCHER, N. M., DOMINGUES, L. G., FESIT, D. G., GATTI, L. V., GLOOR, E., HASE, F., KIVI, R., LIU, Y., MILLER, J. B., MORINO, I., SUSSMANN, R., STRONG, K., UCHINO, O., WANG, J., AND ZAHN, A. (2017) Consistent regional fluxes of CH_4 and CO_2 inferred from GOSAT proxy $XCH_4 : XCO_2$ retrievals, 2010–2014, *Atmospheric Chemistry and Physics*, 17, 4781–4797. Available at: https://doi.org/10.5194/acp-17-4781-2017 [Accessed 17 January 2021].

GANESAN, A. L.; RIGBY, M., LUNT, M.F., PARKER, R. J., BOESCH, H., GOULDING, N., UMEZAWA, T., ZAHN, A; CHATTERJEE, A., PRINN, R. G., TIWARI, Y. K., VAN DER SCHOOT, M. AND KRUMMEL, P. B. (2017) Atmospheric observations show accurate reporting and little growth in India's methane emissions, *Nature Communications*, 8, 836. Available at: https://doi.org/10.1038/s41467-017-00994-7 [Accessed 17 January 2021].

GANESAN, A. L., SCHWIETZKE, S., POULTER, B., ARNOLD, T., LAN, X., RIGBY, M., VOGEL, F. R., VAN DER WERF, G. R., JANSSENS-MAENHOUT, G., BOESCH, H., PANDEY, S, MANNING, A. J., JACKSON, R. B. NISBET, E.G. AND MANNING, M. R. (2019) Advancing scientific understanding of the global methane budget in support of the Paris Agreement. *Global Biogeochemical Cycles*, 33 (12). Available at: https://doi.org/10.1029/2018GB006065 [Accessed 17 January 2021].

GHGSAT (2020a) *GHGSat D - Claire* [online]. Available at: https://www.ghgsat.com/our-platforms/claire/ [Accessed 17 January 2021].

GHGSAT (2020b) *GHGSat C1 - Iris* [online]. Available at: https://www.ghgsat.com/our-platforms/iris/ [Accessed 17 January 2021].

HIGHWAYS ENGLAND (2017) *Our strategy to improve air quality* [online]. Available at: https://assets.publishing.service.gov.uk/government/uploads/system/uploads/attachment_data/file/634933/N160081_Air_Quality_Strategy_Final_V18.pdf [Accessed 17 January 2021].

HM GOVERNMENT (2018) *A Green Future: Our 25 Year Plan to Improve the Environment* [online]. Available at: https://assets.publishing.service.gov.uk/government/uploads/system/uploads/attachment_data/file/693158/25-year-environment-plan.pdf [Accessed 17 January 2021].

INNOCENTI, F., ROBINSON, R., GARDINER, T., FINLAYSON, J. AND CONNOR, A. (2017) Differential absorption lidar (DIAL) measurements of landfill methane emissions, *Remote Sensing*, 9 (9), 953. Available at: https://doi.org/10.3390/rs9090953 [Accessed 17 January 2021].

JONES, P.D., HARPHAM, C. AND BRIFFA, K. R. (2013) Lamb weather types derived from reanalysis products. *International Journal of Climatology*, 33, 1129–1139. Available at: https://doi.org/10.1002/joc.3498 [Accessed 17 January 2021].

KELLY, R. (2019) *First Use of High-Resolution Satellite Data to Derive UK Top-Down City-Scale NO_2 Emissions*, Undergraduate Dissertation, School of Earth and Environment, University of Leeds.

KIM, J., JEONG, U., AHN, M.-H., KIM, J. H., PARK, R. J., LEE, H., SONG, C. H., CHOI, Y. S., LEE, K.-H., YOO, J.-M., JEONG, M.-J., PARK, S. K., LEE, K.-M., SONG, C.-K., KIM, S.-W., KIM, Y.-J., KIM, S.-W., KIM, M., GO, S., LIU, X., CHANCE, K., AL-SAADI, J., VEIHELMANN, B., BHARTIA, P. K., TORRES, O., GONZÁLEZ ABAD, G., HAFFNER, D. P., KO, D. H., LEE, S. H., WOO, J.-H., CHONG, H., PARK, S. S., NICKS, D., CHOI, W. J., MOON, K.-J., CHO, A., YOON, J., KIM, S.-K., HONG, H., LEE, K., LEE, H., LEE, S., CHOI, M., PEPIJN VEEFKIND, J., LEVELT, P. F., EDWARDS, D. P., KANG, M., EO, M., BAK, J., BAEK, K., KWON, H.-A., YANG, J., PARK, J., HAN, K. M., KIM, B.-R., SHIN, H.-W., CHOI, H., LEE, E., CHONG, J., CHA, Y., KOO, J.-H., IRIE, H., HAYASHIDA, S., KASAI, Y., KANAYA, Y., LIU, C., LIN, J., CRAWFORD, J. H., CARMICHAEL, G. R., NEWCHURCH, M. J., LEFER, B. L., HERMAN, J. R., SWAP, R. J., LAU, A. K. H., KUROSU, T. P., JAROSS, G., AHLERS, B., DOBBER, M., McELROY, C. T. AND CHOI, Y. (2020) New Era of Air Quality Monitoring from Space: Geostationary Environment Monitoring Spectrometer (GEMS). *Bulletin of the American Meteorological Society*, 101, E1–E22. Available at: https://doi.org/10.1175/BAMS-D-18-0013.1 [Accessed 17 January 2021].

LEGISLATION (2008) *Climate Change Act 2008* [online]. Available at: http://www.legislation.gov.uk/ukpga/2008/27/contents [Accessed 17 January 2021].

LEGISLATION (2010) *The Environmental Permitting (England and Wales) Regulations 2010* [online]. Available at: http://www.legislation.gov.uk/ukdsi/2010/9780111491423/contents [Accessed 17 January 2021].

LINEHAN, T. (2020) *Statistics from satellite imagery data: Report for CSO Remote Sensing and Satellite Imagery Group*, Central Statistics Office (Ireland), Report under review.

LIU, L., ZHANG, X., WONG, A. Y. H., XU, W., XUEJUN, L., LIU, X., LI, Y., HUAN, M., LU, X., ZHAO, L., WANG, Z., WU, X. AND WEI, J. (2019) Estimating global surface ammonia concentrations inferred from satellite retrievals, *Atmospheric Chemistry and Physics*, 19, 12051–12066. Available at: https://doi.org/10.5194/acp-19-12051-2019 [Accessed 17 January 2021].

LORENTE, A., BORSDOFF, T., BUTZ, A., HASEKAMP, O., AAN DE BRUGH, J., SCHNEIDER, A., HASE, F., KIVI, R., WUNCH, D., POLLARD, D. F., SHIOMI, K., DEUTSCHER, N. M., VELAZCO, V. A., ROEHL, C. M., WENNBERG, P. O., WARNEKE, T. AND LANDGRAF, J. (2020) Methane retrieved from TROPOMI: improvement of the data product and validation of the first two years of measurements, *Atmospheric Measurement Techniques*, under review as of 17 January 2021. Available at: https://doi.org/10.5194/amt-2020-281 [Accessed 17 January 2021].

MAASAKKERS, J. D., ELFARSDÓTTIR, A., LORENTE, A., PANDEY, S., HOUWELING, S., JERVIS, D., McKEEVER, J., VARON, D., SCARPELLI, T., CUSWORTH, D. H., DUREN, R., THORPE, A. K, GAUTAM, R., OMARA, M., GUANTER, L AND ABEN, I. (2020) *Using TROPOMI to guide fine-resolution satellite instruments towards methane point sources*, presentation at 16th International Workshop on Greenhouse Gas Measurements from Space, June 2020. Available at: https://cdn.eventsforce.net/files/ef-xnn67yq56ylu/website/9/2_728_joannes_maasakkers-_using_tropomi_to_guide_fine-resolution_satellite_instruments_towards_methane_point_sources.pdf [Accessed 17 January 2021].

METHANESAT (2020) *About MethaneSAT* [online]. Available at: https://www.methanesat.org/about-methanesat/ Accessed 17 January 2021].

MØNSTER, J., SAMUELSSON, J., KJELDSEN, P. AND SCHEUTZ, C. (2015) Quantification of methane emissions from 15 Danish landfills using the mobile tracer dispersion method, *Waste Management*, 35, 177-186. Available at: http://dx.doi.org/10.1016/j.wasman.2014.09.006 [Accessed 17 January 2021].

MYHRE, G., SHINDELL, D., BRÉON, F.-M., COLLINS, W., FUGLESTVEDT, J., HUANG, J., KOCH, D., LAMARQUE, J.-F., LEE. D., MENDOZA, B., NAKAJIMA T., ROBOCK A., STEPEHENS G., TAKEMURA, T. AND ZHANG, H. (2013) *Anthropogenic and Natural Radiative Forcing* [online]. Available at: http://www.climatechange2013.org/images/report/WG1AR5_Chapter08_FINAL.pdf In: *Climate Change 2013: The Physical Science Basis. Contribution of Working Group I to the Fifth Assessment Report of the Intergovernmental Panel on Climate Change* [Accessed 17 January 2021]

NATIONAL CENTRE FOR EARTH OBSERVATION (2020) *Using Sentinel-5P to monitor Air Quality changes since the Coronavirus outbreak: a UK Expert View* [online]. Available at: https://www.nceo.ac.uk/article/using-sentinel-5p-to-monitor-air-quality-changes-since-the-coronavirus-outbreak-a-uk-expert-view/ [Accessed 17 January 2021].

NATIONAL STATISTICS (2020) *Air Quality Statistics* [online]. Available at:, https://www.gov.uk/government/statistics/air-quality-statistics. [Accessed 17 January 2021].

NETHERLANDS INSTITUTE FOR SPACE RESEARCH (2019) *Algorithm Theoretical Baseline Document for Sentinel-5 Precursor Methane Retrieval* [online]. Available at: https://sentinel.esa.int/documents/247904/2476257/Sentinel-5P-TROPOMI-ATBD-Methane-retrieval [Accessed 17 January 2021]

PALMER, P. I., O'DOHERTY, S., ALLEN, G., BOWER, K., BÖSCH, H., CHIPPERFIELD, M. P., CONNORS, S., DHOME, S., FENG, L., FINCH, D. P., GALLAGHER, M. W., GLOOR, E., GONZI, S., HARRIS, N. R. P., HELFER, C., HUMPAGE, N., KERRIDGE, B., KNAPPETT, D., JONES, R. L., LE BRETON, M., LUNT, M. F., MANNING, A. J., MATTHIESEN, S., MULLER, J. B. A., MULLINGER, N., NEMITZ, E., O'SHEA, S., PARKER, R. J., PERCIVAL, C. J., PITT, J., RIDDICK, S. N., RIGBY, M., SEMBHI, H., SIDDANS, R., SKELTON, R. L., SMITH, P., SONDERFELD, H., STANLEY, K., STAVERT, A. R., WENGER, A., WHITE, E., WILSON, C. AND

YOUNG, D. (2018) A measurement-based verification framework for UK greenhouse gas emissions: an overview of the Greenhouse gAs Uk and Global Emissions (GAUGE) project, Atmospheric Chemistry and Physics, 18, 11753–11777. Available at: https://doi.org/10.5194/acp-18-11753-2018 [Accessed 17 January 2021].

PANDEY, S., HOUWELING, S., KROL, M., ABEN, I., MONTEIL, G., NECHITA-BANDA, N., DLUGOKENCKY, E. J., DETMERS, R., HASEKAMP, O., XU, X., RILEY, W. J., POULTER, B., ZHANG, Z, McDONALD, K. C., WHITE, J. W. C., BOUSQUET, P. AND RÖCKMANN, T. (2017) Enhanced methane emissions from tropical wetlands during the 2011 La Niña. *Scientific Reports,* 7, 45759. Available at: https://doi.org/10.1038/srep45759 [Accessed 17 January 2021].

PANDEY, S., GAUTAM, R., HOUWELING, S., VAN DER GON, H. D., SADAVARTE, P., BORSDOFF, T., HASEKAMP, O., LANGRAF, J., TOL, P., VAN KEMPEN, T., HOOGEVEEN, R., VAN HESS, R., HAMBURG, S. P., MAASAKKERS, J. D. AND ABEN, I. (2019) Satellite observations reveal extreme methane leakage from a natural gas well blowout. *Proceedings of the National Academy of Sciences of the Unites States of America*, 116, 26376-26381. Available at: https://doi.org/10.1073/pnas.1908712116 [Accessed 17 January 2021].

PARKER, R. J., BOESCH, H., BYCKLING, K., WEBB, A. J., PALMER, P. I., FENG, L., BERGAMASCHI, P., CHEVALLIER, F., NOTHOLT, J., DEUTSCHER, N., WARNEKE, T., HASE, F., SUSSMANN, R., KAWAKAMI, S., KIVI, R., GRIFFITH, D. W. T. AND VELAZCO, V. (2015) Assessing 5 years of GOSAT Proxy XCH_4 data and associated uncertainties, *Atmospheric Measurement Techniques*, 8, 4785-4801. Available at: https://doi.org/10.5194/amt-8-4785-2015 [Accessed 17 January 2021].

PARKER, R. J., BOESCH, H., McNORTON, J., COMYN-PLATT, E., GLOOR, M., WILSON, C., CHIPPERFIELD, M. P., HAYMAN, G. D. AND BLOOM, A. A. (2018) Evaluating year-to-year anomalies in tropical wetland methane emissions using satellite CH_4 observations*, Remote Sensing of Environment*, 211, 261-275. Available at: https://doi.org/10.1016/j.rse.2018.02.011 [Accessed 17 January 2021].

POPE, R. J., SAVAGE, N. H., CHIPPERFIELD, M. P., ARNOLD, S. R. AND OSBORNE, T. J. (2014) The influence of synoptic weather regimes on UK air quality: analysis of satellite column NO_2, *Atmospheric Science Letters*, 15 (3), 211-217. Available at: https://doi.org/10.1002/asl2.492 [Accessed 17 January 2021].

POPE, R. J., CHIPPERFIELD M. P., SAVAGE, N.H., ORDÓÑEZ, C., NEAL, L. S., LEE, L. A., DHOMSE, S. S., RICHARDS, N. A. D. AND KESLAKE, T. D. (2015) Evaluation of a regional air quality model using satellite column NO_2: treatment of observation errors and model boundary conditions and emissions. *Atmospheric Chemistry and Physics*, 15, 5611-5626. Available at: https://doi.org/10.5194/acp-15-5611-2015 [Accessed 17 January 2021].

POPE, R. J. AND PROVOD B. J. (2016a) Detection of the Yorkshire power stations from space: an air quality perspective. *Weather*, 71 (2), 40-44. Available at: https://doi.org/10.1002/wea.2651 [Accessed 17 January 2021].

POPE, R. J., MARSHALL, A. M. AND O'KANE, B. O. (2016b) Observing UK Bonfire Night pollution from space: analysis of atmospheric aerosol, *Weather*, 71 (11), 288-291. Available at: https://doi.org/10.1002/wea.2914 [Accessed 17 January 2021].

POPE, R. J., ARNOLD S. R., CHIPPERFIELD M. P., LATTER, B. G., SIDDANS, R. AND KERRIDGE B. J. (2018) Widespread changes in UK air quality observed from space. *Atmospheric Science Letters*, 19 (*5*), e817. Available at: https://doi.org/10.1002/asl.817 [Accessed 17 January 2021].

POPE, R. J., GRAHAM, A. M., CHIPPERFIELD M. P. AND PEPIJN VEEFKIND, J. (2019) High resolution satellite observations give new view of UK air quality. *Weather*,

74 (9), 316-320. Available at: https://doi.org/10.1002/wea.3441 [Accessed 17 January 2021].

QUALITY ASSURANCE FOR ESSENTIAL CLIMATE VARIABLES (2020a) *What is QA4ECV?* [online]. Available at: http://www.qa4ecv.eu/ [Accessed 17 January 2021].

QUALITY ASSURANCE FOR ESSENTIAL CLIMATE VARIABLES (2020b) *QA4ECV Essential Climate Variables* [online]. Available at: http://www.qa4ecv.eu/ecvs [Accessed 17 January 2021].

RICARDO ENERGY & ENVIRONMENT (2015) *Investigating the Feasibility of Innovative Technologies to Improve Air Quality Monitoring over the Medium to Long Term: Stage 1 and Stage 2 Report* [online]. Available at: https://uk-air.defra.gov.uk/assets/documents/reports/cat20/1607061156_DEFRA_innovative_tech_Final.pdf [Accessed 17 January 2021].

RICHMOND, B., MISRA, A., BROOMFIELD, M., BROWN, P., KARAGIANNI, E., MURRELS, T., PANG, Y., PASSANT, N., PEARSON, B., STEWART, R., THISTLETHWAITE, G., WAKELING, D., WALKER, C., WILTSHIRE, J., HOBSON, M., GIBBS, M., MISSELBROOK, T., DRAGOSITS, U. AND TOMLINSON, S. (2019), *UK Informative Inventory Report (1990 to 2017)* [online]. Available at: http://uk-air.defra.gov.uk/reports/cat09/1904121008_GB_IIR_2019_v2.0.pdf [Accessed 17 January 2021].

ROWE, E. C., MITCHELL, Z., TOMLINSON, S., LEVY, P., BANIN, L. F., SAWICKA, K., MARTÍN HERNANDEZ, C. AND DORE, A. (2020) *Trends Report 2020: Trends in critical load and critical level exceedances in the UK* [online]. Available at: https://uk-air.defra.gov.uk/library/reports?report_id=1001 [Accessed 17 January 2021].

ROYAL COLLEGE OF PHYSICIANS (2016) *Every breath we take: The lifelong impact of air pollution* [online]. Available at: https://www.rcplondon.ac.uk/file/2912/download Accessed 17 January 2021].

ROYAL NETHERLANDS METEOROLOGICAL INSTITUTE (2017) *Sentinel-5 precursor/TROPOMI Level 2 Product User Manual: Methane* [online]. Available at: http://www.tropomi.eu/sites/default/files/files/Sentinel-5P-Level-2-Product-User-Manual-Methane.pdf [Accessed 17 January 2021]

ROYAL NETHERLANDS METEOROLOGICAL INSTITUTE (2019) *S5P Mission Performance Centre Nitrogen Dioxide [L2 NO$_2$] Readme*. Available at: http://www.tropomi.eu/sites/default/files/files/publicSentinel-5P-Nitrogen-Dioxide-Level-2-Product-Readme-File.pdf. [Accessed 17 January 2021].

SCHNEISING, O., BUCHWITZ, M., REUTER, M., BOVENSMAN, H., BURROWS, J. P., BORSDOFF, T., DEUTSCHER, N. M., FEIST, D., GRIFFITH, D. W. T., HASE, F. HERMANS, C., IRACI, L. T., KIVI, R., LANGRAF, J., MORINO, I., NOTHOLT, J., PETRI, C., POLLARD, D. F., ROCHE, S., SHIOMI, K., STRONG, S., SUSSMANN, R., VELAZCO, V. A., WARNEKE, T. AND WUNCH, D. (2019) A scientific algorithm to simultaneously retrieve carbon monoxide and methane from TROPOMI onboard Sentinel-5 Precursor, *Atmospheric Measurement Techniques*, 12, 6771-6802. Available at: https://doi.org/10.5194/amt-12-6771-2019 [Accessed 17 January 2021]

SCHNEISING, O., BUCHWITZ, M., REUTER, M., VANSELOW, S., BOVENSMANN, H., AND BURROWS, J. P. (2020) Remote sensing of methane leakage from natural gas and petroleum systems revisited, *Atmospheric Chemistry and Physics,* 20, 9169–9182. Available at: https://doi.org/10.5194/acp-20-9169-2020 [Accessed 17 January 2021]

SCHROTH, M. H., EUGSTER, W., GÓMEZ, K. E., GONZALEZ-GIL, G., NIKLAUS, P. A. AND OESTER, P. (2012) Above- and below-ground methane fluxes and

methanotrophic activity in a landfill-cover soil, *Waste Management*, 32, 879-889. Available at: https://doi.org/10.1016/j.wasman.2011.11.003 [Accessed 17 January 2021].

SCIENTIFIC AMERICAN (2019) *Private Space Race Targets Greenhouse Gas Emitters* [online]. Available at: https://www.scientificamerican.com/article/private-space-race-targets-greenhouse-gas-emitters/ [Accessed 17 January 2021].

SCOTTISH GOVERNMENT (2019) *Cleaner Air for Scotland Strategy – An Independent Review: Final report to the Scottish Government* [online]. Available at: https://www.gov.scot/binaries/content/documents/govscot/publications/independent-report/2019/08/cleaner-air-scotland-strategy-independent-review/documents/cleaner-air-scotland-strategy-independent-review/cleaner-air-scotland-strategy-independent-review/govscot%3Adocument/cleaner-air-scotland-strategy-independent-review.pdf [Accessed 17 January 2021].

SHEEHAN, A, BEDDOWS, A., GREEN, D. AND BEEVERS, S. (2019) *Geospatial estimation of non-exhaust emissions using remote earth observation*, poster at the Air quality, past, present and future conference, November 2019, London, UK.

SHENG, J.-X., JACOB, D. J., TURNER, A. J., MAASAKKERS, J. D., BENMERGUI, J., BLOOM, A. A., ARNDT, C., GAUTAM, R., ZAVALA-ARAIZA, D., BOESCH, H. AND PARKER, R. J. (2018) 2010–2016 methane trends over Canada, the United States, and Mexico observed by the GOSAT satellite: contributions from different source sectors, *Atmospheric Chemistry and Physics,* 18, 12257-12267. Available at: https://doi.org/10.5194/acp-18-12257-2018 [Accessed 17 January 2021]

SIDDANS, R., KNAPPETT, D., KERRIDGE, B., WATERFALL, A., HURLEY, J., LATTER, B., BOESCH, H. AND PARKER, R. (2017), Global height-resolved methane retrievals from the Infrared Atmospheric Sounding Interferometer (IASI) on MetOp, *Atmospheric Measurement Techniques*, 10, 4135-4164. Available at: https://doi.org/10.5194/amt-10-4135-2017 [Accessed 17 January 2021].

SOLERA GARCÍA, M. A., TIMMIS, R. J., VAN DIJK, N., WHYATT, J. D., LEITH, I. D., LEESON, S. R., BRABAN, C. F., SHEPPARD, L. J, SUTTON, M. A., AND TANG, Y. S. (2017) Directional passive ambient air monitoring of ammonia for fugitive source attribution; a field trial with wind tunnel characteristics, *Atmospheric Environment*, 107, 576-585. Available at: https://doi.org/10.1016/j.atmosenv.2017.07.043 [Accessed 17 January 2021].

SONDERFELD, H., BÖSCH, H, JEANJEAN, A. P. R., RIDDICK, S. N., ALLEN, G., ARS, S., DAVIES, S., HARRIS, N., HUMPAGE, N., LEIGH, R. AND PITT, J. (2017) CH_4 emission estimates from an active landfill site inferred from a combined approach of CFD modelling and in situ FTIR measurements, *Atmospheric Measurement Techniques*, 10, 3931-3946. Available at: https://doi.org/10.5194/amt-10-3931-2017 [Accessed 17 January 2021].

TANG, Y. S., BRABAN, C. F., DRAGOSITS, U., DORE, A. J., SIMMONS, I., VAN DIJK, N., POSKITT, J., DOS SANTOS PEREIRA, G., KEENAN, P. O., CONOLLY, C., VINCENT, K., SMITH, R. I., HEAL, M. R. AND SUTTON, M. A. (2018) Drivers for spatial, temporal and long-term trends in atmospheric ammonia and ammonium in the UK, *Atmospheric Chemistry and Physics*, 18, 705–733. Available at: https://doi.org/10.5194/acp-18-705-2018 [Accessed 17 January 2021].

TOBÍAS, A., CARNERERO, C., RECHE, C., MASSAGUÉ, J., VIA, M., CRUZ MINGUILLÓN, M., ALASTUEY, A. AND QUEROL, X. (2020) Changes in air quality during the lockdown in Barcelona (Spain) one month into the SARS-CoV-2 epidemic, *Science of the Total Environment*, 726, 138540, 4pp. Available at: https://doi.org/10.1016/j.scitotenv.2020.138540 [Accessed 17 January 2021].

TROPOSPHERIC EMISSIONS MONITORING OF POLLUTION (2020) *Welcome to TEMPO* [online]. Available at: http://tempo.si.edu/index.html [Accessed 17 January 2021].

TURNER, A. J., JACOB, D. J., WECHT, K. J., MAASAKKERS, J. D., LUNDGREN, E., ANDREWS, A. E., BIRAUD, S. C., BOESCH, H., BOWMAN, K. W., DEUTSCHER, N. M., DUBEY, M. K., GRIFFITH, D. W. T., HASE, F., KUZE, A., NOTHOLT, J., OHYAMA, H., PARKER, R., PAYNE, V. H., SUSSMANN, R., SWEENEY, C., VELAZCO, V. A., WARNEKE, T., WENNBERG, P. O. AND WUNCH, D. (2015) Estimating global and North American methane emissions with high spatial resolution using GOSAT satellite data, *Atmospheric Chemistry and Physics*, 15, 7049-7069. Available at: https://doi.org/10.5194/acp-15-7049-2015 [Accessed 17 January 2021].

TROPOSPHERIC EMISSION MONITORING INTERNET SERVICE (2020) *Tropospheric NO_2 from satellites - archive* [online]. Available at: http://www.temis.nl/airpollution/no2.html [Accessed 17 January 2021].

UK CENTRE FOR ECOLOGY AND HYDROLOGY (2020a), *DELTA active sampler system* [online]. Available at: https://www.ceh.ac.uk/services/delta-active-sampler-system [Accessed 17 January 2021].

UK CENTRE FOR ECOLOGY AND HYDROLOGY (2020b) *Air sampler systems for environmental monitoring: ALPHA sampler* [online]. Available at: https://www.ceh.ac.uk/services/delta-active-sampler-system [Accessed 17 January 2021].

UNITED NATIONS ECONOMIC COMMISSION FOR EUROPE (2020) *Protocol to Abate Acidification, Eutrophication and Ground-level Ozone: The 1999 Gothenburg Protocol to Abate Acidification, Eutrophication and Ground-level Ozone* [online]. Available at: http://www.unece.org/env/lrtap/multi_h1.html [Accessed 17 January 2021].

UNIVERSITY OF EAST ANGLIA (2020), *Lamb Weather Types* [online]. Available at: https://crudata.uea.ac.uk/cru/data/lwt/ [Accessed 17 January 2021].

VAN DAMME, M., CLARISSE, L., HEALD, C. L., HURTMANS, D., NGADI, Y., CLERBAUX, C., DOLMAN, A. J., ERISMAN, J. W. AND COHEUR, P.-F. (2014a) Global distributions, time series and error characterization of atmospheric ammonia (NH_3) from IASI satellite observations, *Atmospheric Chemistry and Physics*, 14, 2905-2922. Available at: https://doi.org/10.5194/acp-14-2905-2014 [Accessed 17 January 2021].

VAN DAMME, M., WICHINK KRUIT, R. J., SCHAPP, M., CLARISSE, L., CLERBAUX, C., COHEUR, P.-F., DAMMERS, E., DOLMAN, A. J. AND ERISMAN, J. W. (2014b) Evaluating 4 years of atmospheric ammonia (NH_3) over Europe using IASI satellite observations and LOTOS-EUROS model results, *Journal of Geophysical Research: Atmospheres*, 119, 9549–9566, Available at: https://doi.org/10.1002/2014JD021911 [Accessed 17 January 2021].

VAN DAMME, M., WHITBURN, S., CLARISSE, L., CLERBAUX, C., HURTMANS, F. AND COHEUR, P.-F. (2017) Version 2 of the IASI NH_3 neural network retrieval algorithm: near-real-time and reanalysed datasets, *Atmospheric Measurement Techniques*, 10, 4905-4914. Available at: https://doi.org/10.5194/amt-10-4905-2017 [Accessed 17 January 2021].

VAN DAMME, M., CLARISSE, L., WHITBURN, S., HADJI-LAZARO, J., HURTMANS, D., CLERBAUX, C., COHEUR, P.-F. (2018) Industrial and agricultural ammonia point sources exposed, *Nature*, 564, 99-103. Available at: https://doi.org/10.1038/s41586-018-0747-1 [Accessed 17 January 2021].

VARON, D. J., JACOB, D. J., MCKEEVER, J., JERVIS, D., DURAK, B. O. A., XIA, Y., and HUANG, Y. (2018) Quantifying methane point sources from fine-scale satellite observations of atmospheric methane plumes, *Atmospheric Measurement Techniques.*, 11, 5673–5686. Available at: https://doi.org/10.5194/amt-11-5673-2018 [Accessed 17 January 2021].

VARON, D. J., McKEEVER, J., JERVIS, D., MAASAKKERS, J. D., PANDEY, S., HOUWELING, S. ABEN, I., SCARPELLI, T. AND JACOB, D. J. (2019) Satellite discovery of anomalously large methane point sources from oil/gas production, *Geophysical Research Letters*, 46, 13507–13516. Available at: https://doi.org/10.1029/2019GL083798 [Accessed 17 January 2021].

VEEFKIND, J. P., ABEN I., McMULLEN, K., FÖRSTER, H., DE VRIES, J., OTTER, G., CLASS, J., ESKES, H. J., DE HAAN, J. F., KLEIPOOL, Q., VAN WEELE, M., HASEKAMP, O., HOOGEVEEN, R., LANDGRAF, J., SNEL, R., TOL, P., INGMANN, P., VOORS, R., KRUIZINGA, B., VINK, R., VISSER, H. AND LEVELT, P. F. (2012) TROPOMI on the ESA Sentinel-5 Precursor: a GMES Mission for global observations of atmospheric composition for climate, air quality and ozone layer applications. *Remote Sensing Environment,* 120, 70-83. Available at: https://doi.org/10.1016/j.rse.2011.09.027 [Accessed 17 January 2021].

VOHRA, K., MARAIS, E. A., SUCKRA, S., KRAMER, L., BLOSS, W. J., SAHU, R., GAUR, A., TRIPATHI, S. N., VAN DAMME, M., CLARISSE, L. AND COHEUR, P.-F. (2020) Long-term trends in air quality in major cities in the UK and India: A view from space, submitted for publication in *Atmospheric Chemistry and Physics.* Preprint available at: https://doi.org/10.5194/acp-2020-342 [Accessed 17 January 2021].

WELSH GOVERNMENT (2019), *Agricultural small area statistics, 2002 to 2018: tables* [online]. Available at: https://gov.wales/agricultural-small-area-statistics-2002-2018 [Accessed 17 January 2021].

WORLD METEOROLOGICAL ORGANIZATION (2020) *Observing Systems Capability Analysis and Review Tool* [online]. Available at https://www.wmo-sat.info/oscar/ [Accessed 17 January 2021].

WHITBURN, S., VAN DAMME, M., KAISER, J. W., VAN DER WERF, G. R., TURQUETY, S., HURTMANS, CLARISSE, L., CLERBAUX, C. AND COHEUR, P.-F. (2015) Ammonia emissions in tropical biomass burning regions: Comparison between satellite-derived emissions and bottom-up fire inventories, *Atmospheric Environment*, 121, 42-54. Available at: http://dx.doi.org/10.1016/j.atmosenv.2015.03.015 [Accessed 17 January 2021].

WHITBURN, S., VAN DAMME, M., CLARISSE, L., BAUDUIN, S., HEALD, C. L., HADJI-LAZARO, J., HURTMANS, D., ZONDIO, M. A., CLERBAUX, C. AND COHEUR, P.-F. (2016) A flexible and robust neural network IASI-NH_3 retrieval algorithm, *Journal of Geophyiscal Research: Atmospheres*, 121 (11), 6581-6599. Available at: https://doi.org/10.1002/2016JD024828 [Accessed 17 January 2021].

List of abbreviations

ADMS	Atmospheric Dispersion Modelling System
AIRS	Atmospheric Infrared Sounder
AOD	Aerosol Optical Depth
ALPHA	Adapted Low-cost Passive High Absorption [sampler]
API	Application programming interface
AOI	Area of interest
AQUM	Air Quality in the Unified Model
CAMS	Copernicus Atmospheric Monitoring Service
CEDA	Centre for Environmental Data Analysis
CEOS	Committee on Earth Observation Satellites
CFC	Chlorofluorocarbon
CH_4	Methane
CO	Carbon monoxide
CO_2	Carbon dioxide
CO2M	Carbon Dioxide Monitoring
CPU	Central Processing Unit
CRC	Carbon reduction commitment
CROME	Crop Map of England
CrIS	Cross-track Infrared Sounder
DAERA	Department of Agriculture, Environment and Rural Affairs [Northern Ireland]
Defra	Department for Agriculture, Food and Rural Affairs
DELTA	Denuder for Long-Term Atmospheric [sampler]
DIAL	Differential absorption lidar
DJF	December, January and February (*i.e.* meteorological Winter)
DPAS	Directional Passive Air Sampler
ECMWF	European Centre For Medium-Range Weather Forecasts
ECV	Essential climate variable(s)
EDF	Environmental Defense Fund (except when used in Table 5.1)
EMEP	European Monitoring and Evaluation Programme [network]
Envisat	Environmental Satellite
E-PRTR	European Pollutant and Transfer Register
ERS	European Remote Sensing
ESA	European Space Agency
EU	European Union
EUMETSAT	European Organisation for the Exploitation of Meteorological Satellites
FPA	Framework Partnership Agreement
FTIR	Fourier transform infrared [spectroscopy]
GAUGE	Greenhouse Gas UK and Global Emissions [project]
GEMS	Geostationary Environment Monitoring Spectrometer
GEO-KOMPSAT-2B	Geostationary Korea Multi Purpose Satellite-2B
GEOS	Goddard Earth Observing System
GHG	Greenhouse gas(es)
GHG-CCI	Greenhouse Gas Climate Change Initiative
GOME	Global Ozone Monitoring Experiment
GOSAT	Greenhouse Gases Observing Satellite
GPU	Graphics processing unit
HAPS	High-altitude platform stations
HCFC	Hydrochlorofluorocarbon
HPC	High performance computing [system]

IASI	Infrared Atmospheric Sounded Interferometer
IASI-NG	Infrared Atmospheric Sounded Interferometer - New Generation
IDL	Interactive Data Language
IRS	Infrared Sounder
IUP	Institute of Environmental Physics [at University of Bremen]
JJA	June, July and August (*i.e.* meteorological Summer)
JNCC	Joint Nature Conservation Committee
JPSS	Joint Polar Satellite System
KARI	Korea Aerospace Research Institute
KMNI	Royal Netherlands Meteorological Institute
L1	Level 1 [product]
L2	Level 2 [product]
L3	Level 3 [product]
L4	Level 4 [product]
LAQN	London Air Quality Network
MAM	March, April and May (*i.e.* meteorological Spring)
MANDE	Mini Annular Denuder [flux sampler]
MetOp	Meteorological Operational Satellite Programme
MetOp-SG	Meteorological Operational Satellite Programme – Second Generation
MODIS	Moderate Resolution Imaging Spectroradiometer
MOPITT	Measurements of Pollution in the Troposphere
$MtCO_2e$	Megatonnes of carbon dioxide equivalent
MTG-S	Meteosat Third Generation – Sounding
NAEI	National Atmospheric Emissions Inventory
NASA	National Aeronautics and Space Administration
NCEO	National Centre for Earth Observation
NDACC	Network for the Detection of Atmospheric Composition Change
NECD	National Emissions Ceilings Directive
NetCDF	Network common data format
NERC	Natural Environment Research Council
NH_3	Ammonia
NIEA	Northern Ireland Environment Agency
NMVOCs	Non-methane volatile organic compounds
N_2O	Nitrous oxide
NF_3	Nitrogen trifluoride
NO	Nitrogen oxide
NO_x	Nitrogen oxides
NO_2	Nitrogen dioxide
NOAA	National Oceanic and Atmospheric Administration
NPP	National Polar-orbiting Operational Environmental Satellite System Preparatory Project
NRW	Natural Resources Wales
O_3	Ozone
OMI	Ozone Monitoring Instrument
PM	Particulate matter
ppb	Parts-per-billion
QA	Quality assurance
QA4ECV	Quality Assurance for Essential Climate Variables
QC	Quality control
RAM	Random access memory
SCIAMACHY	Scanning Imaging Absorption Spectrometer for Atmospheric Chartography
SEPA	Scottish Environment Protection Agency
SF_6	Sulphur hexaflouride
SO_2	Sulphur dioxide

SON	September, October and November (*i.e.* meteorological Autumn)
SRON	Netherlands Institute for Space Research
SWIR	Short wave-infrared
TANSO-FTS	Thermal And Near infrared Sensor for carbon Observation - Fourier Transform Spectrometer
TCCON	Total Carbon Column Observing Network
$TCNO_2$	Tropospheric column nitrogen dioxide
TEMIS	Tropospheric Emissions Monitoring Internet Service
TEMPO	Tropospheric Emissions: Monitoring of Pollution
TIFF	Tagged Image File Format
TROPOMI	Tropospheric Measuring Instrument
UAS	Unmanned aerial system
UCL	University College London
UK	United Kingdom
UKCEH	UK Centre for Ecology & Hydrology
UKEAP	UK Eutrophying & Acidifying [Network]
UKRI	UK Research and Innovation
UNECE	United Nations Economic Commission for Europe
UV	Ultraviolet
UVSat	UV Satellite Data and Science Group
WGS	World Geodetic System
WMO	World Meteorological Organization

Annex: Stakeholders engaged

Stakeholders from the following companies, organisations, Government bodies, etc., were engaged with during the delivery of the project. The authors would like to thank them for the time and input, which was essential for the completion of this report.

Note that the stakeholders are listed in alphabetical order.

- Airbus
- AVS-UK Ltd
- Central Statistics Office Ireland
- Centre for Earth Observation Instrumentation
- Defra / Department for Transport Joint Air Quality Unit
- Defra Chief Scientist's Office
- Defra Earth Observation Centre of Excellence
- Department for Environment, Food & Rural Affairs (Defra)
- EarthSense
- Environmental Protection Agency, Ireland
- Highways England
- Joint Nature Conservation Committee (JNCC)
- King's College London
- MetOffice
- National Centre for Earth Observation
- National Physical Laboratory
- Natural England
- Natural Resources Wales
- Northern Ireland Environment Agency / Northern Ireland Department of Agriculture, Environment and Rural Affairs
- Public Health England
- RAL Space - Science and Technology Facilities Council
- Satellite Applications Catapult
- Scottish Environmental Protection Agency
- Scottish Government
- Surrey Satellite Technology Limited
- UCL
- UK Centre For Ecology & Hydrology

- Université Libre de Bruxelles
- University of Birmingham
- University of Edinburgh
- University of Leicester
- University of Leeds
- University of Manchester
- University of Oxford
- Welsh Government

Would you like to find out more about us or your environment?

Then call us on

03708 506 506 (Monday to Friday, 8am to 6pm)

Email: enquiries@environment-agency.gov.uk

Or visit our website

www.gov.uk/environment-agency

incident hotline

0800 807060 **(24 hours)**

floodline

0345 988 1188 **(24 hours)**

Find out about call charges (https://www.gov.uk/call-charges)

Environment first

Are you viewing this onscreen? Please consider the environment and only print if absolutely necessary. If you are reading a paper copy, please don't forget to reuse and recycle.